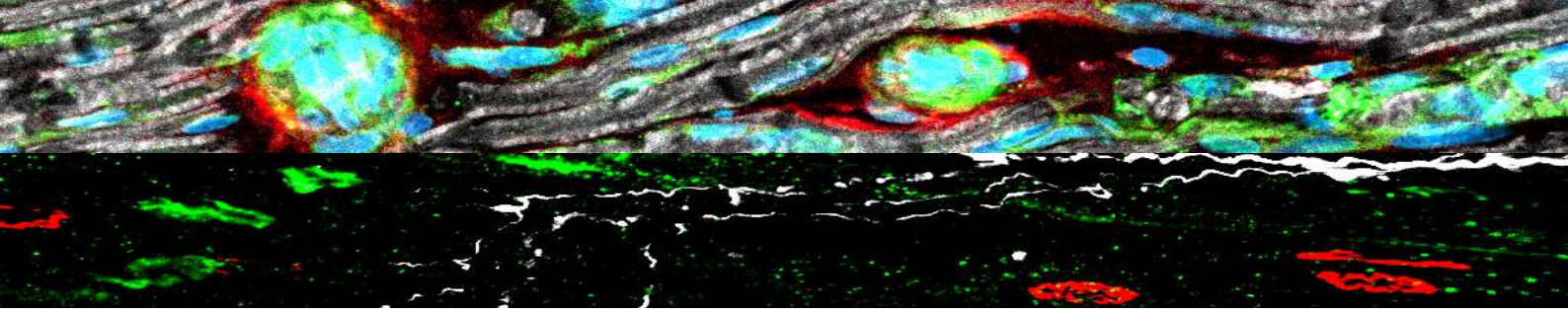

Tesis de Doctorado en Ciencias Biológicas
PEDECIBA Biología - Neurociencias
Universidad de la República

Microambiente celular neurodegenerativo en un modelo de Esclerosis Lateral Amiotrófica

Estudiante:

Emiliano Trias
Laboratorio de Neurodegenración
Institut Pasteur de Montevideo

Orientador:

Luis Barbeito, M.D.
Laboratorio de Neurodegeneración
Institut Pasteur de Montevideo

Co-orientador:

Joseph S. Beckman, Ph.D.
Linus Pauling Institute
Oregon State University

Tribunal:

Raúl E. Russo, Ph.D.
Dep. de Neurofisiología Celular y Molecular
Instituto de Investigaciones Biológicas Clemente Estable, Uruguay

Marcelo Hill, M.D., Ph.D.
Lab. de Inmunobiología, Facultad de Medicina, UdelaR, Uruguay
Lab. de Inmunoregulación e Inflamación, Institut Pasteur de Montevideo

Felipe Court, Ph.D.
Centro de Biología Integrativa, Universidad Mayor, Chile

Montevideo, 4 de diciembre de 2017

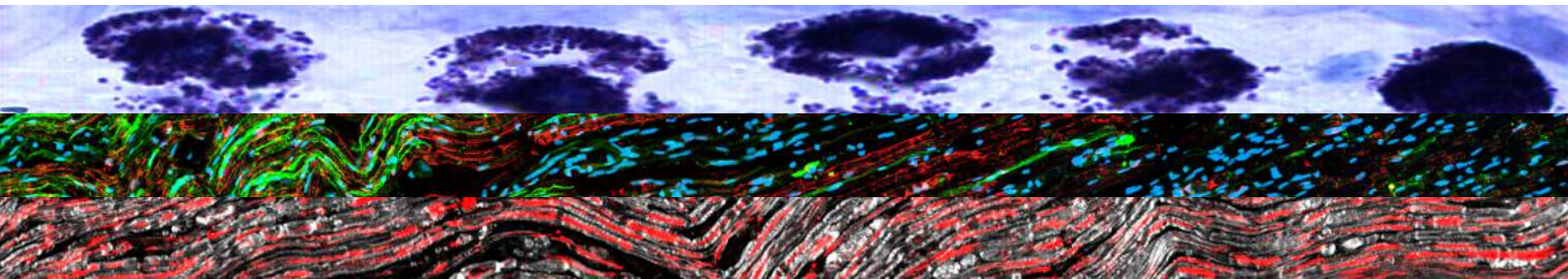

Agradecimientos

A todos aquellos que siempre apoyan esta carrera…

…a Jime
…mi familia
…mis amigos

…a todos los integrantes del Laboratorio de Neurodegeneración
…a los colegas de todos aquellos laboratorios en los que me ha tocado trabajar estos años

…a los miembros del tribunal, quienes amablemente han aceptado evaluar este trabajo

…a Joe y su familia

…especialmente a Luis

Índice

Publicaciones y manuscritos durante el Proyecto de Doctorado **5**

Resumen **6**

Abstract **7**

Introducción **8**

Antecedentes **13**

El microambiente celular neurodegenerativo **14**

Los astrocitos contribuyen a la patogenia de la ELA **15**

La ELA inducida por mutaciones de SOD1 se desarrolla por mecanismos "no autónomos celulares" **17**

La microglía contribuye a la patogenia de la ELA **17**

Significación de fenotipos gliales aberrantes en la ELA **19**

El componente inmune de la ELA **20**

La inflamación a lo largo de la vía motora periférica y el rol de las células de Schwann **21**

Hipótesis **25**

Objetivo **25**

Objetivos Específicos **26**

Resultados **28**

Publicación 1 ..... **29**

Phenotypically aberrant astrocytes that promote motoneuron damage in a model of inherited amyotrophic lateral sclerosis 32

Publicación 2 ..... **38**

Phenotypic transition of microglia into astrocyte-like cells associated with disease onset in a model of inherited ALS 41

Publicación 3 ..... **49**

Focal transplantation of aberrant glial cells carrying the $SOD1^{G93A}$ mutation into rat spinal cord induces extensive gliosis ..... **¡Error! Marcador no definido.**

Publicación 4 ..... **63**

Post-paralysis tyrosine kinase inhibition with masitinib abrogates neuroinflammation and slows disease progression in inherited amyotrophic lateral sclerosis 66

Publicación 5 78

Evidence for mast cells contributing to neuromuscular pathology in an inherited model of ALS 80

Manuscrito 1 94

Evidence for mast cell and neutrophil-driven sciatic nerve pathology associated to paralysis progression in an inherited ALS model..... 96

Discusión..... 109

Conclusiones 118

Referencias 119

Publicaciones y manuscritos durante el Proyecto de Doctorado

1) **Trias, E.,** Varela, V., Barreto-Núñez, R., Ibarburu, S., Kovacs, M.,. . . Barbeito, L. (2018). ***Evidence for mast cell and neutrophil-driven sciatic nerve pathology associated to paralysis progression in an inherited ALS model***. To be sumitted φ

2) Beilby, P.*, **Trias, E.***, Barreto-Núñez, R., Ibarburu, S., . . . Beckman, J.S. (2018). ***Glial cell senescnece in Amyotrophic Lateral Sclerosis***. To be sumitted.

3) **Trias, E**., Ibarburu, S., Barreto-Nunez, R., Varela, V., Moura, I. C., Dubreuil, P., . . . Barbeito, L. (2017). ***Evidence for mast cells contributing to neuromuscular pathology in an inherited model of ALS***. *JCI Insight, 2*(20). doi: 10.1172/jci.insight.95934 φ

4) Ibarburu, S.*, **Trias, E.***, Lago, N., Peluffo, H., Barreto-Núñez, R., . . . Barbeito, L. (2017). ***Focal Transplantation of Aberrant Glial Cells Carrying the SOD1^{G93A} Mutation into Rat Spinal Cord Induces Extensive Gliosis.*** Neuroimmunomodulation, doi: 10.1159/000480639. https://doi.org/10.1159/000480639 φ

5) **Trias, E**., Ibarburu, S., Barreto-Nunez, R., & Barbeito, L. (2017***). Significance of aberrant glial cell phenotypes in pathophysiology of amyotrophic lateral sclerosis***. *Neurosci Lett, 636*, 27-31. doi: 10.1016/j.neulet.2016.07.052

6) **Trias, E**., Ibarburu, S., Barreto-Nunez, R., Babdor, J., Maciel, T. T., Guillo, M., . . . Barbeito, L. (2016). ***Post-paralysis tyrosine kinase inhibition with masitinib abrogates neuroinflammation and slows disease progression in inherited amyotrophic lateral sclerosis.*** *J Neuroinflammation, 13*(1), 177. doi: 10.1186/s12974-016-0620-9 φ

7) Williams, J. R., **Trias, E**., Beilby, P. R., Lopez, N. I., Labut, E. M., Bradford, C. S., . . . Beckman, J. S. (2016). ***Copper delivery to the CNS by CuATSM effectively treats motor neuron disease in SOD(G93A) mice co-expressing the Copper-Chaperone-for-SOD***. *Neurobiol Dis, 89*, 1-9. doi: 10.1016/j.nbd.2016.01.020

8) Diaz-Amarilla, P., Miquel, E., Trostchansky, A., **Trias, E**., Ferreira, A. M., Freeman, B. A., . . . Rubbo, H. (2016***). Electrophilic nitro-fatty acids prevent astrocyte-mediated toxicity to motor neurons in a cell model of familial amyotrophic lateral sclerosis via nuclear factor erythroid 2-related factor activation***. *Free Radic Biol Med, 95*, 112-120. doi: 10.1016/j.freeradbiomed.2016.03.013

9) **Trias, E**., Diaz-Amarilla, P., Olivera-Bravo, S., Isasi, E., Drechsel, D. A., Lopez, N., . . . Barbeito, L. (2013). ***Phenotypic transition of microglia into astrocyte-like cells associated with disease onset in a model of inherited ALS***. *Front Cell Neurosci, 7*, 274. doi: 10.3389/fncel.2013.00274 φ

10) Diaz-Amarilla, P., Olivera-Bravo, S., **Trias, E**., Cragnolini, A., Martinez-Palma, L., Cassina, P., . . . Barbeito, L. (2011). ***Phenotypically aberrant astrocytes that promote motoneuron damage in a model of inherited amyotrophic lateral sclerosis***. *Proc Natl Acad Sci U S A, 108*(44), 18126-18131. doi: 10.1073/pnas.1110689108 φ

φ Estas publicaciones y manuscritos forman parte del capítulo “Resultados” de esta tesis.

Resumen

La Esclerosis Lateral Amiotrófica es una enfermedad neurodegenerativa caracterizada por la degeneración de motoneuronas y parálisis progresiva de músculos esqueléticos. No existen tratamientos efectivos que logren detener o al menos retrasar la progresión de los síntomas. Nuestro grupo ha contribuido de manera significativa en la comprensión de los mecanismos moleculares y celulares que subyacen a la progresión de la parálisis. Se han mostrado evidencias de que las células gliales, astrocitos y microglías, juegan un rol preponderante en la respuesta neuroinflamatoria y la muerte de las motoneuronas. En este proyecto de doctorado nos propusimos estudiar con mayor profundidad cómo se constituye un microambiente celular neurodegenerativo que rodea a las motoneuronas a lo largo de toda la vía motora. Hallamos evidencias de que un tipo de células gliales aberrantes, previamente descritas por nuestro grupo, se generan a partir de la transición fenotípica de células microgliales en la médula espinal, mediante un mecanismo parcialmente dependiente de la activación del receptor CSF1R. Otro hallazgo significativo ha sido la identificación de una interacción entre los axones motores y mastocitos, tanto en el nervio ciático como en las terminales neuromusculares, sugiriendo un mecanismo patogénico de tipo inflamatorio que acelera la axonopatía distal característica de la ELA. Demostramos además la posible contribución de macrófagos y neutrófilos a la degeneración axonal y la denervación de las placas motoras. Finalmente, durante el transcurso de este proyecto, logramos identificar un fármaco inhibidor de receptores de tirosin-quinasas, masitinib, que es capaz de inhibir la actividad neurotóxica de microglía, los macrófagos y los mastocitos mediante la inhibición de los receptores CSF1R y c-Kit. Se destaca que el tratamiento sistémico con masitinib, iniciado después del comienzo de la parálisis, resultó en una disminución significativa de la denervación periférica y la muerte de motoneuronas, enlenteciendo de forma significativa la progresión de la enfermedad. Como resultado de nuestros estudios, masitinib ha sido ensayado en pacientes con ELA, con resultados promisorios que deben ser confirmados.

Abstract

Amyotrophic Lateral Sclerosis is a neurodegenerative disease characterized by the degeneration of motoneurons and progressive paralysis of skeletal muscles. There are no effective treatments to stop or at least delay the progression of symptoms. Our group has contributed significantly to the understanding of the molecular and cellular mechanisms underlying disease progression. Evidence show that glial cells, astrocytes and microglia, play a predominant role in the neuroinflammatory response and death of motoneurons. In this Ph.D. project, we aim to better understand how the neurodegenerative cellular microenvironment is constituted in the surrounding of the motoneurons along the entire motor pathway. We found evidence that aberrant glial cells, previously described by our group, are generated from the phenotypic transition of microglial cells in the spinal cord, through a mechanism partially dependent on the activation of the CSF-1R receptor. Another significant finding has been the identification of an interaction between motor axons and mast cells, both in the sciatic nerve and in neuromuscular junctions, suggesting a pathogenic mechanism of an inflammatory cell type that accelerates the distal axonopathy characteristic of ALS. We also demonstrate the possible contribution of macrophages and neutrophils to axonal degeneration and denervation of motor endplates. Finally, we identified a drug inhibitor of tyrosine kinase receptors, masitinib, that blocks the neurotoxic activity of microglia, macrophages and mast cells by inhibiting CSF-1R and c-Kit receptors. Remarkably, the systemic treatment with masitinib after disease onset resulted in a significant decrease of peripheral denervation and motoneurons death, significantly slowing the disease progression. As a result of our preclinical studies, masitinib has been tested in ALS patients, with promising results that must be confirmed.

Introducción

El aumento actual de la esperanza de vida resulta en un incremento de las enfermedades neurodegenerativas, un grupo de enfermedades asociadas a la edad con una prevalencia estimada entre 1,5 y 2,5 % de la población general, pudiendo elevarse al 50% en personas con más de 85 años. Constituyen un grupo de varias decenas de enfermedades caracterizadas por la degeneración y muerte de poblaciones neuronales específicas, con el consiguiente deterioro funcional de las partes afectadas, lo que resulta en enfermedades bien conocidas como Enfermedad de Alzheimer, Enfermedad de Parkinson, Esclerosis Lateral Amiotrófica (ELA) o la enfermedad de Huntington, entre otras. Todas tienen como característica su cronicidad y progresión ineluctable. Luego de décadas de investigación biomédica no existen tratamientos efectivos para curar o tratar dichas enfermedades. Durante mucho tiempo, el foco de estudio estuvo casi exclusivamente en las poblaciones neuronales vulnerables sin considerar su entorno celular, lo que incluye a las diferentes poblaciones de células gliales y células inflamatorias provenientes, en la mayoría de los casos, del sistema hematopoyético. Actualmente, consideramos que el componente inflamatorio de las patologías neurodegenerativas es un concepto emergente en neurociencias que podría dar lugar al desarrollo de nuevas estrategias terapéuticas inmunomoduladoras[1].

La neuroinflamación es una respuesta inmunológica innata del Sistema Nervioso Central (SNC) frente a estímulos nocivos, envejecimiento, trauma, infecciones o enfermedades neurodegenerativas. Las células gliales –microglía y astrocitos- son los principales tipos celulares que contribuyen a la respuesta inmune innata, muchas veces asistidos por monocitos y linfocitos provenientes de la periferia[2,3]. Las células gliales tienen la capacidad de detectar el microambiente a través de receptores específicos de reconocimiento de patrones moleculares, tanto de agentes infecciosos como de daño tisular estéril[4-6]. La activación neuroinflamatoria implica la liberación de centenas de mediadores químicos, profundos cambios fenotípicos y transcripcionales, cambios en la actividad neuronal y sináptica y neurovasculares. En la mayoría de las veces, la respuesta adaptativa es exitosa, logrando reparar el daño o la

infección. Una respuesta significativa en la neuroinflamación está mediada por el inflamasoma (s), complejos proteicos que resultan en la producción de citoquinas pro-inflamatorias IL-1β e IL-18, citoquinas con alto potencial inflamatorio y que pueden desencadenar respuestas neuroinflamatorias complejas[7-9]. Al igual que las células gliales, las neuronas también tienen capacidad de expresar y liberar citoquinas, quemoquinas y otros mediadores propios del sistema inmunológico, contribuyendo con un factor neurogénico de la neuroinflamación[3]. Los pioneros trabajos de Patrick y Edith McGeer a este campo han sido significativos y han cambiado la forma de entender los procesos neurodegenerativos[1,10-14]. Sumado a esto, las células inmunitarias como los monocitos o linfocitos, tienen la capacidad de infiltrar el sistema nervioso y establecer contactos funcionales con células neurales[15,16]. Normalmente estas respuestas son beneficiosas y logran contener o reparar el daño[17,18]. Sin embargo, en condiciones de neurodegeneración, las respuestas neuroinflamatorias pierden su regulación normal y se convierten en un mecanismo patogénico crónico auto-perpetuado que lleva a la muerte neuronal y neurodegeneración[19-23]. Más importante aún, las propias células gliales inflamatorias podrían convertirse en responsables de propagar el proceso neurodegenerativo a lo largo del neuroeje, lo que podría explicar la progresión ineluctable de estas enfermedades.

Es probable que la neuroinflamación exagerada y mantenida en el tiempo sea una factor de riesgo considerable para el desarrollo ulterior de enfermedades neurodegenerativas, precediendo en meses o años, la aparición de los síntomas neurológicos. En este contexto, la comprensión de la neuroinflamación, tanto a nivel del SNC como del sistema nervioso periférico (SNP) podría permitir el diagnóstico precoz de la neurodegeneración e intervenciones terapéuticas oportunas con fármacos que controlen o disminuyan la inflamación deletérea.

En nuestro trabajo de tesis hemos usado un modelo animal de ELA como una forma de estudiar la neurodegeneración y, en particular, comprender los mecanismos neuroinflamatorios y los cambios más relevantes en el microambiente celular degenerativo que rodea a las neuronas más vulnerables.

Es probable que la inflamación crónica en la fase preclínica de esta enfermedad, lleve a cambios fenotípicos de las células gliales, infiltración de células foráneas o cambios neurovasculares o incluso en la composición de la matriz extracelular, que lleven finalmente a un compromiso de los contactos sinápticos y luego de la supervivencia de poblaciones neuronales vulnerables.
En la ELA degeneran las motoneuronas superiores localizadas en la corteza cerebral y las inferiores, localizadas en el tronco cerebral y médula espinal. La mayor parte de los casos son esporádicos y no reconocen causas genéticas. Sin embargo, un 10-20% de los casos de ELA son familiares y están asociados a mutaciones en genes específicos[24,25]. Entre las más estudiadas, diferentes mutaciones en los genes de la superóxido dismutasa 1 (SOD1), TDP-43, FUS o C9Orf72[25]. En 1994, Gurney y colaboradores marcaron un hito en el estudio de la ELA, generando un modelo de ratón que sobreexpresa una mutación puntual, G93A, de la SOD1 humana[26]. Estos ratones desarrollan, luego de 90 días de vida, una neurodegeneración muy similar a la observada en los pacientes con ELA. Al igual que los pacientes, los animales muestran una degeneración y muerte progresiva de motoneuronas del asta ventral de la médula espinal y la corteza motora, acompañada de reactividad glial que se correlaciona con la parálisis. A nivel del SNP, presentan una masiva denervación de las placas motoras, atrofia muscular y degeneración axonal. Los ratones alcanzan una parálisis completa luego de 25-30 días de progresión[26]. Años más tarde otros grupos desarrollarían modelos murinos similares, sobreexpresando otras mutaciones en diferentes genes asociados a la ELA, que comparten la característica de desarrollar una enfermedad neurodegenerativa progresiva[27-29]. Estos modelos murinos dispararon exponencialmente las investigaciones en el campo de la neurodegeneración.

En los animales que sobreexpresan diferentes mutaciones de la SOD1 el proceso patológico no parece ser provocado por la pérdida de actividad catalítica de la SOD1 mutada[30], sino que ha sido ligado a una ganancia de función asociada a una química redox alterada, agregación de proteica mutante y transmisión tipo priónica, disfunción mitocondrial, estrés de retículo, alteraciones en el transporte axonal y neuroinflamación[31,32]. Además, se ha demostrado tanto en los modelos animales como en los modelos murinos, que

el plegamiento de la SOD1 está alterado en la ELA, produciéndose especies de SOD1 mutada mal plegada que se vuelve neurotóxica[33].

Nuestro trabajo de tesis tiene como antecedentes una serie de investigaciones previas llevadas a cabo durante ya varias décadas entre el grupo de Luis Barbeito y el grupo de Joseph Beckman. Estos autores demostraron los principales mecanismos por los cuales las mutaciones de SOD1 inducen muerte de motoneuronas[34-36] y activación de células gliales[37-39]. En una sucesión de publicaciones se describió un mecanismo patogénico novedoso por lo cual las mutaciones SOD1 inducen en motoneuronas la liberación de FGF1 y la expresión del receptor $P75^{NTR}$ iniciando una vía patogénica amplificada por las células gliales que cambian su fenotipo y producen factores apoptóticos para motoneuronas como el óxido nítrico y el NGF[19,39-43]. Estas investigaciones pioneras abrieron el camino para la concepción de intervenciones terapéuticas originales basadas en la modulación de la toxicidad de la SOD1 mutada así como en la interferencia de la toxicidad mediada por astrocitos que rodean las motoneuronas[44-47].

Nuestro trabajo también se basa en contribuciones previas y de gran importancia de otros autores, mostrando la contribución de las células gliales en la patogenia de la ELA. La hipótesis excitotóxica de la ELA se basa en que los astrocitos disfuncionales pierden su capacidad de recaptar el glutamato por una falla en la expresión del transportador GLT1[48,49]. Analizando tejido postmortem humano, McGeer y colaboradores demuestran la compleja reacción neuroinflamatoria en la ELA, con participación de células gliales e inmunitarias[50]. El equipo dirigido por Jean Pierre Julien demuestra la activación y neurotoxicidad de microglías a través de factores sistémico pro-inflamatorios[51-53]. El grupo liderado por Stanley Appel analiza la contribución de células inmunoreguladoras y de la autoinmunidad en la ELA[54-56]. Finalmente, el equipo de Don Cleveland demuestra con gran elegancia el mecanismo patogénico no-autónomo celular en modelos murinos de ELA, demostrando cómo el entorno glial de las motoneuronas influye en el proceso degenerativo[57-64].

Hoy en día, se considera que la ELA se caracteriza por la constitución de un componente neuroiflamatorio crónico en el cual las células gliales desempeñan un rol fundamental, pero dialogan constantemente con células inflamatorias inmunitarias. En el año 2005, se postuló hipótesis de que el ambiente inflamatorio crónico en la ELA sería capaz de modificar progresivamente el fenotipo normal de las células gliales generando fenotipos “aberrantes”, los que a su vez, amplificarían la neuroinflamación contribuyendo a la muerte de las motoneuronas y la progresión lesional de la ELA[37,39]. Durante mis estudios de postgrado he dedicado mis esfuerzos a la identificación de estos fenotipos celulares aberrantes neurotóxicos e inflamatorios, con la premisa de que su caracterización permitiría la concepción de nuevos fármacos que pudieran enlentecer el curso de la ELA. La profundización del concepto de microambiente celular degenerativo, me llevó a estudiar los fenómenos inflamatorios a lo largo de la trayectoria de axones motores en el SNP, pudiendo hacer aportes sobre la interacción de estos con mastocitos y células inmune asociadas, así como a su modulación farmacológica.

En este trabajo de Tesis, se describe nuestra contribución a la comprensión de los mecanismos patogénicos, nuevos tipos celulares que contribuyen al establecimiento del microambiente celular neurodegenerativo en un modelo murino de ELA. Se presentan las publicaciones realizadas en el capítulo “Resultados” y su análisis e integración en el capítulo “Discusión”.

Antecedentes

La **Esclerosis Lateral Amiotrófica** (ELA) fue descrita en 1869 por el neurólogo J.M. Charcot como un síndrome clínico de parálisis y atrofia muscular progresiva y la lesión de los fascículos axonales antero-laterales (esclerosis lateral) de la médula. En particular, la denominación de Charcot incorpora la expresión ***esclerosis lateral*** que indica la pérdida masiva de fibras nerviosas acompañada de una cicatrización glial (esclerosis) en la región lateral de la médula espinal, donde transcurre la *vía cortico-espinal o piramidal*, que controla los movimientos voluntarios[65]. La ELA es una enfermedad degenerativa que afecta principalmente a las motoneuronas superiores e inferiores del SNC. La enfermedad afecta principalmente a individuos de edad media y avanzada (40-70 años). El 90% de los pacientes con ELA fallecen en un lapso de 3 a 5 años, como consecuencia de parálisis generalizada y paro respiratorio. Para personas entre 60 y 69 años, la incidencia de ELA es de 15 casos cada 100.000, por lo que la misma se incrementa con el envejecimiento progresivo de la población. Los síntomas característicos de ELA son debilidad y atrofia muscular progresiva, seguido por parálisis progresiva, como consecuencia de la pérdida incesante de motoneuronas; fasciculaciones asociadas a la denervación muscular y exaltación de los reflejos tendinosos, que reflejan la pérdida de control inhibitorio por la degeneración de la vía cortico-espinal[66].

Aproximadamente el 90 % de los casos de ELA se clasifican como esporádicos, ya que carecen de antecedentes familiares de la enfermedad. El restante 10% de los casos de ELA son hereditarios y usualmente se comporta como un rasgo autosómico dominante. En un 10-20% de los casos hereditarios de ELA, la enfermedad es causada por mutaciones en el gen que codifica el enzima citosólica Cu/Zn Superóxido Dismutasa-1 (SOD1). Se han identificado más de 100 mutaciones en el gen que codifica para SOD1 capaces de generar la enfermedad[67]. La identificación y aislamiento de estas mutaciones a partir de pacientes con ELA hereditaria ha permitido el desarrollo de modelos animales murinos de la enfermedad[68-70]. En estos animales, la sobreexpresión de

algunas mutaciones de SOD1 recapitulan fenómenos fisiopatológicos similares a los que ocurren en el ser humano, como la muerte de motoneuronas, la degeneración muscular y la subsiguiente parálisis progresiva hasta la muerte.

El microambiente celular neurodegenerativo

Los modelos murinos de ELA han permitido un estudio más profundo de los mecanismos moleculares y celulares que subyacen a la muerte de las motoneuronas en esta paradigmática y progresiva enfermedad. Durante décadas el estudio de estas patologías estuvo enfocado en las poblaciones de neuronas que mueren, las motoneuronas; sin embargo, en las últimas décadas, el número de investigaciones en otros tipos celulares implicados en la degeneración de las neuronas motoras y la progresión de la enfermedad se ha incrementado exponencialmente.

Para poder entender por qué mueren las motoneuronas en la ELA es necesario saber qué rol cumplen las células gliales que les brindan soporte en el microambiente que las rodea, en la corteza motora, la médula espinal, así como a lo largo del axón en el SNP. Dos de los principales tipos celulares implicados en la muerte de las neuronas en las enfermedades neurodegenerativas son los astrocitos y la microglía, y en ellos profundizaremos más adelante. Además, en los últimos años hemos aprendido que las células gliales dialogan permanentemente entre sí, así como con otros tipos celulares, y en particular, durante la neurodegeneración, con células inmunes derivadas del linaje hematopoyético. Este diálogo de varios actores es fundamental para la constitución de la neuroinflamación crónica, un factor fundamental para comprender cómo y por qué degeneran las neuronas. Este componente neuroinflamatorio comienza a formarse en etapas tempranas, mucho antes de que los síntomas se hagan presentes, y tiene la capacidad de hacerse crónico y ser clave en el componente progresivo e invasivo que caracteriza a las enfermedades neurodegenerativas. La progresión ineluctable y devastadora que caracteriza a la ELA puede en gran parte, ser explicado por la constitución de un microambiente celular neurodegenerativo que comienza

formándose en secciones puntuales del SNC o el SNP y progresa rápidamente hacia segmentos o compartimentos contiguos.

Este concepto del microambiente celular que favorece el crecimiento, la proliferación y la migración de células de su entorno, o en el caso de la neurodegeneración, promueve la muerte de neuronas, está inspirado en el microambiente celular que rodea a los tumores malignos promoviendo su crecimiento, invasividad y capacidad metastásica[71-73].

Los astrocitos contribuyen a la patogenia de la ELA

Durante los últimos 15 años, nuestro laboratorio ha estudiado el papel patogénico de las células gliales, especialmente de los astrocitos, en la muerte de motoneuronas de la médula espinal que ocurre en la ELA[19,39]. Estos estudios han logrado demostrar que los astrocitos, son capaces de expresar un fenotipo neurotóxico, el cual es suficiente para inducir la muerte de motoneuronas en cultivo, a través de la liberación de mediadores como el NGF y NO[19,39,40,43,74]. Los astrocitos son las células más numerosas del SNC. Se encuentran en contacto directo con las neuronas, formando una conocida sinapsis tripartita[75], y proveen soporte estructural, metabólico y trófico, a la vez que participan activamente en la modulación de la excitabilidad neuronal y la neurotransmisión, ya que cuentan con la capacidad de controlar los niveles extracelulares de iones así como la liberación y recaptación de neurotransmisores[76,77]. Los astrocitos son capaces de proveer soporte trófico a las motoneuronas en cultivo[41,78,79], produciendo y liberando una gran cantidad de factores tróficos y moléculas pequeñas. Frente al daño, los astrocitos sufren una serie de cambios morfológicos y fisiológicos conocidos como astrocitosis o gliosis. Las células astrocitarias responden al daño que sufre el sistema nervioso, proliferando y adoptando un fenotipo reactivo caracterizado por la prolongación de procesos cortos y gruesos gracias a una redistribución de la proteína glial fibrilar acídica (GFAP)[80]. Además, durante la respuesta de activación, los astrocitos reactivos expresan una gran cantidad de marcadores típicos como proteínas del citoesqueleto, marcadores de membrana, proteasas

y son capaces de liberar una serie de factores de crecimiento y citoquinas anti- y pro-inflamatorias[81-83]. Tanto por liberación de factores solubles inflamatorios, citoquinas, etc, así como por contacto directo, los astrocitos interactúan de forma compleja con otras células gliales como las microglías o los oligodendrocitos y células del sistema inmune que pueden infiltrar el SNC durante el daño agudo o crónico[3,84-86].

En el 2002, Cassina y colaboradores y Pehar y colaboradores, demostraron que la exposición de astrocitos de la médula espinal a peroxinitrito generaba una transformación fenotípica que inducía la muerte de motoneuronas embrionarias por apoptosis[41]. La exposición a peroxinitrito induce una reacción astrocitaria típica que se mantiene por largo tiempo, e induce la expresión de iNOS en las células astrocitarias en cultivo y la acumulación de daño nitro-oxidativo[42]. Al cultivar motoneuronas embrionarias sobre las monocapas de astrocitos reactivos, se produce una muerte por apoptosis significativa de las mismas, un fenómeno que es significativamente prevenido cuando se hace el experimento tratando el cultivo con inhibidores de la iNOS o “scavengers” de superóxido y peroxinitrito[41]. Esta constituye una de las primeras evidencias de que las células gliales pueden sufrir transformaciones fenotípicas duraderas en el tiempo que transforman a estas células, por lo general protectoras, en tóxicas para las motoneuronas. En el 2005, Cassina, Pehar y colaboradores volvieron a demostrar que la muerte por apoptosis de las motoneuronas puede ser un mecanismo patogénico en la ELA dependiente de la activación “aberrante” de los astrocitos. Observaron que estas células gliales pueden sufrir un proceso de activación crónica cando son expuestos al factor de crecimiento de fibroblastos 1 (FGF1). Las motoneuronas son grandes productoras de FGF1, y liberan al neuropilo durante la degeneración. Este factor actúa sobre el receptor FGFR1 en los astrocitos, produciendo una activación glial, lo que lleva a una liberación de NGF y produce la muerte de las motoneuronas a través del receptor p75, el cual es re-expresado por las motoneuronas durante el proceso neurodegenerativo. Estos mecanismos patogénicos celulares de muerte neuronal, aportaron evidencias significativas de que los astrocitos juegan un rol fundamental en la neurodegeneración en la ELA. Durante los últimos 20 años una gran cantidad de evidencia experimental

se ha acumulado, mostrando que las células gliales y el ambiente que rodea a las neuronas que mueren en las diferentes patologías degenerativas juegan un papel clave, contribuyendo a los mecanismos patogénicos y la progresión ineluctable de estas enfermedades[62].

La ELA inducida por mutaciones de SOD1 se desarrolla por mecanismos "no autónomos celulares"

En el año 2003, el grupo de Cleveland demuestra que la muerte de las motoneuronas en los modelos de ELA expresando mutaciones de la SOD1, es un fenómeno "no autónomo celular"[61]. Esto quiere decir que la expresión de la mutación en células gliales vecinas a las motoneuronas, podían ejercer neurotoxicidad sin necesidad de que la mutación fuera expresada en las en estas últimas[57]. En animales con quimerismo en la expresión de SOD1, se logró determinar que cuando el 100% de las motoneuronas expresan mutaciones de la SOD1 humana y se encuentran rodeadas de células gliales que no sobre-expresan la mutación, no se produce muerte significativa de las neuronas, gracias al ambiente propicio en el que se encuentran, y la enfermedad se retrasa significativamente o no se desarrolla. Por otro lado, cuando las motoneuronas no sobreexpresan mutaciones de la SOD1 humana pero, el microambiente que las rodea, en su mayoría está constituido por células que sobre-expresan la mutación, se observa una toxicidad significativa sobre las motoneuronas por parte de las células gliales que las rodean[61]. Esta serie de elegantes experimentos demostraron, por primera vez, que el microambiente celular que rodea a las motoneuronas puede ser detrimental o, por el contrario, protector para el desarrollo de la neurodegeneración[61-63].

La microglía contribuye a la patogenia de la ELA

Otro tipo de célula glial que ha ganado terreno como factor celular patogénico en la neurodegeneración en las últimas décadas es la microglía. Las células microgliales son una parte fundamental del microambiente celular que rodea a las neuronas en el SNC y son los efectores inmunes del mismo. Como tales, responden a cualquier condición patológica que involucre la activación del

sistema inmune[87]. La microglía puede presentar diversos estados de activación, los cuales dependen del ambiente en el que se encuentren. Dicha activación es una respuesta al daño que sufre el tejido nervioso; está caracterizada por la proliferación y una transformación en células fagocíticas, con morfología similar a la de los macrófagos en la periferia[88]. El estado activado de la microglía ha sido reportado en diversos estudios en las diferentes patologías neurodegenerativas, incluyendo la ELA en sus distintos estadios[1,89]. En la etapa asintomática y terminal de la ELA, se han descrito cúmulos de microglía proliferante en estado fagocítico adyacente a las motoneuronas[90-92]. En el 2006, Boillée y colaboradores, demostraron que la microglía juega un rol preponderante en el microambiente celular degenerativo que rodea a las motoneuronas durante la progresión de la ELA[58]. Estos autores redujeron los niveles de expresión de la SOD1 humana mutada en las poblaciones celulares que expresan CD11b, una integrina expresada exclusivamente en el linaje mieloide. Los ratones que sobre-expresan diferentes mutaciones de la SOD1 humana, pero presentan una población de células microgliales con bajos niveles es SOD1 humana, presentan una progresión de la enfermedad más lenta[58]. Siguiendo la misma línea de pensamiento, otros autores han demostrado que la microgliosis contribuye de forma significativa a la muerte de las motoneuronas y la progresión de la enfermedad. Utilizando una aproximación farmacológica, Kriz y colaboradores administraron minociclina en la dieta de ratones ELA que sobre-expresan la mutación SOD1[51]. Más allá de su capacidad antibacteriana la minociclina es capaz de inhibir la microgliosis y disminuir la inflamación en el SNC[93]. Los ratones SOD1 que son administrados diariamente con este antibiótico presentan un retraso en el comienzo de los síntomas, además de una progresión de la enfermedad significativamente más lenta[51]. En otro estudio, se demostró que trasplantando microglía “wild-type” en ratones que sobre-expresan la mutación G93A de la SOD1 se logra modificar el curso de la enfermedad, disminuyendo la gliosis y enlenteciendo la progresión de la enfermedad[94]. Además, se demostró que la microglía que sobreexpresa las mutaciones de SOD1 produce y libera factores nitro-oxidativos con actividad neurotóxica para motoneuronas. Estos experimentos sugieren que la microglía SOD1 en el ambiente celular que rodea a las motoneuronas presenta actividad

neurotóxica y la modificación de esta actividad tóxica puede promover una protección significativa para las neuronas[94].

Significación de fenotipos gliales aberrantes en la ELA

¿Existe un fenotipo celular específico y diferente las células gliales convencionales que promueva selectivamente la muerte de las motoneuronas en la ELA? Esta pregunta había movilizado durante años a nuestro laboratorio, hasta que en el año 2011 se reporta el aislamiento de una población de células gliales con características "aberrantes" de la médula espinal de ratas SOD1^{G93A} durante la fase sintomática de la enfermedad[21]. Estas células, a las que en un comienzo denominamos AbAs (acrónimo de ***Ab****errant* ***A****strocytes* en inglés), representan un tipo celular nunca antes descrito, directamente asociado a la fase progresiva de la enfermedad. Las AbAs se caracterizan por una alta tasa proliferativa, expresión de marcadores moleculares atípicos y son selectivamente tóxicas para las motoneuronas embrionarias *in vitro*[20,21]. En la médula espinal, las AbAs espinales expresan marcadores astrocitarios (GFAP, S100β) y microgliales (Iba1, CD163), sugiriendo un origen microglial de dichas células[20]. Este fue el primer reporte de que las células microgliales podrían sufrir una transformación fenotípica y constituirse en mediadores patogénicos en la enfermedad. La sección resultados del presente proyecto comienza con la publicación de Díaz-Amarilla y colaboradores donde se describe el aislamiento de las células AbAs, a modo introductorio, para luego pasar a la primera publicación, directamente asociada a este proyecto de doctorado, referida al origen celular de las células gliales aberrantes.

En este contexto, el descubrimiento de las células AbAs y su origen microglial ha permitido hacer un replanteo profundo de la teoría de la neurodegeneración predominante hasta ahora, ya que la enfermedad, en particular su progresión a lo largo del neuroeje, podría deberse a la aparición de células neurotóxicas e invasivas anormales en diferentes regiones del SNC. Si el efecto deletéreo de estas células pudiera ser detenido farmacológicamente, la progresión de la ELA podría enlentecerse significativamente.

El componente inmune de la ELA

Está ampliamente aceptado que la constitución de un ambiente inflamatorio crónico de carácter sistémico es una de las características más importantes de la ELA. La construcción de esta inflamación crónica está orquestada por el diálogo entre las células gliales y las células del linaje hematopoyético, entre ellas, monocitos, linfocitos, mastocitos, neutrófilos, entre otros, tanto en el SNC como en el SNP. En el primero, la infiltración de células inmunes está limitada por la barrera hematoencefálica y hematoespinal, que impiden que el parénquima sea invadido masivamente por células potencialmente tóxicas para el sistema. Sin embargo, durante la progresión de la ELA, la barrera se encuentra comprometida, se vuelve permeable[95,96], lo que permite que diversos tipos celulares como monocitos y linfocitos participen del proceso neurodegenerativo en el microambiente que rodea a las motoneuronas. En el 2012, Butovsky y colaboradores demostraron en un modelo murino de ELA que los monocitos circulantes en estos animales con un perfil de expresión $Ly6C^{hi}CCR2^{+}$ infiltran la médula espinal de los ratones, reclutados por un aumento de los niveles de CCL2, contribuyendo a la muerte de las motoneuronas. La atenuación genética del fenotipo de estos monocitos neurotóxicos, así como de microglía con fenotipo proinflamatoria es suficiente para enlentecer el curso de la enfermedad de forma significativa[15]. Más recientemente, Murdock y colaboradores, mostraron que los pacientes con ELA presentan niveles más altos de monocitos, neutrófilos y linfocitos CD4 circulantes, y el aumento de estos tipos celulares se correlaciona directamente con una progresión más rápida de la enfermedad[16]. De la misma forma, otros grupos han mostrado que los pacientes con ELA presentan altos niveles de linfocitos CD8 citotóxicos y células NK circulantes[97,98]. Por otro lado, recientemente se ha demostrado que durante el curso de la enfermedad, los pacientes presentan linfocitos T reguladores (Treg) deficientes. De hecho, esta disfunción se correlaciona directamente con la progresión y la severidad de los síntomas, es decir, que cuánto más rápido progresa la enfermedad, mayor es la deficiencia observada en los linfocitos Treg para cumplir su función[99]. Este descubrimiento está siendo evaluado como potencial estrategia terapéutica, ya que los Treg una vez aislados y expandidos en cultivo, vuelven a adquirir sus

funciones normales, al mismo nivel que los Treg de pacientes controles. Por este motivo el trasplante autólogo de Treg podría constituir una nueva terapia para ayudar a tratar la ELA y controlar la inflamación sistémica característica de esta enfermedad. Finalmente se ha demostrado que los mastocitos pueden infiltrar la médula espinal de los pacientes con ELA durante la fase sintomática de la enfermedad, y a través del diálogo con la microglía, podrían contribuir a la degeneración de las motoneuronas[100].

La inflamación a lo largo de la vía motora periférica y el rol de las células de Schwann

La ELA es una enfermedad donde el componente periférico de la vía motora se ve severamente afectado como producto de la neurodegeneración[101,102]. De hecho, muchos autores consideran a la ELA como una axonopatía distal. Este concepto viene dado por la observación de que la denervación y degeneración de las NMJs es precedida de un déficit en la conducción de los impulsos en nervios periféricos, mucho tiempo antes de que los síntomas comiencen[102]. En 1996, Kennel y colaboradores mostraron que en los ratones $SOD1^{G93A}$ la pérdida de función en las placas motoras comienza varias semanas antes de que los síntomas motores clínicos se hagan presentes y que ocurra la pérdida de motoneuronas en la médula espinal[103]. Estos autores muestran que la pérdida de función e integridad de las NMJs en los modelos animales no proviene de la degeneración de los somas neuronales centrales, sino que es un fenómeno de comienzo distal donde se pierde la integridad de los axones, provocando una denervación temprana de las placas motoras en los músculos esqueléticos[103]. Utilizando diferentes modelos murinos de ELA, Frey y colaboradores lograron evidenciar una pérdida selectiva de conexiones sinápticas antes del comienzo de los síntomas. En particular, las fibras musculares que presentan mayor denervación son las fibras de contracción rápida, mientras que las lentas, no lo hacen hasta avanzado los síntomas[104]. Fischer y colaboradores mostraron un escenario similar, estudiando un paciente con parálisis muscular progresiva diagnosticado con ELA pero que murió repentinamente por otra causa. Observaron que si bien no había una

degeneración de las motoneuronas, existían signos de denervación y reinervación de las placas motoras en el músculo, sugiriendo un comienzo distal de la ELA[102].

Un transporte axonal deficiente a lo largo de la vía motora en etapas tempranas de la vida podría ser una de las causas que lleve a la degeneración axonal en la ELA. Williamson y Cleveland observaron que el transporte de ciertas proteínas, se ve significativamente enlentecido meses antes de que la patología pueda ser detectada clínicamente[105]. Otros autores también han contribuido con observaciones similares, sugiriendo que el transporte defectuoso podría generar la agregación tóxica de proteínas a lo largo de la vía motora, induciendo procesos neurotóxicos que contribuyan a una degeneración temprana de los axones motores[106]. El transporte axonal de mitocondrias a lo largo de la vía motora, es otro proceso que se ve afectado en los modelos murinos de ELA, contribuyendo a la neurodegeneración distal[107]. Por tanto, los mecanismos de muerte retrógrada, como consecuencia de la degeneración axonal temprana en la ELA, podrían explicar, en parte, la muerte de las motoneuronas y el proceso neurodegenerativo progresivo en esta enfermedad[108].

Aún se desconoce si la respuesta inflamatoria a lo largo de la vía motora es causa o consecuencia del proceso degenerativo de la motoneurona. El grupo dirigido por Appel observó que la denervación de las placas motoras, así como la degeneración axonal, que ocurre antes del comienzo clínico de la enfermedad, precede a la infiltración de células inmunitarias y la conformación de la inflamación crónica en el SNP[109]. Sin embargo, una vez comenzado el proceso neurodegenerativo, se ha demostrado que el microambiente celular inflamatorio que se constituye alrededor de los axones motores y las NMJs, contribuye con la progresión de la enfermedad, y su modulación genética o farmacológica constituye una estrategia terapéutica válida para enlentecer el curso de la enfermedad[110]. Otro punto a tener en cuenta es que la denervación de las placas motoras parece preceder a la degeneración axonal de los nervios periféricos. Esta degeneración de las fibras motoras se podría generar debido a los mecanismos de muerte retrógrada. Esta muerte o degeneración retrógrada

(en inglés "*dying-back*") está acompañada de una gran infiltración de células hematopoyéticas proinflamatorias y activación del complemento[111]. Es importante notar que aún hoy en día, se sigue investigando si esta inflamación es completamente detrimental para el sistema o bien podría tener un rol dual, degenerativo/regenerativo[112,113].

Aún siguen sin conocerse cuáles son las causas que disparan esta denervación y la atrofia de los músculos en la ELA. Las NMJs o sinapsis musculares están constituidas por una terminal presináptica, el axón que llega desde las motoneuronas de la médula espinal, y una terminal postsináptica, la hendidura sináptica efectora, en la fibra muscular. Al igual que sucede en el SNC, las NMJs están rodeadas y protegidas por un tipo particular de células glial, las células de Schwann terminales o presinápticas, las cuales poseen excelentes propiedades de adaptabilidad morfológica y estructural, que aseguran la estabilidad de las NMJs, contribuyen al mantenimiento y reparación en caso de ser necesario[114]. Sin embargo, se conoce muy poco sobre el papel que desempeñan las células de Schwann terminales en la ELA. El equipo de R. Robitaille ha mostrado recientemente que en los modelos murinos de ELA, las células de Schwann terminales poseen una actividad alterada a la hora de decodificar la función de las placas motoras, incluso cuando la estructura de la NMJ se observa inalterada en etapas asintomáticas de la enfermedad. Las células de Schwann presentan dificultades para censar una liberación aumentada de neurotransmisores por parte de las terminales presinápticas, estando esta dificultad de control asociada a una actividad aumentada de los receptores muscarínicos en las células gliales. Esta disfunción de las células de Schwann persiste durante las etapas presintomáticas tardías y sintomáticas[115].

Aún se desconoce si en los nervios periféricos que degeneran, las células de Schwann, las cuales mielinizan los axones motores en el SNP, desempeñan un rol central en estos eventos degenerativos. Keller y colaboradores han reportado un aumento significativo de GFAP en las células de Schwann en el nervio ciático de ratones $SOD1^{G93A}$. Esta expresión aumenta progresivamente a medida que la patología avanza. Sin embargo, este fenómeno podría ser una

consecuencia del daño axonal y se desconoce su rol patogénico. A diferencia de lo que ocurre en el SNC, donde la sobreexpresión de SOD1 humana mutada en las células gliales desempeña una función neurotóxica[57,58,62,63], Lobsiger y colaboradores demostraron que la expresión de la SOD1 mutada en las células de Schwann podría tener un efecto protector. Inesperadamente, cuando se bloquea la expresión de SOD1 mutada en esta población, se produce una degeneración acelerada en un modelo murino de ELA[116]. Por lo tanto, más estudios serán necesarios para comprender de manera más certera el rol que desempeñan las células de Schwann en el proceso neurodegenerativo de la vía motora periférica.

Finalmente, también se ha reportado que la denervación de la NMJ en la ELA se acompaña de un infiltrado de macrófagos[110]. Se desconoce si la infiltración de células hematopoyéticas proinflamatoria podría ser dependiente de la axonopatía distal o de respuesta adaptativa de las células de Schwann. Por tanto, comprender cómo dialogan las células inflamatorias con las células de Schwann y las NMJs, puede ayudarnos a comprender de forma más global cuáles son los procesos celulares que desencadenan la progresión ineluctable de la ELA y nos permitirá desarrollar nuevas y mejores estrategias terapéuticas.

Hipótesis

Nuestra hipótesis establece la constitución de un ambiente celular inflamatorio patológico que, por un lado, genera muerte neuronal, y por otro, se autoperpetúa y se extiende espacialmente a lo largo del neuroeje, tanto en el SNC como en el SNP. En la médula espinal, este microambiente estaría conformado por astrocitos, microglía y fenotipos gliales de tipo “aberrante” que pueden emerger como consecuencia de la neuroinflamación crónica. En el SNP, debido a la mayor permeabilidad de las barreras neurovasculares, los tipos celulares candidatos para constituir el microambiente degenerativo son las células inmunológicas, como los monocitos, macrófagos y mastocitos. Estas células actuarían en interacción con las células de Schwann, reconocidas por su alta plasticidad y su papel clave en el crecimiento y mielinización de axones y en el establecimiento y mantenimiento de sinapsis neuromusculares. Como la proliferación, migración y activación de muchos de estos tipos celulares está mediado en parte por receptores de tirosin-quinasas, como CSF-1R y c-Kit, predecimos que fármacos que inhiban estos receptores podrían controlar la neuroinflamación y sus efectos deletéreos en la ELA, convirtiéndose en una nueva estrategia terapéutica para detener o enlentecer el avance de la parálisis.

Objetivo

El objetivo general fue caracterizar los tipos celulares no neuronales que participan en el proceso de muerte neuronal y degeneración axonal, constituyendo un microambiente que denominamos “celular neurodegenerativo” en un modelo de ELA. Se puso especial foco en los procesos patológicos que subyacen a la progresión de la parálisis. En la médula espinal, se identificaron y caracterizaron el conjunto de células gliales relacionadas espacial y funcionalmente, que interactúan entre sí para perpetuar y propagar el estado patológico que subyace a la muerte de motoneuronas. En la vía motora periférica, se investigó el papel de distintos tipos celulares

inflamatorias que interactúen con los axones motores y las terminales neuromusculares. Finalmente, se intentó utilizar los conocimientos patogénicos para concebir nuevas estrategias terapéuticas que pudieran enlentecer la progresión de la ELA, utilizando fármacos antineoplásicos, que bloqueen la respuesta inflamatoria de las células del microambiente.

Objetivos Específicos

- **Determinar el origen celular y la actividad inflamatoria de las células gliales aberrantes que emergen en la médula espinal durante la parálisis.** Mediante aislamiento por citometría de flujo, "*cell sorting*" y caracterización inmunocitoquímica e histológica, hemos investigado el origen de las células gliales aberrantes y aquellos factores que contribuyen a su transformación fenotípica. En otra aproximación, hemos investigado si el trasplante focal de células gliales aberrantes aisladas en cultivo es capaz de inducir reactividad glial y toxicidad para motoneuronas a lo largo del neuroeje.
- **Determinar el efecto del fármaco inhibidor de tirosin-quinasa, masitinib sobre la neuroinflamación y la progresión de la parálisis.** El masitinib es un inhibidor de tirosin-quinasas de clase III con especificidad para los receptores c-Kit y CSF-1R expresados en mastocitos y microglías, respectivamente. Hemos investigado si la inhibición de estos receptores por tratamiento sistémico con masitinib tiene un efecto sobre la neuroinflamación y sobre la supervivencia de las ratas $SOD1^{G93A}$. En ensayos de cultivo celular hemos analizado el papel clave de CSF1R en la generación de glía aberrante.
- **Determinar la contribución de los mastocitos y otras células inmunes en la degeneración de la vía motora periférica.** Los mastocitos son células con capacidad de orquestar respuestas inflamatorias crónica, interactuando con macrófagos y neutrófilos. Se investigará su potencial contribución en la inflamación que acompaña a la degeneración de los axones motores en la periferia, desde la raíz ventral a las terminales motoras neuromusculares. Se analizarán sus

interacciones con los axones motores, las células de Schwann, macrófagos y neutrófilos. Se utilizará el masitinib para prevenir la infiltración de mastocitos.

Resultados

Publicación 1

Phenotypically aberrant astrocytes that promote motoneuron damage in a model of inherited amyotrophic lateral sclerosis

Pablo Díaz-Amarilla, Silvia Olivera-Bravo, Emiliano Trias, Andrea Cragnolini, Laura Martínez-Palma, Patricia Cassina, Joseph Beckman and Luis Barbeito

Resumen

Nuestro grupo había reportado previamente que los astrocitos derivados de neonatos $SOD1^{G93A}$ son tóxicos para las motoneuronas embrionarias cuando estas son cultivadas sobre las monocapas de células gliales[19]. Sin embargo, una de las preguntas fundamentales para entender la muerte de las motoneuronas en el contexto del microambiente neurodegenerativo, era si existe una población de astrocitos especialmente tóxicos para las motoneuronas durante la fase sintomática de la ELA y en este caso, si es posible aislar esta población neurotóxica de células gliales de animales sintomáticos**.** En el año 2011, nuestro grupo logró identificar, en las zonas de degeneración de motoneuronas, un nuevo tipo de célula glial, las células gliales aberrantes, nunca antes descrito en la literatura, que aparecen en forma simultánea con el comienzo de la parálisis muscular y expresan un fenotipo inflamatorio neurotóxico[20,21].

Resultados

- A partir del cultivo de ratas $SOD1^{G93A}$ sintomáticas, es posible aislar una población de células gliales con características o fenotipo aberrante. Luego de 15-20 días de realizado el cultivo de la médula espinal en degeneración, se obtiene una monocapa de células con un fenotipo similar a los astrocitos. Estas células crecen en forma de monocapa, muestran una alta tasa proliferativa, no muestran signos de senescencia replicativa y pueden ser pasadas y mantenidas en cultivo durante varias semanas. Estos cultivos de células proliferantes no pueden ser obtenidos de la médula espinal de animales no transgénicos de la misma edad (6 meses).

- Cuando son comparadas con astrocitos cultivados de animales neonatos no transgénicos y $SOD1^{G93A}$, es posible observar que las células gliales aberrantes expresan diversos marcadores de astrocitos. Muestran una alta expresión S100β, bajos niveles de GFAP, altos niveles de Cx43, vimentina y glutamina sintasa. Sin embargo, carecen del transportador de glutamato GLT-1. Además, en comparación con astrocitos cultivados de neonatos, presentan niveles de proliferación significativamente más altos. No presentan marcadores de células microgliales como Iba1 y CD86, o de progenitores celulares como NG2 u Olig2.
- Estas células gliales aberrantes presentan niveles de toxicidad para motoneuronas nunca antes descritos para un fenotipo glial en la literatura. Cuando motoneuronas embrionarias purificadas son cultivadas sobre las monocapas de células gliales aberrantes, se obtiene una muerte neuronal cercana al 85-90%, en comparación, un 50% de toxicidad obtenida de astrocitos $SOD1^{G93A}$ cultivados de animales neonatos. Además, las células gliales aberrantes liberan factores altamente tóxicos para motoneuronas embrionarias purificadas. Cuando los cultivos de estas neuronas son tratadas con diluciones 1/10 – 1/1000 se observa toxicidad significativamente más alta cuando es comparada con los niveles de muerte observados con el medio condicionado de astrocitos SOD1 neonatales. Además, esta neurotoxicidad es específica de motoneuronas. Cuando neuronas aisladas y cultivadas de hipocampo son tratadas con diluciones similares de medio condicionado de células gliales aberrantes, no se observa muerte neuronal significativa.
- En la médula espinal, identificamos células de tipo astrocitario en el microambiente que rodea a las motoneuronas en degeneración. Estas células que recuerdan a las obtenidas en cultivo, expresan altos niveles de GFAP, S100β y Cx43. La aparición de estas células en los alrededores de las motoneuronas está directamente asociado a la progresión de la enfermedad, aumentando significativamente su número a medida que la enfermedad progresa.

- Las células gliales aberrantes en la médula espinal, al igual que lo observado en cultivo, presentan altos niveles de proliferación celular, evidenciado por la marcación de Ki67 y la incorporación de BrdU.

Conclusiones

Este trabajo responde una pregunta clave para la mejor comprensión de la patogenia de la ELA. La muerte masiva de motoneuronas durante la fase progresiva de la enfermedad, podría estar asociada a la aparición de fenotipos gliales aberrantes, proliferantes y altamente neurotóxicos, en el microambiente celular que rodea a las neuronas motoras que degeneran en la médula espinal de las ratas $SOD1^{G93A}$. Queda por responder la pregunta de si estos fenotipos gliales aberrantes son propios de los modelos murinos de ELA o bien pueden ser hallados durante el proceso neurodegenerativo en pacientes.

Phenotypically aberrant astrocytes that promote motoneuron damage in a model of inherited amyotrophic lateral sclerosis

Pablo Díaz-Amarilla[a], Silvia Olivera-Bravo[a], Emiliano Trias[a], Andrea Cragnolini[b], Laura Martínez-Palma[c], Patricia Cassina[c], Joseph Beckman[d,e], and Luis Barbeito[a,b,1]

[a]Instituto de Investigaciones Biológicas Clemente Estable, Montevideo 11600, Uruguay; [b]Institut Pasteur de Montevideo, Montevideo 11600, Uruguay; [c]Facultad de Medicina, Universidad de la República, Montevideo 11800, Uruguay; and [d]Department of Biochemistry and Biophysics, Environmental Health Sciences Center, and [e]Linus Pauling Institute, Oregon State University, Corvallis, OR 97331

Edited by Don W. Cleveland, University of California at San Diego, La Jolla, CA, and approved September 23, 2011 (received for review July 1, 2011)

Motoneuron loss and reactive astrocytosis are pathological hallmarks of amyotrophic lateral sclerosis (ALS), a paralytic neurodegenerative disease that can be triggered by mutations in Cu-Zn superoxide dismutase (SOD1). Dysfunctional astrocytes contribute to ALS pathogenesis, inducing motoneuron damage and accelerating disease progression. However, it is unknown whether ALS progression is associated with the appearance of a specific astrocytic phenotype with neurotoxic potential. Here, we report the isolation of astrocytes with aberrant phenotype (referred as "AbA cells") from primary spinal cord cultures of symptomatic rats expressing the SOD1^{G93A} mutation. Isolation was based on AbA cells' marked proliferative capacity and lack of replicative senescence, which allowed oligoclonal cell expansion for 1 y. AbA cells displayed astrocytic markers including glial fibrillary acidic protein, S100β protein, glutamine synthase, and connexin 43 but lacked glutamate transporter 1 and the glial progenitor marker NG2 glycoprotein. Notably, AbA cells secreted soluble factors that induced motoneuron death with a 10-fold higher potency than neonatal SOD1^{G93A} astrocytes. AbA-like aberrant astrocytes expressing S100β and connexin 43 but lacking NG2 were identified in nearby motoneurons, and their number increased sharply after disease onset. Thus, AbA cells appear to be an as-yet unknown astrocyte population arising during ALS progression with unprecedented proliferative and neurotoxic capacity and may be potential cellular targets for slowing ALS progression.

neurodegeneration | glial cells

Amyotrophic lateral sclerosis (ALS) is a paradigmatic disease of upper and lower motoneurons leading to progressive paralysis and death. Mice and rats expressing human Cu-Zn superoxide dismutase (SOD1) mutations develop a motor syndrome with symptoms and pathological features of the human disease (1–3). Current evidence indicates that mutant SOD1 leads to motoneuron loss because of a toxic gain of function secondary to misfolding of the protein. Mutant SOD1 activates several pathogenic mechanisms including altered redox chemistry, protein aggregation, endoplasmic reticulum stress, mitochondria dysfunction, defective axonal transport, and inflammation (4, 5). Motoneuron degeneration and prominent astrogliosis are pathological hallmarks of ALS both in patients and in animal models (6). In rats expressing the SOD1^{G93A} mutation, astrogliosis coincides with the disappearance of ventral motoneurons and a striking loss of the astrocytic glutamate transporter 1 (GLT1), also known as "excitatory amino acid transporter 2" (EAAT2) (3, 4).

Mutant SOD1 toxicity involves a non–cell-autonomous mechanism mediated at least in part by disrupted communication between motoneurons and surrounding glial cells (5, 7–13). Although astrocytes and microglia become activated in the spinal cord of symptomatic ALS animal models, the selective ablation of either proliferating GFAP-expressing astrocytes (14) or microglia (15) failed to modify disease progression, suggesting the involvement of a different glial cell type specifically contributing to motoneuron pathology. In addition, the pathogenic role of NG2 oligodendrocyte precursors that proliferate at the end-stage of ALS models (16, 17) remains unknown.

Although the expression of mutant SOD1 restricted to astrocytes is not sufficient to induce motoneuron degeneration in transgenic (Tg) mice (18), genetic excision of mutant SOD1 in astrocytes extended survival and decreased microglia activation, with no effect on disease onset (13). In addition, astrocytes expressing mutant SOD1 exert direct and selective toxicity to motoneurons by secreting soluble factors (12, 19, 20). Human astrocytes derived from the spinal cord of persons with sporadic and familial ALS also can kill motoneurons in culture (21), indicating that astrocytic toxicity is not restricted to animal models expressing mutant SOD1. However, it remains unknown whether all astrocytes are intrinsically neurotoxic for motoneurons or whether instead toxicity is restricted to a specific subclass of astrocytes. Because astrocytes expressing mutant SOD1 are more prone to enter an activated inflammatory and metastable state (22), we hypothesized that a subpopulation of astrocytes might follow a phenotypic transition deleterious to motoneuron survival. The aim of this study was to determine whether such pathogenic subtype of astrocytes occurs in a model of ALS in rats and might be isolated.

Results

Establishment of Astrocyte Cultures from Symptomatic SOD1^{G93A} Rats. To isolate glial cell populations occurring during the symptomatic stage of ALS, we established primary cultures from spinal cord of symptomatic 175-d-old Tg SOD1^{G93A} rats. Identical cultures from non-Tg littermates prepared in the same way yielded only a few cells at day 2 in vitro that proliferated slowly in the following days but failed to reach confluence or survive subsequent passages (Fig. 1, *Insets*). In contrast, cultures from Tg rats yielded numerous cells that proliferated rapidly at day 7 in vitro (Fig. 1) and formed clusters of elongated flat cells resembling astrocytes and often associated with numerous ionized calcium-binding adaptor molecule 1 (Iba1)-positive microglial cells (arrows in Fig. 1, and Fig. S1*C*). At day 10 in vitro, a 3- to 4-mm layer of agarose was polymerized on top of the cell layer.

Author contributions: P.D.-A., S.O.-B., A.C., P.C., and L.B. designed research; P.D.-A., S.O.-B., E.T., A.C., L.M.-P., P.C., and L.B. performed research; P.D.-A., S.O.-B., E.T., A.C., L.M.-P., P.C., J.B., and L.B. analyzed data; and P.D.-A., S.O.-B., E.T., J.B., and L.B. wrote the paper.

The authors declare no conflict of interest.

This article is a PNAS Direct Submission.

[1]To whom correspondence should be addressed. E-mail: barbeito@pasteur.edu.uy.

This article contains supporting information online at www.pnas.org/lookup/suppl/doi:10.1073/pnas.1110689108/-/DCSupplemental.

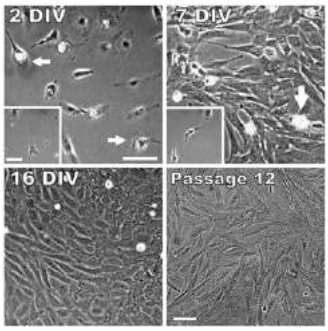

Fig. 1. Establishment of AbA cell cultures. Representative phase-contrast microphotographs of the establishment of primary spinal cord cultures prepared from symptomatic SOD1^{G93A} rats or non-Tg littermates (*Insets*). The cells were plated in a culture flask and observed under a phase-contrast microscope at 2, 7, and 16 days in vitro (DIV) and after replating at passage 12. Note the increased cell number in the culture of the symptomatic rat spinal cord compared with the culture from the non-Tg littermate. Microglial cells (arrows) disappeared progressively with successive passages. (Scale bars: 50 μm.)

Although agarose did not attach to the cultured cells, it further stimulated the intrinsic proliferating potential of Tg astrocytes but failed to stimulate proliferation of non-Tg astrocytes. After 6 d under the agarose layer (day 16 in vitro), the population of cells with astrocytic phenotype in the Tg cultures increased sharply and organized into a monolayer bearing sparse microglial cells (Fig. S1*C*). In contrast, only a few viable cells were found in non-Tg cultures (Fig. 1). After withdrawal of agarose, Tg cells continued proliferating vigorously, yielding highly homogeneous monolayers of flat, fusiform to polygonal cells devoid of microglia (Fig. 1). These cells were passaged successfully and propagated for 1 y without undergoing replicative senescence. Because of these distinctive features, we referred to these cells as "aberrant astrocytes" (AbA cells).

When grown in defined medium to oligodendrocytes (23), cultures from Tg rats yielded NG2 cells but also abundant S100β^{+} astrocytes (Fig. S1*A*). These results show that AbA cells do not arise from the NG2 oligodendrocyte precursors also known to proliferate in the spinal cord of symptomatic ALS mice (16, 17).

AbA cells were generated systematically from more than 10 independent cultures prepared from different symptomatic Tg rats, suggesting that they represent a common cell type resident in the degenerating spinal cord during the symptomatic phase of the disease.

Expression of Astrocytic Markers in AbA Cells. We next assessed the expression of astrocytic markers in AbA cell cultures from passages 8–15. Because we were unable to grow and passage astrocytes from non-Tg adult rats, the phenotypic features of AbA cells were compared with primary spinal cord astrocytes prepared from neonatal SOD1^{G93A} rats and non-Tg littermates. Among the antigenic markers listed in Table S1, we found that both AbA cells and neonatal astrocytes expressed most of the typical astrocytic markers such as GFAP, vimentin, S100β, connexin 43 (Cx43), and glutamine synthase, but GLT1 protein was not detected in AbA cells. NG2 glycoprotein was not expressed in AbA cells immediately after culture establishment, but it increased gradually, beginning after passage 4 (Fig. S1*B*). AbA cells were negative for A2B5, oligodendrocyte transcription factor 2, and CD68 antigen clone (ED1), which are expressed by glial precursors, oligodendrocyte progenitor cells, and phagocytic microglia, respectively (Table S1).

AbA cells displayed weak and diffuse perinuclear GFAP labeling and intense staining for S100β, in contrast with the filamentous GFAP and low S100β expression in neonatal astrocytes (Fig. 2*A*). GFAP levels in AbA cells were decreased by 60% in comparison with neonatal astrocytes, as estimated by Western blotting (Fig. 2*B*). AbA cells displayed processes and increased GFAP staining when challenged with forskolin (10 μM; Fig. S1*D*), a recognized stimulus that promotes astrocyte differentiation in vitro (24). AbA cells expressed Cx43 in a cytoplasmic and patchy surface distribution (Fig. 2*A*) at levels increased fivefold in comparison with control astrocytes (Fig. 2*B*). The expression of glutamine synthase (Fig. 2*B* and Fig. S1*D*) and vimentin (Fig. S1*D*) in AbA cells was comparable to that found in neonatal SOD^{G93A} astrocytes.

AbA Cell Proliferation. The growth of AbA cells through passage 10 was faster than that of Tg and non-Tg neonatal astrocytes (Fig. 2*C*). The doubling times, calculated during the linear phase of the growth curve, were 30 h for AbA cells, 52 h for non-Tg astrocytes, and 49 h for Tg astrocytes. AbA cell numbers con-

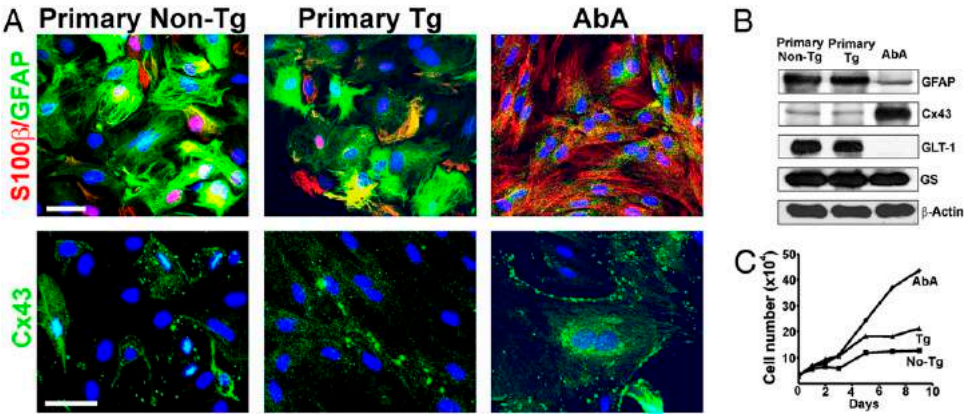

Fig. 2. Expression of astrocyte markers and proliferation in AbA cells. Cultures of AbA cells were compared with non-Tg or SOD1^{G93A} Tg primary neonatal spinal cord astrocytes. (*A*) Confocal imaging of cells immunostained against GFAP (green) and S100β (red) (*Upper*) and Cx43 (green) (*Lower*). In upper panels, yellow staining indicates cells expressing both GFAP and S100β. (Scale bars: 50 μm.) Note AbA cells' low GFAP immunoreactivity but increased S100β and Cx43 immunoreactivity compared with neonatal astrocytes. (*B*) Western blotting analysis of astrocytic markers in AbA cells compared with primary astrocytes. AbA cells' differential protein expression pattern is evidenced by decreased GFAP, absent GLT1, and augmented Cx43. (*C*) Growth of AbA cells (passage 10) and primary neonatal astrocytes was assessed over 9 d. The growth rate of AbA cells was almost twice that of primary astrocytes.

tinued increasing after reaching confluence at day 5 in vitro, suggesting a defect in contact inhibition.

AbA Cells Specifically Induced Motoneuron Death. Because astrocytes carrying the $SOD1^{G93A}$ mutation have been shown specifically to induce motoneuron death (10–12), we assessed the neurotoxic potential of AbA cells by plating embryonic motoneurons (25) on top of confluent AbA or neonatal astrocyte monolayers. The survival rate after 2 d was <10% for motoneurons in cocultures with AbA cells but was 60% for neurons cocultured with Tg cells and was 100% for neurons cultured with non-Tg neonatal astrocytes (Fig. 3*A*). These data suggest that AbA cells exert a marked nonpermissive environment for motoneuron growth and differentiation.

We next investigated whether AbA cell toxicity was mediated by soluble factors secreted to the conditioned media (CM), as previously described for mutant primary astrocytes (12). Increasing dilutions of CM from AbA cells or neonatal astrocyte cultures having similar cell number were added to embryonic motoneuron cultures maintained with glial cell-derived neurotrophic factor (GDNF) as the trophic factor. As expected, CM from neonatal non-Tg astrocytes did not cause motoneuron death (100% survival in Fig. 3*B*). In contrast, after exposure to AbA CM in a range of dilutions from 1:10 to 1:1,000, the number of motoneurons was significantly lower than the number surviving after addition of CM from neonatal Tg astrocytes, which reduced motoneuron survival significantly only at dilutions up to 1:100. Thus, the neurotoxic potential of AbA CM is at least 10-fold greater than that of Tg astrocyte CM (Fig. 3*B*). Notably, the neurotoxicity of AbA CM was specific to motoneurons, because even a 1:10 dilution failed to kill primary cultures of embryonic hippocampal neurons (Fig. 3*C*).

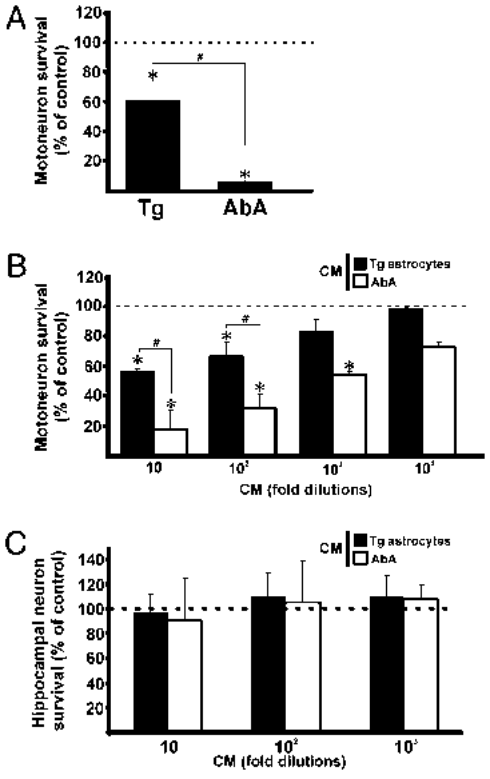

Fig. 3. AbA cells specifically induced motoneuron death. (*A*) Embryonic motoneurons were seeded on top of confluent feeder layers of neonatal astrocytes or AbA cells, and survival was assessed 48 h later. Note that the survival rate of motoneurons maintained on top of AbA cells was <10% but was 100% for non-Tg (100%, dotted line) and 60% for Tg neonatal astrocytes. (*B*) CM from neonatal astrocytes or AbA cells was added to pure motoneurons 24 h after plating. The final fold dilution is indicated in each condition. CM from non-Tg astrocytes did not induce motoneuron death; thus it was taken as a control (100%, dotted line). Note that CM from AbA cells exerted significant motoneuron loss at dilutions up to 1:1,000, whereas Tg astrocyte CM was neurotoxic at dilutions up to 1:100. (*C*) Lack of neurotoxic activity of increasing dilutions of AbA CM in primary cultures of hippocampal neurons. Data are shown as mean ± SD; in *A* and *B*, $^{\#}P < 0.01$ and $^{*}P < 0.05$ with respect to CM from non-Tg astrocytes.

Identification of AbA-Like Cells in the Degenerating Spinal Cord. We used immunohistochemistry to S100β/Cx43 to determine whether AbA-like cells were present in the degenerating spinal cord of $SOD1^{G93A}$ rats. S100β staining was low or moderate in non-Tg and Tg asymptomatic rats. In contrast, S100β increased dramatically during the symptomatic stage of Tg rats, being localized in the nuclei and cytoplasm in a population of hypertrophic astrocytes that expressed GFAP restricted to cell bodies and proximal processes. Typically, these cells were observed in the ventral spinal cord, near damaged motoneurons, and at the boundary between gray and white matter. Cx43 staining also increased dramatically in symptomatic rats and colocalized with S100β hypertrophic astrocytes (Fig. 4*A*). Such astrocytes appeared at the time of disease onset, and their number increased sharply at disease end stage (Fig. 4*B*). In the ventral horn of symptomatic rats, S100β did not colocalize with NG2 oligodendrocyte precursors previously described in ALS mice (Fig. 4*C*; Manders coefficient ≤ 0.02), suggesting that S100β cells constitute a different cell population. Furthermore, $S100\beta^{+}$ or $Cx43^{+}$ AbA-like cells surrounding motoneurons were labeled with the proliferation markers Ki67 or BrdU in animals systemically injected with the nucleotide (Fig. S2*C*). The number of $Ki67^{+}$ proliferating AbA-like cells in the ventral cord region enriched in motoneurons represented 20 ± 5% of cells, compared with 33 ± 8% proliferating NG2 cells and 43 ± 10% microglia (Fig. S2*B*).

Discussion

Neuronal degeneration in ALS begins as a focal process that spreads contiguously through the upper and lower motoneurons (26), suggesting an acquired pathogenic mechanism in which motoneuron pathology and inflammation actively propagate in the CNS. Here we report the isolation of a type of astrocyte with aberrant phenotypic features (AbA cells) and an unprecedented toxicity to motoneurons in vitro from symptomatic $SOD1^{G93A}$ rats. Notably, AbA cells exhibit a distinctive pattern of astrocytic markers with an increased proliferation rate and a lack of replicative senescence. Proliferating AbA-like astrocytes were localized near motoneurons in the spinal cord of symptomatic $SOD1^{G93A}$ rats, suggesting a link between the appearance of pathogenic AbA cells and the rapid progression of paralysis characteristic of the $SOD1^{G93A}$ rat model.

The proliferative potential of AbA cells after isolation from the Tg spinal cord was strong enough to allow their oligoclonal expansion in conditions where age-matched non-Tg rats yielded few cells with limited growth potential. The AbA proliferation rate was almost twice that of the neonatal astrocytes but still was far below that of the C6 astrocyte cell line (27). Thus, AbA cells do not appear to be fully transformed cells, even though they do not follow replicative senescence. Cultured AbA cells are almost undistinguishable morphologically from primary neonatal astrocytes and exhibit a set of distinctive antigenic markers of undifferentiated astrocytes including high S100β and Cx43 expression and low levels of nonfilamentous GFAP. As a prototypic subunit of the calcium-binding S100 proteins, S100β is known to exert paracrine effects in astrocytes that contribute to proliferation, migration, differentiation, and neurotoxicity (28–30). Intracellular S100β can interact with GFAP monomers to prevent their assembly into filaments (31), possibly contributing to the

NEUROSCIENCE

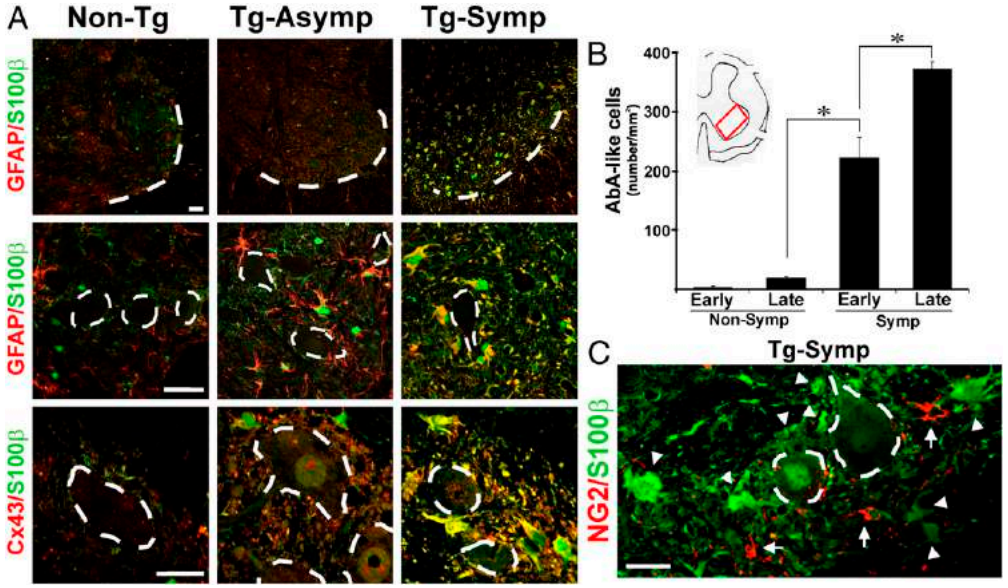

Fig. 4. Identification of AbA-like cells in the degenerating spinal cord. (*A*) Representative microphotographs of GFAP (red), S100β (green), and Cx43 (red) immunostaining in lumbar spinal cord sections from non-Tg, asymptomatic (Tg-Asymp), and symptomatic (Tg-symp) SOD1^{G93A} rats. Dotted lines in the top row indicate the border between gray and white matter in low-magnification representative microphotographs. The perimeter of large motoneurons has been drawn in the middle and bottom rows. Note that S100β was up-regulated in the spinal cord of symptomatic rats and especially was expressed in a population of hypertrophic cells with astrocyte morphology. Most of these cells displayed colocalization of S100β and GFAP (yellow). Cx43 immunoreactivity also was increased in Tg-symp spinal cords, being colocalized with S100β in most hypertrophic AbA-like cells (yellow in bottom row). (Scale bars: 50 μm in GFAP/S100β and 20 μm in Cx43/S100β.) (*B*) Increased number of AbA-like cells in the ventral horn of Tg rats during the progression of the disease. *Inset* shows the ventral horn area analyzed. Data are shown as mean ± SD; *$P < 0.05$. (*C*) Representative confocal immunostaining against NG2 and S100β in the ventral horn of a Tg-symp rat showing that AbA cells are not stained for NG2. (Scale bar: 20 μm.)

diffuse GFAP distribution in AbA cells. Forskolin, which induces astrocytic process growth and differentiation (24), also increased process growth and GFAP expression in AbA cells, further indicating their astrocytic phenotype.

Another distinctive marker of AbA cells is the high expression of the gap junction protein Cx43, which also is found in cultured neonatal astrocytes (32) and is known to modulate their proliferation, migration, and differentiation (33). Cx43 also can form hemichannels opened to the extracellular space in inflammatory astrocytes (34, 35), which can release extracellular ATP (34, 36). Thus, the high levels of Cx43 in AbA cells may explain their potential to trigger glial activation and excitotoxic degeneration of motoneurons (37). The blunted levels of astroglial glutamate transporter GLT1 protein in AbA cells suggest that these cells recapitulate a defect in GLT1 expression previously described in ALS patients (38) and SOD1^{G93A} rats (3). Because GLT1 is expressed in differentiated astrocyte endings to uptake synaptic glutamate, accumulation of AbA cells around motoneurons may promote further excitotoxic damage in vivo.

Furthermore, AbA cells do not appear to be derived from NG2 oligodendrocyte progenitors that recently have been reported to proliferate in the ALS spinal cord after disease onset (16, 17). AbA-like cells in the spinal cord of symptomatic rats are NG2$^-$ and display a morphology and location distinct from that of typical NG2 cells. In addition, AbA cells were NG2$^-$ when first established in culture, and the glycoprotein was expressed only after more than four passages. Characteristic AbA cells coexisted with and were easily distinguishable from NG2$^+$ cells when primary cultures of the spinal cord were prepared in a defined medium that favors oligodendrocyte differentiation.

AbA cells represent a population of glial cells with undifferentiated features. Thus, their generation in the spinal cord could be associated with the overt inflammatory microenvironment that accompanies motoneuron loss, particularly in the SOD1^{G93A} animal models (39). Such a milieu may promote the recruitment and phenotypic transition of glial cells or precursors (40), leading to the generation of AbA cells. A similar proliferative and immature phenotype of astrocytes can be found following defective function in paired box 6 (Pax6) transcription factor (41) and in pathological conditions leading to aberrant specification of glial precursors (42).

Previous studies have shown that astrocytes bearing the SOD1^{G93A} mutation induce apoptosis of motoneurons both in coculture conditions and through soluble factors found in the culture media (10–12, 19, 20), whereas non-Tg astrocytes provided excellent trophic support. However, we show here that AbA cells display an unprecedented toxicity to motoneurons that greatly exceeds that of neonatal Tg astrocytes expressing mutant SOD1. The complete failure of motoneurons to survive when plated on a confluent layer of AbA cells suggests that AbA cells create a nonpermissive microenvironment for motoneuron growth. This effect could be mediated at least in part by the accumulation of specific extracellular matrix proteins that are known to be up-regulated in ALS rats (43). In addition, the AbA cell CM were >10-fold more potent than neonatal Tg astrocytes in inducing motoneuron death. Because AbA cell CM were applied in the presence of GDNF, which supports motoneuron survival, it is unlikely the toxicity is caused solely by decreased trophic activity. Rather, AbA cells appear to be a subclass of astrocytes producing active soluble factors that kill motoneurons. Although the mechanism of AbA neurotoxicity is under active investigation, the possibility exists that AbA cells produce cytokines, excitotoxins, or trophic factors such as nerve-growth factor that may kill motoneurons specifically (8).

Hypertrophic AbA-like cells strongly expressing S100β and Cx43 were identified in the degenerating spinal cord, suggesting a common phenotype with AbA cells isolated in culture. Moreover, BrdU$^+$ and Ki67$^+$ AbA-like cells were found systematically in close contact with degenerating motoneurons, suggesting that they proliferate in the ventral horn as the rat becomes paralytic. Evidence for the occurrence of astrocytic-like BrdU$^+$ nuclei

coexisting with dividing NG2 cells was provided previously by Kang et al. (17) in SOD1^{G93A} mouse spinal cord. Although AbA-like cells represented only about 20% of the proliferating glial cells in the ventral cord gray matter, they were more closely associated with degenerating motoneurons than were NG2^{+} cells and frequently were associated with proliferating microglia. Perineuronal S100β^{+} astrocytes were described previously in ALS patients (44), suggesting that AbA cells also may occur in human terminal disease. S100β can form heterodimers with S100A6, which is up-regulated specifically in reactive astrocytes occurring in ALS patients and mutant SOD1 Tg animals (45). The increased expression of Cx43 in AbA cells is intriguing. Although increased astrocytic expression of Cx43 has not been reported in ALS, neurogenic activation of spinal cord astrocytes is known to induce Cx43 (46) following axotomy and spinal cord injury (47). The fact that blocking Cx43 in spinal cord injury improved recovery (48) anticipates a pathogenic role of Cx43 up-regulation in ALS.

In conclusion, the present study addressed one key question about ALS pathogenesis: the identification and isolation of an astrocyte population with the potential to mediate motoneuron disease. Such astrocytes were abundant in the symptomatic phase of disease and typically localized close to motoneurons, suggesting a link between the emergence of pathogenic AbA cells and the rapidly progressing neurodegeneration characteristic of the SOD1^{G93A} rat model. Thus, AbA cells represent an intriguing cell target for further understanding the pathogenesis of neurodegenerative diseases.

Materials and Methods

Details for materials and methods used in this study are provided in *SI Materials and Methods*.

Animals. Male hemizygous NTac:SD-TgN(SOD1^{G93A})L26H rats (Taconic), originally developed by Howland, et al. (3), were bred locally as outbred Sprague-Dawley background. The onset of symptomatic disease (~160 d) and lifespan (180 d) in our colony were delayed considerably compared with the original report (3).

Establishment of Aba Cell Cultures. AbA cells were obtained from adult spinal cord of symptomatic SOD1^{G93A} rats (175 d) according to the procedures described by Saneto and De Vellis (49) with minor modifications (25). Adult age-matched non-Tg rats were used as controls. Briefly, animals were killed by deeply anesthesia, and spinal cord was dissected on ice. After the meninges were removed carefully, spinal cord was chopped finely and dissociated with 0.25% trypsin in calcium-free buffer for 5 min at 37 °C. Trypsinization was stopped by adding DMEM/10% (vol/vol) FBS in the presence of 50 μg/mL DNaseI and mechanical disaggregation by repeated pipetting. The resulting extract was passed through an 80-μm mesh to eliminate tissue debris and then was spun. The pellet was resuspended in culture medium [DMEM/10% (vol/vol) FBS, Hepes (3.6 g/L), penicillin (100 IU/mL), and streptomycin (100 μg/mL)] and then was plated in a 25-cm^2 tissue culture flask. Because large amounts of fat hindered cell counting, the cells isolated from individual spinal cords were plated in individual culture flasks. Culture medium was removed after 24 h and then was replaced every 48 h. At day 10 in vitro, 3 mL of a 1% agarose solution maintained at 37 °C was layered on top of the cells according to procedures described by Hassell, et al. (50). Although the agarose layer did not attach to the cell layer, it facilitated astrocyte proliferation. At day 20 in vitro, agarose was withdrawn as an entire piece, and AbA cells were passaged every week. To do so, the monolayer was incubated at 37 °C with 0.25% trypsin without calcium. After 5 min, the cells were harvested in DMEM/10% (vol/vol) FBS and spun at 250 × *g* for 10 min. The resultant pellet was resuspended in DMEM/10% (vol/vol) FBS and plated at a density of 1 × 10^6 cells per 25-cm^2 culture flask. After confluence, each flask yielded up to 2 × 10^6 cells, and 1 wk after seeding each bottle was divided in two bottles. AbA cells were cultured in the same medium during the entire procedure.

In some experiments, primary cultures from spinal cord of symptomatic Tg rats were plated on 0.1 mg/mL polylysine-covered plates and maintained in oligodendrocyte-defined medium (Neurobasal medium supplemented with B-27) for 2 d (23).

Primary Cell Cultures. Heterozygous Tg and non-Tg astrocytes were prepared from spinal cords of 1-d-old pups according the methods described by Saneto and De Vellis (49) with minor modifications (25). Motoneuron cultures were prepared from embryonic day 15 wild-type rat spinal cords and purified by immunopanning (25). Motoneurons were seeded on polyornithine-laminin–coated substrate and maintained in Neurobasal medium supplemented with GDNF (1 ng/mL) (Sigma). After 24 h in vitro, motoneurons were treated with dilutions of CM. Survival was assessed after 48 h. For preparation of CM, confluent neonatal astrocyte and AbA monolayers were incubated in complete L15 medium for 24 h. Respective supernatants were centrifuged at 1,000 × *g* for 15 min and were applied immediately to motoneuron cultures. For coculture experiments, motoneurons were plated on confluent AbA or neonatal astrocyte monolayers and were maintained for 48 h in complete L15 medium supplemented as previously described (25). Hippocampal neuronal cultures were obtained from embryonic day18 embryos as described in *SI Materials and Methods*.

Western Blots. Protocols for Western blotting are described in *SI Materials and Methods*.

Assessment of Cell Proliferation. Cell proliferation was assessed as described in *SI Materials and Methods* by counting the number of viable nuclei.

Immunolabeling. Methanol-fixed cultured cells or paraformaldehyde perfusion-fixed free-floating spinal cord sections were processed for immunocytochemistry or immunohistochemistry as described in *SI Materials and Methods* and Table S1. Quantification of AbA-like cells in the ventral horn of spinal cord sections was done by direct counting of hypertrophic cells that surround motoneurons and exhibit cytoplasmic S100β.

Statistical Snalysis. Statistical studies were performed using statistical tools of Origin 8.0. Descriptive statistics were used for each group, and one-way ANOVA, followed by Scheffé post hoc comparison if necessary, was used among groups. All experiments were performed in duplicate or triplicate and were replicated at least three times. All results are presented as mean ± SD. $P < 0.05$ was considered significant.

ACKNOWLEDGMENTS. We thank Luc Dupuis and José Gonzales Aguilar for help in proofreading and criticism of the manuscript. This work was funded by the program for development of basic sciences (PEDECIBA), Innovation and Research National Agency (ANII) and Institut Pasteur de Montevideo. Partial funding also came from National Institutes of Health National Institute on Environmental Health Sciences Grant P30ES000210, National Institute of Neurological Disorders and Stroke Grant R01NS058628A, and National Center for Complementary and Alternative Medicine Grant NCCAM P01AT002034; and from the Amyotrophic Lateral Sclerosis Association (to J.B.).

1. Gurney ME, et al. (1994) Motor neuron degeneration in mice that express a human Cu,Zn superoxide dismutase mutation. *Science* 264:1772–1775.
2. Bruijn LI, et al. (1997) ALS-linked SOD1 mutant G85R mediates damage to astrocytes and promotes rapidly progressive disease with SOD1-containing inclusions. *Neuron* 18:327–338.
3. Howland DS, et al. (2002) Focal loss of the glutamate transporter EAAT2 in a transgenic rat model of SOD1 mutant-mediated amyotrophic lateral sclerosis (ALS). *Proc Natl Acad Sci USA* 99:1604–1609.
4. Bruijn LI, Miller TM, Cleveland DW (2004) Unraveling the mechanisms involved in motor neuron degeneration in ALS. *Annu Rev Neurosci* 27:723–749.
5. Boillée S, Vande Velde C, Cleveland DW (2006) ALS: A disease of motor neurons and their nonneuronal neighbors. *Neuron* 52:39–59.
6. Hall ED, Oostveen JA, Gurney ME (1998) Relationship of microglial and astrocytic activation to disease onset and progression in a transgenic model of familial ALS. *Glia* 23:249–256.
7. Cassina P, et al. (2008) Mitochondrial dysfunction in SOD1G93A-bearing astrocytes promotes motor neuron degeneration: Prevention by mitochondrial-targeted antioxidants. *J Neurosci* 28:4115–4122.
8. Barbeito LH, et al. (2004) A role for astrocytes in motor neuron loss in amyotrophic lateral sclerosis. *Brain Res Brain Res Rev* 47:263–274.
9. Clement AM, et al. (2003) Wild-type nonneuronal cells extend survival of SOD1 mutant motor neurons in ALS mice. *Science* 302:113–117.
10. Vargas MR, Pehar M, Cassina P, Beckman JS, Barbeito L (2006) Increased glutathione biosynthesis by Nrf2 activation in astrocytes prevents p75NTR-dependent motor neuron apoptosis. *J Neurochem* 97:687–696.
11. Di Giorgio FP, Carrasco MA, Siao MC, Maniatis T, Eggan K (2007) Non-cell autonomous effect of glia on motor neurons in an embryonic stem cell-based ALS model. *Nat Neurosci* 10:608–614.
12. Nagai M, et al. (2007) Astrocytes expressing ALS-linked mutated SOD1 release factors selectively toxic to motor neurons. *Nat Neurosci* 10:615–622.

13. Yamanaka K, et al. (2008) Astrocytes as determinants of disease progression in inherited amyotrophic lateral sclerosis. *Nat Neurosci* 11:251–253.
14. Lepore AC, et al. (2008) Selective ablation of proliferating astrocytes does not affect disease outcome in either acute or chronic models of motor neuron degeneration. *Exp Neurol* 211:423–432.
15. Gowing G, et al. (2008) Ablation of proliferating microglia does not affect motor neuron degeneration in amyotrophic lateral sclerosis caused by mutant superoxide dismutase. *J Neurosci* 28:10234–10244.
16. Magnus T, et al. (2008) Adult glial precursor proliferation in mutant SOD1G93A mice. *Glia* 56:200–208.
17. Kang SH, Fukaya M, Yang JK, Rothstein JD, Bergles DE (2010) NG2+ CNS glial progenitors remain committed to the oligodendrocyte lineage in postnatal life and following neurodegeneration. *Neuron* 68:668–681.
18. Gong YH, Parsadanian AS, Andreeva A, Snider WD, Elliott JL (2000) Restricted expression of G86R Cu/Zn superoxide dismutase in astrocytes results in astrocytosis but does not cause motoneuron degeneration. *J Neurosci* 20:660–665.
19. Di Giorgio FP, Boulting GL, Bobrowicz S, Eggan KC (2008) Human embryonic stem cell-derived motor neurons are sensitive to the toxic effect of glial cells carrying an ALS-causing mutation. *Cell Stem Cell* 3:637–648.
20. Marchetto MC, et al. (2008) Non-cell-autonomous effect of human SOD1 G37R astrocytes on motor neurons derived from human embryonic stem cells. *Cell Stem Cell* 3:649–657.
21. Haidet-Phillips AM, et al. (2011) Astrocytes from familial and sporadic ALS patients are toxic to motor neurons. *Nat Biotechnol* 29:824–828.
22. Hensley K, et al. (2006) Primary glia expressing the G93A-SOD1 mutation present a neuroinflammatory phenotype and provide a cellular system for studies of glial inflammation. *J Neuroinflammation*, 3:2, 1–9.
23. Yang Z, Watanabe M, Nishiyama A (2005) Optimization of oligodendrocyte progenitor cell culture method for enhanced survival. *J Neurosci Methods* 149:50–56.
24. Abe K, Saito H (1997) Developmental changes in cyclic AMP-stimulated stellation of cultured rat cortical astrocytes. *Jpn J Pharmacol* 75:433–438.
25. Cassina P, et al. (2002) Peroxynitrite triggers a phenotypic transformation in spinal cord astrocytes that induces motor neuron apoptosis. *J Neurosci Res* 67:21–29.
26. Ravits JM, La Spada AR (2009) ALS motor phenotype heterogeneity, focality, and spread: Deconstructing motor neuron degeneration. *Neurology* 73:805–811.
27. Fukumoto H, Kakihana M, Suno M (1994) Characterization of C6-10A glioma cells highly responsive to beta-adrenergic receptor agonist-induced NGF synthesis/secretion. *Glia* 12:151–160.
28. Donato R, et al. (2009) S100B's double life: Intracellular regulator and extracellular signal. *Biochim Biophys Acta* 1793:1008–1022.
29. Hu J, Ferreira A, Van Eldik LJ (1997) S100beta induces neuronal cell death through nitric oxide release from astrocytes. *J Neurochem* 69:2294–2301.
30. Raponi E, et al. (2007) S100B expression defines a state in which GFAP-expressing cells lose their neural stem cell potential and acquire a more mature developmental stage. *Glia* 55:165–177.
31. Frizzo JK, et al. (2004) S100B-mediated inhibition of the phosphorylation of GFAP is prevented by TRTK-12. *Neurochem Res* 29:735–740.
32. Bennett MV, Contreras JE, Bukauskas FF, Sáez JC (2003) New roles for astrocytes: Gap junction hemichannels have something to communicate. *Trends Neurosci* 26:610–617.
33. Homkajorn B, Sims NR, Muyderman H (2010) Connexin 43 regulates astrocytic migration and proliferation in response to injury. *Neurosci Lett* 486:197–201.
34. Orellana JA, et al. (2009) Modulation of brain hemichannels and gap junction channels by pro-inflammatory agents and their possible role in neurodegeneration. *Antioxid Redox Signal* 11:369–399.
35. Sáez JC, Retamal MA, Basilio D, Bukauskas FF, Bennett MV (2005) Connexin-based gap junction hemichannels: Gating mechanisms. *Biochim Biophys Acta* 1711:215–224.
36. Garré JM, et al. (2010) FGF-1 induces ATP release from spinal astrocytes in culture and opens pannexin and connexin hemichannels. *Proc Natl Acad Sci USA* 107: 22659–22664.
37. Gandelman M, Peluffo H, Beckman JS, Cassina P, Barbeito L (2010) Extracellular ATP and the P2X7 receptor in astrocyte-mediated motor neuron death: Implications for amyotrophic lateral sclerosis. *J Neuroinflammation*, 7:33, 1–9.
38. Lin CL, et al. (1998) Aberrant RNA processing in a neurodegenerative disease: The cause for absent EAAT2, a glutamate transporter, in amyotrophic lateral sclerosis. *Neuron* 20:589–602.
39. Hensley K, et al. (2006) On the relation of oxidative stress to neuroinflammation: Lessons learned from the G93A-SOD1 mouse model of amyotrophic lateral sclerosis. *Antioxid Redox Signal* 8:2075–2087.
40. Buffo A, et al. (2008) Origin and progeny of reactive gliosis: A source of multipotent cells in the injured brain. *Proc Natl Acad Sci USA* 105:3581–3586.
41. Sakurai K, Osumi N (2008) The neurogenesis-controlling factor, Pax6, inhibits proliferation and promotes maturation in murine astrocytes. *J Neurosci* 28:4604–4612.
42. Bain JM, Ziegler A, Yang Z, Levison SW, Sen E (2010) TGFbeta1 stimulates the overproduction of white matter astrocytes from precursors of the "brain marrow" in a rodent model of neonatal encephalopathy. *PLoS ONE* 5:e9567.
43. Mizuno H, Warita H, Aoki M, Itoyama Y (2008) Accumulation of chondroitin sulfate proteoglycans in the microenvironment of spinal motor neurons in amyotrophic lateral sclerosis transgenic rats. *J Neurosci Res* 86:2512–2523.
44. Migheli A, et al. (1999) S-100beta protein is upregulated in astrocytes and motor neurons in the spinal cord of patients with amyotrophic lateral sclerosis. *Neurosci Lett* 261:25–28.
45. Hoyaux D, et al. (2002) S100A6 overexpression within astrocytes associated with impaired axons from both ALS mouse model and human patients. *J Neuropathol Exp Neurol* 61:736–744.
46. Rohlmann A, et al. (1993) Facial nerve lesions lead to increased immunostaining of the astrocytic gap junction protein (connexin 43) in the corresponding facial nucleus of rats. *Neurosci Lett* 154:206–208.
47. Lee IH, Lindqvist E, Kiehn O, Widenfalk J, Olson L (2005) Glial and neuronal connexin expression patterns in the rat spinal cord during development and following injury. *J Comp Neurol* 489:1–10.
48. Cronin M, Anderson PN, Cook JE, Green CR, Becker DL (2008) Blocking connexin43 expression reduces inflammation and improves functional recovery after spinal cord injury. *Mol Cell Neurosci* 39:152–160.
49. Saneto R, De Vellis J (1987) Neuronal and glial cells: Cell culture of the central nervous system. *Neurochemistry: A Practical Approach*, eds, Turner AJ, Brachelard HS (IRL, Oxford), pp 27–63.
50. Hassell JR, Kane BP, Etheredge LT, Valkov N, Birk DE (2008) Increased stromal extracellular matrix synthesis and assembly by insulin activated bovine keratocytes cultured under agarose. *Exp Eye Res* 87:604–611.

Publicación 2

Phenotypic transition of microglia into astrocyte-like cells associated with disease onset in a model of inherited ALS

Emiliano Trias, Pablo Díaz-Amarilla, Silvia Olivera-Bravo, Eugenia Isasi, Derek A. Drechsel, Nathan Lopez, C. Samuel Bradford, Kyle E. Ireton, Joseph S. Beckman and Luis Barbeito

Resumen

El hallazgo de un fenotipo glial aberrante altamente neurotóxico que puede ser aislado de la médula espinal degenerante fue sorprendente y cambió nuestro paradigma sobre el estudio de las células gliales en la ELA. La descripción de estas células proliferantes que se sitúan en los alrededores de las motoneuronas durante el proceso neurodegenerativo, aportó nuevas evidencias sobre la conformación de un microambiente celular inflamatorio característico de los modelos animales de ELA. Sin embargo, el origen de estas células aberrantes permanecía desconocido. La presente publicación es referida al origen de la glía aberrante.

Resultados

- Observamos una población de células que presentan una alta tasa proliferativa, marcadas por una alta expresión de Ki67 y que expresan simultáneamente marcadores astrocitarios y microgliales (GFAP e Iba1) en el microambiente celular que rodea a las motoneuronas durante la fase sintomática de la enfermedad.
- Esta población glial aberrante no fue observada en animales no transgénicos o transgénicos durante la fase sintomática. Además, las células con fenotipo aberrante, expresan altos niveles de nitración, evidenciado por una alta expresión de nitro-tirosina (NO_2Tyr).
- Siguiendo el protocolo de cultivo descrito por Díaz-Amarilla y colaboradores[21], realizamos cultivos de médula espinal sintomática y analizamos los primeros estadios del cultivo. El análisis por citometría de flujo indica que inmediatamente luego de establecerse el cultivo

primario, el 99% de las células expresan el marcador de membrana CD11b.

- Luego de 15 días en cultivo, una subpoblación de células comienza una transformación fenotípica que culmina en la monocapa de células gliales aberrantes previamente descritas, expresando marcadores astrocitarios. Para determinar que el origen de estas células fuera microglial y no una contaminación con células astrocitarias o progenitores gliales, realizamos un ensayo de "*cell sorting*". Luego de 5 días en cultivo, las células fueron marcadas con CD11b unido a FITC, y seleccionadas por "*cell sorting*". Las células fueron recultivadas y se siguió su transformación fenotípica. Luego de 12-15 días en cultivo, las células seleccionadas sufren una transformación fenotípica a células gliales aberrantes y se disponen en forma de monocapa. Estas células transformadas muestran un fenotipo similar y los mismos niveles de proliferación que las células obtenidas del cultivo original.
- Durante el proceso de transformación fenotípica, observamos una disminución de la expresión de los marcadores microgliales Iba1 y CD11b y un aumento progresivo de dos marcadores astrocitarios, GFAP y S100β. De hecho, pueden observarse zonas de transición donde se ve una coexpresión de ambos tipos de marcadores gliales. Una vez completada la transición fenotípica se pierde completamente la expresión de los marcadores típicos de células microgliales.
- Para determinar el origen microglial de las células gliales aberrantes, llevamos a cabo otro experimento confirmatorio. A los 3 días de cultivada la médula espinal de animales sintomáticos, las células fueron tratadas con 25 mM de Leucin-metil-ester, un compuesto utilizado para depletar células microgliales de los cultivos primarios. Cuando las células son tratadas con esta droga al comienzo del cultivo, se genera una muerte masiva del cultivo y no ocurre una transformación fenotípica. Cuando el tratamiento es realizado sobre monocapas de células ya transformadas a los 20 días post-cultivo, el leucin-metil-ester no tiene efecto alguno sobre las células, sugiriendo una transformación total de las células microgliales a células gliales aberrantes.

Conclusiones

Nuestros resultados apoyan el concepto de que las células gliales aberrantes se originan a partir de células microgliales con fenotipo inflamatorio que proliferan en los alrededores de las neuronas en degeneración. Mostramos que la microglía aislada de estos animales SOD1 sintomáticos tiene la capacidad de sufrir una transformación fenotípica hacia células gliales aberrantes, las cuales se vuelven altamente tóxicas para motoneuronas. Una mejor comprensión de los factores que podrían promover estos fenómenos de transformación fenotípica en el ambiente inflamatorio degenerante podría abrirnos las puertas a considerar aproximaciones terapéuticas dirigidas a estos fenotipos gliales.

frontiers in
CELLULAR NEUROSCIENCE

ORIGINAL RESEARCH ARTICLE
published: 24 December 2013
doi: 10.3389/fncel.2013.00274

Phenotypic transition of microglia into astrocyte-like cells associated with disease onset in a model of inherited ALS

Emiliano Trias[1], Pablo Díaz-Amarilla[1], Silvia Olivera-Bravo[1], Eugenia Isasi[1], Derek A. Drechsel[2,3], Nathan Lopez[2,3], C. Samuel Bradford[2,3], Kyle E. Ireton[2,3,5], Joseph S. Beckman[2,3,4] and Luis Barbeito[5]*

[1] *Instituto de Investigaciones Biológicas Clemente Estable, Montevideo, Uruguay*
[2] *Department of Biochemistry and Biophysics, Oregon State University, Corvallis, OR, USA*
[3] *Environmental Health Sciences Center, Oregon State University, Corvallis, OR, USA*
[4] *Linus Pauling Institute, Oregon State University, Corvallis, OR, USA*
[5] *Institut Pasteur de Montevideo, Montevideo, Uruguay*

Edited by:
Ricardo Tapia, Universidad Nacional Autónoma de México, Mexico

Reviewed by:
Ricardo Tapia, Universidad Nacional Autónoma de México, Mexico
Jie Zhang, University of Texas Health Science Center at San Antonio, USA

Correspondence:
Luis Barbeito, Institut Pasteur de Montevideo, Mataojo 2020, Montevideo 11400, Uruguay
e-mail: barbeito@pasteur.edu.uy

Microglia and reactive astrocytes accumulate in the spinal cord of rats expressing the Amyotrophic lateral sclerosis (ALS)-linked SOD1^{G93A} mutation. We previously reported that the rapid progression of paralysis in ALS rats is associated with the appearance of proliferative astrocyte-like cells that surround motor neurons. These cells, designated as Aberrant Astrocytes (AbA cells) because of their atypical astrocytic phenotype, exhibit high toxicity to motor neurons. However, the cellular origin of AbA cells remains unknown. Because AbA cells are labeled with the proliferation marker Ki67, we analyzed the phenotypic makers of proliferating glial cells that surround motor neurons by immunohistochemistry. The number of Ki67^{+}AbA cells sharply increased in symptomatic rats, displaying large cell bodies with processes embracing motor neurons. Most were co-labeled with astrocytic marker GFAP concurrently with the microglial markers Iba1 and CD163. Cultures of spinal cord prepared from symptomatic SOD1^{G93A} rats yielded large numbers of microglia expressing Iba1, CD11b, and CD68. Cells sorted for CD11b expression by flow cytometry transformed into AbA cells within two weeks. During these two weeks, the expression of microglial markers largely disappeared, while GFAP and S100β expression increased. The phenotypic transition to AbA cells was stimulated by forskolin. These findings provide evidence for a subpopulation of proliferating microglial cells in SOD1^{G93A} rats that undergo a phenotypic transition into AbA cells after onset of paralysis that may promote the fulminant disease progression. These cells could be a therapeutic target for slowing paralysis progression in ALS.

Keywords: microglia, astrocytes, AbA cells, ALS, phenotypic transformation, neurodegeneration

INTRODUCTION

Amyotrophic lateral sclerosis (ALS) may be considered as a paradigm of neurodegeneration involving the progressive death of upper and lower motor neurons (Cleveland and Rothstein, 2001; Boillee et al., 2006a). A consistent neuropathological feature of ALS is the extensive inflammation around motor neurons and axonal degeneration, evidenced by the accumulation of reactive astrocytes, activated microglia and lymphocytes (Engelhardt et al., 1993; Barbeito et al., 2004; Ilieva et al., 2009; Graber et al., 2010). Neuroinflammation is evident in rodent models of inherited ALS overexpressing mutant Cu/Zn superoxide dismutase (SOD1) and in ALS human patients (Gurney et al., 1994; Bruijn et al., 1997; Howland et al., 2002; McGeer and McGeer, 2002; Appel, 2009). Several studies suggest that glial cells, including astrocytes and microglia, play a pathogenic role in ALS through promoting motor neuron death and spreading paralysis after disease onset (Hall et al., 1998; Barbeito et al., 2004; Sargsyan et al., 2005; Boillee et al., 2006b; Papadeas et al., 2011). These observations suggest that therapeutics targeting the inflammatory response of glial cells could slow ALS progression.

We have recently reported the isolation of astrocytes-like glial cells with an aberrant phenotype (AbA cells) from primary spinal cord cultures of symptomatic transgenic rats expressing the SOD1^{G93A} mutation (Diaz-Amarilla et al., 2011). Isolation was based on AbA cell's marked proliferative capacity and lack of replicative senescence. These cells secrete soluble factors that induce motor neuron death with a higher potency than neonatal transgenic astrocytes. Aberrant astrocytes only appear after disease onset in SOD1^{G93A} rats and are localized adjacent to motor neurons, suggesting a link between generation of AbA cells and the progression of paralysis. However, the origin of AbA cells remains unknown. Because AbA cells actively proliferate in the degenerating spinal cord, we hypothesized they could originate from glial progenitors with a high proliferative potential. Previous studies have identified phagocytic microglia as well as NG2^{+} glial progenitors that proliferate during the active phase of motor neuron degeneration in ALS mice and rats (Magnus et al., 2008; Kang et al., 2010; Sanagi et al., 2010). Because we have previously shown that AbA cells do not express NG2 (Diaz-Amarilla et al., 2011), we examined whether AbA cells might be derived from

microglia proliferating adjacent to motoneurons. In this study, we have characterized both *in vivo* and *ex vivo* the phenotype of proliferating glial cells in symptomatic ALS rats and found evidence that neurotoxic AbA cells result from a phenotypic transition from activated microglial cells.

MATERIALS AND METHODS

ANIMALS

All procedures using laboratory animals were performed in accordance with the international guidelines for the use of live animals and were approved by the Institutional Animal Committee. Male hemizygous NTac:SD-TgN(SOD1^{G93A})L26H rats (Taconic), originally developed by Howland et al. (2002), were bred locally by crossing with wild-type Sprague–Dawley female rats. Male SOD1^{G93A} progenies were used for further breeding to maintain the line. Rats were housed in a centralized animal facility with a 12-h light-dark cycle with ad libitum access to food and water. Symptomatic disease onset was determined by periodic clinical examination for abnormal gait, typically expressed as subtle limping or dragging of one hind limb. Rats were killed when they reached the end stage of the disease. Both the onset of symptomatic disease (160–170 d) and lifespan (180–195 d) in our colony were delayed considerably compared with earlier reports (Howland et al., 2002). This study was carried out in strict accordance with the IIBCE Bioethics Committee's requirements and under the current ethical regulations of the Uruguayan Law N° 18.611 for animal experimentation that follows the Guide for the Care and Use of Laboratory Animals of the National Institutes of Health (USA). All surgery was performed under 90% ketamine – 10% xylazine anesthesia, and all efforts were made to minimize suffering, discomfort or stress.

CELL CULTURE FROM END-STAGE SYMPTOMATIC SOD1^{G93A} RATS

Microglia cells were obtained from adult spinal cord of symptomatic SOD1^{G93A} rats (175 d) according to the procedures described by Diaz-Amarilla et al. (2011) with minor modifications. Adult age-matched non-Tg rats were used as controls. Briefly, animals were killed by deeply anesthesia, and spinal cord was dissected on ice. After the meninges were removed carefully, spinal cord was chopped finely and dissociated with 0.25% trypsin in calcium-free buffer for 5 min at 37°C. Trypsin treatment was stopped by adding DMEM/10% (vol/vol) FBS in the presence of 50 μg/mL DNaseI and mechanical disaggregation by repeated pipetting. The resulting extract was passed through an 80-μm mesh to eliminate tissue debris and then was spun. The pellet was resuspended in culture medium [DMEM/10% (vol/vol) FBS, Hepes (3.6 g/L), penicillin (100 IU/mL), and streptomycin (100 μg/mL)] and then was plated in a 25-cm^2 tissue culture flask. Because large amounts of fat hindered cell counting, the cells isolated from individual spinal cords were plated in individual culture flasks. Culture medium was removed after 24 h and then was replaced every 48 h.

LEUCINE-METHYL ESTER TREATMENT

Leucine-Methyl Ester (Leu-OMe, Sigma) was prepared in DMEM, pH adjusted to 7.4. Cultures from transgenic symptomatic rats were treated 3 days after plated with 25 mM of Leu-OMe during 1 h. Then, the cells were washed three times with PBS and fixed with cold methanol during 5 min (n = 3).

IMMUNOCYTOCHEMICAL STAINING OF CULTURED CELLS

Cultured cells were fixed with absolute methanol at -20°C for 5 min on ice and then were washed three times with 10 mM PBS (pH 7.4). Non-specific binding was blocked by incubating fixed cells with 5% BSA in PBS for 1 h at room temperature. Corresponding primary antibodies were diluted in blocking solution and incubated overnight at 4°C in a wet closed chamber. The primary antibodies for microglia recognition were rabbit anti-Iba1 (1:200, Abcam), rabbit anti-CD11b (1:200, Abcam), and mouse anti-CD68 (1:300, Abcam). The antibodies used for astrocyte recognition were mouse anti-GFAP (1:500, Sigma), rabbit anti-GFAP (1:500, Sigma), mouse anti-S100β(1:400, Sigma). After washing, sections were incubated in a 1,000-fold dilution of secondary antibodies conjugated to Alexa Fluor 488 and/or Alexa Fluor 546 (1:1000, Invitrogen). Antibodies were detected by confocal microscopy using a confocal Olympus FV300 microscope.

ANALYSIS OF MICROGLIAL MARKERS EXPRESSION

After isolation of the symptomatic spinal cord, cells were plated in 35-mm dishes at 1.2 × 10^4 cells/cm^2. 7 days after plating, cells were fixed and stained with microglia specific markers as described above. The analysis was performed manually in using the cell counter tool of the Image J software. Values were expressed as a percentage (± SD) of the total number of DAPI$^+$ nuclei. Only healthy nuclei with clearly defined limiting membranes were counted. Cell counts were performed in duplicate.

FORSKOLIN TREATMENT

After 20 days *in vitro*, 35 mm dishes were treated with 10 μM of forskolin (FSK; Sigma) during 3 h. Then, the cells were fixed using cold methanol and stained as described above.

FLOW CYTOMETRIC ISOLATION

After 7 days *in vitro* the cells were incubated at 37°C with 0.25% trypsin without calcium. After 5 min, the cells were harvested in DMEM/10% (vol/vol) FBS and spun at 250 × *g* for 10 min. The resultant pellet was washed three times in PBS at 37°C. After that, the cells were re-suspended in blocking solution (PBS; 5% FBS, and 1% BSA). The cells were labeled at 4°C for 15 min with mouse anti-CD11b-FITC (1:100, Abcam) and sorted using the MoFlo^{TM} XDP–Beckman Coulter. After sorting, the cells were re-plated in a 25 cm^2 bottle with DMEM/10% FBS.

IMMUNOHISTOCHEMICAL STAINING OF RAT SPINAL CORDS

Animals were deeply anesthetized and transcardial perfusion was performed with 0.9% saline and 4% paraformaldehyde in 0.1 M PBS (pH 7.2–7.4) at a constant flow of 1 mL/min. Fixed spinal cord was removed, post-fixed by immersion for 24 h, and then transverse sectioned serially (30–50 μm) on a vibrating microtome. Serial sections were collected in 100 mM PBS for immunohistochemistry. After citrate antigen retrieval, free-floating sections were permeabilized for 15 min at room temperature with 0.1% Triton X-100 in PBS, passed through washing buffered solutions, blocked with 5% BSA:PBS for 1 h at room temperature, and incubated overnight at 4°C in a solution of 0.1% Triton X-100

and PBS containing the primary antibodies, mouse anti-Iba1 (1:200, Abcam), mouse anti CD163 (1:100, Serotec) for microglia recognition, and rabbit anti-GFAP (1:500, Sigma) for astrocyte recognition. A rabbit anti-Ki67 (1:400, Abcam) was used as a proliferation marker. The expression of nitrotyrosine was recognized with a mouse anti-NO_2-Tyr (1:300, Millipore) antibody. The immunoreactivity was completely blocked by pre-incubation of the primary antibody with free nitrotyrosine (10 mM). No antigen retrieval was needed to detect nitrotyrosine. After washing, sections were incubated in 1:1,000-diluted secondary antibodies conjugated to Alexa Fluor 488 and/or Alexa Fluor 546 (Invitrogen). Antibodies were detected by confocal microscopy using a confocal Olympus FV300 microscope.

QUANTITATIVE ANALYSIS OF ABA CELLS IN THE DEGENERATING SPINAL CORD

The number of proliferating cells labeled with Ki67 and also stained for the astrocytic marker GFAP or microglial marker Iba1 was assessed by counting the respective double-positive cells in the gray matter of the lumbar cord of symptomatic or asymptomatic $SOD1^{G93A}$ rats. Quantification was performed only in the ventral horn, comparing the cell numbers in Rexed laminae VII and IX, which display low and high density of large motor neurons, respectively. Double-positive cells were counted in a perimeter of 100 μm, surrounding motor neurons. The analysis was performed manually in 10 histological sections per animal (two different rats for each condition) using the cell counter tool of the Image J software. Values were expressed as a ratio of double-positive cells per motor neuron. The number of double-positive cells labeled with Iba1 or CD163 and GFAP assessed by counting the respective double-positive cells in the gray matter of the lumbar cord of asymptomatic and symptomatic $SOD1^{G93A}$ rats. Quantification was performed only in the ventral horn, comparing the cell numbers in Rexed laminae VII and IX, which display low and high density of large motor neurons, respectively. Values were expressed as the number of double-positive cells per mm^2.

RESULTS

GLIAL PROLIFERATION ADJACENT TO DEGENERATING MOTOR NEURONS

The number of proliferating glia as identified by $Ki67^+$ nuclei sharply increased in the ventral horn of $SOD1^{G93A}$ symptomatic rats and accumulated near surviving motor neurons as well as at sites of apparent motor neuron loss (**Figure 1**). This population of $Ki67^+$ cells had large cell bodies (30–50 μm) with processes embracing motor neurons and expressed GFAP and Iba1 (**Figure 1A**, upper panels). Both Ki67/GFAP and Ki67/Iba1-positive cells displayed morphological features of AbA cells in culture (Diaz-Amarilla et al., 2011) and could be easily differentiated from astrocytes and microglia from non-transgenic or Tg asymptomatic rat's spinal cord. These large GFAP/Ki67 or Iba1/Ki67 cells were rarely observed in asymptomatic or non-transgenic rats (**Figure 1A**, lower panels). Due to the antigen retrieval procedure, motor neuron cell bodies were non-specifically labeled with Ki67 in all experimental conditions. The ratio of GFAP/Ki67 cells and Iba1/Ki67 cells to motor neurons in symptomatic rats was 2.7 and 2.9 respectively, whereas the ratio was < 0.3 in asymptomatic animals for both markers (**Figure 1B**).

CO-EXPRESSION OF MICROGLIAL AND ASTROCYTIC MARKERS IN ABA CELLS

While astrocytes and microglial cells constituted two separate cell populations in asymptomatic rats, being typically detected by GFAP and Iba1 respectively, most AbA cells surrounding the motor neurons in symptomatic rats were surprisingly co-labeled with both markers as well as CD163 (**Figure 2A**). 70% of the GFAP-positive AbA cells in the ventral horn exhibited microglial markers, as compared as <1% in asymptomatic rats. The number of cells labeled with Iba1/GFAP or CD163/GFAP was similar (∼100 cells per mm^2) in symptomatic rats, suggesting the same cells expressed both microglial markers (**Figure 2B**). Detection of the microglial markers required the use of strong antigen retrieval methods, which made motor neuron to artifactually stained with CD163.

Both peri-neuronal AbA cells as well as motor neurons were strongly stained for nitrotyrosine in symptomatic rats, consistent with the production of peroxynitrite (**Figure 2C**). This immunoreactivity was completely blocked by preincubation of the primary antibody with free nitrotyrosine (data not shown).

CHARACTERIZATION OF FIRST STAGES OF ABA CELLS *IN VITRO*

Because AbA cells can be cultured from symptomatic rats (Diaz-Amarilla et al., 2011), we determined the time course of microglial and astrocytic marker expression. Soon after primary cultures of spinal cord were established (DIV2–DIV7), most of the cells displayed the morphology of phagocytic microglia and were fluorescently labeled with the microglia markers CD11b, CD68, and Iba1 (**Figure 3A**). The detailed morphology of cultured cells closely corresponded to the typical features of microglial cells previously reported (Kreutzberg, 1996; **Figure 3B**). No immunoreactivity for GFAP or S100β was detected in cultures since the establishment of cultures and until 10–12 DIV (data not shown). Microglial cells were also analyzed by flow cytometry (FACS) using FITC-labeled CD11b antibodies. FACS analysis showed that > 99% of cells of the primary spinal cord culture of symptomatic rats belonged to the microglia lineage. The purity of this culture was also determined by counting $CD68^+$ and $Iba1^+$ cells and found to be > 98% (**Figure 3C**).

PHENOTYPIC TRANSFORMATION OF MICROGLIA INTO ABA CELLS *IN VITRO*

To confirm that AbA cells were derived from microglia cell progenitors, $CD11b^+$ expressing cells were FACS-sorted and re-established in culture until DIV15. Sorted cells displayed the typical microglia morphology and phenotypic marker until DIV10. This population of cells progressively transitioned into astrocyte-like cells forming monolayers between DIV10 and DIV15, while losing the morphology and phenotypic markers of microglia (**Figure 4A**). At this time, transition zones in the border separating the microglial and the astrocyte-like cells expressed both microglial (Iba1 and CD11b) and astrocytic (GFAP) markers (**Figure 4B**). These transition zones were transient because most cells expressed S100β without microglial markers by DIV15. The treatment of

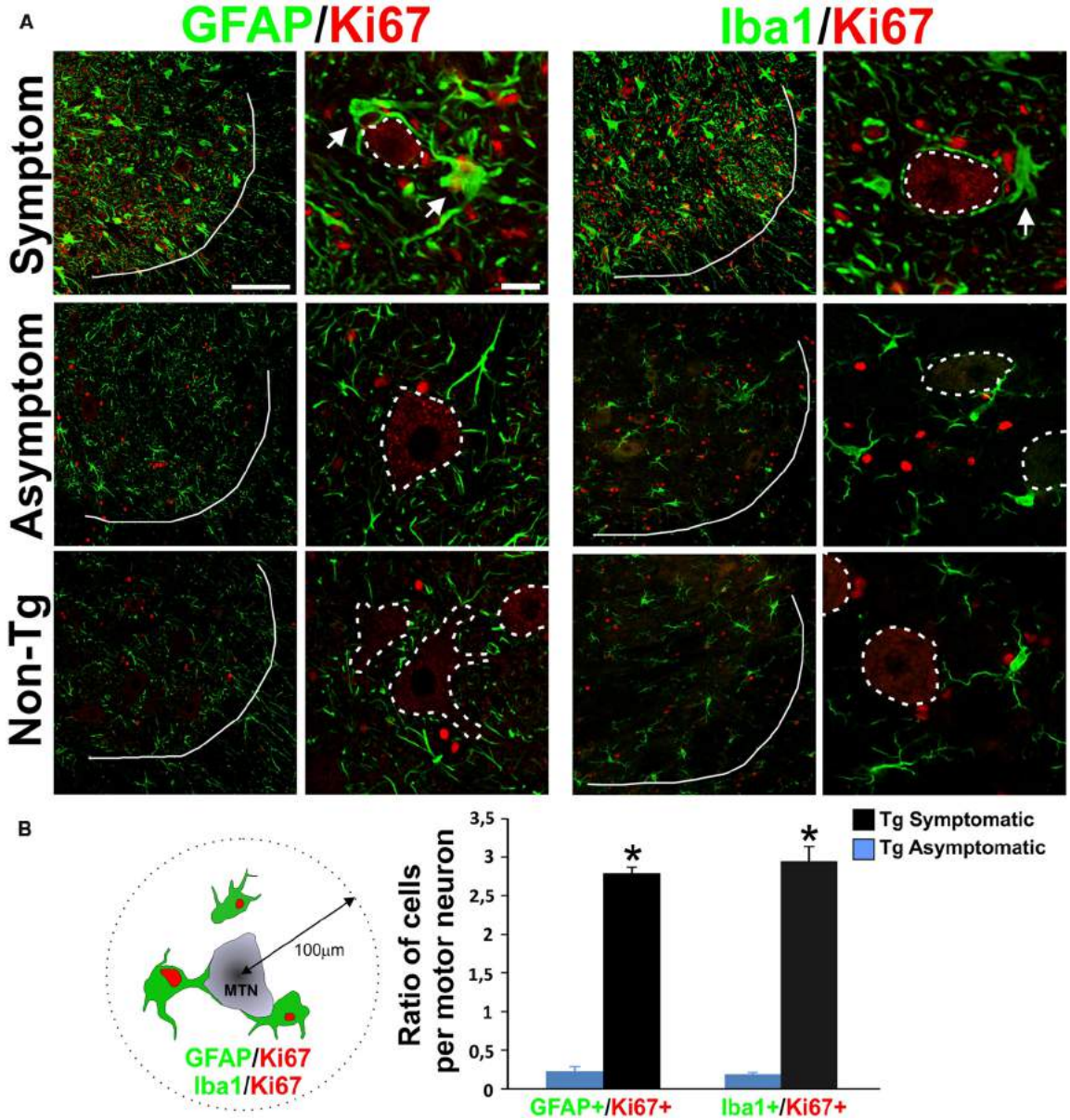

FIGURE 1 | Characterization of proliferative astrocytes and microglia in the degenerating lumbar spinal cord. **(A)** Photomicrographs showing GFAP/Ki67 and Iba1/Ki67 stained lumbar spinal cord sections measured in symptomatic (upper panels), asymptomatic (middle panels) $SOD1^{G93A}$ rats, and non-transgenic rats (lower panels). Low magnification panels show the notorious increase in the number of $Ki67^{+}$ red nuclei and the appearance of large $GFAP^{+}$ and $Iba1^{+}$ cells (green) in the symptomatic rats, as compared to low cell proliferation in asymptomatic or non-Tg rats. A white line indicates the border between white and grey matter. The high magnification images show that GFAP/Ki67 and Iba1/Ki67 cells are typically located around the motor neurons (indicated as dotted lines) and their processes closely embrace the neuronal cell body. The arrows indicate double-labeled cells. Note the unspecific binding of Ki67 antibody to motor neuron cell bodies. **(B)** Ratio of GFAP/Ki67 and Iba1/Ki67-positive cells per motor neuron in symptomatic and asymptomatic rats. The scheme at the left shows the methods used to count the cells in a perimeter of 100 μm around motor neurons. The counting was performed in 10 histological sections per animal. Two different rats were used for each condition. Data are shown as mean ± SD; $*P < 0.05$. Scale bars: 100 μm for low magnification panels; 20 μm for high magnification panels.

the cultures with 10 μM FSK, which is known to induce astrocytic processes growth and differentiation (Abe and Saito, 1997), accelerated the transition from microglia to AbA cells, while down-regulating the expression of Iba1 and promoting the growth of processes stained with GFAP (**Figure 4C**). To further confirm the microglia to astrocyte phenotypic switch, we treated the cultures with Leu-OMe, a compound used to selectively deplete microglia from primary cell cultures (Uliasz et al., 2012). **Figure 4D** shows that microglia from ALS rats were completely killed by 25 mM of Leu-OMe at DIV3, whereas there was no toxicity at DIV20 after the cells had undergone the phenotypic transition to an AbA morphology.

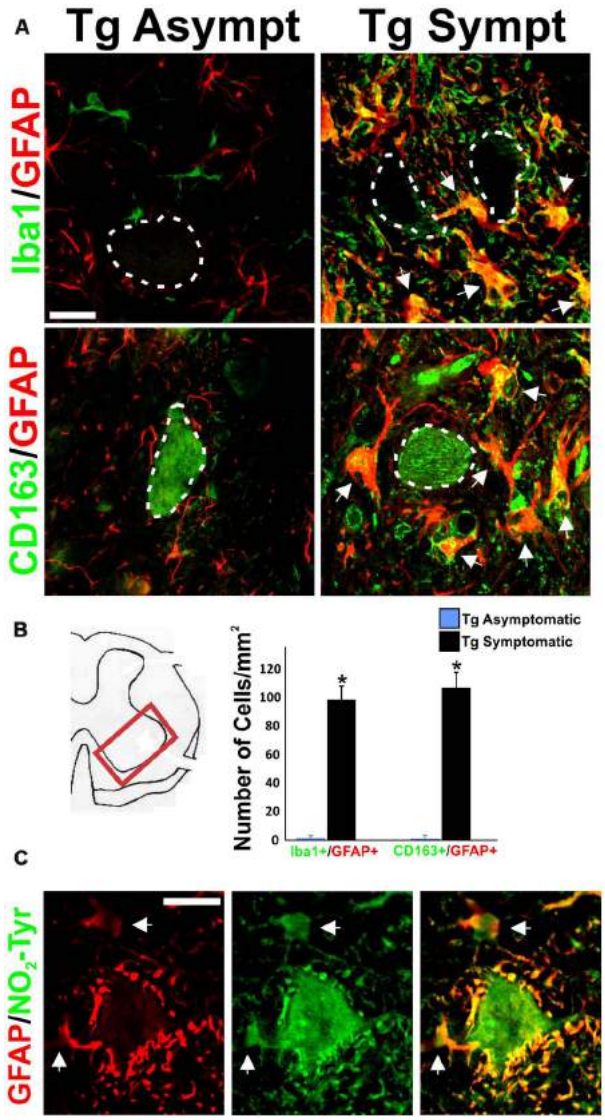

FIGURE 2 | Concurrent expression of microglia and astrocytic markers in AbA cells.(A) Representative image of GFAP (red), Iba1 (green), and CD163 (green) in lumbar spinal cord sections from transgenic asymptomatic (Tg-asymp) and symptomatic (Tg-sympt) $SOD1^{G93A}$ rats. Dotted lines indicate motor neuron cells bodies, which artifactually stained for CD163. Note that microglia and astrocytes in asymptomatic rat expressed GFAP and Iba1 in well-segregated cell populations. In comparison, most of the $Iba1^{+}$ and $CD163^{+}$ cells also expressed GFAP in symptomatic animals (arrows). **(B)** Quantification of cells expressing Iba1/GFAP and CD163/GFAP in the lumbar spinal cord. The counting was performed in 10 histological sections per animal. Two different rats were used for each condition. Data are shown as mean ± SD; $^{*}P < 0.05$. **(C)** Representative confocal immunostaining against GFAP (red) and nitrotyrosine (NO_2–Tyr, green) in the ventral horn of a symptomatic rat showing the intense nitration of Perineuronal AbA cells (arrows). Scale bars: 20 μm.

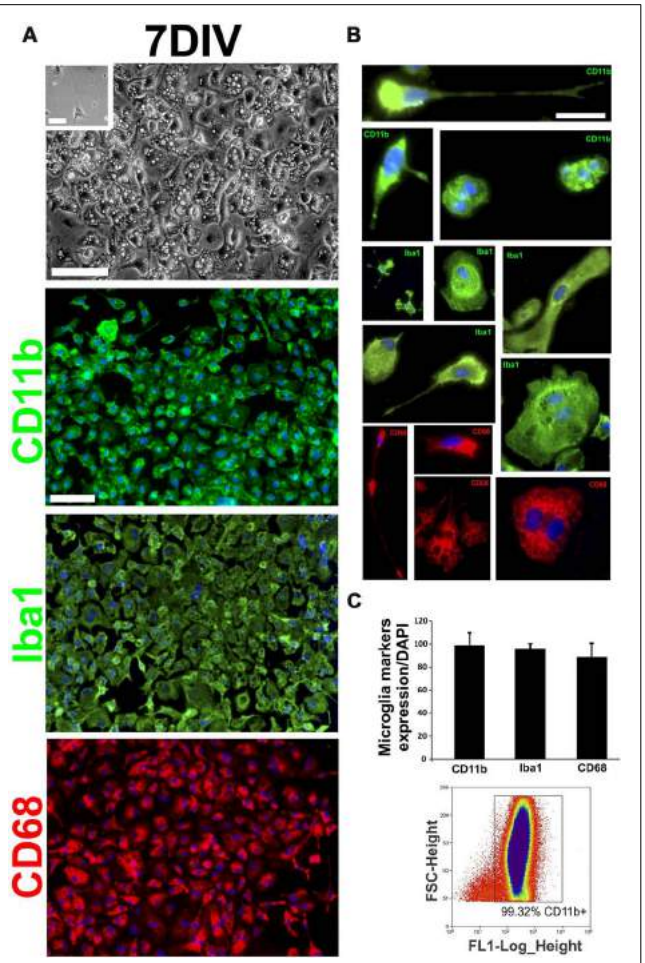

FIGURE 3 | Characterization of first stages of AbA cells *in vitro*. Primary cultures of the spinal cord of symptomatic rats were established as in (Diaz-Amarilla et al., 2011) and the cell phenotypes were analyzed on DIV7. **(A)** The upper panel shows a representative phase-contrast image of the culture at DIV7. The inset shows the same culture obtained from non-Tg littermates where no cells could be grown. The lower panels show confocal images of cells immunostained for typical microglia markers such as CD11b, CD68, and Iba1 at 7 DIV. Scale bars: 50 μm. **(B)** Characterization of different typical microglia phenotypes present at 7 DIV, cultured from Tg symptomatic rats. Scale bar: 25 μm. **(C)** Quantification of the microglia markers expression (CD11b, CD68, and Iba1) in culture at 7 DIV, counting cell positive for microglia marker respect to the total number of nuclei labeled with DAPI (upper panel). Typical data from flow cytometry showing that 99% of cells were $CD11b^{+}$. The data are representative of three independent experiments.

DISCUSSION

Glial cells expressing mutant SOD1 are now well established to be toxic to motor neurons in rodent models as well as in ALS patients (Barbeito et al., 2004; Nagai et al., 2007; Yamanaka et al., 2008; Haidet-Phillips et al., 2011). AbA cells are the most toxic cells yet identified to motor neurons (Diaz-Amarilla et al., 2011). These distinctive glial cells are directly associated with motor neuron disease, because they actively proliferate after the onset of progressive paralysis and make intimate contact with degenerating motor neurons. By analyzing the population of proliferating $Ki67^{+}$ glial cells in the ventral horn of symptomatic SOD1 rats, we found that AbA cells most likely originate from microglia. Notably, purified microglia isolated from the spinal cord of symptomatic rats spontaneously transformed into AbA cells.

The extremely rapid progression of paralysis in $SOD1^{G93A}$ rats is characterized by prominent neuroinflammation associated with

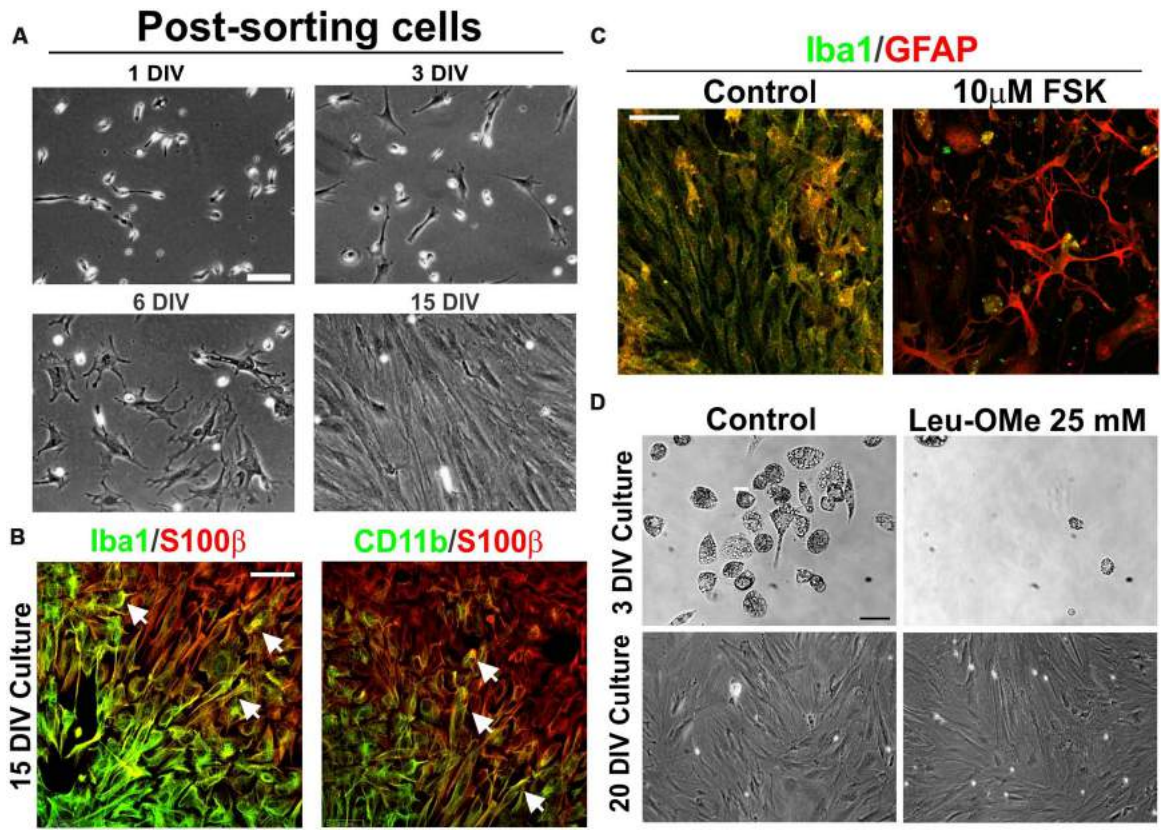

FIGURE 4 | Phenotypic transition of microglia into AbA cells in culture. **(A)** Microglia cell cultures (7 DIV) from symptomatic spinal cord were dissociated and stained with FITC-labeled CD11b. After FACS sorting, cells were re-plated and analyzed for phenotypic transition at DIV15. Scale bar: 50 μm. **(B)** Confocal image showing transition zones observed at 15 DIV. Note the segregation of astrocytic S100β staining with the microglia Iba1 or CD11b markers, which coincides with the morphological change of cells. The co-localization of astrocytic and microglia markers was found in a few cells in the border between these zones. Scale bar: 50 μm. **(C)** Treatment of cultures at DIV15 with foskolin (10 μM, 3 h) down regulated Iba1 expression and stimulated GFAP expression and growth of processes. Scale bars: 50 μm. **(D)** Differential effect of 25 μM of Leucine-Methyl Ester (Leu-OMe) before and after the phenotypic transition. Treatment with Leu-OMe was applied to cultures at DIV3 and DIV20 to assess the toxicity. Toxicity of Leu-OMe was restricted to the microglia phenotype. This experiment was repeated with three independent isolations of AbA cells. Scale bars: 20 μm

microglia activation (Sanagi et al., 2010; Philips and Robberecht, 2011). This inflammatory response is consistent with the sharp increase in cell proliferation others and we have observed with Ki67-staining in symptomatic animals (Schaefer et al., 2005; Pun et al., 2006). Previously, BrdU incorporation was used to demonstrate increased cell proliferation in ALS rats of NG2-positive glial progenitor cells (Magnus et al., 2008), which can potentially differentiate into astrocytes. Our results indicate that microglia more likely gave rise to AbA cells expressing astrocytic markers in regions adjacent to motor neurons.

The finding that spinal AbA cells co-express astrocytic GFAP with two different microglia markers Iba1 or CD163 was surprising because such a mixed phenotype is rarely observed. Co-expression of both markers has been observed in neoplastic glioblastoma multiforme cells (Huysentruyt et al., 2011; Persson and Englund, 2012). These human astroglial tumor cells seem to acquire phagocytic properties as a consequence of the dramatic inflammatory conditions occurring in tumors (Persson and Englund, 2012). Similarly, spinal AbA cells may originate from a phenotypic transition of inflammatory microglia into astrocytes-like cells in the degenerating cellular environment of the ventral horn. Other reports have shown aberrant features of microglial cells in symptomatic $SOD1^{G93A}$ rats, including formation of microglia clusters (Howland et al., 2002) and multi-nucleated giant cells (Fendrick et al., 2007). Based on the morphology, localization, high proliferation rate, and other phenotypic features, spinal AbA cells are distinct from previously described M1 or M2 microglia (Kigerl et al., 2009; Durafourt et al., 2012; Liao et al., 2012). It is uncertain whether the phenotypic transition is specific for mutant SOD1 microglia or might also be observed in other CNS insults where phagocytic microglia accumulate around dying neurons (Beyer et al., 2000; Sanagi et al., 2010; Neher et al., 2012). For example, ameboid microglia-like cells expressing markers of oligodendrocyte and monocyte lineages have been described in hippocampus following acute neuronal damage (Fiedorowicz et al., 2008). AbA cells represent a novel pathological phenotype of microglia/macrophages derived from their prominent plasticity following activation (Schwartz et al., 2006; Luo and Chen, 2012). This phenotypic transformation of microglia may explain why the ablation of dividing

astrocytes did not alter astrogliosis in SOD1 mice (Lepore et al., 2008).

Further evidence that AbA cells derive from activated microglia was provided in cell culture experiments showing that purified endogenous microglia can transition to astrocyte-like cells. Microglia expressing CD11b, Iba1, and CD68 represented more than 98% of cells isolated from the spinal cord of symptomatic $SOD1^{G93A}$ rats. Moreover, FACS sorting of these cells using CD11b antibodies resulted in typical microglia cultures that also transitioned to AbA cells after 2 weeks, showing not only that AbA cells are originated from microglia but also the phenotypic change occurs *in vitro*.

Because the phenotypic switch is associated to sustained cell proliferation and a critical cell density, we suggest that inflammatory mediators secreted by the activated microglia induced the transformation. Previous reports have shown the ability of microglia to be progenitors for different neural cell types, including astrocytes *in vitro* (Yokoyama et al., 2004). This property in turn may be related to their hematopoietic origin (Yokoyama et al., 2006). Compared to AbA cells growing in the degenerating spinal cord, the concurrent expression of astrocytic and microglia markers by cultured AbA cells is only transiently in restricted to the borders of the transition zones. Therefore, it appears that activated microglial cells in degenerating spinal cord are prone to transition to astrocyte-like phenotype both in culture conditions as well as *in vivo*, in the cellular niche surrounding the motor neurons. These cells may play a role in the killing and subsequent phagocytosis of motor neurons.

Spinal AbA cells also show a number of aberrant features including high levels of S100β and Cx43 expression (Diaz-Amarilla et al., 2011) that may be relevant for neuronal toxicity through secreted S100 proteins as well as extracellular ATP released through connexin hemichannels. Activation of the extracellular ATP receptor/channel P2X7 has recently been shown to induce motor neuron death and to induce the neurotoxic phenotypes of astrocytes in culture (Gandelman et al., 2010, 2013). Furthermore, endogenous nitration of tyrosine near the ATP binding pocket of HSP90 activates P2X7, which induces motor neuron apoptosis (Franco et al., 2013).

We also showed that spinal AbA cells are strongly stained for nitrotyrosine especially in the distal perineuronal processes, consistent with the production of peroxynitrite. Microglia bearing mutant SOD1 has been shown to damage motor neurons through the production of peroxynitrite (Thonhoff et al., 2012).Because their microglia origin, spinal AbA cells may have primed to generate superoxide and hence peroxynitrite on the exterior face of the plasma membrane in close proximity to motor neurons (Beckman et al., 2001).

CONCLUSION

Taken together, the present work supports the concept that aberrant astrocyte-like cells in the degenerating spinal cord are derived from activated microglia that proliferate around damaged motor neurons. The present study provides evidence that microglia isolated from the spinal cord of ALS–SOD rats developing paralysis have the potential to transition into an astrocyte-like phenotype. The proliferating spinal AbA cells concurrently express markers of both microglia and astrocytes lineages. Because the appearance of AbA cells is closely associated to the progression of paralysis in $SOD1^{G93A}$ rats, a better understanding of the mediators inducing the phenotypic transition may provide another avenue of intervention to slow the progressive spread of disease in ALS patients.

AUTHOR CONTRIBUTIONS

Emiliano Trias, Pablo Díaz-Amarilla, Silvia Olivera-Bravo, Joseph S. Beckman, and Luis Barbeito designed research; Emiliano Trias, Pablo Díaz-Amarilla, Silvia Olivera-Bravo, Eugenia Isasi, Derek A. Drechsel, Nathan Lopez, C. Samuel Bradford, and Kyle E. Ireton performed research; Emiliano Trias, Pablo Díaz-Amarilla, C. Samuel Bradford, Joseph S. Beckman, and Luis Barbeito analyzed data; and Emiliano Trias, Joseph S. Beckman, and Luis Barbeito wrote the paper.

ACKNOWLEDGMENTS

This work was funded by the program for development of basic sciences (PEDECIBA), Innovation and Research National Agency (ANII), and FOCEM-Mercosur funding. Partial funding also came from National Institute on Environmental Health Sciences Grant P30ES000210, National Institute of Neurological Disorders and Stroke Grant R01NS058628A, and National Center for Complementary and Alternative Medicine Grant NCCAM P01AT002034; and from the ALS Association (to Joseph S. Beckman).

REFERENCES

Abe, K., and Saito, H. (1997). Developmental changes in cyclic AMP-stimulated stellation of cultured rat cortical astrocytes. *Jpn. J. Pharmacol.* 75, 433–438. doi: 10.1254/jjp.75.433

Appel, S. H. (2009). CD4+ T cells mediate cytotoxicity in neurodegenerative diseases. *J. Clin. Invest.* 119, 13–15. doi: 10.1172/JCI38096

Barbeito, L. H., Pehar, M., Cassina, P., Vargas, M. R., Peluffo, H., Viera, L., et al. (2004). A role for astrocytes in motor neuron loss in amyotrophic lateral sclerosis. *Brain Res. Brain Res. Rev.* 47, 263–274. doi: 10.1016/j.brainresrev.2004.05.003

Beckman, J. S., Estevez, A. G., Crow, J. P., and Barbeito, L. (2001). Superoxide dismutase and the death of motoneurons in ALS. *Trends Neurosci.* 24, S15–S20. doi: 10.1016/S0166-2236(01)00004-2

Beyer, M., Gimsa, U., Eyupoglu, I. Y., Hailer, N. P., and Nitsch, R. (2000). Phagocytosis of neuronal or glial debris by microglial cells: upregulation of MHC class II expression and multinuclear giant cell formation in vitro. *Glia* 31, 262–266. doi: 10.1002/1098-1136(200009)31:3<262::AID-GLIA70>3.0.CO;2-2

Boillee, S., Vande Velde, C., and Cleveland, D. W. (2006a). ALS: a disease of motor neurons and their non-neuronal neighbors. *Neuron* 52, 39–59. doi: 10.1016/j.neuron.2006.09.018

Boillee, S., Yamanaka, K., Lobsiger, C. S., Copeland, N. G., Jenkins, N. A., Kassiotis, G., et al. (2006b). Onset and progression in inherited ALS determined by motor neurons and microglia. *Science* 312, 1389–1392. doi: 10.1126/science.1123511

Bruijn, L. I., Becher, M. W., Lee, M. K., Anderson, K. L., Jenkins, N. A., Copeland, N. G., et al. (1997). ALS-linked SOD1 mutant G85R mediates damage to astrocytes and promotes rapidly progressive disease with SOD1-containing inclusions. *Neuron* 18, 327–338. doi: 10.1016/S0896-6273(00)80272-X

Cleveland, D. W., and Rothstein, J. D. (2001). From Charcot to Lou Gehrig: deciphering selective motor neuron death in ALS. *Nat. Rev. Neurosci.* 2, 806–819. doi: 10.1038/35097565

Diaz-Amarilla, P., Olivera-Bravo, S., Trias, E., Cragnolini, A., Martinez-Palma, L., Cassina, P., et al. (2011). Phenotypically aberrant astrocytes that promote motoneuron damage in a model of inherited amyotrophic lateral sclerosis. *Proc. Natl. Acad. Sci. U.S.A.* 108, 18126–18131. doi: 10.1073/pnas.1110689108

Durafourt, B. A., Moore, C. S., Zammit, D. A., Johnson, T. A., Zaguia, F., Guiot, M. C., et al. (2012). Comparison of polarization properties of human adult microglia and blood-derived macrophages. *Glia* 60, 717–727. doi: 10.1002/glia.22298

Engelhardt, J. I., Tajti, J., and Appel, S. H. (1993). Lymphocytic infiltrates in the spinal cord in amyotrophic lateral sclerosis. *Arch. Neurol.* 50, 30–36. doi: 10.1001/archneur.1993.00540010026013

Fendrick, S. E., Xue, Q. S., and Streit, W. J. (2007). Formation of multinucleated giant cells and microglial degeneration in rats expressing a mutant Cu/Zn superoxide dismutase gene. *J. Neuroinflammation* 4, 9. doi: 10.1186/1742-2094-4-9

Fiedorowicz, A., Figiel, I., Zaremba, M., Dzwonek, K., and Oderfeld-Nowak, B. (2008). The ameboid phenotype of NG2 (+) cells in the region of apoptotic dentate granule neurons in trimethyltin intoxicated mice shares antigen properties with microglia/macrophages. *Glia* 56, 209–222. doi: 10.1002/glia.20605

Franco, M. C., Ye, Y., Refakis, C. A., Feldman, J. L., Stokes, A. L., Basso, M., et al. (2013). Nitration of Hsp90 induces cell death. *Proc. Natl. Acad. Sci. U.S.A.* 110, E1102–E1111. doi: 10.1073/pnas.1215177110

Gandelman, M., Levy, M., Cassina, P., Barbeito, L., and Beckman, J. S. (2013). P2X7 receptor-induced death of motor neurons by a peroxynitrite/FAS-dependent pathway. *J. Neurochem.* 126, 382–388. doi: 10.1111/jnc.12286

Gandelman, M., Peluffo, H., Beckman, J. S., Cassina, P., and Barbeito, L. (2010). Extracellular ATP and the P2X7 receptor in astrocyte-mediated motor neuron death: implications for amyotrophic lateral sclerosis. *J. Neuroinflammation* 7, 33. doi: 10.1186/1742-2094-7-33

Graber, D. J., Hickey, W. F., and Harris, B. T. (2010). Progressive changes in microglia and macrophages in spinal cord and peripheral nerve in the transgenic rat model of amyotrophic lateral sclerosis. *J. Neuroinflammation* 7, 8. doi: 10.1186/1742-2094-7-8

Gurney, M. E., Pu, H., Chiu, A. Y., Dal Canto, M. C., Polchow, C. Y., Alexander, D. D., et al. (1994). Motor neuron degeneration in mice that express a human Cu,Zn superoxide dismutase mutation. *Science* 264, 1772–1775. doi: 10.1126/science.8209258

Haidet-Phillips, A. M., Hester, M. E., Miranda, C. J., Meyer, K., Braun, L., Frakes, A., et al. (2011). Astrocytes from familial and sporadic ALS patients are toxic to motor neurons. *Nat. Biotechnol.* 29, 824–828. doi: 10.1038/nbt.1957

Hall, E. D., Oostveen, J. A., and Gurney, M. E. (1998). Relationship of microglial and astrocytic activation to disease onset and progression in a transgenic model of familial ALS. *Glia* 23, 249–256. doi: 10.1002/(SICI)1098-1136(199807)23:3<249::AID-GLIA7>3.0.CO;2-#

Howland, D. S., Liu, J., She, Y., Goad, B., Maragakis, N. J., Kim, B., et al. (2002). Focal loss of the glutamate transporter EAAT2 in a transgenic rat model of SOD1 mutant-mediated amyotrophic lateral sclerosis (ALS). *Proc. Natl. Acad. Sci. U.S.A.* 99, 1604–1609. doi: 10.1073/pnas.032539299

Huysentruyt, L. C., Akgoc, Z., and Seyfried, T. N. (2011). Hypothesis: are neoplastic macrophages/microglia present in glioblastoma multiforme? *ASN Neuro.* 3, e00064. doi: 10.1042/AN20110011

Ilieva, H., Polymenidou, M., and Cleveland, D. W. (2009). Non-cell autonomous toxicity in neurodegenerative disorders: ALS and beyond. *J. Cell Biol.* 187, 761–772. doi: 10.1083/jcb.200908164

Kang, S. H., Fukaya, M., Yang, J. K., Rothstein, J. D., and Bergles, D. E. (2010). NG2+ CNS glial progenitors remain committed to the oligodendrocyte lineage in postnatal life and following neurodegeneration. *Neuron* 68, 668–681. doi: 10.1016/j.neuron.2010.09.009

Kigerl, K. A., Gensel, J. C., Ankeny, D. P., Alexander, J. K., Donnelly, D. J., and Popovich, P. G. (2009). Identification of two distinct macrophage subsets with divergent effects causing either neurotoxicity or regeneration in the injured mouse spinal cord. *J. Neurosci.* 29, 13435–13444. doi: 10.1523/JNEUROSCI.3257-09.2009

Kreutzberg, G. W. (1996). Microglia: a sensor for pathological events in the CNS. *Trends Neurosci.* 19, 312–318. doi: 10.1016/0166-2236(96)10049-7

Lepore, A. C., Dejea, C., Carmen, J., Rauck, B., Kerr, D. A., Sofroniew, M. V., et al. (2008). Selective ablation of proliferating astrocytes does not affect disease outcome in either acute or chronic models of motor neuron degeneration. *Exp. Neurol.* 211, 423–432. doi: 10.1016/j.expneurol.2008.02.020

Liao, B., Zhao, W., Beers, D. R., Henkel, J. S., and Appel, S. H. (2012). Transformation from a neuroprotective to a neurotoxic microglial phenotype in a mouse model of ALS. *Exp. Neurol.* 237, 147–152. doi: 10.1016/j.expneurol.2012.06.011

Luo, X. G., and Chen, S. D. (2012). The changing phenotype of microglia from homeostasis to disease. *Transl. Neurodegener.* 1:9. doi: 10.1186/2047-9158-1-9

Magnus, T., Carmen, J., Deleon, J., Xue, H., Pardo, A. C., Lepore, A. C., et al. (2008). Adult glial precursor proliferation in mutant SOD1G93A mice. *Glia* 56, 200–208. doi: 10.1002/glia.20604

McGeer, P. L., and McGeer, E. G. (2002). Inflammatory processes in amyotrophic lateral sclerosis. *Muscle Nerve* 26, 459–470. doi: 10.1002/mus.10191

Nagai, M., Re, D. B., Nagata, T., Chalazonitis, A., Jessell, T. M., Wichterle, H., et al. (2007). Astrocytes expressing ALS-linked mutated SOD1 release factors selectively toxic to motor neurons. *Nat. Neurosci.* 10, 615–622. doi: 10.1038/nn1876

Neher, J. J., Neniskyte, U., and Brown, G. C. (2012). Primary phagocytosis of neurons by inflamed microglia: potential roles in neurodegeneration. *Front. Pharmacol.* 3:27. doi: 10.3389/fphar.2012.00027

Papadeas, S. T., Kraig, S. E., O'Banion, C., Lepore, A. C., and Maragakis, N. J. (2011). Astrocytes carrying the superoxide dismutase 1 (SOD1G93A) mutation induce wild-type motor neuron degeneration in vivo. *Proc. Natl. Acad. Sci. U.S.A.* 108, 17803–17808. doi: 10.1073/pnas.1103141108

Persson, A., and Englund, E. (2012). Phagocytic properties in tumor astrocytes. *Neuropathology* 32, 252–260. doi: 10.1111/j.1440-1789.2011.01266.x

Philips, T., and Robberecht, W. (2011). Neuroinflammation in amyotrophic lateral sclerosis: role of glial activation in motor neuron disease. *Lancet Neurol.* 10, 253–263. doi: 10.1016/S1474-4422(11)70015-70011

Pun, S., Santos, A. F., Saxena, S., Xu, L., and Caroni, P. (2006). Selective vulnerability and pruning of phasic motoneuron axons in motoneuron disease alleviated by CNTF. *Nat. Neurosci.* 9, 408–419. doi: 10.1038/nn1653

Sanagi, T., Yuasa, S., Nakamura, Y., Suzuki, E., Aoki, M., Warita, H., et al. (2010). Appearance of phagocytic microglia adjacent to motoneurons in spinal cord tissue from a presymptomatic transgenic rat model of amyotrophic lateral sclerosis. *J. Neurosci. Res.* 88, 2736–2746. doi: 10.1002/jnr.22424

Sargsyan, S. A., Monk, P. N., and Shaw, P. J. (2005). Microglia as potential contributors to motor neuron injury in amyotrophic lateral sclerosis. *Glia* 51, 241–253. doi: 10.1002/glia.20210

Schaefer, A. M., Sanes, J. R., and Lichtman, J. W. (2005). A compensatory subpopulation of motor neurons in a mouse model of amyotrophic lateral sclerosis. *J. Comp. Neurol.* 490, 209–219. doi: 10.1002/cne.20620

Schwartz, M., Butovsky, O., Bruck, W., and Hanisch, U. K. (2006). Microglial phenotype: is the commitment reversible? *Trends Neurosci.* 29, 68–74. doi: 10.1016/j.tins.2005.12.005

Thonhoff, J. R., Gao, J., Dunn, T. J., Ojeda, L., and Wu, P. (2012). Mutant SOD1 microglia-generated nitroxidative stress promotes toxicity to human fetal neural stem cell-derived motor neurons through direct damage and noxious interactions with astrocytes. *Am. J. Stem Cells* 1, 2–21.

Uliasz, T. F., Hamby, M. E., Jackman, N. A., Hewett, J. A., and Hewett, S. J. (2012). Generation of primary astrocyte cultures devoid of contaminating microglia. *Methods Mol. Biol.* 814, 61–79. doi: 10.1007/978-1-61779-452-0_5

Yamanaka, K., Chun, S. J., Boillee, S., Fujimori-Tonou, N., Yamashita, H., Gutmann, D. H., et al. (2008). Astrocytes as determinants of disease progression in inherited amyotrophic lateral sclerosis. *Nat. Neurosci.* 11, 251–253. doi: 10.1038/nn2047

Yokoyama, A., Sakamoto, A., Kameda, K., Imai, Y., and Tanaka, J. (2006). NG2 proteoglycan-expressing microglia as multipotent neural progenitors in normal and pathologic brains. *Glia* 53, 754–768. doi: 10.1002/glia.20332

Yokoyama, A., Yang, L., Itoh, S., Mori, K., and Tanaka, J. (2004). Microglia, a potential source of neurons, astrocytes, and oligodendrocytes. *Glia* 45, 96–104. doi: 10.1002/glia.10306

Conflict of Interest Statement: The authors declare that the research was conducted in the absence of any commercial or financial relationships that could be construed as a potential conflict of interest.

Received: 18 July 2013; paper pending published: 05 November 2013; accepted: 09 December 2013; published online: 24 December 2013.

Citation: Trias E, Díaz-Amarilla P, Olivera-Bravo S, Isasi E, Drechsel DA, Lopez N, Bradford CS, Ireton KE, Beckman JS and Barbeito L (2013) Phenotypic transition of microglia into astrocyte-like cells associated with disease onset in a model of inherited ALS. Front. Cell. Neurosci. 7:274. doi: 10.3389/fncel.2013.00274

This article was submitted to the journal Frontiers in Cellular Neuroscience.

Publicación 3

Focal transplantation of aberrant glial cells carrying the SOD1^{G93A} mutation into rat spinal cord induces extensive gliosis

Sofía Ibarburu*, Emiliano Trias*, Natalia Lago, Hugo Peluffo, Romina Barreto-Núñez, Valentina Varela, Joseph S. Beckman, Luis Barbeito

Resumen

El hallazgo de que la progresión de la enfermedad está directamente asociada a la aparición de fenotipos gliales aberrantes brinda nuevas oportunidades para comprender el rol que estas células desempeñan en la orquestación de la neuroinflamación. Por este motivo diseñamos una serie de experimentos para responder la pregunta de si las células gliales aberrantes son capaces de inducir neuroinflamación y toxicidad hacia motoneuronas cuando son trasplantadas en la médula espinal de ratas no transgénicas. Luego de 7 días, las ratas fueron sacrificadas y se realizó un análisis inmunohistoquímico para analizar marcadores de inflamación y daño en el microambiente que rodea a las motoneuronas.

Resultados

- Para los trasplantes, utilizamos un pasaje 15-20 de células gliales aberrantes. Estos pasajes de células presentan niveles de proliferación exacerbada y son altamente tóxicas para motoneuronas en cultivo. Esto las hace excelentes candidatos para estudiar su capacidad de inducir inflamación y toxicidad en el ambiente en el que se encuentren. Por ser aisladas de animales SOD1^{G93A}, en cultivo, estas células presentan altos niveles de expresión de la SOD1 humana mutada; además, una subpoblación de estas células expresa altos niveles de SOD1 humana mal plegada. Al ser inyectadas en animales no transgénicos, la expresión de las diferentes formas de SOD1 humana nos permitirá reconocer a las células una vez inyectadas en la médula.
- Las células trasplantadas en la médula espinal se localizan en el sitio cercano a la inyección. Al igual que lo observado in vitro, una

subpoblación de células expresa altos niveles de SOD1 humana, mientras que las células que se localizan en el centro del agregado de células inyectadas, presentan niveles elevados de SOD1 humana mal plegada. No observamos migración significativa de estas células hacia sitios adyacentes del inyectado.

- El trasplante de células gliales aberrantes indujo altos niveles de microgliosis y astrocitosis en el sitio del trasplante. En la periferia del agregado de células aberrantes se puede observar altos niveles de expresión de marcadores astrocitarios, GFAP, S100β, nestina y vimentina, y microgliales, CD68, Iba1, lectina y MHC de clase II. Ninguna de las células que rodean al agregado celular trasplantado presenta niveles de SOD1 humana, lo que sugiere una reactividad glial local inducida por el trasplante. Además, las células gliales aberrantes trasplantadas inducen una reactividad microglial que se esparce hacia toda la médula espinal desde el sitio de inyección, evidenciado por altos niveles de expresión de Iba1. Esta inducción de la reactividad glial no fue observada con el trasplante de microglía no transgénica o el vehículo.
- El trasplante de células gliales aberrantes induce una significativa reactividad glial, astrocitaria y microglial a lo largo del neuroeje, tanto en el lado inyectado como en el contralateral. Este efecto no es producido por los controles. Incluso a nivel cervical, del lado de la médula trasplantada con células aberrantes, se observan niveles de gliosis significativamente aumentados cuando se lo compara a la inyección de los controles.
- Finalmente, las células gliales aberrantes inyectadas en la médula espinal de ratas no transgénicas, inducen una incipiente toxicidad para las motoneuronas cercanas al sitio del trasplante, algo que queda evidenciado por la acumulación de ubiquitina en los somas de las motoneuronas.

Conclusiones

Estos resultados muestran por primera vez que las células gliales aberrantes tienen la potencialidad de inducir y propagar la neuroinflamación y la toxicidad

para las motoneuronas cuando son trasplantadas en el SNC de ratas no transgénicas. Las células gliales aberrantes no solo indujeron reactividad glial en sitios cercanos al que fueron trasplantadas, sino que indujeron una gliosis significativa a lo largo del neuroeje, incluso llegando esta reactividad glial a nieves cervicales. El trasplante de células gliales aberrantes podría constituir un modelo válido y novedoso para estudiar el potencial neurotóxico de esta sub-población celular. Por ser células que expresan altos niveles de SOD1 mal plegada, también pueden servir como modelo para analizar la toxicidad de tipo priónica que inducen las especies de SOD1 mal plegadas. Para esto, el trasplante de células gliales aberrantes debería ser realizado en animales que sobreexpresen diferentes especies de SOD1 humana, ya que la progresión de tipo priónica inducida por las especies mal plegadas de SOD1 no ocurre entre proteínas de diferentes especies. Este trasplante constituye un modelo válido de “screening” para la búsqueda de nuevos fármacos que tengan la capacidad de modular la actividad tóxica de las células gliales aberrantes.

Original Paper

NeuroImmunoModulation

Neuroimmunomodulation
DOI: 10.1159/000480639

Received: June 22, 2017
Accepted after revision: August 17, 2017
Published online: November 1, 2017

Focal Transplantation of Aberrant Glial Cells Carrying the SOD1^{G93A} Mutation into Rat Spinal Cord Induces Extensive Gliosis

Sofía Ibarburu[a] Emiliano Trias[a] Natalia Lago[b] Hugo Peluffo[b, c]
Romina Barreto-Núñez[a] Valentina Varela[a] Joseph S. Beckman[a] Luis Barbeito[a]

[a]Laboratorio de Neurodegeneración, Institut Pasteur de Montevideo, [b]Laboratorio de Neuroinflamación y Terapia Génica, Institut Pasteur de Montevideo, and [c]Departamento de Histología y Embriología, Facultad de Medicina, Universidad de la República, Montevideo, Uruguay; [d]Linus Pauling Institute, Oregon State University, Corvallis, OR, USA

Keywords
Aberrant glial cells · Neuroinflammation · Motor neuron damage · Microgliosis · Asotrcytosis

Abstract
Objective: We aimed to determine the potential of aberrant glial cells (AbAs) isolated from the spinal cord of adult SOD1^{G93A} symptomatic rats to induce gliosis and neuronal damage following focal transplantation into the lumbar spinal cord of wild-type rats. ***Methods:*** AbAs were obtained from the spinal cords of SOD1^{G93A} symptomatic rats. One hundred thousand cells were injected using a glass micropipette into the lumbar spinal cords (L3–L5) of syngeneic wild-type adult rats. Equal volumes of culture medium or wild-type neonatal microglia were used as controls. Seven days after transplantation, immunohistochemistry analysis was carried out using astrocytic and microglia cell markers. Transplanted SOD1^{G93A} AbAs were recognized by specific antibodies to human SOD1 (hSOD1) or misfolded human SOD1. ***Results:*** Seven days after transplantation, AbAs were mainly detected in the medial region of the lumbar ventral horn as a well-limited cell cluster formed at the site of injection by their immunoreactivity to either misfolded SOD1 or normally folded hSOD1. Compared with controls, transplanted AbAs were surrounded by marked microgliosis and reactive astrocytes. Marked microgliosis was observed to extend bilaterally up to the cervical cord. Motor neurons close to AbA transplants were surrounded by activated glial cells and displayed ubiquitin aggregation. ***Conclusions:*** AbAs bearing mutant SOD1^{G93A} have the potential to induce neuroinflammation along the spinal cord and incipient damage to the motor neurons. The emergence of AbAs during amyotrophic lateral sclerosis pathogenesis may therefore be a mechanism to boost neuroinflammation and spread motor neuron damage along the neuroaxis.

Background

It is well recognized that glial cells play a key role in the pathogenesis of amyotrophic lateral sclerosis (ALS), a fatal neurodegenerative paralytic disease leading to progressive paralysis [1]. While most ALS cases are sporadic, a small number correspond to hereditary familial cases, some of them caused by mutations in the SOD1 [2]. Mice

Sofía Ibarburu and Emiliano Trias contributed equally to this work.

E-Mail karger@karger.com
www.karger.com/nim

Luis Barbeito
Institut Pasteur de Montevideo
Mataojo 2020, Montevideo CP 11.000 (Uruguay)
E-Mail barbeito@pasteur.edu.uy

and rats overexpressing different SOD1 mutations have become valuable in the approach for studying ALS disease mechanisms and drug discovery [2–4]. However, the pathogenic processes underlying motor neuron degeneration in ALS are multifactorial and unsettled, despite decades of research. An important concept in ALS is the non-cell-autonomous mechanisms leading to motor neuron degeneration, implying that glial cells expressing SOD1 mutations may trigger the degeneration and death of neighboring motor neurons [5, 6]. In this context, the mechanisms underlying glial activation and the spread of motor neuron damage in ALS also remain largely unknown.

We have previously shown that the rapid spread of paralysis in rats carrying the ALS-linked $SOD1^{G93A}$ mutation coincides with the emergence of aberrant glial cells exhibiting an astrocyte-like phenotype (AbA cells/AbAs) derived from activated microglia [7, 8], which suggests a link between AbAs and the progression of paralysis. AbAs are characterized by a distinctive pattern of astrocyte and microglial markers, simultaneously expressing the astrocytic markers GFAP and S100β and the microglial markers Iba1, CD11b, and CD163, and their localization in the surroundings of degenerating motor neurons [7, 9]. AbAs secrete soluble factors that induce motor neuron death with a higher potency than neonatal transgenic astrocytes. Pharmacological inhibition of AbAs by treating of $SOD1^{G93A}$ rats with the CSF-1R kinase inhibitor masitinib was found to result in unprecedented survival protection, even when the drug was administered after the onset of paralysis [10]. While AbAs appear as a distinct but relevant glial cell type associated with rapid paralysis progression in ALS rats, it remains unknown whether AbAs isolated in cell culture are neurotoxic or inflammatory in vivo after their transplantation into the spinal cord. Evidence of an aberrant glial phenotype has been recently described in a rat model of ischemia with reperfusion.

AbAs can be isolated from primary cultures of the spinal cord from transgenic $SOD1^{G93A}$ rats (aged 5–6 months) exhibiting advanced paralysis [7, 9]. These cultures yield high numbers of phagocytic microglia that actively proliferate before transitioning after a few passages to a confluent layer of flat, astrocyte-like cells. Once established in culture, AbAs express high levels of the transgene $SOD1^{G93A}$ as well as typical astrocytic markers such as S100β, connexin-43, and glutamine synthase [7]. We reasoned that one approach to further understand the pathogenic role of AbAs was to isolate these cells from the spinal cord of $SOD1^{G93A}$ rats, and then transplant them into the lumbar spinal cord of wild-type syngeneic rats. Such an experimental approach would allow us to determine the ability of AbAs to induce the activation of host microglia or astrocytes, or toxicity to motor neurons. Because transplanted AbAs express the human $SOD1^{G93A}$ mutation at high levels, the cells could be tracked using specific antibodies to SOD and to its misfolded form. Here, we report that transplantation of $SOD1^{G93A}$-bearing AbAs induces extensive microglia activation all along the spinal cord and incipient damage to the motor neurons. These findings support the concept that the emergence of AbAs during ALS pathogenesis may boost neuroinflammation and spread motor neuron damage along the neuroaxis.

Methods

Animals

Male $SOD1^{G93A}$ rat progeny were used for further breeding to maintain the transgenic line. The rats were housed in a centralized animal facility with a 12-h light-dark cycle with ad libitum access to food and water. Perfusion with fixatives was performed under 90 mg/kg ketamine – 10 mg/kg xylazine anesthesia and all efforts were made to minimize animal suffering, discomfort, or stress. All procedures using laboratory animals were performed in accordance with national and international guidelines and were approved by the Institutional Animal Committee for Animal Experimentation. This study was carried out in strict accordance with the Institut Pasteur de Montevideo Committee's requirements and under the current ethics regulations of the Uruguayan Law No. 18.611 for animal experimentation that follows the Guide for the Care and Use of Laboratory Animals of the National Institutes of Health (USA). All experiments were performed on 7 animals per experimental group.

AbA Cell Culture

AbAs were obtained according to the procedures described by Díaz-Amarilla et al. [7], with minor modifications. Briefly, $SOD1^{G93A}$ symptomatic rats were deeply anesthetized and sacrificed by decapitation, and then the spinal cord was removed and dissected on ice. After careful removal of the meninges, the spinal cord was chopped finely and dissociated with 0.25% trypsin in calcium-free buffer PBS for 15 min at 37°C. Trypsinization was stopped by adding DMEM/10% (vol/vol) FBS and mechanical disaggregation was performed by repeated pipetting. The resulting extract was passed through an 80-μm mesh to eliminate tissue debris, and then spun. The pellet was resuspended in culture medium: DMEM/10% (vol/vol) FBS, HEPES (3.6 g/L), penicillin (100 IU/mL), and streptomycin (100 μg/mL), and then plated in a 25-cm^2 tissue culture flask. Culture medium was removed after 48 h and then replaced every 48 h. Cells were passed and maintained during at least 20 passages. Before transplantation into the spinal cord, AbAs were stained in vitro with the tracer pkh26 (Sigma) according to the manufacturer instructions. Briefly, pkh26 dye was added to cell suspension for 5 min at 37°C, and its incorporation was stopped by adding 10% FBS. Cells were visualized at 2, 4, and 7 days in vitro after labeling to ensure the permanence of the dye.

Neonatal Wild-Type Microglia Cultures

Purified neonatal microglia were obtained from mixed glial cell culture as described by Ni and Aschner [11], with minor modifications. Briefly, mixed glial cells were prepared from the spinal cords of 1-day-old wild-type pups according to the procedures of Saneto and De Vellis [12], with minor modifications [13]. Cells were plated at a density of 2×10^4 cells/cm^2 in 35-mm Petri dishes, and maintained in DMEM/10% FBS, HEPES (3.6 g/L), penicillin (100 IU/mL), and streptomycin (100 μg/mL). After mixed glial cultures were confluent, the flask was shaken at 100 rpm for 1 h at 37°C. The medium was collected, place in a conical tube, and centrifuge at 2,500 *g* for 5 min at 4°C. The microglial cell pellet was resuspended in culture medium: DMEM/10% (vol/vol) FBS, HEPES (3.6 g/L), penicillin (100 IU/mL), and streptomycin (100 μg/mL), and placed in a 25-cm^2 culture flask.

Immunocytochemistry of AbAs

AbAs (passage 20) were fixed using 4% paraformaldehyde (PFA) at 4°C for 20 min, and then washed 3 times with 10 mM PBS (pH 7.4). Fixed cells were permeabilized during 20 min with 0.1% Triton X-100 in PBS. Blockade of nonspecific binding was done incubating fixed cells with 5% BSA during 1 h at room temperature. Primary antibodies against hSOD1 (rabbit polyclonal, 1/500) and misfolded SOD1 (mouse monoclonal MEDIMABS, 1/200) were diluted in 1% BSA and incubated overnight at 4°C. After several washes, cells were incubated with goat anti-rabbit and goat anti-mouse secondary antibodies conjugated to Alexa Fluor 488 or Alexa Fluor 546, respectively (Thermo Fisher Scientific, 1/1,000). Images were acquired by confocal microscopy using a ZEISS LSM 800 microscope.

Transplantation of AbAs into the Lumbar Spinal Cord of Wild-Type Rats

Cell transplants were performed in wild-type rats from the same inbred SOD1^{G93A} colony to assure syngeneic conditions and minimize the rejection of grafted cells. As reported in the literature [14], cell transplants were performed following a dorsal laminectomy to expose the spinal cord at the L3–L5 level. Laminectomy was performed under appropriate conditions of asepsis and anesthesia using ketamine-xylazine (90 and 10 mg/kg i.p., respectively). Animals were shaved and disinfected with iodine, and a longitudinal incision was made in the skin and muscles, extending from the lower thoracic part to the sacral vertebrae, in order to access the lumbar portion. Using a micromanipulator-stabilized glass micropipette attached to an infusion pump (Quintessential Stereotaxic Nanoinjector, Stoelting Co., Wood Dale, IL, USA), 3 μL of a suspension containing 100,000 AbAs, or neonatal microglia at an injection rate of 0.4 μL/min were injected. Equal volumes of culture medium were injected as a vehicle control. Once the injections were completed, the muscular and cutaneous planes were closed with sutures and the wound disinfected. Animals were kept in a thermostable environment until their full recovery.

Immunohistochemistry of Rat Spinal Cord

Seven days after injection, animals were deeply anesthetized and transcardial perfusion was performed with 0.04% sodium citrate in 0.1 M PBS and 4% PFA. Fixed spinal cord was dissected, postfixed overnight by immersion in 4% PFA, and then sectioned (20 μm) in a cryostat (Leica). Sections were permeabilized and blocked to prevent nonspecific binding with 5% BSA/0.5% Triton X-100 in PBS, and then incubated overnight at 4°C with primary antibodies: rabbit anti-hSOD1 (1/500), mouse anti-misfolded SOD1 (MEDIMABS, 1/200), mouse anti-GFAP (Sigma, 1/400), mouse anti-Nestin (Thermo Fisher Scientific, 1/200), mouse anti-S100β (Sigma, 1/400), mouse anti-Iba1 (Millipore, 1/300), mouse anti-CD68 (Abcam, 1/300), isolectin-biotin probe (Thermo Fisher Scientific, 1/200), mouse anti-MHCII (Abcam, 1/300), rabbit anti-Ki67 (Abcam, 1/300), and an Nissl-Alexa Fluor 555 probe (Thermo Fisher Scientific, 1/200) in a 1% BSA solution with 0.5% Triton X-100. After washing several times with PBS, sections were incubated for 2 h at room temperature with secondary antibodies conjugated to Alexa Fluor 488, 546, and/or 633 (Thermo Fisher Scientific, 1/1,000) or streptavidin/Alexa Fluor 633 (Thermo Fisher Scientific, 1/1,000). Images were acquired by confocal microscopy using a ZEISS LSM 800 microscope.

Quantitative Analysis of Microglia and Astrocytes

The number of Iba1+ and GFAP+ cells was performed by counting the respective positive cells in the ventral horn of the lumbar and cervivcal spinal cord of the injected animals. The analysis was assessed manually in at least 8 histological sections (30-μm) per animal ($n = 3$) using the cell counter tool of ImageJ software. Values were expressed as the ratio of Iba+ or GFAP+ cells with respect to vehicle. Statistical studies were performed using the statistical tools of the free software PAST3. All results are reported as the mean ± SEM, with $p < 0.01$ considered significant.

Analysis of Motor Neuron Number and Size

Analysis of motor neuron number and size was based on a stereological approach as described by Trias et al. [10]. Briefly, the number of motor neurons stained with Nissl was assessed by counting the positive cells in the gray matter of the lumbar spinal cord. The longest axis (length) of each soma was used to quantify the mean size of the motor neuron soma. The analysis was performed manually in at least 8 histological 30-μm sections per animal (4 different rats were used for each condition) using ImageJ software.

Statistical Analysis

Statistical analyses were performed using Past3 software. A two-sample test (Student *t* test) was made between groups. All results were expressed as mean ± standard error of the mean (SEM), with $p < 0.01$ considered statistically significant.

Results

Characterization of AbA Cell Transplants

AbAs were isolated from the spinal cord of symptomatic SOD1^{G93A} rats and expanded in culture during 20 passages. As previously reported by Díaz-Amarilla et al. [7], AbAs do not undergo replicative senescence, and, after passages 15–20, they showed a sustained replicative phenotype. Figure 1a shows the phenotype of cultured AbAs before transplantation. The cells predominantly expressed hSOD1, but a subpopulation also expressed misfolded SOD1 species recognized by specific antibod-

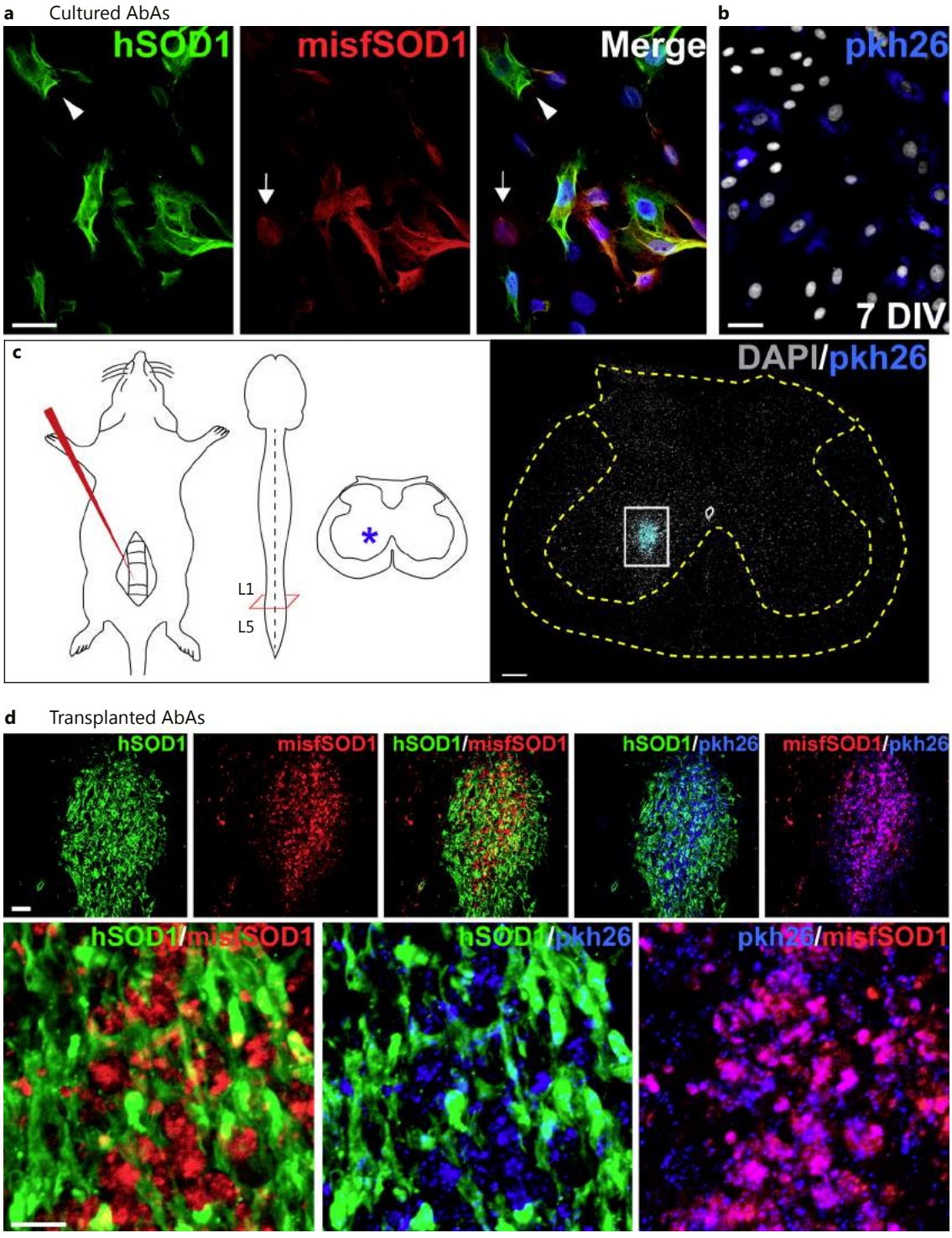

1

(For legend see next page.)

Color version available online

ies. To locate transplanted cells into the host tissue, AbAs were labelled with the fluorescent dye pkh26 before grafting. This was retained in cultured cells for at least 1 week (Fig. 1b), but did not label newborn cells resulting from cell proliferation.

After transplantation of AbAs into the lumbar cord, cells were clearly detected in the medial region of the ventral horn as a well-limited cluster of cells that remained close to the injection site (Fig. 1c, box). There was no apparent infiltration or migration of AbAs to the neighboring tissue, nor was there any apparent cell differentiation into astrocytes or neuronal phenotypes, as suggested by the lack of colocalization of hSOD1 with specific cell markers. Transplanted AbAs displayed immunoreactivity to misfolded SOD1, intermixed with a separate subpopulation of cells displaying immunoreactivity for native hSOD1. As shown in Figure 1d (lower panels), AbAs carrying the tracer pkh26 largely colocalized with mis-

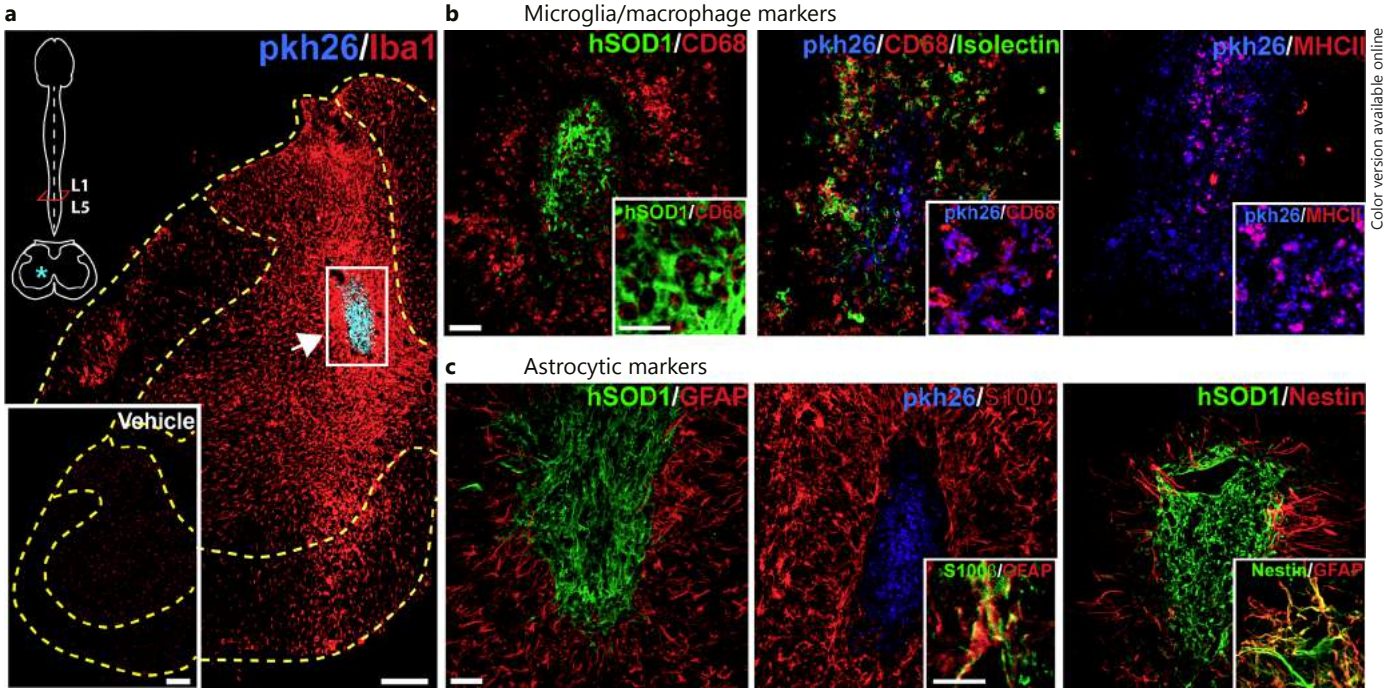

Fig. 2. Characterization of gliosis surrounding transplanted aberrant glial cells (AbAs). **a** Microgliosis produced by AbAs in the dorsal and ventral horn of the lumbar spinal cord. The cluster of transplanted pkh26-positive cells is shown in the box. Note the accumulation of Iba1+ microglia surrounding AbAs. **Inset** The lack of microgliosis induced by the injection of cell-free culture medium. **b** Confocal images: the close interaction of transplanted hSOD1+ or pkh26+ AbAs with host microglia expressing CD68, isolectin, and MHC ll. **c** Confocal images: the interaction of transplanted hSOD1+ or pkh26+ AbAs with host GFAP-, nestin- and S100β-expressing astrocytes. **Insets** Colocalization of the different markers at high magnification. Scale bars, 20 μm (**insets**), 50 μm (**b**, **c**), and 200 μm (**a**).

Fig. 1. Characterization of transplantation of aberrant glial cells (AbAs). **a** Representative confocal images: AbAs (passage 20) immunostained with rabbit anti-hSOD1 and mouse anti-misfolded SOD1 antibodies. Note the different subpopulations of AbAs expressing hSOD1 (white arrowhead), misfolded SOD1 (white arrow), or both. **b** AbAs were stained with pkh26 fluorescent dye before transplantation. After 7 days in vitro (DIV), pkh26 labeling remained in a subpopulation of cells, but was not observed in newborn cells. **c** Schematic representation: transplantation of AbAs into wild-type rat spinal cord. Seven days after transplantation, AbAs were detected in the medial region of the ventral horn as a well-limited cluster of cells (pkh26, white box). **d** Representative confocal images: AbA cell clusters (upper panels) showing the expression of both hSOD1 and misfolded SOD1. Note that the expression of misfolded SOD1 was only observed in pkh26-positive cells. Lower panels: magnification of AbA clusters. Scale bars, 20 μm (**a**, **b**, **d**, lower panel), 50 μm (**d**, upper panel), and 200 μm (**c**).

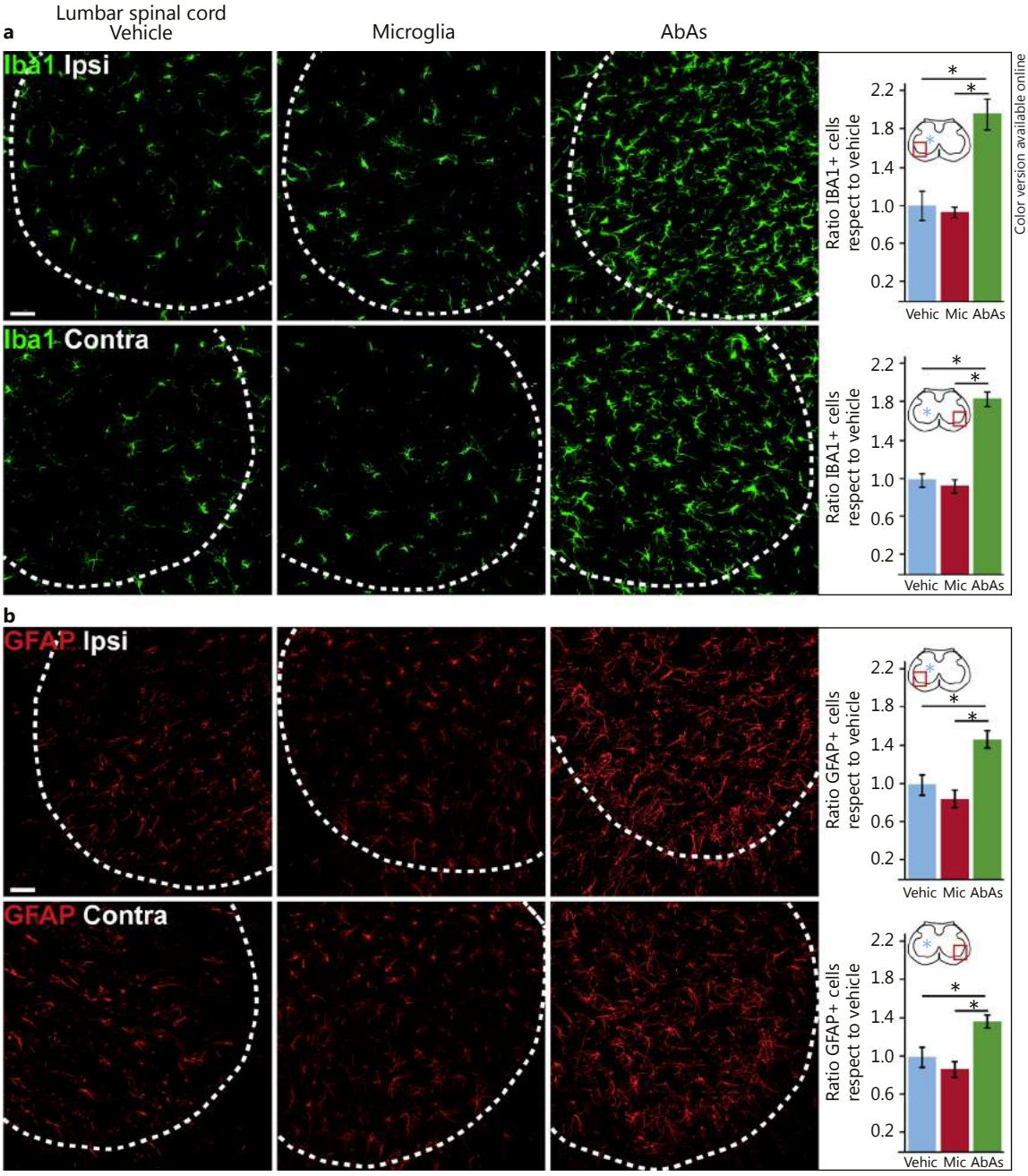

Fig. 3. AbA transplantation induces gliosis in the lumbar cord. Seven days after the transplantation of AbAs, neonatal microglia, or vehicle, microgliosis and astrocytosis were assessed in the lumbar cord segments adjacent to the transplantation sites. White dotted lines delimit grey and white matter. **a** Confocal images: Iba1+ microglia in ipsilateral (Ipsi) and contralateral (Contra) ventral horns. The graphs show the Iba1+ cell quantitation in different experimental conditions, expressed as the ratio with respect to vehicle. **b** Confocal images: GFAP+ astrocytes in Ipsi and Contra ventral horns. The graphs show the GFAP+ cell quantitation in different experimental conditions, expressed as the ratio with respect to vehicle. Note the significant increase of microglia and astrocytes after the transplantation of AbAs. Data are shown as mean ± SEM. * $p < 0.01$ was considered significant. Scale bars, 50 μm.

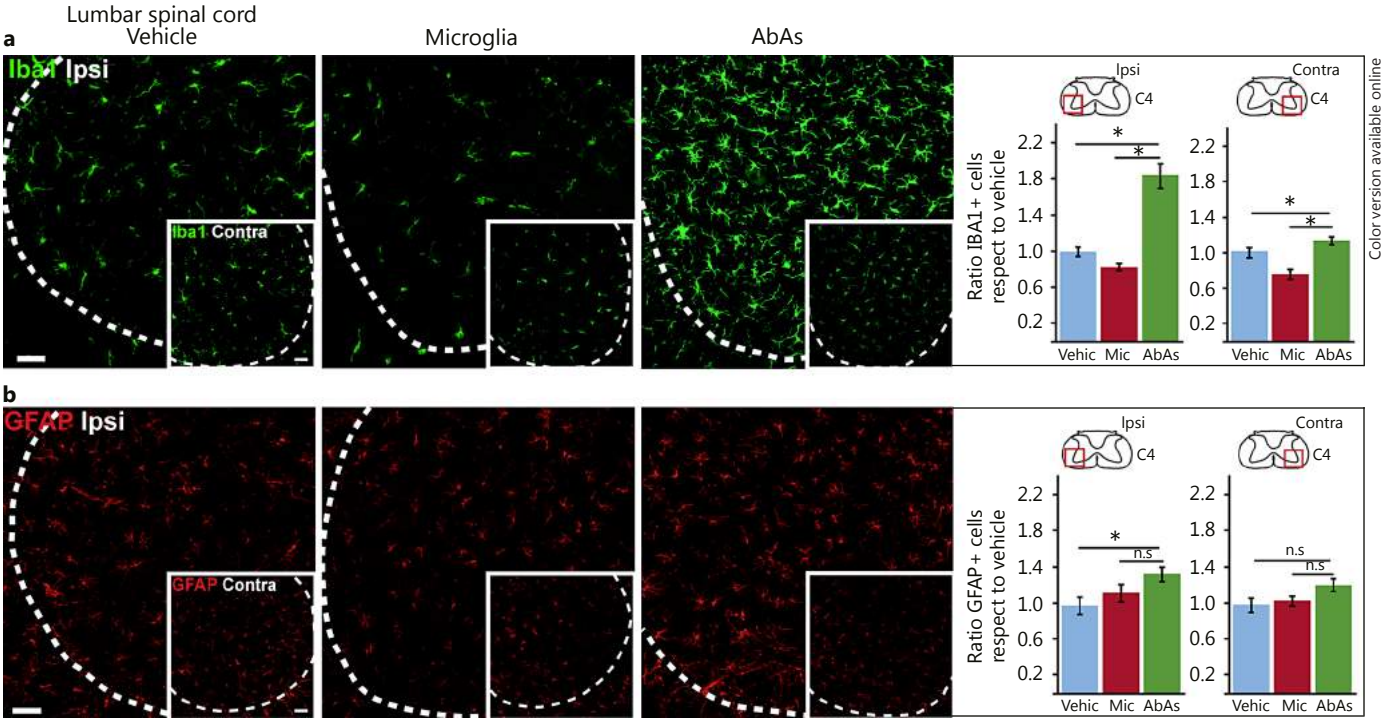

Fig. 4. AbA transplantation induces gliosis in the cervical spinal cord. Microgliosis and astrocytosis were assessed in the cervical cord segments 7 days after the transplantation of AbAs, neonatal microglia, or vehicle in the lumbar cord. White dotted lines delimit grey and white matter. **a** Confocal images: Iba1+ microglia in ipsilateral (Ipsi) and contralateral (Contra, inset) ventral horns. The graphs show the Iba1+ cell quantitation in different experimental conditions, expressed as the ratio with respect to vehicle. **b** Confocal images: GFAP+ astrocytes in Ipsi and Contra (inset) ventral horns. The graphs show the GFAP+ cell quantitation in different experimental conditions, expressed as the ratio with respect to vehicle. Data are shown as mean ± SEM. * $p < 0.01$ was considered significant. Scale bars, 50 μm.

folded SOD1, but not with normally folded hSOD1, suggesting that misfolded SOD1 accumulated in the original transplanted cells.

Transplanted AbAs Induced Host Microgliosis and Astrogliosis

One week after transplantation, AbAs appeared surrounded by numerous Iba1+ microglia (Fig. 2a). The Iba1 cell density was highest at the proximity of AbAs but also extended along the needle track. To determine whether host microglia and astrocyte activation was specifically induced by AbA transplantation, control experiments were performed by transplanting neonatal wild-type microglia or cell-free culture medium into a condition similar to that used for the AbA transplants. As shown in Figure 2a (inset), no comparable microgliosis was observed in either control conditions. A subpopulation of CD68+, isolectin+, or MHC ll host phagocytic microglia/macrophages was found mainly infiltrating the core of transplanted AbAs and interacting with pkh26+/misfolded SOD1+ cells (Fig. 2b). Some CD68+ and MHC ll+ phagocytic cells displayed immunoreactivity to pkh26, suggesting the engulfment of the grafted AbAs (Fig. 2b, inset).

In addition, transplanted AbAs were surrounded by GFAP+ reactive astrocytes bearing long processes that were restricted to the surroundings of the transplant, without penetrating the transplant core. GFAP+ reactive astrocytes also expressed S100β and nestin (Fig. 2c). Surprisingly, AbAs did not display immunoreactivity to GFAP, S100 β, or Iba1, which is in agreement with their dedifferentiation after several passages [7].

Focal Lumbar Cord AbA Transplantation Induced Extensive Microgliosis along the Spinal Cord

We analyzed whether focal AbA transplantation in the lumbar cord could induce gliosis in adjacent lumbar segments and more distally at the cervical cord level. Figure

3 shows lumbar spinal cord segments adjacent to transplantation sites. The AbA transplants, but not the neonatal microglia and vehicle injections, induced marked host microgliosis and astrocytosis bilaterally, with respect to the injection site. The numbers of microglia and astrocytes induced by AbAs increased by 85 and 40%, respectively, when compared with controls.

We analyzed whether focal AbA transplantation in the lumbar cord could induce gliosis at the cervical cord level. Compared with control transplants, AbAs elicited a robust Iba1+ microglial reaction in the grey matter of the cervical spinal cord, both at the ipsilateral and contralateral sides of the injection (Fig. 4a). Microglia cells were consistently larger with hypertrophic cell bodies, with respect to controls, with the number increasing by 80% on the ipsilateral side (Fig. 4a). Compared to controls, the increase in GFAP+ astrocytes in the cervical cord was moderate, and was observed only on the ipsilateral side (Fig. 4b).

Transplanted AbAs Induced Ubiquitin Aggregation in Neighboring Motor Neurons

Because AbAs in culture secrete potent soluble factors that kill motor neurons [7], we investigated whether the transplantation of AbAs induces damage to the motor neurons located adjacent to the transplant sites. As observed in Figure 5a, there was no overt loss or change in size of the ventral-horn motor neurons. In contrast, they were consistently surrounded by activated microglia and astrocytes, some displaying active proliferation as assessed by Ki67 expression (Fig. 5b–d). Remarkably, motor neurons in adjacent segments of AbA transplants displayed punctuate ubiquitin aggregates (Fig. 5d), a characteristic early pathological feature of motor neuron degeneration in ALS murine models and humans [15, 16]. Motor neuron ubiquitination or associated exaggerated gliosis was not observed in transplant control conditions (Fig. 5d).

Discussion

Transplanted AbAs derived from adult paralytic $SOD1^{G93A}$ rats initiate an extensive host microglia and astrocytic reactive response in the wild-type rat spinal cord. The AbA-induced neuroinflammatory response propagated rostrally from the lumbar injection site throughout the cervical spinal cord, and was associated with incipient motor neuron damage assessed by ubiquitin aggregation, suggesting that AbAs could be capable of eliciting an ALS-like pathology. While this study only focused on the short-term behavior of AbAs, the possibility exists that engrafted AbAs could continue to proliferate over weeks or months, leading to a more robust pathological motor and/or inflammatory phenotype.

Transplantation of relatively few AbAs into the lumbar cord of nontransgenic rats did not cause extensive damage in the spinal cord or overt motor deficits, suggesting that, for 1 week after the injection, at least, the cells have limited direct neurotoxic activity in the host spinal cord. Rather, most of the transplanted cells remained grouped at the site of injection and showed a limited migratory capacity. Remarkably, they retained their proliferative potential and ability to attract a massive number of Iba1+, CD68+, and lectin+ microglia/macrophages as well as GFAP+ astrocytes to the site of injection and adjacent regions. This scenario strongly suggests that engrafted AbAs express or produce factors that promote microglia proliferation and migration, and astrocyte activation. AbA-induced neuroinflammation was specific because it was not reproduced by control experiments using transplants of wild-type neonatal microglia or cell-free culture medium. Our results are in agreement with previous studies showing neuroinflammation and motor neuron death induced by spinal cord transplantation of glial-restricted precursors bearing $SOD1^{G93A}$ [14, 17, 18]. Further work is needed to determine whether $SOD1^{G93A}$ AbAs can also induce motor neuron death if transplants are left for longer.

We found that focal AbA transplantation into the lumbar spinal cord induced extensive microgliosis, not only at the grafting site but also in upper segments of the spinal cord. The magnitude of AbA-induced microglia activation suggests an exceptional ability of AbAs to boost neuroinflammation. Although the identification of specific inflammatory factors secreted by AbAs was beyond the objective of this study, we speculate that colony-stimulating factor (M-CSF) and interleukin (IL)-34 are among the proteins potentially secreted by AbAs. We have previously shown that aberrant microglial cells from symptomatic ALS rats are responsive to M-CSF through the tyrosine kinase receptor CSF-1R [10]. Accordingly, the pharmacological inhibition of CSF-1R decreases microglia reactivity and extends the life span of ALS mice [10, 19]. Astrocytes are another major source of M-CSF and IL-34, both factors being potent agonists of the CSF-1R [20, 21]. In support of this hypothesis, previous studies have shown that the intraperitoneal administration of M-CSF to ALS mice induced microglia proliferation, also exacerbating disease progression [22]. Monocyte chemoattractant pro-

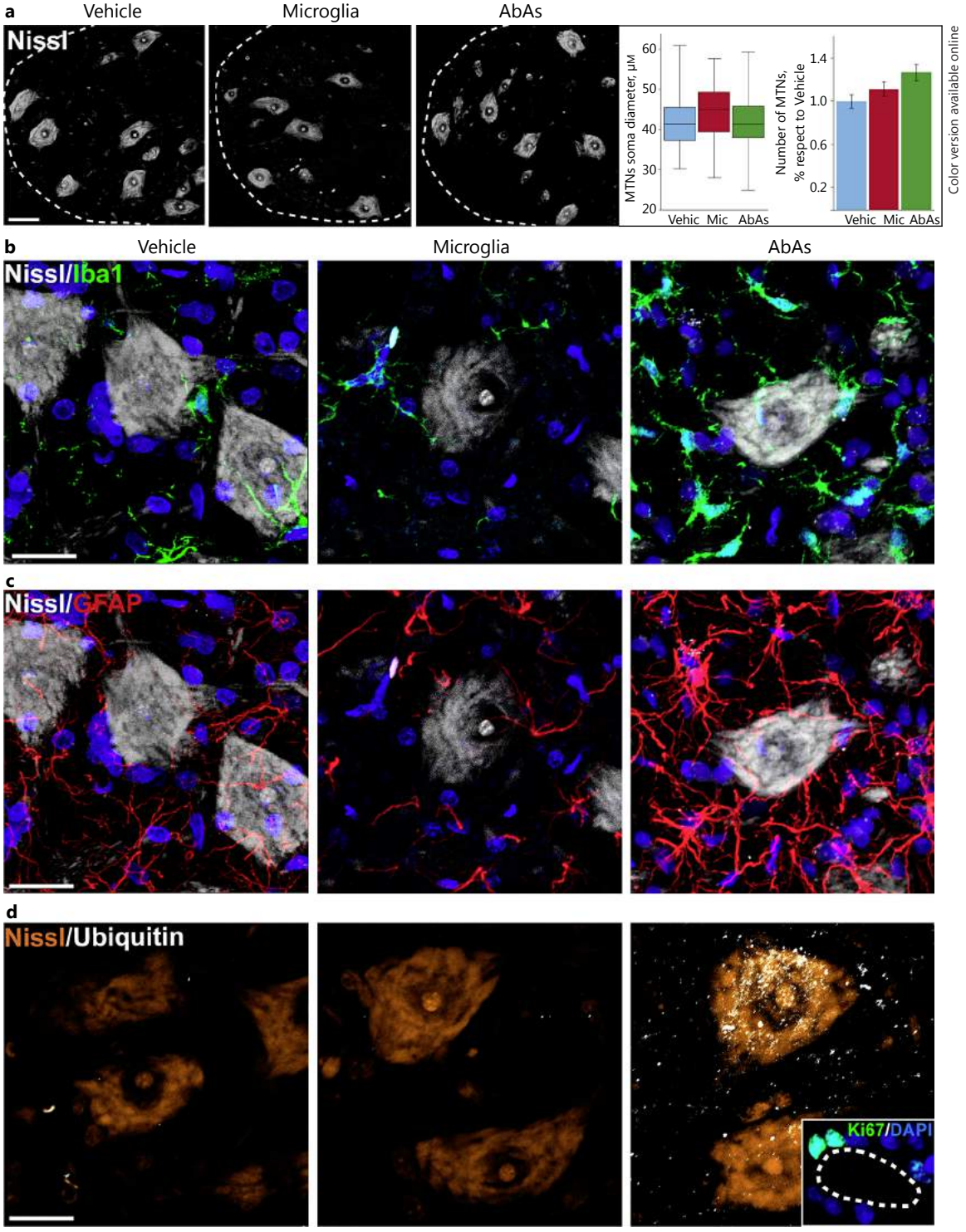

Fig. 5. AbA transplantation induces incipient motor neuron damage. Motor neuron morphology and gliosis were analyzed in the ventral horns at the level of the transplantation site. **a** Representative confocal images: motor neuron morphology. The graphs (right) show the size and comparative number of motor neurons with respect to the vehicle condition. Representative confocal images show Iba1+ microgliosis (**b**) and GFAP+ astrocytes (**c**) surrounding the motor neurons. **d** Representative confocal images: ubiquitin+ aggregates inside motor neuron somas in rats with transplanted AbAs. **Inset** Proliferating Ki67+ cells that surround motor neurons in the AbAs condition. Few or no Ki67+ cells were detected in transplanted controls. White dotted lines delimit the motor neuron somas. Scale bars, 20 µm.

tein-1 (MCP-1) is another factor influencing microgliosis activation that could be secreted by AbAs. MCP-1 is increased in the cerebrospinal fluid and serum of ALS patients, being mainly expressed in glial cells [23, 24]. Finally, misfolded SOD1 could be a major protein secreted by AbAs, activating innate immunity responses. Misfolded SOD1 could be secreted in exosomes from AbAs, as is the case for primary transgenic astrocytes [25], thus initiating an additional pathological mechanism.

One unexpected finding of our study was the accumulation of misfolded SOD1, but no normally folded protein, in cells that were originally transplanted as indicated by their retention of dye pkh26. Changes in SOD1 folding may be associated with cell damage or stress, affecting a subpopulation of transplanted cells. AbAs forming misfolded SOD1 may have a relevant pathogenic role in ALS pathology, both in familial and sporadic cases [26, 27], generating the aggregated template for massive SOD1 aggregation. Furthermore, recent studies showed that aggregated hSOD1 species can spread from cell to cell in culture systems, and even transmit prion-like disease when inoculated into the spinal cord [28–30]. However, spreading SOD1 aggregation is not transmitted from a misfolded human SOD1 template to the rodent wild-type SOD1 [31], thus discarding a possible transmission route from the transplanted AbAs to the host cells in our experimental setting.

Conclusion

The study addressed a significant aspect of ALS pathogenesis by further characterizing the biology of AbAs that emerge during the progression of paralysis in the rat model of ALS expressing $SOD1^{G93A}$. We provide evidence of the significant inflammatory and neurotoxic potential of AbAs when they are focally engrafted into the lumbar spinal cord of wild-type rats. Experimental data indicate that AbA-induced microgliosis and astrocytosis extended bilaterally over the spinal cord, suggesting a mechanism likely mediated by the secretion of soluble factors. Transplants of AbAs may also constitute a valuable model to study the generation, prion-like transmission and proinflammatory activity of misfolded SOD1 as well as to screen for novel drugs for the treatment of ALS

Acknowledgments

This work was supported by Institut Pasteur de Montevideo – FOCEM Mercosur (COF 03/11), the Amyotrophic Lateral Sclerosis Association (00482), Agencia Nacional de Investigación e Innovación (ANII), Programa de Desarrollo de las Ciencias Básicas (PEDECIBA) and Sistema Nacional de Investigadores (SNI). We want to thank the staff from the Departamento de Histología y Embriología and animal facility (URBE) of the Facultad de Medicina, UdelaR, Montevideo, Uruguay, and also the staff from the Transgenic and Experimental Animal Unit from Institut Pasteur de Montevideo.

Statement of Ethics

All procedures performed in studies involving animals were in accordance with the ethical standards of the institution at which the studies were conducted.

Disclosure Statement

The authors have no conflicts of interest.

Author Contributions

S.I., E.T., N.L., H.P., and L.B. designed the study. S.I., E.T., R.B.-N., N.L., H.P., and V.V. performed experiments. S.I., E.T., J.S.B., and L.B. analyzed data. S.I., E.T., J.S.B., and L.B. prepared the manuscript. All authors contributed to discussion of the results and edited and approved the final version.

References

1 Rowland LP, Shneider NA: Amyotrophic lateral sclerosis. N Engl J Med 2001;344:1688–1700.
2 Rosen DR, et al: Mutations in Cu/Zn superoxide dismutase gene are associated with familial amyotrophic lateral sclerosis. Nature 1993;362:59–62.
3 Gurney ME, et al: Motor neuron degeneration in mice that express a human Cu,Zn superoxide dismutase mutation. Science 1994;264:1772–1775.
4 Howland DS, et al: Focal loss of the glutamate transporter EAAT2 in a transgenic rat model of SOD1 mutant-mediated amyotrophic lateral sclerosis (ALS). Proc Natl Acad Sci USA 2002;99:1604–1609.
5 Boillee S, Vande Velde C, Cleveland DW: ALS: a disease of motor neurons and their nonneuronal neighbors. Neuron 2006;52:39–59.
6 Barbeito LH, et al: A role for astrocytes in motor neuron loss in amyotrophic lateral sclerosis. Brain Res Brain Res Rev 2004;47:263–274.
7 Diaz-Amarilla P, et al: Phenotypically aberrant astrocytes that promote motoneuron damage in a model of inherited amyotrophic lateral sclerosis. Proc Natl Acad Sci USA 2011;108:18126–18131.
8 Trias E, et al: Significance of aberrant glial cell phenotypes in pathophysiology of amyotrophic lateral sclerosis. Neurosci Lett 2017;636:27–31.

9 Trias E, et al: Phenotypic transition of microglia into astrocyte-like cells associated with disease onset in a model of inherited ALS. Front Cell Neurosci 2013;7:274.
10 Trias E, et al: Post-paralysis tyrosine kinase inhibition with masitinib abrogates neuroinflammation and slows disease progression in inherited amyotrophic lateral sclerosis. J Neuroinflamm 2016;13:177.
11 Ni M, Aschner M: Neonatal rat primary microglia: isolation, culturing, and selected applications. Curr Protoc Toxicol 2010, DOI: 10.1002/0471140856.
12 Saneto RP, De Vellis J: Neuronal and glial cells: cell culture of the central nervous system. In: Turner AJ, Brachelard HS, editors. Neurochemistry: A Practical Approach. Washington, DC: Oxford University Press; 1987. pp. 27–63.
13 Cassina P, et al: Peroxynitrite triggers a phenotypic transformation in spinal cord astrocytes that induces motor neuron apoptosis. J Neurosci Res 2002;67:21–29.
14 Papadeas ST, et al: Astrocytes carrying the superoxide dismutase 1 (SOD1G93A) mutation induce wild-type motor neuron degeneration in vivo. Proc Natl Acad Sci USA 2011;108:17803–17808.
15 Leigh PN, et al: Ubiquitin-immunoreactive intraneuronal inclusions in amyotrophic lateral sclerosis. Morphology, distribution, and specificity. Brain 1991;114:775–788.
16 Huang C, et al: Mutant TDP-43 in motor neurons promotes the onset and progression of ALS in rats. J Clin Invest 2012;122:107–118.
17 Haidet-Phillips AM, et al: Astrocytes from familial and sporadic ALS patients are toxic to motor neurons. Nat Biotechnol 2011;29:824–828.
18 Ramirez-Jarquin UN, et al: Chronic infusion of SOD1G93A astrocyte-secreted factors induces spinal motoneuron degeneration and neuromuscular dysfunction in healthy rats. J Cell Physiol 2017;232:2610–2615.
19 Martinez-Muriana A, et al: CSF1R blockade slows the progression of amyotrophic lateral sclerosis by reducing microgliosis and invasion of macrophages into peripheral nerves. Sci Rep 2016;6:25663.
20 Frei K, et al: Production of macrophage colony-stimulating factor by astrocytes and brain macrophages. J Neuroimmunol 1992;40:189–195.
21 Mizuno T, et al: Interleukin-34 selectively enhances the neuroprotective effects of microglia to attenuate oligomeric amyloid-beta neurotoxicity. Am J Pathol 2011;179:2016–2027.
22 Gowing G, et al: Macrophage colony stimulating factor (M-CSF) exacerbates ALS disease in a mouse model through altered responses of microglia expressing mutant superoxide dismutase. Exp Neurol 2009;220:267–275.
23 Baron P, et al: Production of monocyte chemoattractant protein-1 in amyotrophic lateral sclerosis. Muscle Nerve 2005;32:541–544.
24 Wilms H, et al: Intrathecal synthesis of monocyte chemoattractant protein-1 (MCP-1) in amyotrophic lateral sclerosis: further evidence for microglial activation in neurodegeneration. J Neuroimmunol 2003;144:139–142.
25 Basso M, et al: Mutant copper-zinc superoxide dismutase (SOD1) induces protein secretion pathway alterations and exosome release in astrocytes: implications for disease spreading and motor neuron pathology in amyotrophic lateral sclerosis. J Biol Chem 2013;288:15699–15711.
26 Kato S, et al: New consensus research on neuropathological aspects of familial amyotrophic lateral sclerosis with superoxide dismutase 1 (SOD1) gene mutations: inclusions containing SOD1 in neurons and astrocytes. Amyotroph Lateral Scler Other Motor Neuron Disord 2000;1:163–184.
27 Sheng Y, et al: SOD1 aggregation and ALS: role of metallation states and disulfide status. Curr Top Med Chem 2012;12:2560–2572.
28 Ayers JI, et al: Prion-like propagation of mutant SOD1 misfolding and motor neuron disease spread along neuroanatomical pathways. Acta Neuropathol 2016;131:103–114.
29 Ayers JI, et al: Experimental transmissibility of mutant SOD1 motor neuron disease. Acta Neuropathol 2014;128:791–803.
30 Grad LI, Fernando SM, Cashman NR: From molecule to molecule and cell to cell: prion-like mechanisms in amyotrophic lateral sclerosis. Neurobiol Dis 2015;77:257–265.
31 Grad LI, et al: Intermolecular transmission of superoxide dismutase 1 misfolding in living cells. Proc Natl Acad Sci USA 2011;108:16398–16403.

Publicación 4

Post-paralysis tyrosine kinase inhibition with masitinib abrogates neuroinflammation and slows disease progression in inherited amyotrophic lateral sclerosis

Emiliano Trias, Sofía Ibarburu, Romina Barreto-Núñez, Joël Babdor, Thiago T. Maciel, Matthias Guillo, Laurent Gros, Patrice Dubreuil, Pablo Díaz-Amarilla, Patricia Cassina, Laura Martínez-Palma, Ivan C. Moura, Joseph S. Beckman, Olivier Hermine, and Luis Barbeito

Resumen

El descubrimiento del origen de las células gliales aberrantes abrió nuevas oportunidades terapéuticas para poder modular farmacológicamente el microambiente degenerativo que se establece en la médula espinal de las ratas SOD1^{G93A}. Uno de los principales receptores que regula la maduración y activación de la microglía, es el receptor 1 del factor estimulante de colonias (CSF-1R)[117]. Este receptor pertenece a la familia de los receptores de tirosin-quinasas de Clase III, entre los que se encuentran además el receptor del factor de crecimiento derivado de plaquetas (PDGF-R, subunidades α y β), el receptor del factor de crecimiento de células madre/mastocitos (CD117 o c-Kit) y el receptor de tirosin-quinasa de tipo *fms* (CD135 o FLT-3)[118,119]. La inhibición farmacológica o genética del receptor CSF-1R en animales es suficiente para, prácticamente, depletar las células microgliales que pueblan el SNC. De esta manera, el receptor de la microglía, CSF-1R se convierte en un blanco interesante para intentar bloquear la proliferación de la microglía durante la fase sintomática de la ELA y la aparición de las células gliales aberrantes en el modelo de rata de SOD1^{G93A}. Fue por esto, que comenzamos a trabajar con un inhibidor de la clase III de receptores de tirosin-quinasas, el masitinib. Esta droga es un potente inhibidor de c-Kit pero también inhibe de muy buena manera CSF-1R y PDGF-R. Nuestra hipótesis establece que el masitinib es capaz de modular la proliferación y activación de células gliales aberrantes en cultivo. Además, utilizando una aproximación terapéutica, la administración de masitinib a ratas sintomáticas, podría inhibir la microgliosis masiva que ocurre durante la fase sintomática de la enfermedad, enlenteciendo, de esta manera,

la aparición de las células gliales aberrantes, protegiendo a las motoneuronas y enlenteciendo la progresión de la ELA.

Resultados

- El masitinib inhibe la proliferación de la microglía aberrante dependiente de CSF1, aislada de la médula espinal de ratas SOD1 sintomáticas. Dosis incrementales de masitinib 0.1 – 1 μM, inhiben significativamente la proliferación y la capacidad migratoria de la microglía adulta, incluso cuando la proliferación es estimulada utilizando 30 ng/ml de CSF1.
- El tratamiento con el inhibidor de tirosin-quinasas bloquea el perfil pro-inflamatorio que muestra la microglía adulta aberrante en cultivo, disminuyendo los niveles de expresión de IL-1β, Cox2, IL6, TNFα e iNOS. Además, el tratamiento con masitinib previene significativamente la transición fenotípica que sufre el cultivo de microglía luego de 15 días en cultivo. Las pocas células que logran una transición fenotípica no poseen una tasa proliferativa significativa y mueren a los pocos días.
- Luego de comenzado los síntomas clínicos (onset) las ratas SOD1 fueron administradas diariamente por vía oral (gavage) con 30 mg/kg de masitinib. Luego de 20 días de tratamiento los signos histopatológicos fueron analizados por inmunohistoquímica.
    - El tratamiento con masitinib durante 20 días previene de forma significativa la emergencia de las células gliales aberrantes GFAP+/S100β+ en el microambiente inflamatorio que rodea a las motoneuronas en degeneración.
    - Cuando la médula espinal de ratas $SOD1^{G93A}$ es cultivada para obtener células gliales aberrantes, luego de 20 días de tratamiento con masitinib, es posible aislar un bajo número de células microgliales en comparación con los animales tratados con vehículo. Las pocas células que se obtienen no poseen una capacidad proliferativa que les permita alcanzar la confluencia ni hacer una transición fenotípica hacia células gliales aberrantes. Las pocas células que logran aislarse mueren en cultivo luego de 10 días.

- El tratamiento durante 20 días con masitinib previene de forma significativa la microgliosis en la médula espinal de las ratas sintomáticas, evidenciado por la marcación para Iba1, CD68 y CD206.
- El masitinib previene la muerte masiva de motoneuronas que ocurre entre el comienzo de los síntomas y la fase terminal de la enfermedad. Además, previene la atrofia de los somas neuronales de forma significativa.

Utilizando la misma aproximación experimental, realizamos un ensayo pre-clínico administrando ratas $SOD1^{G93A}$ desde el día que comienzan los síntomas motores, con 30 mg/kg de masitinib hasta la fase terminal de la enfermedad. El tratamiento con el inhibidor de tirosin-quinasas retrasó de forma significativa la progresión de la ELA, en aproximadamente un 40 %.

Conclusiones

Nuestros resultados muestran que la inhibición del receptor de tirosin-quinasas CSF-1R con masitinib es capaz de bloquear el fenotipo de glías aberrantes, inhibir la neuroinflamación, retrasando en forma significativa la progresión de la enfermedad, un resultado que no tiene precedentes en otros ensayos pre-clínicos que utilizan modelos animales de ELA. Esto posiciona al masitinib como un potencial fármaco para el tratamiento de la ELA.

Cabe destacar que, basado en nuestros estudios pre-clínicos llevados a cabo en el modelo de rata $SOD1^{G93A}$, la empresa ABScience, realizó un ensayo clínico fase 3 en 400 pacientes, utilizando el masitinib como terapia para la ELA asociado con el fármaco riluzole. Los resultados preliminares de este ensayo sugieren que el masitinib actúa enlenteciendo la progresión de la parálisis en un sub-grupo mayoritario de pacientes.

Trias et al. Journal of Neuroinflammation (2016) 13:177
DOI 10.1186/s12974-016-0620-9

Journal of Neuroinflammation

RESEARCH Open Access

Post-paralysis tyrosine kinase inhibition with masitinib abrogates neuroinflammation and slows disease progression in inherited amyotrophic lateral sclerosis

Emiliano Trias[1], Sofía Ibarburu[1†], Romina Barreto-Núñez[1†], Joël Babdor[2,3,4,5], Thiago T. Maciel[2,3,4,5,6,7], Matthias Guillo[2,3,4,5], Laurent Gros[8], Patrice Dubreuil[7,8,9], Pablo Díaz-Amarilla[10], Patricia Cassina[11], Laura Martínez-Palma[11], Ivan C. Moura[2,3,4,5,6,7], Joseph S. Beckman[12], Olivier Hermine[2,3,4,5,6,7,8,13,14*] and Luis Barbeito[1*]

Abstract

Background: In the SOD1^{G93A} mutant rat model of amyotrophic lateral sclerosis (ALS), neuronal death and rapid paralysis progression are associated with the emergence of activated aberrant glial cells that proliferate in the degenerating spinal cord. Whether pharmacological downregulation of such aberrant glial cells will decrease motor neuron death and prolong survival is unknown. We hypothesized that proliferation of aberrant glial cells is dependent on kinase receptor activation, and therefore, the tyrosine kinase inhibitor masitinib (AB1010) could potentially control neuroinflammation in the rat model of ALS.

Methods: The cellular effects of pharmacological inhibition of tyrosine kinases with masitinib were analyzed in cell cultures of microglia isolated from aged symptomatic SOD1^{G93A} rats. To determine whether masitinib prevented the appearance of aberrant glial cells or modified post-paralysis survival, the drug was orally administered at 30 mg/kg/day starting after paralysis onset.

Results: We found that masitinib selectively inhibited the tyrosine kinase receptor colony-stimulating factor 1R (CSF-1R) at nanomolar concentrations. In microglia cultures from symptomatic SOD1^{G93A} spinal cords, masitinib prevented CSF-induced proliferation, cell migration, and the expression of inflammatory mediators. Oral administration of masitinib to SOD1^{G93A} rats starting after paralysis onset decreased the number of aberrant glial cells, microgliosis, and motor neuron pathology in the degenerating spinal cord, relative to vehicle-treated rats. Masitinib treatment initiated 7 days after paralysis onset prolonged post-paralysis survival by 40 %.

Conclusions: These data show that masitinib is capable of controlling microgliosis and the emergence/expansion of aberrant glial cells, thus providing a strong biological rationale for its use to control neuroinflammation in ALS. Remarkably, masitinib significantly prolonged survival when delivered after paralysis onset, an unprecedented effect in preclinical models of ALS, and therefore appears well-suited for treating ALS.

Keywords: ALS, Aberrant glial cells, Neurodegeneration, Masitinib, M-CSF

* Correspondence: ohermine@gmail.com; barbeito@pateur.edu.uy
†Equal contributors
[2]Imagine Institute, Hôpital Necker, 24 boulevard du Montparnasse, 75015 Paris, France
[1]Institut Pasteur de Montevideo, Mataojo 2020, Montevideo 11.400, Uruguay
Full list of author information is available at the end of the article

Background

Amyotrophic lateral sclerosis (ALS) is a paralytic neurodegenerative disease characterized by the progressive degeneration of upper and lower motor neurons. Survival after diagnosis varies between 1 and 5 years or more, largely determined on the rate of spread of motor neuron pathology. Paralysis progression in rodent models of ALS appears to be modulated by glial cells that proliferate and express inflammatory mediators in the degenerating spinal cord [1–4]. In the SOD1^{G93A} mutant rat model of ALS, a rapid spread of paralysis is associated with marked glial cell activation and the emergence of aberrant glial cells that actively proliferate around degenerating motor neurons [4, 5]. Furthermore, aberrant glial cells display a marked neurotoxic potential on cultured motor neurons [4], suggesting that they might directly contribute to the rapid spread of paralysis of ALS rats. It remains unknown, however, whether pharmacologically downregulation of aberrant glial cells could slow paralysis progression in the rat model of ALS.

We have theorized that aberrant glial cells proliferating in the ALS spinal cord could be sensitive to tyrosine kinase inhibitors that target the family of type III growth factor receptors including PDGF-R, c-Kit, FLT3, and CSF-1R. These receptors synergistically signal cell proliferation and the migration of cancer and hematopoietic cells, including macrophages [6]. In particular, while M-CSF/CSF-1R signaling is critical for the mononuclear phagocytic system [7, 8], a recent report indicates that damaged motor neurons induce the expansion of spinal cord microglia by expressing M-CSF [9]. Thus, we have explored whether the inhibition of CSF-1R and related kinase receptors could modulate neuroinflammation and slow disease spreading in an inherited rat model of ALS.

Among candidate tyrosine kinase inhibitors, masitinib (AB1010) was found to be a highly selective kinase inhibitor [10, 11] and shown to prevent central nervous system (CNS) neuroinflammation in multiple sclerosis [12], stroke [13], and Alzheimer's disease [14]. Thus, we aimed to characterize the effects of masitinib on cultured aberrant glial cells and determine its therapeutic potential after oral administration to SOD1^{G93A} rats. Because aberrant glial cells emerge only after paralysis onset [4], the drug treatment was initiated following overt disease onset to better simulate the clinical condition of ALS patients. We found that masitinib inhibited glial cell activation in SOD1^{G93A} rats and prolonged survival, indicating a promising therapeutic approach to ALS.

Methods

Animals

Male SOD1^{G93A} progeny were used for further breeding to maintain the line. Rats were housed in a centralized animal facility with a 12-h light-dark cycle with ad libitum access to food and water. Perfusion with fixatives was performed under 90 % ketamine—10 % xylazine anesthesia and all efforts were made to minimize animal suffering, discomfort, or stress. All procedures using laboratory animals were performed in accordance with the national and international guidelines and were approved by the Institutional Animal Committee for animal experimentation. Male hemizygous NTac:SD-TgN (SOD1-^{G93A})L26H rats (Taconic), originally developed by Howland et al. [15], were bred locally by crossing with wild-type nontransgenic Sprague-Dawley female rats.

Determination of disease onset and end-stage

All rats were weighed and evaluated for motor activity daily. Disease onset was determined for each animal when pronounced muscle atrophy was accompanied by abnormal gait, typically expressed as subtle limping or dragging of one hind limb. End-stage was defined by a lack of righting reflexes or the inability to reach food and water.

Masitinib post-paralysis survival trial

Only transgenic rats showing weakness and gait alterations in hind limbs as first clinical sign were selected for masitinib treatment studies. Male and female rats were divided randomly into the masitinib or vehicle-treated groups. Masitinib mesylate (AB1010) freshly prepared in drinking sterilized water was administrated daily at a dose of 30 mg/kg using a curved stainless steel gavage needle with 3-mm ball tip. Dosing was defined in accordance to previous studies in a rat model of stroke that was shown to be safe for chronic treatments [13]. Rats were treated from day 1 or day 7 post-paralysis during 20 days or until end-stage, when they were euthanized.

Immunohistochemical staining of rat spinal cords

After 20 days of treatment using 30 mg/kg/day of masitinib, starting after paralysis onset, animals were deeply anesthetized and transcardial perfusion was performed with 0.9 % saline and 4 % paraformaldehyde in 0.1 M PBS (pH 7.2–7.4). Fixed spinal cord was removed, post-fixed by immersion for 24 h, and then transverse sectioned (30 μm) in a Leica cryostat. Serial sections were collected in 100 mM PBS for immunohistochemistry. Free-floating sections were permeabilized for 30 min at room temperature with 0.3 % Triton X-100 in PBS, passed through washing buffered solutions, blocked with 5 % BSA:PBS for 1 h at room temperature, and incubated overnight at 4 °C in a solution of 0.3 % Triton X-100 and PBS containing the primary antibodies, rabbit anti-GFAP (1:500, Sigma), mouse anti-S100β (1:400, Sigma), rabbit anti-Iba1 (1:300, abcam), rabbit anti-

CD206 (1:300 abcam), mouse anti-CD68 (1:200, abcam), mouse anti-ChAT (choline acetyltransferase) (1:300, Millipore). After washing, sections were incubated in 1:1000-diluted secondary antibodies conjugated to Alexa Fluor 488 and/or Alexa Fluor 633 (1:1000, Invitrogen). Antibodies were detected by confocal microscopy using a confocal LEICA TCS-SP5-DMI6000 or a confocal ZEISS LSM 780.

Analysis of glial cells in the lumbar spinal cord of hind limb symptomatic rats

The number of aberrant glial cells co-expressing the astrocytic markers GFAP and S100β or the microglia markers Iba-1, CD206, and CD68 were assessed by counting the respective positive cells for the different markers in gray matter from the lumbar cord of $SOD1^{G93A}$ asymptomatic or symptomatic rats that had been treated with either vehicle or masitinib. The analysis was performed manually in at least 20 histological sections per animal (four different rats for each condition) using the cell counter tool of the ImageJ software. For aberrant glial cell counting, values were expressed as the number of GFAP+/S100β+ cells in each ventral horn of the spinal cord in masitinib-treated rats relative to vehicle-treated rats. For microgliosis analysis, the number of Iba1+, CD206+, or CD68+ cells was assessed via manual counting using the ImageJ software tools. Only microglia cells present in the grey matter of the ventral horn of the spinal cord were taken into consideration. Statistical studies were performed using statistical tools of the free Software PAST3. Descriptive statistics were used for each group, and Kruskal-Wallis analysis or one-way ANOVA, followed by Scheffé post hoc comparison if necessary, was used among groups. All results are presented as mean ± SEM, with $p < 0.01$ considered significant.

Analysis of microgliosis spreading along the degenerating spinal cord of $SOD1^{G93A}$ rats

The spinal cord of hind limb symptomatic rats was dissected at thoracic and cervical levels. Three masitinib-treated rats were compared with three vehicle-treated rats. As previously described, immunohistochemistry was assessed to determine the levels of microgliosis by Iba1 detection. At least ten different 30 μm sections of each rat were visualized using a LEICA TCS-SP5-DMI6000 confocal microscope.

Analysis of motor neuron number and size

The number of motor neurons expressing ChAT was assessed by counting the positive cells in the gray matter of the lumbar spinal cord of non-transgenic compared with symptomatic $SOD1^{G93A}$, vehicle-, and masitinib-treated rats. Motor neuron counting was based on a stereological approach as previously reported [16]. Briefly, ChAT positive cells were quantified on five 30 μm sections taken 300 μm apart from the ventral horn, comparing the cell numbers in Rexed laminae VII and IX, which display low and high density of large motor neurons, respectively. Results are presented as mean ± SEM, with $p < 0.01$ considered significant. The longest axis (length) of each soma was taken into consideration to quantify the mean size of motor neuron soma. The analysis was performed manually in at least 25 histological sections per animal (four different rats for each condition) using the cell counter tool of the ImageJ software. Results are presented as median ± SD, with $p < 0.01$ considered significant. Statistical studies were performed using statistical tools of the free Software PAST3. Descriptive statistics were used for each group, and Kruskal-Wallis analysis or one-way ANOVA, followed by Scheffé post hoc comparison if necessary, was used among groups.

Microglia cell cultures from symptomatic $SOD1^{G93A}$ rats

Microglial cells were obtained from a primary culture adult spinal cord of symptomatic $SOD1^{G93A}$ rats according to the procedures described by Trias et al. [5] with minor modifications. Briefly, animals were euthanized by administering an overdose of ketamine/xylazine, and the spinal cord was dissected on ice. After the meninges were removed, the spinal cord was chopped finely and dissociated with 0.25 % trypsin in calcium-free buffer for 5 min at 37 °C. Trypsin treatment was stopped by adding DMEM/10 % (vol/vol) FBS in the presence of 50 μg/mL DNaseI and mechanical disaggregation by repeated pipetting. The resulting extract was passed through an 80-μm mesh to eliminate tissue debris and was then spun. The pellet was resuspended in culture medium [DMEM/10 % (vol/vol) FBS, Hepes (3.6 g/L), penicillin (100 IU/mL), and streptomycin (100 μg/mL)] and was then plated in a 24-multiwell culture dish. Culture medium was removed after 24 h and subsequently replaced every 24 or 48 h depending on the procedure.

Microglia migratory capacity assay

Primary cultures were plated in high-density 4-multiwell plates during 4 days. After that, and when cells already reached confluence, media was changed to DMEM-0.5 % FBS, thereby, significantly reducing the proliferation rate. A scratch was then made in the monolayer using a 1000 μL tip, and cells were treated with increasing doses of masitinib in DMSO (used as vehicle in control-treated cells). Post-scratch pictures were taken at 24 h using a bright field NIKON microscope attached to a Canon HD camera, and cells that invaded the scratch were counted manually in at least 12 different pictures (three different rats were cultured for this

experiment, $n = 3$) using the cell counter tool of ImageJ software.

Proliferation assay induced by macrophages-colony stimulating factor (M-CSF)

Cells were isolated as described above from the three different symptomatic rat spinal cords and plated in 24-multiwell dishes during 24 h in low serum, DMEM-0.5 % FBS. Cells were then treated with 30 ng/mL of rat M-CSF in PBS-0.1 % BSA (vehicle-treated cells were treated with the same amount of PBS-0.1 % BSA). To determine the inhibitory capacity of masitinib against the tyrosine kinase receptor CSF-1R, cells were treated with increasing doses of the drug (0.01–1 μM) in the presence of M-CSF and compared with vehicle-treated cells for which masitinib was substituted with DMSO. In total, three experimental groups were analyzed: control cells (in DMEM-0.5 % FBS + PBS-0.1 % BSA), vehicle-treated cells (DMEM-0.5 % FBS + M-CSF + DMSO), and masitinib-treated cells (DMEM-0.5 % FBS + M-CSF + masitinib). All wells were treated at the same time with 10 μM of BrdU (Sigma). After 24 h, cells were fixed and immunocytochemistry using anti-BrdU antibody was followed. Briefly, cells were washed and fixed with cold methanol during 5 min at 4 °C, then washed with PBS and treated with 2 M of HCl for 30 min. Cells were blocked using 5 % of BSA in PBS for 1 h, and rat anti-BrdU was incubated for 24 h at 4 °C. After that, the primary antibody was removed, washed with PBS three times for 10 min, and goat anti-rat antibody was incubated for 1 h at room temperature. After washing away the secondary antibody, cells were covered in glycerol mounting medium with 1/2000 DAPI dilution and a cover slip (Sigma). Cells were visualized in an epifluorescence microscope Olympus IX81. BrdU+ nuclei were counted and ratio of DAPI to BrdU labeling was compared among groups. Data were analyzed using analyzing tools of ImageJ software and shown as mean ± SEM, with $p < 0.01$ considered significant.

Cultured microglia treated with masitinib

Microglial cells were plated in a 24-multiwell dish during 24 h and floating fat was removed. Masitinib treatment was started at that time and was repeated every 48 h chronically with each media change. Three doses of masitinib diluted in DMSO were tested, 0.1, 0.5, and 1.0 μM. Vehicle cells were treated with the same amount of DMSO as a control. Microphotographs were taken using a phase contrast microscope equipped with a Canon HD camera. Cells were treated during 15 days until cell transformation into monolayers of aberrant astrocyte cells. Quantitative analysis of the cell number every 48 h was assessed using the "cell counter" of the ImageJ Software. The number of cells in the masitinib-treated plates was compared to vehicle-treated ones. Data are shown as mean ± SEM, with $p < 0.01$ considered significant.

Cell cultures from symptomatic SOD1^{G93A} masitinib-treated rats

After 20 days of treatment with 30 mg/kg/day of masitinib, spinal cords were cultured in p35 dishes (three different treated animals were cultured as described previously). Spinal cords from vehicle-treated animals were cultured as controls. After 24 h, floating fat was removed and pictures were taken every 48 h after every change of culture media, using a phase contrast microscope and a Canon HD camera. Pictures were taken during 10 days. Cells were counted using the tool "cell counter" from ImageJ Software. Data is shown as the number of microglia cells/mm^2 in the masitinib-treated rats and compared to vehicle. Kruskal-Wallis analysis was used among groups. Data are shown as mean ± SEM, with $p < 0.01$ considered significant.

Real-time PCR analysis in microglia cell cultures

Three different end-stage symptomatic rat spinal cords were cultured to obtained microglia as described previously [5]. Cells were plated in p60 dishes during 5 days and treated during 72 h with different doses of masitinib (0.5–1 μM) in DMEM-10 % FBS. An estimated 200,000 cells were processed for each mRNA extraction using RNeasy Micro kit (QIAGEN) according to the manufacturer's instructions. mRNA yields were measured on Nanodrop device (Thermo Scientific) and cDNA were obtained from 0.5 μg of RNA (−80 °C), 4 μL of iScript reverse transcription Supermix for RT-qPCR (BIORAD, −20 °C) in a final volume of 20 μL filled with nuclease free water. The Thermo cycler was set as follows: priming 5 min at 25 °C followed by 30 min at 42 °C for reverse transcription and 5′ at 85 °C for RT inactivation. RT-qPCR was performed on reverse transcribed cDNA using SsoAdvanced™ Universal SYBR® Green Supermix (BIO-RAD) on a CFX96 Touch™ real-time PCR detection system. For each well, 5 μL of diluted DNA was added to 20 μL of mix (containing 1 μL of each primer, 12.5 μL of SsoAdvanced™ Universal SYBR® Green Supermix, 5.5 μL of nuclease free water). Each sample was run in duplicate. The cycling parameters were as follows: 30 s at 95 °C then 40 cycles at 95 °C for 10 and 30 s at 60 °C. Cq values were obtained for every cycle. Primers were designed on NCBI Primer-BLAST following the best guidelines to exclude genomic DNA amplification. The analysis was done using BioRad CFX manager 3.1 with a threshold set at 650 RFU corresponding to the amplification curves linear portion. Variations between samples were normalized using two housekeeping genes PGK1 and HPRT. All primers were validated for

specificity and efficiency. Primers were designed on PrimerBlast. All primers were validated with differentiated bone marrow-derived rat macrophages (BMDM) in vitro and selected for specificity and quantitativity before being tested on primary microglia from $SOD1^{G93A}$ rats (only primers achieving quantitatively up to a dilution factor of 500 were kept). The following primers were used: monocyte chemoattractant protein-1 (**MCP-1**) forward 5′-TGT CTC AGC CAG ATG CAG TTA AT-3′; reverse 5′-TCC AGC CGA CTC ATT GGG AT-3′; Interleukin-6 (**IL-6**) forward 5′-TTC TCT CCG CAA GAG ACT TCC-3′; reverse 5′-TCT CCT CTC CGG ACT TGT GAA-3′; tumor necrosis factor alpha (**TNFα**) forward 5′-ATC CGA GAT GTG GAA CTG GC-3′; reverse 5′-TGG GAA CTT CTC CTC CTT GTT G-3′; inducible nitric oxide synthase (**iNOS**) forward 5′-AGC CTA GTC AAC TAC AAG CCC C-3′; reverse 5′-CAT CCT GTG TTG TTG GGC TG-3′; interleukin-1 beta (**IL-1β**) forward 5′-TAG CAG CTT TCG ACA GTG AGG-3′; reverse 5′-CTC CAC GGG CAA GAC ATA GG-3′; cyclooxygenase-2 (**Cox2**) forward 5′-TGT ACT ACG CCT GAG TTT CTG AC-3′; reverse 5′-GGG ATC CGG GAT GAA CTC TC-3′; ionized calcium-binding adaptor molecule 1 (**Iba1**) forward 5′-CAA GGA TTT GCA GGG AGG AAA A-3′; reverse 5′-TTG AAG GCC TCC AGT TTG GAC-3′; transcription factor Spi-1/PU.1 **(PU.1)** forward 5′-GGA GAC AGG CAG CAA GAA GAA G-3′; reverse 5′-CCT TCA TGT CTC CGC TAC GC-3′; hypoxanthine-guanine phosphoribosyl transferase (**HPRT**) forward 5′-GTC ATG TCG ACC CTC AGT CC-3′; reverse 5′-GCA AGT CTT TCA GTC CTG TCC-3′; phosphoglycerate kinase 1 (**PGK1**) forward 5′-GTC GTG ATG AGG GTG GAC TT-3′; reverse 5′-AAC CGA CTT GGC TCC ATT GT-3′.

Kinase inhibition assay

CSF-1R kinase domain (AA 538–972) was expressed as a *N*-terminus 6HN-tagged protein in Sf21 cells using the BacPAK6 baculovirus expression system (Clontech, Mountain View, CA 94043, USA) and purified by Ni^{2+} affinity chromatography. The analysis of the effect of masitinib on CSF-1R kinase activity was assessed with the *HTRF® KinEASE assay* (Cisbio International, Bagnols-sur-Cèze, France) using a biotinylated poly(-Glu_4Tyr) peptide (1 μM) as substrate. Kinase assays were performed at an ATP concentration of 100 μM (CSF-1R Km_{ATP} = 52 μM) in kinase buffer (50 mM HEPES pH 7.5, 5 mM $MgCl_2$, 1 mM $MnCl_2$, 1 mM DTT, 0.01 % Brij-35) for 30 min at room temperature in the presence of various masitinib concentrations (0 to 10 μM). Reactions were stopped by addition of EDTA, and samples were incubated for 1 h with an anti-phospho peptide-Eu^{3+} antibody (emission 620 nm) and streptavidin XL-665 (emission 665 nm) according to manufacturer's instructions. After incubation, the obtained signal is proportional to the concentration of phosphorylated peptide in the sample. All measurements were performed on a BMG Labtech Pherastar FS apparatus. Results are expressed in delta fluorescence (DF) unit defined as follow DF % = [(ratio – ratio blank) / (ratio blank)] × 100, where ratio = (665 nm/620 nm) × 10^4. Each experiment was performed in duplicate and repeated three times.

Statistics analysis and survival curves

Survival curves were compared by Kaplan-Meier analysis with the log-rank test using PAST3 software. Quantitative data were expressed as mean ± SEM and Student's *t* test or ANOVA followed by Scheffé post hoc comparison if necessary were used for statistical analysis, with $p < 0.01$ considered significant.

Results

Masitinib prevents M-CSF-induced proliferation in cultured microglia

To determine the effect of tyrosine kinase inhibition with masitinib, we used microglia isolated from the primary spinal cord cultures of symptomatic $SOD1^{G93A}$ rats before their transformation into astrocyte-like cells [5]. Microglia appeared as hypertrophic phagocytic cells that actively proliferate in the presence of fetal bovine serum (FBS) or M-CSF (Fig. 1a). Treating cell cultures using pharmacological concentrations of masitinib (0.1–1 μM) dose-dependently abrogated the morphology of hypertrophic phagocytic microglia and also inhibited M-CSF-induced proliferation as measured by BrdU uptake (Fig. 1b). In accordance, masitinib potently inhibited the kinase activity of recombinant CSF-1R with an IC_{50} of 90 ± 35 nM (Fig. 1c), a concentration that is reachable in vivo.

Masitinib prevents $SOD1^{G93A}$ microglia cells inflammatory profile

As predicted by the hypertrophic and phagocytic morphology, primary cultured microglia from symptomatic $SOD1^{G93A}$ spinal cords displayed a robust transcriptional activity for inflammatory genes. After exposure to masitinib during 72 h, the transcription of several genes highly involved in neuroinflammation decreased more than 50 %. In particular, relevant inflammatory transcripts such as IL1β, IL6, Iba1, and Cox2 were downregulated by approximately 80 % (Fig. 2a). In addition, Fig. 2b shows that masitinib inhibited by more than 50 %, the ability of microglia to migrate across a scratch made in the culture dish in low FBS conditions.

Previously, we have reported that hypertrophic microglia from ALS rats follow a phenotypic transition after 12–15 days in culture turning to flat, astrocyte-like cells characterized by being highly toxic for cultured motor

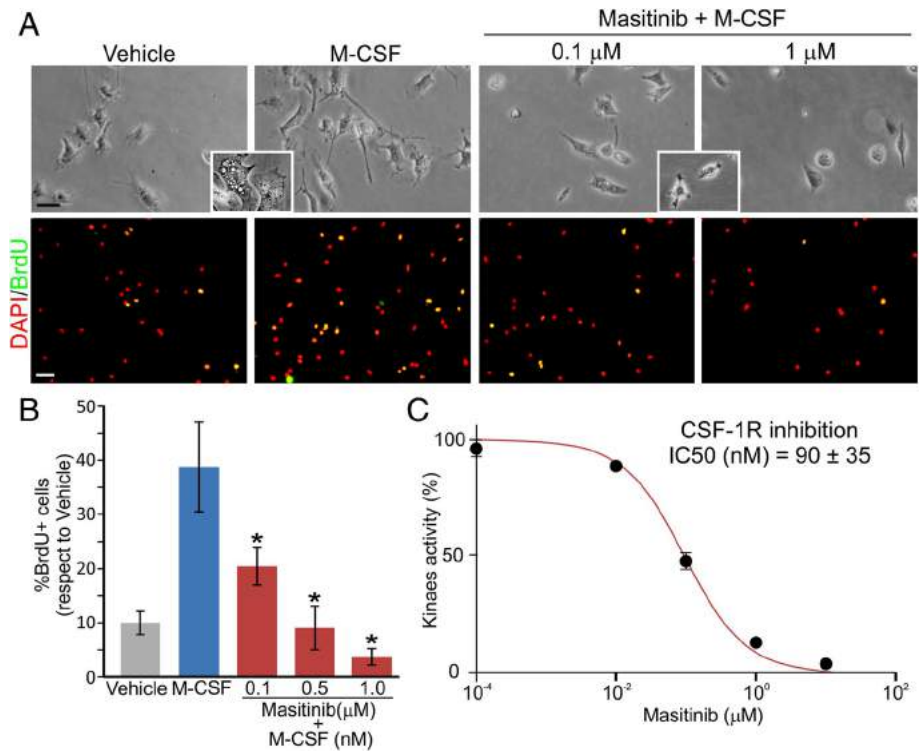

Fig. 1 Masitinib prevented microglia proliferation by inhibiting CSF-1R. **a** Microglia cultured from symptomatic $SOD1^{G93A}$ rat spinal cord in low FBS conditions (0.5 %) adding 30 ng/mL of M-CSF with indicated masitinib concentrations. The *insets* show the hypertrophic vacuolated cells in vehicle and M-CSF conditions and the small rounded cells after masitinib treatment (*scale bars*: contrast 20 μm and DAPI/BrdU 50 μm). **b** The *graph* shows the quantitative BrdU analysis where positive cells were counted and expressed as percentage of total cells stained with DAPI. M-CSF treatment produced a significant increase in microglial proliferation that was blocked by masitinib. **c** Kinase inhibition assay showing that masitinib inhibited CSF-1R with an $IC_{50} = 90 \pm 35$ nM. All data are expressed as mean ± SEM $^*p < 0.01$

neurons [4, 5]. Figure 2c shows that masitinib (0.1–1 μM) potently prevented this phenotypic transformation by more than 50 %, thus preventing the emergence of the aberrant glial cell phenotype in culture.

Post-paralysis masitinib treatment reduces the number of aberrant glial cells and neuroinflammation

We then explored whether chronic treatment with masitinib could reduce the number of aberrant glial cells in the degenerating spinal cord, which were identifiable as large GFAP/S100β-positive cells located around motor neurons as described previously [4]. Rats were orally treated with masitinib (30 mg/kg/day), starting right after paralysis onset and during the next 20 days, corresponding to the average post-paralysis survival in untreated rats (Fig. 5). Only rats that initiated paralysis in the hind limbs were used in the experiments in order to reduce experimental variables. As compared with rats treated with vehicle, masitinib significantly reduced the number of aberrant glial cells in the lumbar spinal cord by 40 % (Fig. 3a).

In accordance, masitinib treatment to symptomatic rats prevented the isolation and subsequent proliferation of microglia in primary cell cultures of the degenerating spinal cord (Fig. 3b). This sharply contrasted with a large number of hypertrophic and phagocytic cells obtained in cultures from vehicle-treated rats, indicating that masitinib treatment reduces inflammatory and proliferative potential of endogenous glial cells.

Post-paralysis masitinib treatment also significantly reduced microgliosis as assessed by the number of cells expressing Iba1+, CD206+, or CD68+ cells in the ventral horn of the lumbar spinal cord, when compared with vehicle-treated animals (Fig. 4a, see Additional file 1: Figure S1A). Remarkably, there was a reduction of hypertrophic Iba1+ microglia cells surrounding motor neurons at thoracic and cervical levels of the degenerating spinal cords, suggesting that masitinib may prevented the spread of neuroinflammation along the neuraxis (see Additional file 1: Figure S1B).

Masitinib ameliorates motor neuron pathology

Because motor neuron death is the main pathological feature of symptomatic rodent models and human ALS, we used the same experimental setting to determine if motor neuron pathology was influenced by masitinib

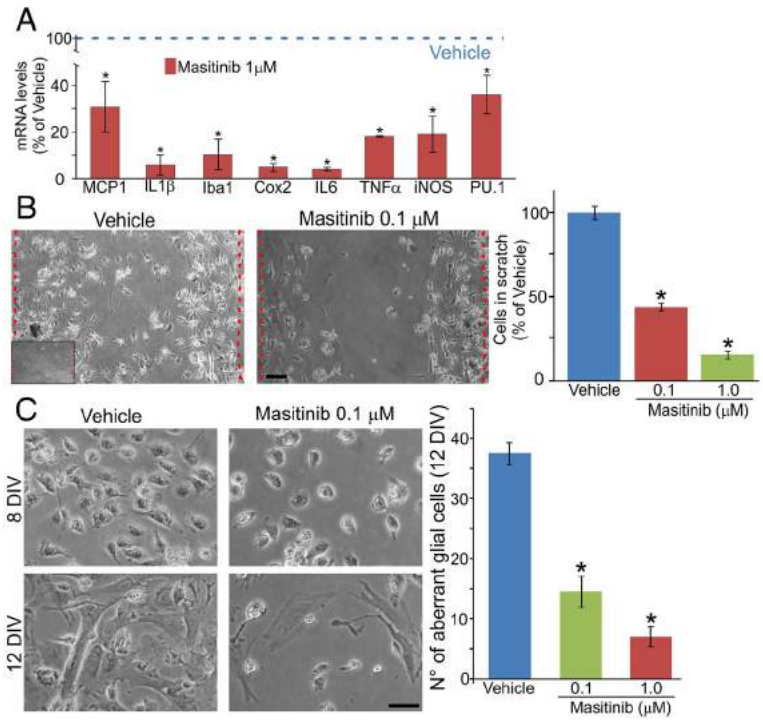

Fig. 2 Masitinib inhibited microglia proinflammatory phenotype and prevented microglia migration and transformation into aberrant glial cells. **a** Real-time PCR analysis showed that the treatment with pharmacological concentration (1 μM) of masitinib during 72 h is sufficient to significantly reduce the expression of several genes involved in inflammatory processes. **b** A confluent monolayer was scratched to determine the migratory capacity of aberrant microglia. After 24 h, cells located between the *dashed lines* were counted. Vehicle-treated microglia covered most of the scratch after 24 h, while masitinib-treated cells showed significantly less migratory capacity. The *inset* shows the open space in the monolayer immediately after making the scratch (*scale bar* 20 μm). The graph to the *right* shows the quantitative analysis of migration. **c** Masitinib prevented microglia transformation into aberrant glial cells in a dose-dependent manner when compared with vehicle-treated cultures. Note how after 12 days in vitro, microglia transition to a flat astrocyte-like cell that reach confluence. Masitinib significantly prevented this transformation and few microglia cells transitioned into aberrant glial cells (*scale bar* 10 μm). The graph to the *right* represents the quantitative analysis showing the number of aberrant glial cells after 12 days in vitro (12DIV). All data are expressed as mean ± SEM $*p < 0.01$

treatment. As shown in Fig. 4b, in vehicle-treated $SOD1^{G93A}$ rat, the number of ventral horn ChAT+ motor neurons decreased by 60 % when measured 20 days after paralysis onset. In comparison, masitinib significantly reduced motor neuron loss to 40 % when administered after paralysis onset. We next analyzed the effect of masitinib treatment on the motor neuron soma diameter in surviving motor neurons. When compared with non-transgenic animals (soma diameter 35.8 ± 8.7 μm), there was a significant reduction in the soma diameter of end-stage symptomatic rats (23.4 ± 5.8 μm). This neuron atrophy was significantly prevented by masitinib treatment (30 ± 10.3 μm) (Fig. 4b).

Masitinib prolongs post-paralysis survival in $SOD1^{G93A}$ rats

Next, we designed two randomized trials using masitinib to determine how the drug affected the survival of $SOD1^{G93A}$ rats with hind limb onset. As shown in Table 1, our rat colony develops disease with a delayed onset (187 ± 15 days for vehicle rats) if compared with that originally described by Howland et al. [15]. In our colony, the post-paralysis survival with hind limb onset has been highly reproducible in non-treated animals (20 ± 3.8 days, Fig. 5). Table 1 shows that there were no significant differences in the pre-treatment parameters analyzed such as age and weight between treated and non-treated animal groups (see Additional file 1: Figure S2C, D).

Masitinib (30 mg/kg/day) was administrated immediately upon abnormal gait onset (day 1) or after day 7. The effect of masitinib treatment was compared against age, weight, and gender-matched control groups treated with vehicle (Fig. 5a, b, see Additional file 1: Figure S2A–D). Without masitinib, the ALS rats died within 3 weeks of paralysis onset (Fig. 5a). Rats in the masitinib day 1 cohort ($n = 14$) had a statistically significant ($p < 0.0006$) difference in the probability of survival when compared with vehicle-treated animals (Kaplan-Meier curves, Fig. 5a).

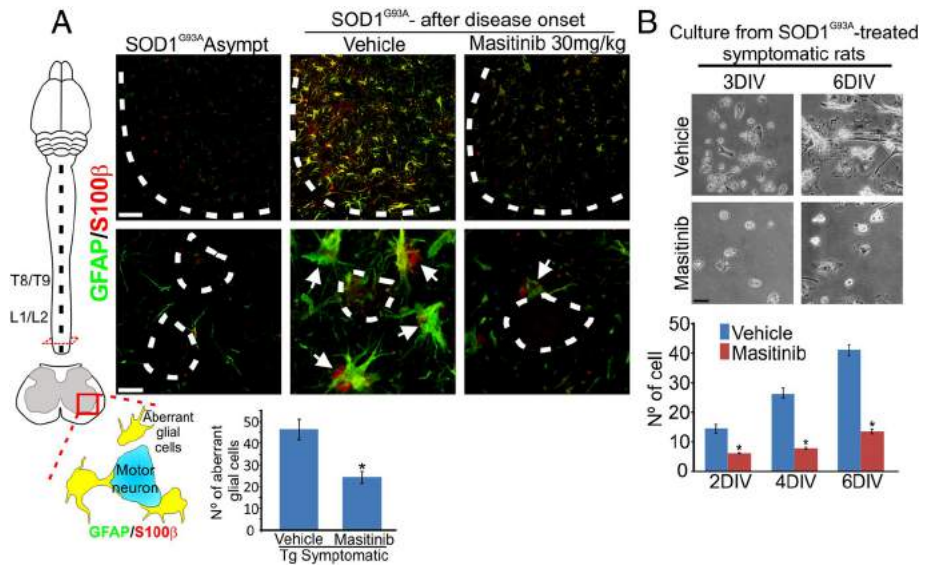

Fig. 3 Masitinib treatment reduced the number of aberrant glial cells in the degenerating spinal cord. **a** Aberrant glial cells expressing GFAP (*green*) and S100β (*red*) in the ventral horn of the spinal cord. *Dotted white lines* mark the border between white and grey matter in the upper images and outline motor neurons in high magnification panels. In the vehicle-treated rats aberrant glial cells (*white arrows*) surround motor neurons as compared with asymptomatic (Tg Asympt) where glial cells express low S100β. Masitinib (30 mg/kg/day) prevented the appearance of aberrant glial cells in the degenerating spinal cord after 20 days treatment. The scheme represents the level of spinal cord segments and Rexed laminae VII and IX where aberrant glial cells were counted (*scale bars* 50 μm in low magnification and 10 μm in high magnification). **b** Spinal cord culture from masitinib-treated rats compared with vehicle-treated rats. Relatively few cells were obtained from the degenerating spinal cord after masitinib treatment when compared with vehicle-treated animals (*scale bar* 15 μm). All data are expressed as mean ± SEM *$p < 0.01$

Remarkably, animals in the masitinib day 7 cohort ($n = 9$) also had a statistically significant ($p < 0.0001$) difference in the probability of survival with respect to controls.

Comparing each cohort's mean survival time also evidenced a survival benefit for masitinib. The mean post-paralysis survival time was respectively 30 ± 8 days and 27 ± 4.3 days for day 1 and day 7 masitinib cohorts, which were both significantly longer than the 20 ± 3.8 days observed for vehicle-treated rats (Fig. 5b, $p < 0.0016$ and 0.0003, respectively). The protective effect of masitinib was equally observed in both female and male rats (see Additional file 1: Figure S2A, B).

Discussion

Tyrosine kinase inhibitors are a well-established class of drugs typically used to suppress or decrease cancer cell proliferation and modulate the associated tumor microenvironment [17, 18]. Here, we show evidence that the tyrosine kinase inhibitor masitinib therapeutically modulates the neuroinflammation associated with the ALS progression. Masitinib reduced microgliosis and the subsequent emergence of aberrant glial cells in the degenerating spinal cord, which is consistent with a potent effect in microglial cell cultures, downregulating proliferation, migration, and inflammatory transcriptional profile. Remarkably, treatment of already paralytic rats with masitinib resulted in an unprecedented increase (~40 %) in post-paralysis survival in both genders. While other drugs modulating glial cell inflammation can prolong survival in ALS models [19], our study is the first one showing a protective effect when the drug is delivered post-paralysis. Such a therapeutic approach is appealing in the clinical setting of ALS where drug treatment is initiated only after overt motor symptoms.

Tyrosine kinase inhibition with masitinib sharply decreased the number microglia cells expressing Iba1, CD206, and CD68 and the appearance of aberrant glial cells in the lumbar spinal cord, thus supporting the concept that preventing the emergence of aberrant glial cells moderates the accelerated paralysis progression characteristic of SOD1^{G93A} rats. Our results also anticipate that tyrosine kinase inhibition could be also protective in other ALS models involving overt glial activation [20, 21]. Indeed, the SOD1^{G93A} rat appears as a useful model to study drugs with post-paralysis effects through the modulation of CNS neuroinflammation, contrasting with SOD1^{G93A} mice where distal axonopathy appears as a more important determinant of post-paralysis survival [15, 22].

The inhibition of receptor and non-receptor tyrosine kinases controlling inflammation and exaggerated glial cell activation appears as the most plausible mechanism of action of masitinib. Compared to previous studies in ALS murine models based on ablation of proliferating

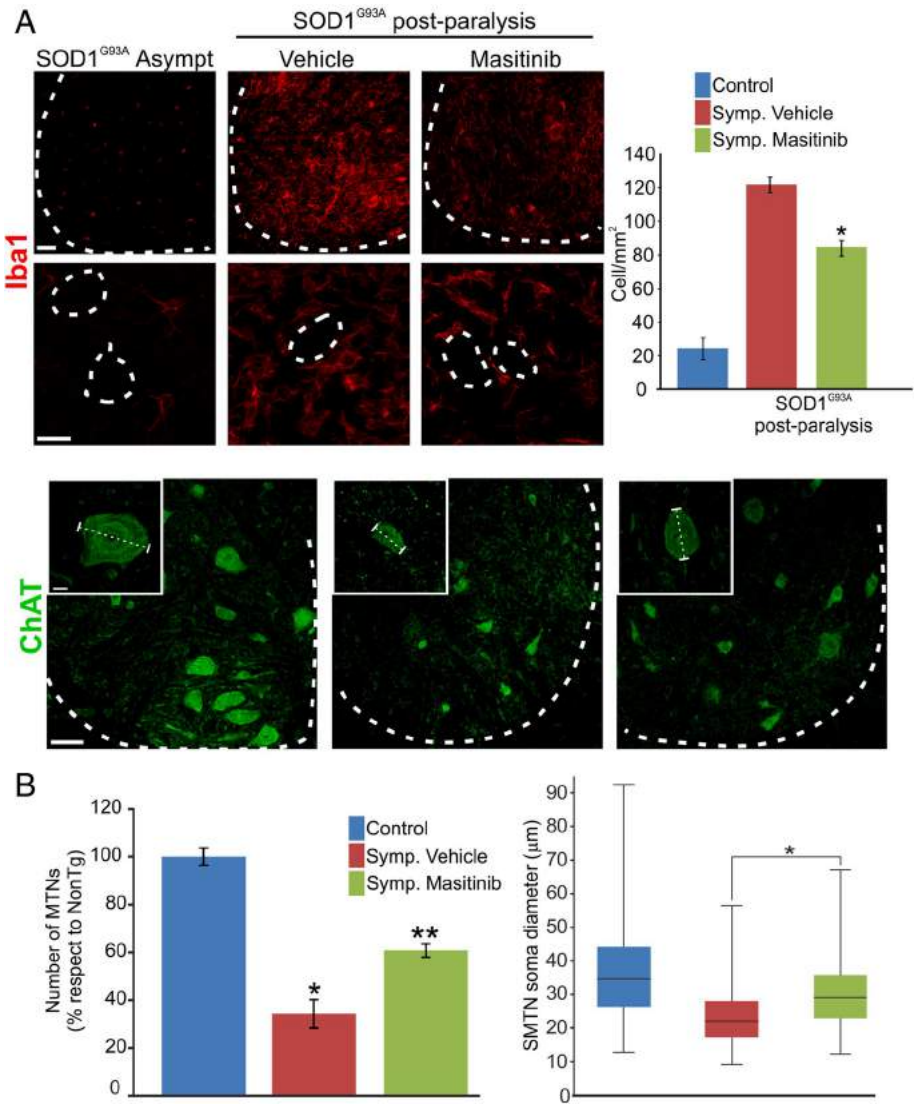

Fig. 4 Masitinib ameliorates microgliosis and motor neuron pathology. **a** Microglia marker Iba1 confocal images. Note the significant reduction of microglial cells in masitinib-treated rat spinal cords when compared with vehicle-treated ones. High magnification panels show a significant reduction in the number of microglial cells that surround motor neurons after masitinib chronic treatment (*scale bars* 50 µm low magnification and 20 µm high magnification). **b** Confocal image of ChAT in the lumbar spinal cord (*dotted line*) indicates the border between white and grey matter (*scale bar* 50 µm). The *graph* below to the *left* represents the quantitative analysis showing the number of motor neurons in the ventral horn in each condition. The *graph* to the *right* represents the quantitation of the motor neuron soma diameter showing the decreased diameter of surviving motor neurons in vehicle-treated rats and the protective effect of masitinib (*insets* in a) (*scale bar* 10 µm). All data are expressed as mean ± SEM $*p < 0.01$, $**p < 0.01$

Table 1 Characteristics of SOD1^{G93A} rats used in the post-paralysis masitinib trial

	Vehicle	Masitinib (>day 1)	Masitinib (>day 7)
Age at onset (days)	187 ± 15	182 ± 25	198 ± 14
Weight at onset (g)	315 ± 56	306 ± 16	323 ± 71
Weight at end-stage (g)	235 ± 13	214 ± 50	211 ± 50
Survival range (days)	174–234	177–249	201–246

The table shows characteristics of the consolidated studies for rats treated with vehicle, masitinib starting 1 (>day 1) and 7 (>day 7) days after paralysis onset. Age and weight values are expressed as mean ± SD. Survival range indicates the age of rats at the time animals reached end-stage of paralysis

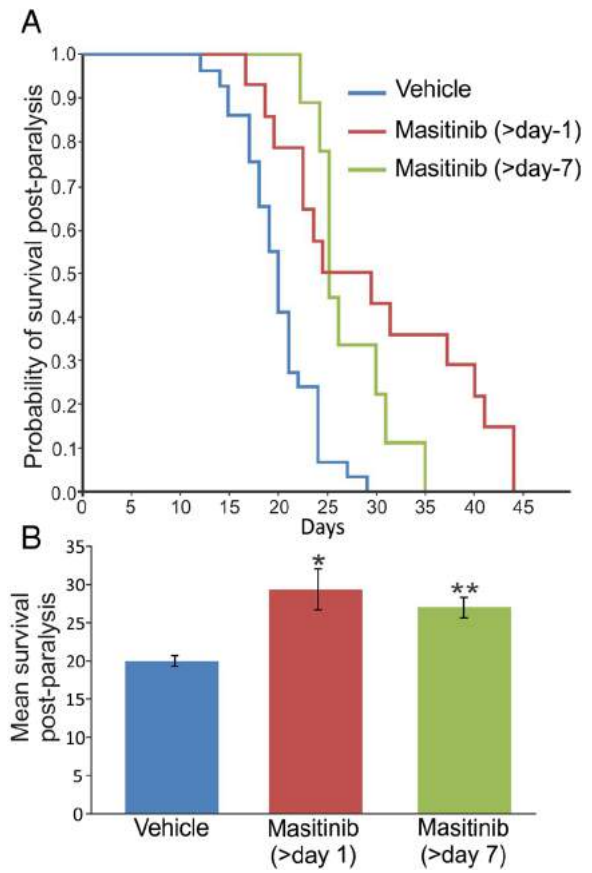

Fig. 5 Masitinib treatment after paralysis onset increased survival of SOD1^{G93A} transgenic rats. **a** Kaplan-Meier survival curves from masitinib-treated and vehicle-treated SOD1^{G93A} rats. SOD1 ^{G93A} transgenic rats were treated with masitinib (30 mg/kg/day) or vehicle (water, $n = 29$, *blue line*) immediately after observation of paralysis onset of one limb (day 1; $n = 14$, *red line*) or starting 7 days after paralysis onset (day 7, $n = 9$, *green line*). There was a statistically significant difference in the probability of survival for both masitinib-treated groups when compared with vehicle-treated group, according to the log-rank test of the Kaplan-Meier analysis ($p < 0.0006$ for masitinib—gait onset vs. vehicle and $p < 0.00025$ for masitinib—7 days onset vs. vehicle). **b** The *graph* shows the mean survival of the three different groups. All data are expressed as mean ± SEM. $p < 0.01$ was considered significant

microglial cells [23–25], treatment with masitinib does not eliminate the proliferating microglia. Rather, it more likely modulates the proliferation and inflammatory signaling underlying the emergence of aberrant glial cells, representing a new pharmacological approach to control detrimental neuroinflammation.

In particular, we found that masitinib inhibits purified recombinant CSF-1R kinase activity at nanomolar concentrations and reduces M-CSF-induced microglia proliferation and migration ability in vitro, suggesting that it regulates a key inflammatory pathway, thus promoting microglia expansion and invasive behavior. Previous reports have shown that activation of CSF-1R by the agonist M-CSF or interleukin 34 potently regulates macrophage/microglia number and inflammatory phenotype in animal models [26, 27]. Recent reports have shown that motor neurons express M-CSF upon damage causing the expansion of surrounding spinal microglial cells [9, 28], thus prompting a pathogenic pathway where motor neuron pathology exacerbates deleterious microgliosis. In accordance, M-CSF levels are elevated in ALS patients as well as in ALS mouse models and may represent a key pathway exacerbating microgliosis and ALS progression [29–31]. Moreover, a recent report has shown that CSF-1R blockade with the drug GW2580 administered to ALS mice several weeks before paralysis onset decreased both microgliosis and slowed disease progression [32].

Although masitinib is a relatively selective kinase inhibitor [33] for CSF-1R, it also targets a few other tyrosine kinases such as PDGF-R, c-Kit, Lyn, and Fyn [10, 11], whose activation may also be associated with the modulation of the neurodegenerative microenvironment. A number of tyrosine kinase inhibitors targeting specific receptors have been approved over the last 5 years for many different types of cancer. However, there are few reports of central nervous system adverse effects or direct neuronal damage. The effect of masitinib, as well as other tyrosine kinase inhibitors, is not selective for a specific cell type, because it blocks several kinases expressed in many cell types. However, masitinib is one of the most selective kinase inhibitors currently in development and as such, potentially exerts a low toxicity profile [11]. In addition, the effects of inhibition of kinase targeted by masitinib are more involved in cell proliferation (c-Kit, PDGF-R, and MCSF/CSF-1R) and immune activation (Lyn, Fyn) than apoptosis. Thus, post-mitotic cells and particularly neurons and resting astrocytes are generally less vulnerable to pharmacological tyrosine kinase inhibition by masitinib as reported previously [13, 34]. Furthermore, inhibition of the non-receptor c-Abl kinase by imatinib has been shown to prevent astrocyte-induced motor neuron death in cell cultures [34], further suggesting an alternative neuroprotective pathway unrelated to neuroinflammation. Such a unique combination of molecular effects could explain our results showing the potent effect of masitinib downregulating the expression of inflammatory mediators, characteristic of deleterious aberrant glial cell phenotype. Thus, further work will be required to decipher the precise tyrosine kinases deregulated in ALS and their pharmacological targeting.

The present study does not establish whether masitinib targets inflammatory cells outside the CNS also known to influence motor neuron degeneration [35, 36]. In particular, masitinib may target the peripheral monocyte/macrophage system, which appears affected in ALS animal models. Immunological downregulation of Ly6C^{hi}

monocytes that infiltrate the degenerative spinal cord attenuates motor neuron loss and delays disease progression in mutant SOD1 mice [37]. Masitinib could also target macrophages that infiltrate and promote degeneration of peripheral motor axons [38]. Moreover, macrophage activation and microgliosis are known to be influenced by mast cells located inside or outside the blood-brain barrier [39]. Because masitinib potently prevents mast cell differentiation and activation [10], it could also indirectly regulate neuroinflammation by targeting mast cells through the inhibition of c-Kit, Lyn, and Fyn. Future studies in patients and animal models are needed to determine alternative mechanisms of action of tyrosine kinase inhibitors and masitinib in ALS.

There are currently no effective treatments for ALS. Riluzole, an anti-glutamatergic drug, is the sole authorized product used in ALS, providing a modest improvement in survival (~3 months) [40]. Over the past 10 years, a number of drugs were identified as providing survival benefits in rodent preclinical trials [19]. However, none of them proved to be clinically better than riluzole in ALS patients. Such incongruence could be explained, at least in part, by the fact that most animal studies that were translated to clinical trials have been started before paralysis onset. Therefore, tyrosine kinase inhibition with masitinib appears unique among other ALS-developmental drugs because it exerts neuroprotection when administrated post-paralysis. A randomized phase III clinical trial testing the effect of masitinib in ALS patients is currently running (Clinicaltrial.gov NCT02588677).

Conclusions

The present study shows that tyrosine kinase inhibition with masitinib is capable of controlling microgliosis, neuroinflammation, and the emergence/expansion of aberrant glial cells in SOD1^{G93A} rats. Remarkably, masitinib significantly prolonged survival when delivered after paralysis onset, an unprecedented effect in preclinical models of ALS, and therefore appears well-suited for treating ALS where drug treatment is initiated only after diagnosis based on overt motor symptoms.

Additional file

Additional file 1: Figures S1. Masitinib inhibited microgliosis along the degenerating spinal cord. **Figure S2.** Masitinib treatment after paralysis onset increased survival of SOD1^{G93A} female and male rats. (DOCX 700 kb)

Abbreviations

ALS, amyotrophic lateral sclerosis; BrdU, bromodeoxyuridine; ChAT, choline acetyltransferase; c-Kit, stem cell growth factor receptor (SCFR); CNS, central nervous system; Cox2, cyclooxygenase-2; CSF-1R, colony-stimulating factor 1 receptor; FBS, fetal bovine serum; FLT3, fms-related tyrosine kinase 3; Iba1, ionized calcium binding adaptor molecule 1; IL1β, interleukin 1 beta; IL6, interleukin 6; M-CSF, macrophages colony-stimulating factor; PDGF-R, platelet-derived growth factor receptor; SOD1, superoxide dismutase 1

Acknowledgements

We want also thank to Colin Mansfield for his critical comments and helpful suggestions revising the manuscript.

Funding

This work was supported by Fondo Clemente Estable–ANII (FCE_1_2011_1_7342), Institut Pasteur de Montevideo–FOCEM Mercosur (COF 03/11), NIH (NS058628) the Amyotrophic Lateral Sclerosis Association (00482), Department of Defense (AL140108), and by ECOS-SUD program (U14S02).

Availability of data and materials

There is no data, software, databases, application/tool available apart from the reported in the present study. Data supporting the conclusions are presented in the manuscript. For other information please contact corresponding author.

Authors' contributions

ET, TTM, ICM, JB, OH, and LB designed the study. ET, SI, RBN, JB, MG, LG, PD, PDA, PC, and LMP performed the experiments. ET, SI, RBN, TTM, LG, and LB analyzed the data. ET, SI, RBN, JB, OH, and LB prepare the manuscript. All authors contributed to discussion of the results and edited and approved the final version.

Competing interests

OH and PD are cofounder and shareholder of AB Science, LG is an employee of AB Science, JB received salary from AB Science, and others declare that they have no competing interests.

Consent for publication

Not applicable.

Ethics approval and consent to participate

All procedures using laboratory animals were performed in accordance with the national and international guidelines and were approved by the Institutional Animal Committee for animal experimentation. This study was carried out in strict accordance with the Instituto de Investigaciones Biológicas Clemente Estable Bioethics Committee's requirements and under the current ethical regulations of the Uruguayan Law No. 18.611 for animal experimentation that follows the Guide for the Care and Use of Laboratory Animals of the National Institutes of Health (USA).

Author details

[1]Institut Pasteur de Montevideo, Mataojo 2020, Montevideo 11.400, Uruguay. [2]Imagine Institute, Hôpital Necker, 24 boulevard du Montparnasse, 75015 Paris, France. [3]INSERM UMR 1163, Laboratory of Cellular and Molecular Mechanisms of Hematological Disorders and Therapeutic Implications, Paris, France. [4]Paris Descartes–Sorbonne Paris Cité University, Imagine Institute, Paris, France. [5]CNRS ERL 8254, Paris, France. [6]Laboratory of Excellence GR-Ex, Paris, France. [7]Equipe Labélisée par la Ligue Nationale contre le cancer, Paris, Cedex, France. [8]AB Science, 3 Avenue Georges V, 75008 Paris, France. [9]CRCM, [Signaling, Hematopoiesis and Mechanism of Oncogenesis], Inserm, U1068, Institut Paoli-Calmettes, Aix-Marseille Univ, UM105, CNRS, UMR7258, Marseille F-13009, France. [10]Laboratorio de Neurobiología Celular y Molecular, Instituto de Investigaciones Biológicas Clemente Estable, Montevideo, Uruguay. [11]Departamento de Histología y Embriología, Facultad de Medicina, Universidad de la República, Montevideo, Uruguay. [12]Linus Pauling Institute, Department of Biochemistry and Biophysics, Environmental Health Sciences Center, Oregon State University, Corvallis, USA. [13]Department of Hematology, Necker Hospital, Paris, France. [14]Centre national de référence des mastocytoses (CEREMAST), Paris, France.

Received: 2 March 2016 Accepted: 9 June 2016
Published online: 11 July 2016

References

1. Barbeito LH, Pehar M, Cassina P, Vargas MR, Peluffo H, Viera L, et al. A role for astrocytes in motor neuron loss in amyotrophic lateral sclerosis. Brain Res Brain Res Rev. 2004;47:263–74.
2. Ilieva H, Polymenidou M, Cleveland DW. Non-cell autonomous toxicity in neurodegenerative disorders: ALS and beyond. J Cell Biol. 2009;187:761–72.

3. Maragakis NJ, Rothstein JD. Mechanisms of disease: astrocytes in neurodegenerative disease. Nat Clin Pract Neurol. 2006;2:679–89.
4. Diaz-Amarilla P, Olivera-Bravo S, Trias E, Cragnolini A, Martinez-Palma L, Cassina P, et al. Phenotypically aberrant astrocytes that promote motoneuron damage in a model of inherited amyotrophic lateral sclerosis. Proc Natl Acad Sci U S A. 2011;108:18126–31.
5. Trias E, Diaz-Amarilla P, Olivera-Bravo S, Isasi E, Drechsel DA, Lopez N, et al. Phenotypic transition of microglia into astrocyte-like cells associated with disease onset in a model of inherited ALS. Front Cell Neurosci. 2013;7:274.
6. Lemmon MA, Schlessinger J. Cell signaling by receptor tyrosine kinases. Cell. 2010;141:1117–34.
7. Chitu V, Stanley ER. Colony-stimulating factor-1 in immunity and inflammation. Curr Opin Immunol. 2006;18:39–48.
8. Hamilton JA. Colony-stimulating factors in inflammation and autoimmunity. Nat Rev Immunol. 2008;8:533–44.
9. Guan Z, Kuhn JA, Wang X, Colquitt B, Solorzano C, Vaman S, et al. Injured sensory neuron-derived CSF1 induces microglial proliferation and DAP12-dependent pain. Nat Neurosci. 2016;19:94–101.
10. Dubreuil P, Letard S, Ciufolini M, Gros L, Humbert M, Casteran N, et al. Masitinib (AB1010), a potent and selective tyrosine kinase inhibitor targeting KIT. PLoS One. 2009;4, e7258.
11. Anastassiadis T, Deacon SW, Devarajan K, Ma H, Peterson JR. Comprehensive assay of kinase catalytic activity reveals features of kinase inhibitor selectivity. Nat Biotechnol. 2011;29:1039–45.
12. Vermersch P, Benrabah R, Schmidt N, Zephir H, Clavelou P, Vongsouthi C, et al. Masitinib treatment in patients with progressive multiple sclerosis: a randomized pilot study. BMC Neurol. 2012;12:36.
13. Kocic I, Kowianski P, Rusiecka I, Lietzau G, Mansfield C, Moussy A, et al. Neuroprotective effect of masitinib in rats with postischemic stroke. Naunyn Schmiedebergs Arch Pharmacol. 2015;388:79–86.
14. Piette F, Belmin J, Vincent H, Schmidt N, Pariel S, Verny M, et al. Masitinib as an adjunct therapy for mild-to-moderate Alzheimer's disease: a randomised, placebo-controlled phase 2 trial. Alzheimers Res Ther. 2011;3:16.
15. Howland DS, Liu J, She Y, Goad B, Maragakis NJ, Kim B, et al. Focal loss of the glutamate transporter EAAT2 in a transgenic rat model of SOD1 mutant-mediated amyotrophic lateral sclerosis (ALS). Proc Natl Acad Sci U S A. 2002;99:1604–9.
16. Thomsen GM, Gowing G, Latter J, Chen M, Vit JP, Staggenborg K, et al. Delayed disease onset and extended survival in the SOD1G93A rat model of amyotrophic lateral sclerosis after suppression of mutant SOD1 in the motor cortex. J Neurosci. 2014;34:15587–600.
17. Zhang J, Yang PL, Gray NS. Targeting cancer with small molecule kinase inhibitors. Nat Rev Cancer. 2009;9:28–39.
18. Ozao-Choy J, Ma G, Kao J, Wang GX, Meseck M, Sung M, et al. The novel role of tyrosine kinase inhibitor in the reversal of immune suppression and modulation of tumor microenvironment for immune-based cancer therapies. Cancer Res. 2009;69:2514–22.
19. Pandya RS, Zhu H, Li W, Bowser R, Friedlander RM, Wang X. Therapeutic neuroprotective agents for amyotrophic lateral sclerosis. Cell Mol Life Sci. 2013;70:4729–45.
20. Lobsiger CS, Cleveland DW. Glial cells as intrinsic components of non-cell-autonomous neurodegenerative disease. Nat Neurosci. 2007;10:1355–60.
21. Yamanaka K, Chun SJ, Boillee S, Fujimori-Tonou N, Yamashita H, Gutmann DH, et al. Astrocytes as determinants of disease progression in inherited amyotrophic lateral sclerosis. Nat Neurosci. 2008;11:251–3.
22. Fischer LR, Culver DG, Tennant P, Davis AA, Wang M, Castellano-Sanchez A, et al. Amyotrophic lateral sclerosis is a distal axonopathy: evidence in mice and man. Exp Neurol. 2004;185:232–40.
23. Lee JC, Seong J, Kim SH, Lee SJ, Cho YJ, An J, et al. Replacement of microglial cells using Clodronate liposome and bone marrow transplantation in the central nervous system of SOD1(G93A) transgenic mice as an in vivo model of amyotrophic lateral sclerosis. Biochem Biophys Res Commun. 2012;418:359–65.
24. Gowing G, Philips T, Van Wijmeersch B, Audet JN, Dewil M, Van Den Bosch L, et al. Ablation of proliferating microglia does not affect motor neuron degeneration in amyotrophic lateral sclerosis caused by mutant superoxide dismutase. J Neurosci. 2008;28:10234–44.
25. Audet JN, Gowing G, Paradis R, Soucy G, Julien JP. Ablation of proliferating cells in the CNS exacerbates motor neuron disease caused by mutant superoxide dismutase. PLoS One. 2012;7, e34932.
26. Smith AM, Gibbons HM, Oldfield RL, Bergin PM, Mee EW, Curtis MA, et al. M-CSF increases proliferation and phagocytosis while modulating receptor and transcription factor expression in adult human microglia. J Neuroinflammation. 2013;10:85.
27. Doring A, Sloka S, Lau L, Mishra M, van Minnen J, Zhang X, et al. Stimulation of monocytes, macrophages, and microglia by amphotericin B and macrophage colony-stimulating factor promotes remyelination. J Neurosci. 2015;35:1136–48.
28. Okubo M, Yamanaka H, Kobayashi K, Dai Y, Kanda H, Yagi H, et al. Macrophage-colony stimulating factor derived from injured primary afferent induces proliferation of spinal microglia and neuropathic pain in rats. PLoS One. 2016;11, e0153375.
29. Henkel JS, Engelhardt JI, Siklos L, Simpson EP, Kim SH, Pan T, et al. Presence of dendritic cells, MCP-1, and activated microglia/macrophages in amyotrophic lateral sclerosis spinal cord tissue. Ann Neurol. 2004;55:221–35.
30. Gowing G, Lalancette-Hebert M, Audet JN, Dequen F, Julien JP. Macrophage colony stimulating factor (M-CSF) exacerbates ALS disease in a mouse model through altered responses of microglia expressing mutant superoxide dismutase. Exp Neurol. 2009;220:267–75.
31. Sargsyan SA, Monk PN, Shaw PJ. Microglia as potential contributors to motor neuron injury in amyotrophic lateral sclerosis. Glia. 2005;51:241–53.
32. Martinez-Muriana A, Mancuso R, Francos-Quijorna I, Olmos-Alonso A, Osta R, Perry VH, et al. CSF1R blockade slows the progression of amyotrophic lateral sclerosis by reducing microgliosis and invasion of macrophages into peripheral nerves. Sci Rep. 2016;6:25663.
33. Davis MI, Hunt JP, Herrgard S, Ciceri P, Wodicka LM, Pallares G, et al. Comprehensive analysis of kinase inhibitor selectivity. Nat Biotechnol. 2011; 29:1046–51.
34. Rojas F, Gonzalez D, Cortes N, Ampuero E, Hernandez DE, Fritz E, et al. Reactive oxygen species trigger motoneuron death in non-cell-autonomous models of ALS through activation of c-Abl signaling. Front Cell Neurosci. 2015;9:203.
35. Beers DR, Henkel JS, Zhao W, Wang J, Appel SH. CD4+ T cells support glial neuroprotection, slow disease progression, and modify glial morphology in an animal model of inherited ALS. Proc Natl Acad Sci U S A. 2008;105: 15558–63.
36. Zhao W, Beers DR, Appel SH. Immune-mediated mechanisms in the pathoprogression of amyotrophic lateral sclerosis. J Neuroimmune Pharmacol. 2013;8:888–99.
37. Butovsky O, Siddiqui S, Gabriely G, Lanser AJ, Dake B, Murugaiyan G, et al. Modulating inflammatory monocytes with a unique microRNA gene signature ameliorates murine ALS. J Clin Invest. 2012;122:3063–87.
38. Chiu IM, Phatnani H, Kuligowski M, Tapia JC, Carrasco MA, Zhang M, et al. Activation of innate and humoral immunity in the peripheral nervous system of ALS transgenic mice. Proc Natl Acad Sci U S A. 2009;106:20960–5.
39. Skaper SD, Giusti P, Facci L. Microglia and mast cells: two tracks on the road to neuroinflammation. FASEB J. 2012;26:3103–17.
40. Miller RG, Mitchell JD, Moore DH. Riluzole for amyotrophic lateral sclerosis (ALS)/motor neuron disease (MND). Cochrane Database Syst Rev. 2012;3, CD001447.

Publicación 5

Evidence for mast cells contributing to neuromuscular pathology in an inherited model of ALS

Emiliano Trias, Sofía Ibarburu,Romina Barreto-Núñez, Valentina Varela, Ivan C. Moura, Patrice Dubreuil, Olivier Hermine, Joseph S. Beckman and Luis Barbeito

Resumen

Luego de demostrar que el masitinib es un fármaco capaz de reducir el daño que sufren las motoneuronas durante la progresión de la ELA, exploramos otros potenciales mecanismos de acción para esta droga. El masitinib fue desarrollado originalmente para bloquear el receptor de tirosin-quinasas c-Kit, clave en la maduración y activación de los mastocitos. Siguiendo una estrategia de "ingeniería inversa" estudiamos la presencia y el potencial rol de los mastocitos durante la progresión de la ELA. Si bien nuestros estudios preliminares mostraron que, durante la fase sintomática de la enfermedad, los mastocitos no infiltran la médula espinal en degeneración, nuestros estudios se enfocaron en el sistema nervioso periférico. En el presente estudio demostramos que los mastocitos infiltran masivamente el compartimiento neuromuscular en el músculo esquelético de las ratas SOD1^{G93A} sintomáticas, teniendo una correlación con la progresión de la parálisis.

Resultados

- Mediante el análisis con azul de toluidina del músculo extensor (EDL) de ratas transgénicas sintomáticas, luego de 15 días de comenzados los síntomas, observamos una infiltración masiva de mastocitos. Además, un porcentaje significativo de estas células se encuentra en estado de degranulación, algo que no ocurre de forma significativa al comienzo de la enfermedad o en animales no sintomáticos. El análisis Inmunohistoquímica de microscopía confocal muestra la expresión de marcadores típicos de mastocitos en estas células, como triptasa, quimasa y el receptor de tirosin-quinasas c-Kit.

- Interesantemente, observamos que la infiltración de mastocitos ocurre en el microambiente que rodea a las NMJs que se están denervando en mayor número que en el parénquima que no contiene placas motoras.
- En los alrededores de las NMJs, lo mastocitos interactúan con células macrofágicas que también infiltran el músculo atrofiado.
- El tratamiento con 30 mg/kg de masitinib durante 15 días, iniciado luego del comienzo clínico de la enfermedad, reduce el número de mastocitos que infiltran el músculo, así como su degranulación. También se reduce el número de macrófagos que infiltran el músculo durante la fase sintomática.
- El tratamiento con masitinib, previene significativamente esta denervación de las placas motoras y por lo tanto pérdida de la función motora.
- El tratamiento con masitinib también previene la disociación de las células de Schwann terminales adyacentes a las NMJs así como la atrofia de la red de capilares del músculo esquelético.

Conclusiones

Este estudio contribuye de manera significativa al entendimiento de los mecanismos patogénicos y el tratamiento de la ELA, ya que la denervación de las NMJs es una de las principales características en esta enfermedad. Los mastocitos parecen orquestar la inflamación que se constituye en el microambiente celular de las placas motoras, lo que acelera la denervación y la atrofia muscular luego del comienzo clínico de la enfermedad.

En este trabajo demostramos que la modulación farmacológica de los mastocitos y los macrófagos puede contribuir al enlentecimiento del proceso neurodegenerativo en el músculo esquelético. Además, aportamos nuevos mecanismos de acción para el masitinib, una droga con potencial uso para el tratamiento en la ELA, ya que presenta propiedades neuroprotectoras, tanto en el SNC como en el SNP a través de la inhibición de diferentes receptores de tirosin-quinasas.

JCI insight

RESEARCH ARTICLE

Evidence for mast cells contributing to neuromuscular pathology in an inherited model of ALS

Emiliano Trias,[1] Sofía Ibarburu,[1] Romina Barreto-Núñez,[1] Valentina Varela,[1] Ivan C. Moura,[2,3,4,5,6,7] Patrice Dubreuil,[7,8,9] Olivier Hermine,[2,3,4,5,6,7,8,10,11] Joseph S. Beckman,[12] and Luis Barbeito[1]

[1]Institut Pasteur de Montevideo, Uruguay. [2]Imagine Institute, Hôpital Necker, Paris, France. [3]INSERM UMR 1163, Laboratory of Cellular and Molecular Mechanisms of Hematological Disorders and Therapeutic Implications, Paris, France. [4]Paris Descartes–Sorbonne Paris Cité University, Imagine Institute, Paris, France. [5]CNRS ERL 8254, Paris, France. [6]Laboratory of Excellence GR-Ex, Paris, France. [7]Equipe Labélisée par la Ligue Nationale contre le cancer, Parisa, France. [8]AB Science, Paris, France. [9]Signaling, Hematopoiesis and Mechanism of Oncogenesis, Cancer Research Center of Marseille (CRCM), Inserm U1068, Institut Paoli-Calmettes, Aix-Marseille University UM105, CNRS UMR7258, Marseille, France. [10]Department of Hematology, Necker Hospital, Paris, France. [11]Centre national de référence des mastocytoses (CEREMAST), Paris, France. [12]Linus Pauling Institute, Department of Biochemistry and Biophysics, Environmental Health Sciences Center, Oregon State University, Corvallis, Oregon, USA.

Evidence indicates that neuroinflammation contributes to motor neuron degeneration in amyotrophic lateral sclerosis (ALS), a fatal neurodegenerative disease leading to progressive muscular paralysis. However, it remains elusive whether inflammatory cells can interact with degenerating distal motor axons, influencing the progressive denervation of neuromuscular junctions (NMJs). By analyzing the muscle extensor digitorum longus (EDL) following paralysis onset in the SOD1^{G93A} rat model, we have observed a massive infiltration and degranulation of mast cells, starting after paralysis onset and correlating with progressive NMJ denervation. Remarkably, mast cells accumulated around degenerating motor axons and NMJs, and were also associated with macrophages. Mast cell accumulation and degranulation in paralytic EDL muscle was prevented by systemic treatment over 15 days with masitinib, a tyrosine kinase inhibitor currently in clinical trials for ALS exhibiting pharmacological activity affecting mast cells and microglia. Masitinib-induced mast cell reduction resulted in a 35% decrease in NMJ denervation and reduced motor deficits as compared with vehicle-treated rats. Masitinib also normalized macrophage infiltration, as well as regressive changes in Schwann cells and capillary networks observed in advanced paralysis. These findings provide evidence for mast cell contribution to distal axonopathy and paralysis progression in ALS, a mechanism that can be therapeutically targeted by masitinib.

Introduction

Amyotrophic lateral sclerosis (ALS) is a neurodegenerative disease characterized by progressive weakness and paralysis, caused by motor neuron degeneration and distal motor axonopathy (1, 2). In general, ALS is a rapidly progressing disease with survival of 3–5 years after the time of diagnose. The cause of ALS remains largely unknown, and there exists an urgent unmet medical need for drugs that can stop or delay disease progression. In the CNS, ALS is typically accompanied by neuroinflammation involving the emergence of reactive microglia, astrocytes, and aberrant glial phenotypes (3–5). Evidence also shows activation of circulating immune cells (6), as well as immune cell infiltration of the ALS-degenerating peripheral nerves containing motor axons (7–10).

Complex, yet not completely understood, mechanisms underlie the progressive retraction of axons from the muscular motor endplates, a key pathological event leading to paralysis in ALS. Most neuromuscular pathological features of familial and sporadic ALS are reproduced in transgenic mice and rats overexpressing the human ALS-linked mutation of the superoxide dismutase-1 (SOD1^{G93A}) (11–13). It is reported that motor neuron degeneration in mutant SOD1 mice starts peripherally by a distal axonopathy of the motor nerve branches innervating the neuromuscular junctions (NMJs) before overt loss of motor neuron cell bodies (2, 14). Altered axonal transport, defective mitochondria function in motor axon terminals, dys-

Conflict of interest: OH and PD are cofounders and shareholders of AB Science.

Submitted: June 27, 2017
Accepted: September 11, 2017
Published: October 19, 2017

Reference information:
JCI Insight. 2017;2(20):e95934.
https://doi.org/10.1172/jci.insight.95934.

functional Schwann cells, and defective stabilization of NMJs have been proposed as potential pathogenic defects triggering the "dying back" of motor axons (15–17). Finally, evidence for such dying back motor neuropathy has also been found in some clinical forms of ALS (2, 16), suggesting a key pathogenic event that could be targeted by therapeutic interventions.

The role of immune cells influencing NMJ alterations in ALS remains unknown. Previous reports have found macrophage infiltration of peripheral nerves and skeletal muscle in ALS patients and transgenic mice (7, 18). However, it remains unknown whether other immune cells interact with motor nerve endings and NMJs. Mast cells are hematopoietic-derived immune cells, whose precursors migrate within tissues reaching maturation and differentiation (19). Mast cells are constitutive immune cells in skeletal muscle, being enriched in tendon regions and perimysium — but in low numbers in the endomysium (20). Mast cells likely play a physiological role in muscle repair and remodeling through the release of different trophic and inflammatory factors, as well as vasoactive mediators (21). Mast cells accumulate in the muscle endomysium following injury or primary myopathies (21, 22), with a potential of causing direct lysis of myofibers through the release of proteases (23). In ALS patients, an increased number of mast cells have been described in CNS regions of active degeneration (e.g., motor and prefrontal cortex and pyramidal tracts; ref. 24), suggesting their contribution to neuroinflammation. Nonetheless, scarce information exists about the behavior of mast cells in ALS-affected muscles, such as whether they have a potential role modulating NMJ innervation or triggering local chronic inflammation.

Masitinib mesylate is a selective tyrosine kinase inhibitor that mainly targets type III growth factor receptors including c-Kit, CSF-1 receptor (CSF-1R), and platelet-derived growth factor receptors (PDGF-R), as well as Lyn and Fyn kinases (25–27). These receptors synergistically signal proliferation and migration of cancer and hematopoietic cells, including macrophages. By targeting c-Kit, Lyn, and Fyn, masitinib is particularly efficient in controlling the survival, differentiation, and degranulation of mast cells and, thus, modulating the mast cell–induced array of proinflammatory and vasoactive effects (25, 28). Accordingly, clinical trials have shown therapeutic effects of masitinib in cases of mastocytosis, a rare disease characterized by abnormal accumulation and activation of mast cells in various tissues and organs (28). Masitinib was also shown to beneficially modulate CNS function in multiple sclerosis (29), stroke (30), and Alzheimer' s disease (31). In addition, a recent phase III clinical trial with masitinib in ALS has shown promising therapeutic effects in a significant group of patients, slowing the deterioration of motor functions and reducing the decline in quality of life (32). However, the mechanisms of action of masitinib remain largely unexplored, considering that the drug acts on multiple organs and cell types expressing type III tyrosine kinase receptors.

The clinical trial of masitinib in ALS was based on a previous study performed in transgenic rats bearing the ALS-linked $SOD1^{G93A}$ mutation, which showed that postparalysis survival of rats can be significantly extended by systemic treatment with masitinib starting up to 7 days after disease onset (27). This result is significant, considering that in this animal model, a fulminant paralysis develops in rats aged 5–6 months, rapidly progressing from abnormal gait to complete loss of motor function in a period of 2–3 weeks (27). The therapeutic effect of masitinib in ALS rats was associated with the inhibition of CSF-1R in microglia and aberrant glial cells that surround degenerating spinal motor neurons (33, 34). Because masitinib is a multifaceted drug affecting multiple immune cell types, we hypothesized that the protective effect of masitinib in ALS likely involves other inflammatory cell types such as mast cells and macrophages in addition to glial cells.

Our primary objective was to search for a morphological interaction between degenerating motor nerve endings and mast cells during the development of paralysis in the hind limb muscle extensor digitorum longus (EDL), a fast-fatigable muscle that becomes largely denervated in the $SOD1^{G93A}$ rat model (35). We also explored whether the pharmacologic reduction of mast cells, by means of systemic treatment with masitinib, could modulate the rate of NMJ denervation. Here, we report a sharp increase in mast cell number and degranulation infiltrating the EDL muscle — starting after paralysis onset — and the protective effect of masitinib preventing progressive NMJ denervation.

Results

Endomysial infiltration and degranulation of mast cells correlate with paralysis progression. In healthy skeletal muscle, mast cells are mainly located at the perimysium and epimysium, with only a small fraction in the endomysium (20). In contrast, endomysial mast cells have been reported to accumulate in response to muscle denervation or myopathies (22, 36), suggesting that mast cells are part of a broader inflammatory reaction. Because

there are no previous studies on the behavior of mast cells in ALS-affected muscles, we analyzed the mast cell number and their phenotypic features in longitudinal sections of the SOD1^{G93A} rat fast-fatigable EDL muscle. The temporal sequence of events was analyzed at the paralysis onset and after 15 days during advanced paralysis stages, and it was compared with nontransgenic (NonTg) age-matched rats. In the NonTg rat muscles, a low density of mast cells resided in the endomysium, typically displaying uniform granularity when stained with toluidine blue. Compared with NonTg EDL muscle, the density of endomysial mast cells increased by 2-fold at paralysis onset (7 vs. 14 cells/mm^2) and then sharply augmented by 5-fold in the following 2 weeks of paralysis progression (7 vs. 39 cells/mm^2) (Figure 1, A–C). During advanced paralysis, endomysial mast cells were grouped and arranged either in line along some interstitial spaces (Figure 1A) or close to neuromuscular elements (see below), typically displaying increased size and with frequent occurrences of explosive degranulation (Figure 1B). The density of degranulating mast cells, a more relevant measure of mast cell activity and influence in the neuromuscular microenvironment, increased by 8-fold in advanced paralysis EDL muscle as compared with NonTg controls (Figure 1C). Additionally, mast cells in EDL muscle displayed strong immunostaining for tryptase, chymase, and the tyrosine kinase receptor c-Kit, with their colocalization being considered as a specific mast cell marker (Figure 1D).

Mast cells cluster together with motor nerve endings, NMJs, and macrophages during paralysis progression. Peripheral sensory and autonomic nerves have been shown to functionally interact with mast cells, being a mechanism underlying neurogenic inflammation (37, 38). However, whether motor nerve terminals interact with mast cells during ALS paralysis progression is presently unknown. Therefore, we used mechanically dissociated EDL muscle preparations to analyze whether the sharp increase of mast cells after paralysis onset was spatially associated with the degenerating motor fibers and NMJs. Figure 2A shows comparative fields of motor nerve branches interacting with motor endplates at different stages of paralysis. In NonTg and SOD1^{G93A} onset EDL muscles, only a few mast cells were found in close proximity of motor nerve endings and NMJs (Figure 2A). By contrast, in the advanced paralysis stage, tryptase- and chymase-expressing mast cells were found clustering near or in close contact with degenerating motor nerve endings and NMJs (Figure 2, A and B). Quantitative analysis performed in the whole-mounted EDL muscle showed a significant increase in mast cell density in those areas surrounding the denervated motor nerve terminals and NMJs (neuromuscular compartment), as compared with muscle parenchyma lacking NMJs (Figure 2B). In advanced paralysis, mast cells also consistently interacted with macrophages expressing CD11b/Iba1 and CD68 (Figure 2C and Supplemental Figure 1; supplemental material available online with this article; https://doi.org/10.1172/jci.insight.95934DS1). Endomysial CD11b$^+$ macrophages also progressively accumulated within degenerating EDL muscle after paralysis onset and localized in close contact with NMJs. In parallel, CSF-1R immunoreactivity augmented near neuromuscular compartments (Supplemental Figure 1).

Postparalysis tyrosine kinase inhibition with masitinib prevents mast cell accumulation into EDL muscle during advanced paralysis. Masitinib has proven to exert therapeutic effects in ALS patients (32) and to prolong postparalysis survival in SOD1^{G93A} rats (27). Because masitinib potently inhibits the stem cell factor/c-Kit pathway in mast cells, we reasoned that systemic administration of masitinib (30 mg/kg/d) during 15 days after paralysis onset could prevent the augmentation of muscular mast cells in symptomatic rats. Moreover, because masitinib is not expected to exert direct neuroprotection on motor nerve terminals, the masitinib-induced mast cell downregulation would serve as evidence for their pathogenic contribution to NMJ denervation. Figure 3A shows representative transversal sections of the EDL muscle in advanced paralysis from SOD1^{G93A} rats treated with vehicle and with masitinib. Compared with vehicle-treated rats, masitinib almost completely prevented mast cell accumulation and degranulation, the cell numbers being nonsignificantly different than those of rats at the onset of paralysis (Figure 3, A and B). Masitinib treatment also prevented the interstitial infiltration of macrophages assessed by CD11b staining in the EDL muscle during advanced paralysis (Figure 3C). These results are consistent with a synergistic action of masitinib-downregulating inflammatory activity of mast cells and inhibiting CSF-1R in macrophages (27).

Masitinib-induced reduction of mast cells was associated with preserved innervation of motor endplates. Paralysis progression in ALS correlates with anatomical contact between muscular nerve terminals and motor endplates (39, 40). Thus, we have analyzed the effect of masitinib-induced downregulation of mast cells on the NMJ innervation pattern in the EDL muscle. Figure 4 shows representative microscopic fields illustrating the sequence of progressive denervation between paralysis onset and advanced paralysis as compared with NonTg EDL muscles. About 35% of EDL muscle motor endplates at onset exhibited denervation, as assessed by NMJ occupancy calculated as motor endplates devoid of presynaptic terminals (yellow colocalization in Figure 4A). Fifteen days

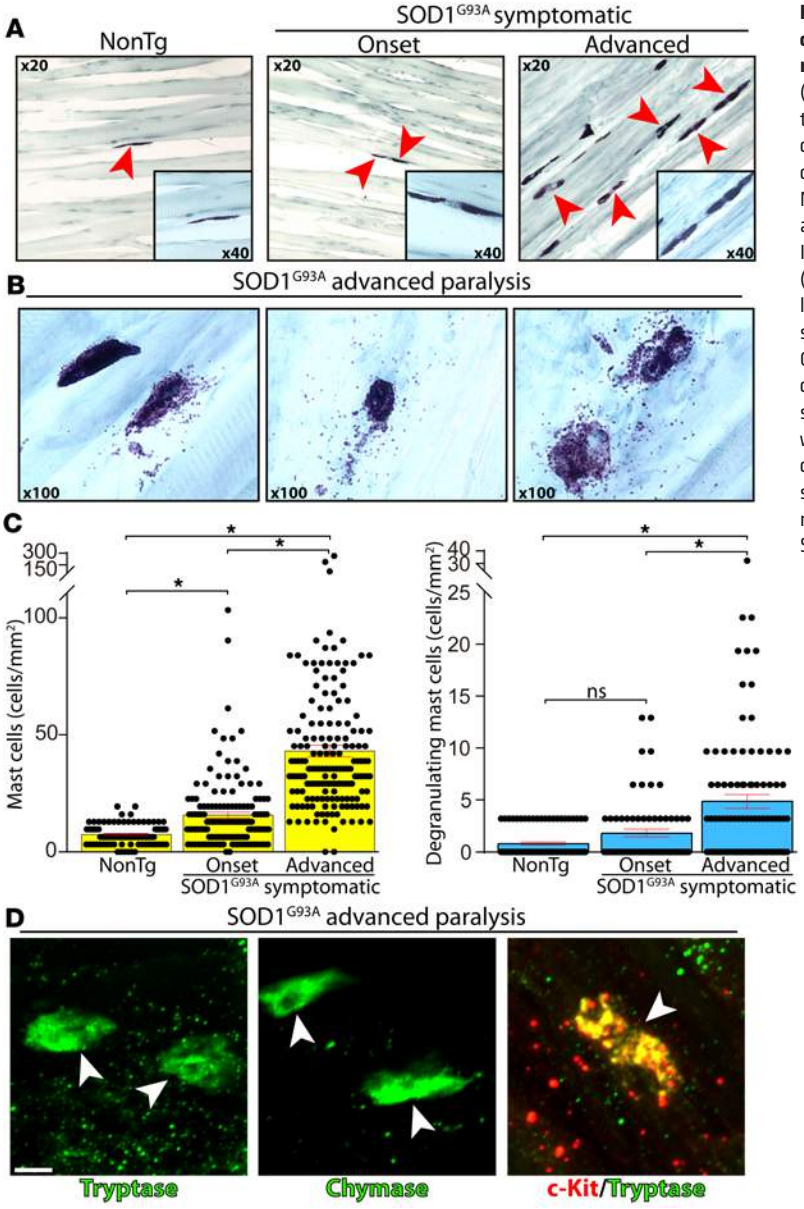

Figure 1. Endomysial infiltration and degranulation of mast cells in the extensor digitorum longus (EDL) muscle of SOD1^{G93A} rats. Longitudinal cryostat sections of NonTg and SOD1^{G93A} rat (onset and advanced paralysis) EDL muscles were stained with toluidine blue to visualize mast cells. (**A**) Few endomysial mast cells were observed in NonTg and mSOD1-onset EDL muscles as compared with numerous mast cells during advanced paralysis. Note the sharp increase in mast cell density between onset and advanced paralysis conditions (arrowheads indicate mast cells). Insets show a 40× magnification of Toluidine blue+ mast cells. (**B**) Representative toluidine blue images of different degranulating mast cell morphologies during the advanced symptomatic stage, displaying the release of metachromatic granules. (**C**) Quantitative analysis showing the significant increase in mast cell number and degranulation correlating with paralysis progression. All quantitative data are expressed as mean ± SEM; data were analyzed by Kruskal-Wallis followed by Dunn's multiple comparison test, $^*P < 0.01$. (**D**) Representative confocal images showing immunoreactivity to tryptase, chymase, and c-Kit in mast cells (arrowheads) from advanced paralysis EDL muscle. Scale bar: 10 μm. n = 4–5 animals/condition.

after paralysis progression, the motor phenotype advanced into advanced paralysis stage and large areas of EDL muscle displayed complete NMJ denervation (data not shown), with the percent of motor endplate denervation being close to 80% (Figure 4B). Remarkably, masitinib treatment significantly prevented motor endplate denervation with respect to vehicle-treated rats, exhibiting similar denervation values to paralysis onset (Figure 4B). The NMJ protection by masitinib was also evidenced in the functional inverted screen motor test (Figure 4C), where treatment improved the latency-to-fall by 15%–25 % from 5–15 days after onset .

Postparalysis masitinib treatment prevented the pathological remodeling of Schwann cells and vascular networks associated to progressive paralysis. Perisynaptic Schwann cells are glial cells at the NMJs that ensure the synapse stability, maintenance, and repair during damage or denervation (41). Perisynaptic Schwann cells respond to ALS-induced denervation with profound morphological and phenotypic changes (17), retracting processes from the NMJs while extending processes to other endplate areas (42). Therefore, we examined whether downregulation of mast cells in masitinib-treated rats was associated to preservation of perisynaptic Schwann cells in the EDL muscle, as analyzed by confocal microscopy followed by 3-D reconstructions. Figure 5A and Supplemental Figure 2 show that NMJ denervation correlated with fewer nestin$^+$ and S100β$^+$ perisynaptic Schwann cells overlapping with NMJs as compared with those in NonTg or paralysis-onset EDL muscles. In comparison, the number of perisynaptic Schwann cells overlapping with NMJs was largely preserved in masitinib-treated rats (Figure 5A), being comparable with the number at the onset of paralysis.

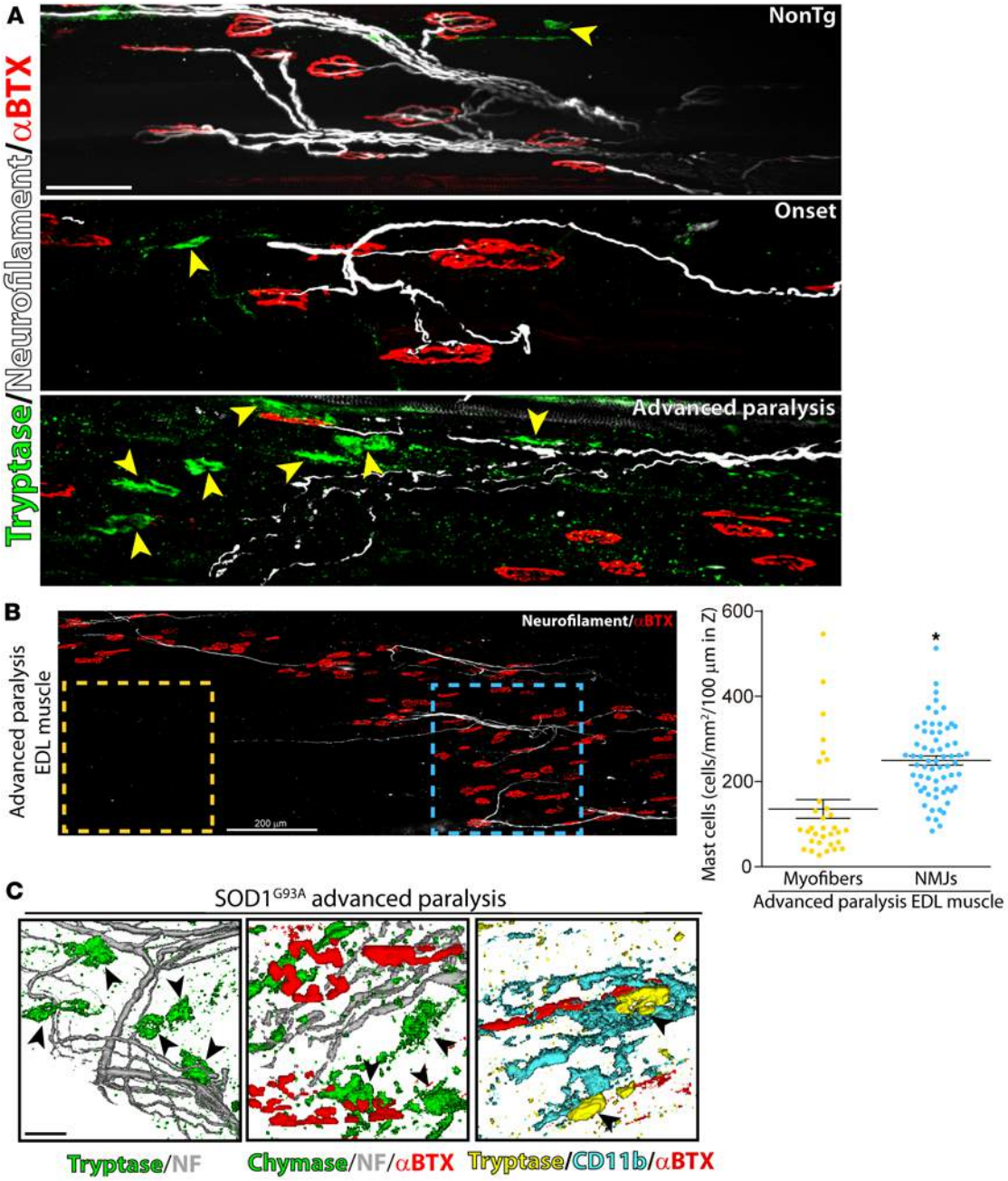

Figure 2. Spatial interaction of mast cells with motor nerve endings, neuromuscular junctions (NMJs), and macrophages during paralysis progression. Whole mount of extensor digitorum longus (EDL) muscles were processed for IHC and visualized in the confocal microscope. (**A**) Representative confocal images showing the interaction of mast cells with motor nerve endings and NMJs. Branches of motor axons were immunostained for anti-neurofilament (NF, white), motor endplates for α-bungarotoxin (α-BTX, red), and mast cells for tryptase (green, yellow arrowheads). Note the clustering of mast cells surrounding degenerating and fragmenting motor nerve endings and denervated NMJs during advanced paralysis (n = 4 animals/condition). (**B**) Comparative analysis of mast cell density in EDL-muscle NMJ compartment (blue square) versus muscle parenchyma devoid of plates (yellow square). The graph shows the cell density expressed as number of cells per mm² in a 100-μm Z-stack. Data are expressed as mean ± SEM: data were analyzed by Mann-Whitney U test, 2-tailed, $^*P < 0.01$. Confocal microphotograph in **B** is a representative image of the EDL muscle from a symptomatic SOD1^{G93A} rat to illustrate the regions used for quantitative analysis. (**C**) Representation of the interaction of chymase$^+$/tryptase$^+$ mast cells (green, arrowheads) with motor nerve endings (gray) and NMJs endplates (α-BTX, red). The right panel shows a representative image of the interaction between CD11b$^+$ macrophage–like cells (blue) with mast cells (yellow) in the surrounding of a NMJ (red). Scale bars: 50 μm (**A**) and 15 μm (**C**). n = 4 animals/condition for **A** and **C**.

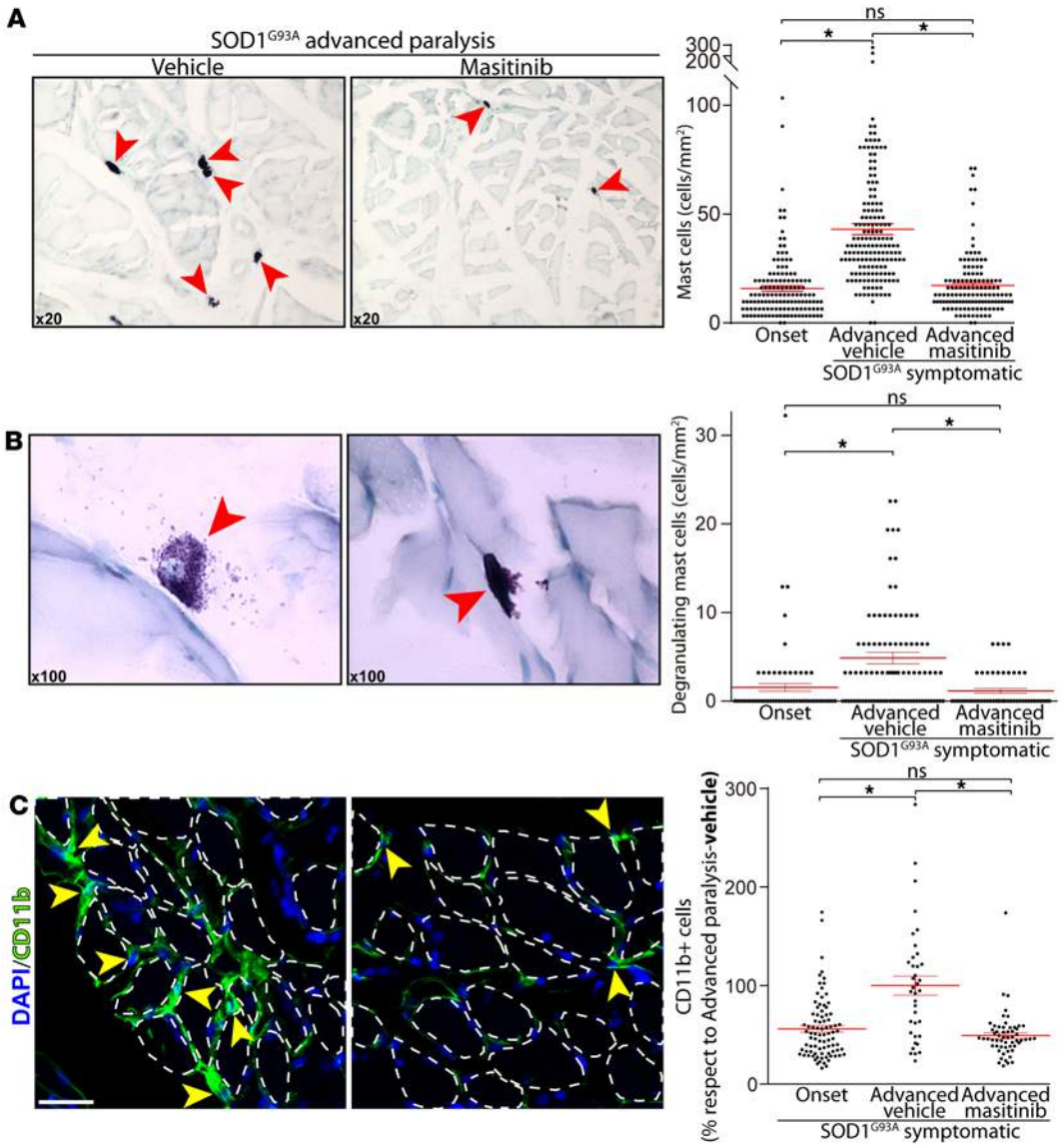

Figure 3. Masitinib treatment reduces mast cell infiltration and degranulation into extensor digitorum longus (EDL) muscle during advanced paralysis. Masitinib (30 mg/kg) or vehicles were orally administered during 15 days after paralysis onset, and rats were processed for histochemical analysis of the EDL muscles. (**A** and **B**) Representative microscopic fields of transversal sections of EDL muscle stained with toluidine blue, showing the number and degranulation of mast cells. Note the sharp reduction in mast cell number, size, and degranulating pictures in masitinib-treated rats as compared with controls. The graphs to the right show the quantitative analysis of the number of total mast cells (upper) and degranulating mast cells (lower) assessed in toluidine blue–stained sections. (**C**) Representative microscopic fields of transversal sections of EDL muscle immunostained with CD11b. Myofibers are delineated by dashed lines. Note the reduction of endomysial macrophage infiltrating the EDL muscles in masitinib-treated rats as compared with controls. The CD11b macrophage–like cell (yellow arrowheads) infiltration area was assessed by IHC. Values for paralysis onset and advanced paralysis–masitinib are expressed as percent respect to advanced paralysis–vehicle. All quantitative data are expressed as mean ± SEM; data were analyzed by Kruskal-Wallis followed by Dunn's multiple comparison test, $^*P < 0.01$. n = 4–5 animals/condition. Scale bar: 25 μm (**C**).

Innervated muscles display a dense network of capillaries that distribute along the interstitial spaces close to myofibrils (43). However, there is scarce knowledge about vascular remodeling occurring in muscles affected in ALS. As shown in Figure 5B, regions with NMJ denervation in EDL muscle 15 days after paralysis onset displayed a systematic reduction of capillary network, suggestive of failing microcirculation. A 15-day treatment with masitinib significantly prevented this pathological vascular remodeling, in parallel with preserved NMJ innervation.

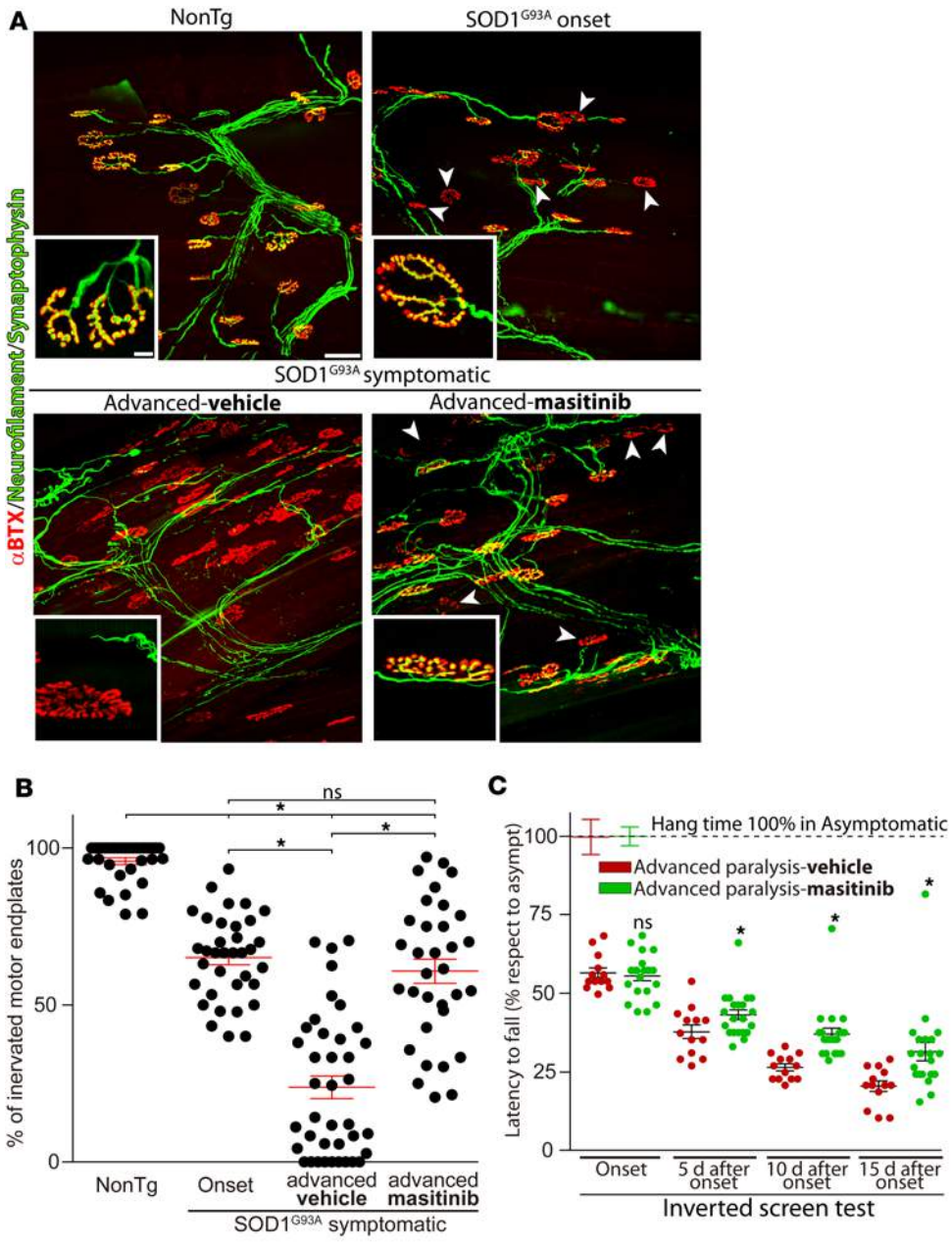

Figure 4. Masitinib treatment prevented neuromuscular junction (NMJ) denervation. (**A**) Masitinib or vehicle was administered as described above and whole mounted extensor digitorum longus (EDL) muscles were processed for IHC. The panels show representative confocal images used to assess the innervation pattern of NMJs in different experimental conditions. α-Bungarotoxin-FITC (α-BTX, red) staining was used to analyze motor endplates. Synaptophysin–Alex Fluor 555 and heavy chain of neurofilaments–Alexa Fluor 555 (green) were used to visualize the motor axon branches and presynaptic terminals. Insets show higher-magnification images of innervated (yellow colocalization) or denervated (red) NMJs. Arrowheads indicate typical denervated motor endplates. Scales bars: 50 μm and 10 μm for insets. (**B**) The graph represents the quantitative analysis of NMJ occupancy defined as the overlapping of synaptophysin and α-BTX staining and expressed as percentage with respect to the nonTg condition. Note the massive loss of innervation occurring between onset and advanced paralysis in vehicle-treated rats and its prevention by masitinib. n = 4–5 animals/condition; at least 100 NMJs were analyzed per muscle, per animal. Data are expressed as mean ± SEM; data were analyzed by Kruskal-Wallis followed by Dunn's multiple comparison test, $^*P < 0.01$. (**C**) The inverted screen test was used to measure motor function. For each animal, hang time from an inverted grid was recorded in seconds and expressed as percent of the value of asymptomatic rats (100%). n = 14 and n = 22 for vehicle- and masitinib-treated groups, respectively. Data are expressed as mean ± SEM; data were analyzed by Mann-Whitney U test, 2-tailed, $^*P < 0.01$.

Discussion

Here, we report that mast cells and macrophages directly interact with degenerating motor nerve endings and motor endplates in symptomatic SOD1^{G93A} rats. In particular, the increased number and degranulation of mast cells correlated with paralysis progression, suggesting mast cells may be deleterious for the maintenance of functional NMJs. Downregulation of mast cells and macrophage infiltration by means of systemic treatment with the tyrosine kinase inhibitor masitinib significantly reduced the rate of NMJ denervation and motor deficits, further indicating inflammation as a relevant pathogenic mechanism aggravating distal axonopathy and paralysis progression in ALS. Masitinib also prevented the rapid pathological remodeling of Schwann cells and capillary networks observed after paralysis onset, which is consistent with a preserved functioning of the EDL muscle. Remarkably, our findings also provide a significant mechanism of action for masitinib at degenerating NMJs, which may have clinical therapeutic relevance for ALS.

Previous studies have not paid attention to mast cell infiltration in affected muscles from ALS patients or animal models. In symptomatic SOD1^{G93A} rats, we found striking changes in the number, phenotype, and spa-

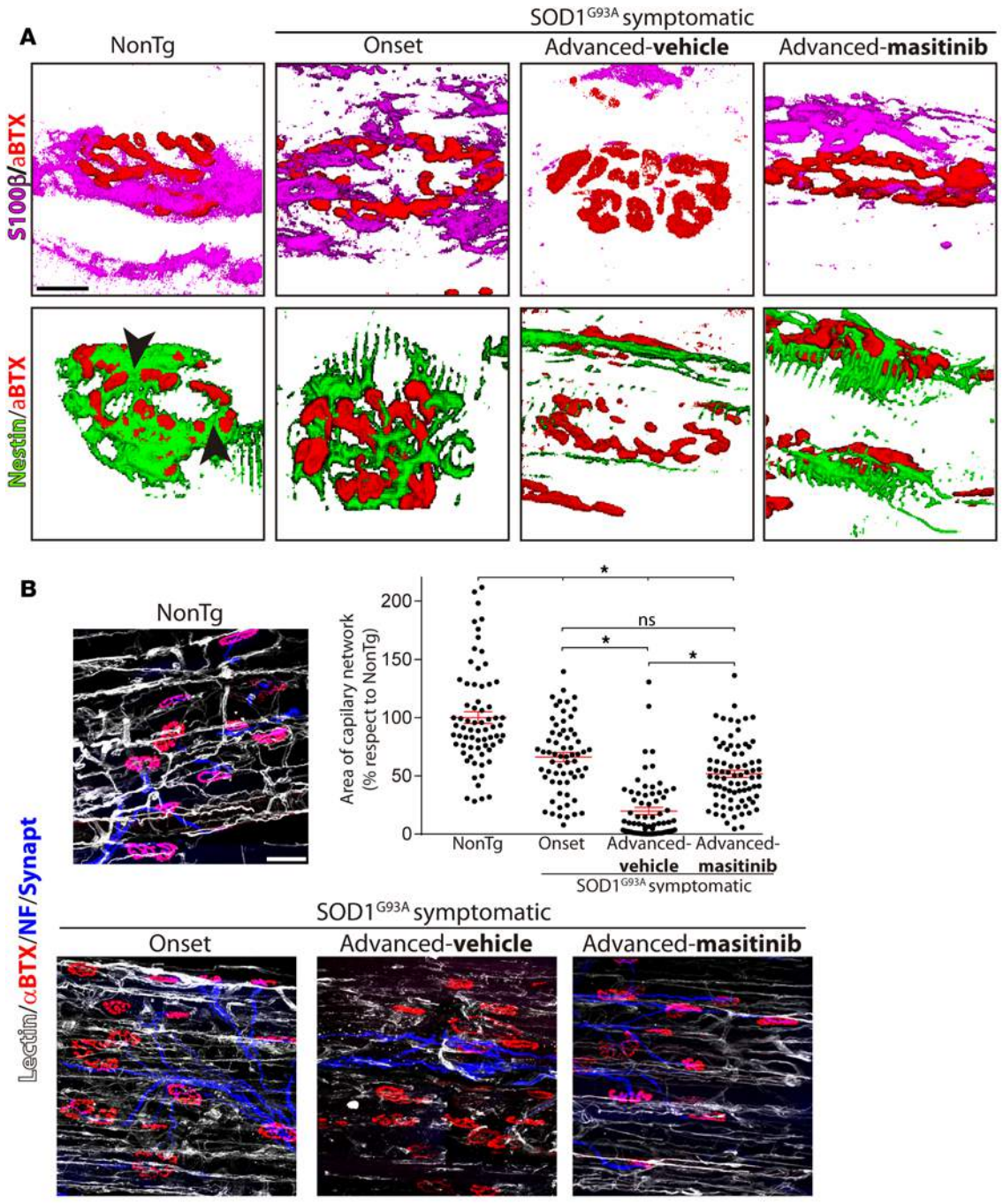

Figure 5. Masitinib prevented perisynaptic Schwann cell and capillary network remodeling in extensor digitorum longus (EDL) muscle during advanced paralysis. Longitudinal cryostat sections of NonTg and SOD1^{G93A} rat (onset and advanced paralysis) EDL muscles were processed for IHC to visualize neuromuscular junctions (NMJs), perisynaptic Schwann cells, and the capillary network. (**A**) Representative 3-D reconstruction of the spatial interactions between α-bungarotoxin$^+$ motor endplates (α-BTX, red) and perisynaptic S100β$^+$ (magenta) and nestin$^+$ (green) Schwann cells. Original confocal images are shown in Supplemental Figure 2. In normal NonTg rat EDL muscle, Schwann cells covered the endplates and filled the spaces between adjacent gutters (arrowheads). In contrast, during the symptomatic phase, most nestin$^+$ and S100β$^+$ cells progressively retracted from the NMJs no longer overlapping the motor endplates. Masitinib treatment prevented the associated retraction of Schwann cells from NMJs observed during advanced paralysis. (**B**) Representative images of capillary network assessed with tomato-isolectin staining (white) in EDL muscle areas with high density of motor nerve terminals (blue) and NMJ (red). Note the loss of capillary networks in symptomatic rats. The graph shows the quantitative analysis of total areas stained by lectin in NMJ-rich regions in different experimental conditions. Data are expressed as mean ± SEM; data were analyzed by Kruskal-Wallis followed by Dunn's multiple comparison test, $^*P < 0.01$. $n = 4$ animals/condition. Scale bars: 50 μm (**A**) and 10 μm (**B**).

tial location of mast cells in rat EDL muscle, installing in a short period of time (2 weeks) after paralysis onset. These changes are consistent with a causal association between the underlying neuromuscular pathology and a complex inflammatory process, likely orchestrated by degranulation of mast cells, further accelerating denervation. In comparison, mast cell degranulation has been described in patients with muscular dystrophy and autoimmune myositis (22, 44), the cells likely inducing injury of myofibers and further recruitment of inflammatory cells through the secretion of proteases (45, 46). It is uncertain if similar mast cell–mediated myofiber toxicity also occurs in ALS. Nonetheless, about half of ALS patients exhibit robust increases in serum creatine kinases (47), indicating sustained myofiber injury potentially mediated by mast cell infiltration. Thus, serum creatine kinase might be a useful biomarker of active mast cell–mediated pathology in ALS patients.

The finding of frequent explosive mast cell degranulation in the EDL muscle during advanced paralysis is intriguing, and it anticipate multiple local responses mediated by secreted proteases, cytokines, trophic factors and vasoactive mediators (48). The release of metachromatic granules indicates the secretion of heparin derivatives, which promote regenerative pathways in muscle, mediated in part by FGF signaling (36). At the same time, heparan sulphate may impair the formation of neuromuscular functions in vitro by direct binding to neural agrin (49). The unregulated or overstimulated mast cells can also lead to fibrosis and collagen deposition via the release of several mediators, such as cytokines and TGFβ (50, 51). In turn, fibrosis could adversely affect motor nerve axon plasticity and growth, as well as NMJ reinnervation. A marked fibrotic process in skeletal muscle of symptomatic $SOD1^{G93A}$ mice has been reported, involving increased deposition of extracellular matrix molecules such as fibronectin and collagen I and -III (52). Mast cells can also release nerve growth factor (NGF) species, leading to the recruitment of T-lymphocytes (53, 54) or deleterious signaling through 75-kD neurotrophin receptor ($p75^{NTR}$) receptors expressed in either motor nerve terminals or Schwann cells (55). Thus, degranulating mast cells have the potential to directly or indirectly trigger damage of myofibers, motor nerve endings, Schwann cells, and capillary networks.

The proposed pathogenic role of mast cells in the neuromuscular compartment appears to be in conflict with a previous report showing that developmental mutation in kit genes, which limits the expression of c-Kit in SOD1G93A mice, results in reduced survival, despite having a decreased number of mast cells in the spinal cord (56). However, this phenotype could be explained by different concomitant developmental alterations of mice, such as defective myelination and neural progenitors that might create increased vulnerability to mutant SOD1 overexpression. This scenario profoundly differs from our finding of detrimental mast cell activity in ALS, which is spatially and temporally restricted to NMJ pathology during postparalysis stages. Therefore, the appropriate functional phenotype or activation of mast cells appears to be of critical importance, as opposed to their absolute number in the neuromuscular compartment. Consequently, a preferred therapeutic strategy would be downregulation of mast cell activity rather than their pharmacological depletion.

Little is known about the mechanisms of chemoattraction and differentiation of mast cell precursors to ALS-affected muscles. Primary myofiber damage associated with denervation or muscle-restricted expression of mutant SOD1 (57) is a plausible mechanism. Alternatively, a currently unknown mechanism of neurogenic recruitment of mast cells can be anticipated, as evidenced by the close spatial interaction between mast cells and degenerating motor nerve endings and denervated NMJs. A bidirectional interaction between nerves and mast cells is a well-recognized mechanism in neurogenic inflammation triggered by sensory and autonomic nerve endings (58, 59). This mechanism is known to be largely mediated by substance P released by axon terminals (60). Substance P does not seem to be expressed in healthy rodent motor neurons but rather is found in significant levels in muscle fibers (61). Other putative mast cell chemoattractant molecules in ALS-affected muscles include TNFα, NGF, and ATP produced by either degenerating motor nerve endings, denervated myofibers, perisynaptic Schwann cells, or inflammatory cells. Finally, intact motor nerve terminals release the neurokinin calcitonin gene related protein (CGRP) (62), also capable of modulating mast cell degranulation through specific receptors (58). It is reported that CGRP expression and release in motor neurons is involved in maintenance of NMJs and inversely correlated to neuronal survival (63). Thus, dysfunctional motor nerve terminals might trigger mast cell accumulation and activation in the neuromuscular compartment during ALS.

Mast cell accumulation in EDL muscle was paralleled by accumulation of $CD11b^+$ macrophage–like cells in the same neuromuscular compartment, suggesting a crosstalk between these immune cells as part of a complex pathological process. Previous studies have described $CD11b^+$ and $CD68^+$ macrophage infiltrates close to NMJs in $SOD1^{G93A}$ rats and mice (7, 64), a scenario that was partially reverted by protective interventions in ALS rats (64). Also, $CD68^+$ macrophages infiltrating the interstitial space between myofibers have been described in the skeletal muscle of ALS patients (18).

As expected, we found that tyrosine kinase inhibition with masitinib treatment downregulated the mast cell recruitment in degenerating EDL muscle, which in turn resulted in a significant and complete interruption of NMJ denervation in the 15 days after paralysis onset. This mechanism of action of masitinib in muscle was unknown and complementary to a previously described effect of the drug-inhibiting neuroinflammation in the lumbar spinal cord of SOD1^{G93A} rats (27). Thus, the significant increase in SOD1^{G93A} rats after paralysis survival, when treated with masitinib at paralysis onset, might be explained by a simultaneous and probably synergist effect of the drug on deleterious inflammation that accelerates paralysis progression.

Neuroprotection by masitinib was originally associated to inhibition of tyrosine kinase receptor CSF-1R in microglia and aberrant glial cells that typically proliferate after paralysis onset (27). Because masitinib inhibits various tyrosine kinases, including c-Kit, CSF-1R, PDGF-R, Lyn, and Fyn, it could potentially downregulate other cell types, including mast cells as well as monocytes and macrophages (25, 26). In particular, c-Kit receptor activation by stem cell factor is needed for the differentiation of mast cells from precursors (65). It is presently unknown whether stem cell factor is upregulated in ALS-affected muscles; however, it could be expressed by Schwann cells, as described previously in neurofibromatosis type-1 (66).

Masitinib treatment also prevented the regressive remodeling of perisynaptic Schwann cells described in ALS (67, 68). Because Schwann cell dissociation from NMJ is mainly caused by the axon retraction from motor plates (17, 68), our results further suggest the halt of distal motor axon degeneration following treatment with masitinib. A potential important finding for ALS pathogenesis is the almost complete disappearance we found of capillaries in EDL muscle areas devoid of NMJ innervation. This loss was prevented by masitinib. Degranulating mast cells could potentially mediate this effect through yet-unknown mechanisms. CNS microvascular pathology has been described in ALS (69) and could lead to local hypoxia further promoting recruitment of mast cells, as has been reported in ischemia-reperfusion of skeletal muscle (70). A similar microcirculation failure has been reported in other neuromuscular pathologies such as spinal muscle atrophy or muscular dystrophy (71, 72).

In conclusion, the present study addressed one key issue about ALS pathogenesis and therapeutics: the identification of mast cells orchestrating inflammation in the cellular microenvironment of the neuromuscular compartment with the potential to accelerate NMJ denervation after paralysis onset. Mast cells were abundant in the endomysium during paralysis progression and typically clustered with macrophages close to motor nerve terminals, suggesting a neurogenic and/or myogenic induction. Moreover, pharmacological downregulation of mast cells and other immune effectors with masitinib prevented not only NMJ denervation, but also regressive changes in Schwann cells and capillary networks. These mechanisms of action make masitinib a potentially novel ALS drug, capable of exerting multifaceted neuroprotection in both central and peripheral nervous systems via selective kinase inhibition.

Methods

Animals. Male SOD1^{G93A} progeny were used for further breeding to maintain the line (Taconic Biosciences Inc., NTac:SD-Tg(SOD1G93A)L26H). Rats were housed in a centralized animal facility with a 12-hour light-dark cycle with ad libitum access to food and water. Perfusion with fixative was performed under 90% ketamine (Phs Pharmaservice) and 10% xylazine (Xylased) anesthesia, and all efforts were made to minimize animal suffering, discomfort or stress.

Experimental conditions. At least 4 rats were analyzed for each experiment. Four different conditions were studied as follows: i) NonTg rats 160–180 days old; ii) transgenic SOD1^{G93A} rats 180–190 days old (symptomatic, onset); iii) transgenic SOD1^{G93A} rats 195–210 days old treated with vehicle (symptomatic, advanced paralysis-vehicle), and iv) transgenic SOD1^{G93A} rats 195–210 days old treated with 30 mg/kg/d of masitinib during 15 days (symptomatic, advanced paralysis-masitinib).

Determination of disease onset and end-stage. As described previously (27), all rats were weighed and evaluated for motor activity daily. Disease onset was determined for each animal when pronounced muscle atrophy was accompanied by abnormal gait, typically expressed as subtle limping or dragging of one hind limb. When necessary, end-stage was defined by a lack of righting reflexes or the inability to reach food and water.

Masitinib administration. As described previously (27), only transgenic rats showing weakness and gait alterations in hind limbs as first clinical sign were selected for masitinib treatment studies. Male and female rats were divided randomly into the masitinib or vehicle-treated groups. Masitinib mesylate (AB1010, manufactured and provided by ABScience), freshly prepared in drinking sterilized water, was administrated daily at a dose of 30 mg/kg using a curved stainless steel gavage needle with 3-mm ball tip

(Kent Scientific Corp). Dosing was defined in accordance with previous studies in the same rat model of ALS that was shown to be safe for chronic treatments (27). Rats were treated from day 1 after paralysis for an additional 15 days, when they were then euthanized.

Inverted screen test. Twelve vehicle- and 16 masitinib-treated rats were placed on a metal grid screen (45 × 30 cm). After placement, the rats were allowed time to grip before the grid was inverted 50 cm over a cage containing fresh bedding. Latency to fall was recorded up to 30 seconds. Three independent measurements were recorded 10 minutes apart during the day of testing, and data of 3 measurements were averaged. Measurements started at approximately 5 months (1 month before onset, approximately) and continued during 15 days after onset. Latency to fall was plotted (percentage with respect to asymptomatic stage), considering the time of grip during the asymptomatic stage as 100%.

IHC of whole mounted muscle. Rats were deeply anesthetized using 90% ketamine and 10% xylazine anesthesia and were fixed by perfusion with 4% paraformaldehyde (MilliporeSigma) in PBS (AppliChem). Extensor digitorium longus (EDL) muscles from the hind limb were dissected. Then, tissues were blocked for 2 hours at room temperature (5% BSA, 0.8% Triton X-100 in PBS), incubated with primary antibodies at 4°C overnight: 1:300 mouse monoclonal anti-nestin (GeneTex, GTX26142), 1:400 mouse monoclonal anti-S100β (MilliporeSigma, S2532), 1:250 mouse monoclonal anti–CSF-1R (Santa Cruz Biotechnology Inc., sc-46662), 1:300 rabbit polyclonal anti-Iba1 (Wako, 019-19741), 1:250 mouse monoclonal anti-CD68 (Abcam, ab31630), 1:200 mouse monoclonal anti-CD11b (BD Biosciences, BD550299), 1:200 rabbit polyclonal anti-Tryptase (Abcam, ab134932), 1:250 mouse monoclonal anti-chymase (Abcam, ab2377), and rat polyclonal anti–c-Kit-Biotin (Abcam, ab25022). Then, tissue was washed with PBS 3 times for 5 minutes, incubated with secondary antibodies (1:500 goat anti–mouse Alexa Fluor 633 [Thermo Fisher Scientific, A21052], 1:500 goat anti–rabbit Alexa Fluor 546 [Thermo Fisher Scientific, A11035] or -633 [Thermo Fisher Scientific, A21071], 1:500 streptavidin-633 [Thermo Fisher Scientific, #S21375] and/or fluorescently labeled α-bungarotoxin-FITC [α-BTX, Thermo Fisher Scientific, B13422]) for 2 hours at room temperature, washed with PBS 3 times for 15 minutes, and whole mounted in DPX mounting medium (MilliporeSigma) on slides. Axon staining was carried out using 1:1,000 heavy chain neurofilament-Alexa Fluor 555 (MilliporeSigma, MAB5256A5), and axon presynaptic terminals were labeled with 1:300 synaptophysin–Alexa Fluor 555 (Abcam, ab206870). Capillary networks were visualized using an isolectin-biotin/streptavidin-633 1:300 probe (Thermo Fisher Scientific, I21414).

Comparative analysis of mast cells in myofiber and NMJ compartments. Tryptase$^+$ mast cells were counted in whole-mounted EDL muscle using a stereological approach, contrasting mast cell number in 2 predefined muscle compartments: the region surrounding the motor end plates (NMJ compartment) versus muscle parenchyma devoid of plates. At least 50 confocal stacks (320 × 320 × 100 μm in Z-stacks) of 4 SOD1^{G93A} symptomatic animals were analyzed as shown in Figure 2B.

NMJ analysis. Structural changes of the NMJ were scored using maximum-intensity projections of images acquired from whole-mounted muscles. Briefly, NMJ innervation analysis was performed taking into consideration those postsynaptic motor endplates occupied by a presynaptic axon terminal, where full innervation was defined as at least 80% of overlapping between pre- and postsynapsis. An average of 100 NMJs per animal was analyzed using the ImageJ software.

Muscle cryopreserved sections. Paraformaldehyde (4%) fixed extensor muscle was dissected and cryopreserved in 30% sucrose (MilliporeSigma) at 4°C. The 72-hour preserved muscle was embedded in TissueTek (Sakura) sectioned (longitudinal and transverse) at 10 μm using a cryostat and collected on gelatin-coated slides. Sections were blocked for 1 hour at room temperature (5% BSA, 0.5% Triton X-100 in PBS), incubated with primary antibodies overnight at 4°C (1:250 mouse monoclonal anti-Chymase [Abcam, ab2377], 1:250 rat polyclonal anti–c-Kit-biotin [Abcam, ab25022], 1:200 rabbit polyclonal anti-tryptase [Abcam, ab134932], and 1:200 mouse monoclonal anti-CD11b [BD Bioscience, 550299]), washed with PBS 3 times for 10 minutes, incubated with secondary antibodies for 2 hours at room temperature (1:500 goat anti–rabbit Alexa Fluor 488 [Thermo Fisher Scientific, A11034], 1:500 goat anti–mouse Alexa Fluor 633 [Thermo Fisher Scientific, A21052], and 1:500 streptavidin-Alexa Fluor 633 [Thermo Fisher Scientific, S21375]), washed with PBS 3 times for 5 minutes, and mounted in DPX.

Toluidine blue staining. For the mast cell analysis based in metachromasia observation, 10-μm sections of paraformaldehyde-fixed extensor muscle were cryostat sliced and mounted in gelatin-coated slides. Sections were washed and hydrated 2 times in distilled water for 10 minutes and embedded in 1% toluidine blue solu-

tion for 10 minutes. Then, slides were washed in distilled water 3 times for 5 minutes and dehydrated during 3 minutes in 70% ethanol, 3 minutes in 95% ethanol, and finally 2 minutes in 100% ethanol. Slides were cleared in xylene twice for 3 minutes each and finally mounted in DPX (MilliporeSigma). Images (10×, 20×, 40×, and 100×) were acquired using an Olympus CX41 microscope connected to a Evolution LC Color camera and using ImagePro Express software for adquicition. The number of toluidine blue$^+$ metachromatic mast cells was counted using the ImageJ software, in at least 40 fields per muscle per animal using a magnification of 10×. Degranulating mast cells, characterized by extensive metachromatic granules being released by an isolated mast cell, were counted using 20× magnification in serial pictures of each muscle section.

Fluorescence Imaging. Fluorescence imaging was performed with a laser scanning confocal microscope (Zeiss LSM 880 or Zeiss LSM 800) with either a 25× (1.2 numerical aperture) objective or 63× (1.3 numerical aperture) oil-immersion objective using Zeiss Zen Black software. Maximum intensity projections of optical sections were created with Zeiss Zen software, as were 3-D reconstructions.

Statistics. Quantitative data were expressed as mean ± SEM. Two-tailed Mann-Whitney test or Kruskal-Wallis followed by Dunn's multiple comparison test were used for statistical analysis, with $P < 0.01$ considered significant. GraphPad Prism 7.03 software was used for statistical analyses.

Study approval. All procedures using laboratory animals were performed in accordance with the national and international guidelines and were approved by the Institutional Animal Committee for animal experimentation. All experimental procedures were approved by the Ethical Committee for the use of Experimental Animals (CEUA) of the Institut Pasteur de Montevideo, Uruguay, and under the current ethical regulations of the Uruguayan Law 18.611 for animal experimentation that follows the Guide for the Care and Use of Laboratory Animals of the National Institutes of Health (National Academies Press, 2011).

Author contributions

ET, LB, OH, and JSB designed the study. ET, SI, RBN, and VV performed experiments. ET, SI, RBN, ICM, PD, and LB analyzed data. ET, OH, JSB, and LB prepared the manuscript. All authors contributed to discussion of the results and edited and approved the final version.

Acknowledgments

This work was supported by Institut Pasteur de Montevideo – FOCEM Mercosur (COF 03/11), the Amyotrophic Lateral Sclerosis Association (00482), Department of Defense (AL140108), Agencia Nacional de Investigación e Innovación (ANII), Programa de Desarrollo de las Ciencias Básicas (PEDECIBA), and ECOS-*Sud* Program (U014S02). Partial funding was received from AB Science. We want to thank Colin Mansfield for his critical comments and helpful suggestions revising the manuscript, the staff from the Transgenic and Experimental Animal Unit from Institut Pasteur de Montevideo, and Pablo Fresia for his advice on statistical analysis. Finally, the authors wish to acknowledge the Confocal Microscopy Facility of the Center for Genome Research and Biocomputing at Oregon State University.

Address correspondence to: Luis Barbeito, Institut Pasteur de Montevideo, Mataojo 2020, Montevideo 11.400, Uruguay. Phone: 00.598.2.522.0910; Email: barbeito@pateur.edu.uy.

1. Rowland LP, Shneider NA. Amyotrophic lateral sclerosis. *N Engl J Med*. 2001;344(22):1688–1700.
2. Fischer LR, et al. Amyotrophic lateral sclerosis is a distal axonopathy: evidence in mice and man. *Exp Neurol*. 2004;185(2):232–240.
3. Ilieva H, Polymenidou M, Cleveland DW. Non-cell autonomous toxicity in neurodegenerative disorders: ALS and beyond. *J Cell Biol*. 2009;187(6):761–772.
4. Philips T, Robberecht W. Neuroinflammation in amyotrophic lateral sclerosis: role of glial activation in motor neuron disease. *Lancet Neurol*. 2011;10(3):253–263.
5. Trias E, Ibarburu S, Barreto-Núñez R, Barbeito L. Significance of aberrant glial cell phenotypes in pathophysiology of amyotrophic lateral sclerosis. *Neurosci Lett*. 2017;636:27–31.
6. Butovsky O, et al. Modulating inflammatory monocytes with a unique microRNA gene signature ameliorates murine ALS. *J Clin Invest*. 2012;122(9):3063–3087.
7. Chiu IM, et al. Activation of innate and humoral immunity in the peripheral nervous system of ALS transgenic mice. *Proc Natl Acad Sci USA*. 2009;106(49):20960–20965.
8. Graber DJ, Hickey WF, Harris BT. Progressive changes in microglia and macrophages in spinal cord and peripheral nerve in the transgenic rat model of amyotrophic lateral sclerosis. *J Neuroinflammation*. 2010;7:8.
9. Martínez-Muriana A, et al. CSF1R blockade slows the progression of amyotrophic lateral sclerosis by reducing microgliosis and invasion of macrophages into peripheral nerves. *Sci Rep*. 2016;6:25663.
10. Nardo G, et al. Immune response in peripheral axons delays disease progression in SOD1(G93A) mice. *J Neuroinflammation*.

2016;13(1):261.
11. Rosen DR. Mutations in Cu/Zn superoxide dismutase gene are associated with familial amyotrophic lateral sclerosis. *Nature*. 1993;364(6435):362.
12. Gurney ME, et al. Motor neuron degeneration in mice that express a human Cu,Zn superoxide dismutase mutation. *Science*. 1994;264(5166):1772–1775.
13. Howland DS, et al. Focal loss of the glutamate transporter EAAT2 in a transgenic rat model of SOD1 mutant-mediated amyotrophic lateral sclerosis (ALS). *Proc Natl Acad Sci USA*. 2002;99(3):1604–1609.
14. Kennel PF, Finiels F, Revah F, Mallet J. Neuromuscular function impairment is not caused by motor neurone loss in FALS mice: an electromyographic study. *Neuroreport*. 1996;7(8):1427–1431.
15. Bilsland LG, Sahai E, Kelly G, Golding M, Greensmith L, Schiavo G. Deficits in axonal transport precede ALS symptoms in vivo. *Proc Natl Acad Sci USA*. 2010;107(47):20523–20528.
16. Dadon-Nachum M, Melamed E, Offen D. The "dying-back" phenomenon of motor neurons in ALS. *J Mol Neurosci*. 2011;43(3):470–477.
17. Arbour D, Vande Velde C, Robitaille R. New perspectives on amyotrophic lateral sclerosis: the role of glial cells at the neuromuscular junction. *J Physiol (Lond)*. 2017;595(3):647–661.
18. Jensen L, Jørgensen LH, Bech RD, Frandsen U, Schrøder HD. Skeletal Muscle Remodelling as a Function of Disease Progression in Amyotrophic Lateral Sclerosis. *Biomed Res Int*. 2016;2016:5930621.
19. Frenzel L, Hermine O. Mast cells and inflammation. *Joint Bone Spine*. 2013;80(2):141–145.
20. Sánchez-Mejorada G, Alonso-deFlorida F. Changes in mast-cell distribution in skeletal muscle after denervation. *Muscle Nerve*. 1992;15(6):716–719.
21. Gorospe JR, Nishikawa BK, Hoffman EP. Recruitment of mast cells to muscle after mild damage. *J Neurol Sci*. 1996;135(1):10–17.
22. Yokota M, et al. Roles of mast cells in the pathogenesis of inflammatory myopathy. *Arthritis Res Ther*. 2014;16(2):R72.
23. Porter JD, et al. A chronic inflammatory response dominates the skeletal muscle molecular signature in dystrophin-deficient mdx mice. *Hum Mol Genet*. 2002;11(3):263–272.
24. Graves MC, et al. Inflammation in amyotrophic lateral sclerosis spinal cord and brain is mediated by activated macrophages, mast cells and T cells. *Amyotroph Lateral Scler Other Motor Neuron Disord*. 2004;5(4):213–219.
25. Dubreuil P, et al. Masitinib (AB1010), a potent and selective tyrosine kinase inhibitor targeting KIT. *PLoS ONE*. 2009;4(9):e7258.
26. Anastassiadis T, Deacon SW, Devarajan K, Ma H, Peterson JR. Comprehensive assay of kinase catalytic activity reveals features of kinase inhibitor selectivity. *Nat Biotechnol*. 2011;29(11):1039–1045.
27. Trias E, et al. Post-paralysis tyrosine kinase inhibition with masitinib abrogates neuroinflammation and slows disease progression in inherited amyotrophic lateral sclerosis. *J Neuroinflammation*. 2016;13(1):177.
28. Lortholary O, et al. Masitinib for treatment of severely symptomatic indolent systemic mastocytosis: a randomised, placebo-controlled, phase 3 study. *Lancet*. 2017;389(10069):612–620.
29. Vermersch P, et al. Masitinib treatment in patients with progressive multiple sclerosis: a randomized pilot study. *BMC Neurol*. 2012;12:36.
30. Kocic I, et al. Neuroprotective effect of masitinib in rats with postischemic stroke. *Naunyn Schmiedebergs Arch Pharmacol*. 2015;388(1):79–86.
31. Piette F, et al. Masitinib as an adjunct therapy for mild-to-moderate Alzheimer's disease: a randomised, placebo-controlled phase 2 trial. *Alzheimers Res Ther*. 2011;3(2):16.
32. Mora J, Barbeito L, Hermine O. Masitinib as an add-on therapy to riluzole is beneficial in the treatment of amyotrophic lateral sclerosis (ALS) with acceptable tolerability: Results from a randomized controlled phase 3 trial. Video Lectures. http://videolectures.net/encals2017_barbeito_mora_hermine_therapy/. Published July 21, 2017. Accessed September 22, 2017.
33. Trias E, et al. Phenotypic transition of microglia into astrocyte-like cells associated with disease onset in a model of inherited ALS. *Front Cell Neurosci*. 2013;7:274.
34. Díaz-Amarilla P, et al. Phenotypically aberrant astrocytes that promote motoneuron damage in a model of inherited amyotrophic lateral sclerosis. *Proc Natl Acad Sci USA*. 2011;108(44):18126–18131.
35. Derave W, Van Den Bosch L, Lemmens G, Eijnde BO, Robberecht W, Hespel P. Skeletal muscle properties in a transgenic mouse model for amyotrophic lateral sclerosis: effects of creatine treatment. *Neurobiol Dis*. 2003;13(3):264–272.
36. Lefaucheur JP, Gjata B, Sebille A. Factors inducing mast cell accumulation in skeletal muscle. *Neuropathol Appl Neurobiol*. 1996;22(3):248–255.
37. Dines KC, Powell HC. Mast cell interactions with the nervous system: relationship to mechanisms of disease. *J Neuropathol Exp Neurol*. 1997;56(6):627–640.
38. Forsythe P, Bienenstock J. The mast cell-nerve functional unit: a key component of physiologic and pathophysiologic responses. *Chem Immunol Allergy*. 2012;98:196–221.
39. Murray LM, Talbot K, Gillingwater TH. Review: neuromuscular synaptic vulnerability in motor neurone disease: amyotrophic lateral sclerosis and spinal muscular atrophy. *Neuropathol Appl Neurobiol*. 2010;36(2):133–156.
40. Fischer LR, Glass JD. Axonal degeneration in motor neuron disease. *Neurodegener Dis*. 2007;4(6):431–442.
41. Sugiura Y, Lin W. Neuron-glia interactions: the roles of Schwann cells in neuromuscular synapse formation and function. *Biosci Rep*. 2011;31(5):295–302.
42. Kang H, Tian L, Mikesh M, Lichtman JW, Thompson WJ. Terminal Schwann cells participate in neuromuscular synapse remodeling during reinnervation following nerve injury. *J Neurosci*. 2014;34(18):6323–6333.
43. Plyley MJ, Sutherland GJ, Groom AC. Geometry of the capillary network in skeletal muscle. *Microvasc Res*. 1976;11(2):161–173.
44. Gorospe JR, Tharp M, Demitsu T, Hoffman EP. Dystrophin-deficient myofibers are vulnerable to mast cell granule-induced necrosis. *Neuromuscul Disord*. 1994;4(4):325–333.
45. Abonia JP, et al. Mast cell protease 5 mediates ischemia-reperfusion injury of mouse skeletal muscle. *J Immunol*. 2005;174(11):7285–7291.
46. Oskarsson B. Myopathy: five new things. *Neurology*. 2011;76(7 Suppl 2):S14–S19.

47. Iłzecka J, Stelmasiak Z. Creatine kinase activity in amyotrophic lateral sclerosis patients. *Neurol Sci*. 2003;24(4):286–287.
48. Krystel-Whittemore M, Dileepan KN, Wood JG. Mast Cell: A Multi-Functional Master Cell. *Front Immunol*. 2015;6:620.
49. Wallace BG. Inhibition of agrin-induced acetylcholine-receptor aggregation by heparin, heparan sulfate, and other polyanions. *J Neurosci*. 1990;10(11):3576–3582.
50. Lee SB, Kalluri R. Mechanistic connection between inflammation and fibrosis. *Kidney Int Suppl*. 2010;Suppl(119):S22–26.
51. Levi-Schaffer F, et al. Nerve growth factor and eosinophils in inflamed juvenile conjunctival nevus. *Invest Ophthalmol Vis Sci*. 2002;43(6):1850–1856.
52. Gonzalez D, Contreras O, Rebolledo DL, Espinoza JP, van Zundert B, Brandan E. ALS skeletal muscle shows enhanced TGF-β signaling, fibrosis and induction of fibro/adipogenic progenitor markers. *PLoS ONE*. 2017;12(5):e0177649.
53. Leon A, et al. Mast cells synthesize, store, and release nerve growth factor. *Proc Natl Acad Sci USA*. 1994;91(9):3739–3743.
54. Levi-Montalcini R, Skaper SD, Dal Toso R, Petrelli L, Leon A. Nerve growth factor: from neurotrophin to neurokine. *Trends Neurosci*. 1996;19(11):514–520.
55. Tomita K, et al. The neurotrophin receptor p75NTR in Schwann cells is implicated in remyelination and motor recovery after peripheral nerve injury. *Glia*. 2007;55(11):1199–1208.
56. Staats KA, et al. C-kit is important for SOD1(G93A) mouse survival independent of mast cells. *Neuroscience*. 2015;301:415–420.
57. Wong M, Martin LJ. Skeletal muscle-restricted expression of human SOD1 causes motor neuron degeneration in transgenic mice. *Hum Mol Genet*. 2010;19(11):2284–2302.
58. Kleij HP, Bienenstock J. Significance of Conversation between Mast Cells and Nerves. *Allergy Asthma Clin Immunol*. 2005;1(2):65–80.
59. Skaper SD, Facci L, Giusti P. Mast cells, glia and neuroinflammation: partners in crime? *Immunology*. 2014;141(3):314–327.
60. White DM. Release of substance P from peripheral sensory nerve terminals. *J Peripher Nerv Syst*. 1997;2(3):191–201.
61. Gundersen K, Oktedalen O, Fonnum F. Substance P in subdivisions of the sciatic nerve, and in red and white skeletal muscles. *Brain Res*. 1985;329(1-2):97–103.
62. Ringer C, Weihe E, Schütz B. Calcitonin gene-related peptide expression levels predict motor neuron vulnerability in the superoxide dismutase 1-G93A mouse model of amyotrophic lateral sclerosis. *Neurobiol Dis*. 2012;45(1):547–554.
63. Sala C, Andreose JS, Fumagalli G, Lømo T. Calcitonin gene-related peptide: possible role in formation and maintenance of neuromuscular junctions. *J Neurosci*. 1995;15(1 Pt 2):520–528.
64. Van Dyke JM, Smit-Oistad IM, Macrander C, Krakora D, Meyer MG, Suzuki M. Macrophage-mediated inflammation and glial response in the skeletal muscle of a rat model of familial amyotrophic lateral sclerosis (ALS). *Exp Neurol*. 2016;277:275–282.
65. Ito T, et al. Stem cell factor programs the mast cell activation phenotype. *J Immunol*. 2012;188(11):5428–5437.
66. Ryan JJ, et al. Role for the stem cell factor/KIT complex in Schwann cell neoplasia and mast cell proliferation associated with neurofibromatosis. *J Neurosci Res*. 1994;37(3):415–432.
67. Loeffler JP, Picchiarelli G, Dupuis L, Gonzalez De Aguilar JL. The Role of Skeletal Muscle in Amyotrophic Lateral Sclerosis. *Brain Pathol*. 2016;26(2):227–236.
68. Liu JX, Brännström T, Andersen PM, Pedrosa-Domellöf F. Distinct changes in synaptic protein composition at neuromuscular junctions of extraocular muscles versus limb muscles of ALS donors. *PLoS ONE*. 2013;8(2):e57473.
69. Garbuzova-Davis S, et al. Amyotrophic lateral sclerosis: a neurovascular disease. *Brain Res*. 2011;1398:113–125.
70. Bortolotto SK, Morrison WA, Han X, Messina A. Mast cells play a pivotal role in ischaemia reperfusion injury to skeletal muscles. *Lab Invest*. 2004;84(9):1103–1111.
71. Shababi M, Lorson CL, Rudnik-Schöneborn SS. Spinal muscular atrophy: a motor neuron disorder or a multi-organ disease? *J Anat*. 2014;224(1):15–28.
72. Ennen JP, Verma M, Asakura A. Vascular-targeted therapies for Duchenne muscular dystrophy. *Skelet Muscle*. 2013;3(1):9.

Manuscrito 1

Evidence for mast cell and neutrophil-driven sciatic nerve pathology associated to paralysis progression in an inherited ALS model

Emiliano Trias, Valentina Varela, Romina Barreto-Núñez, Sofía Ibarburu, Mariángeles Kovacs, Olivier Hermine, Joseph S. Beckman, Luis Barbeito

Resumen

Para complementar el estudio anterior sobre la contribución de los mastocitos en la axonopatía distal de las neuronas motoras, procedimos a investigar si los mastocitos, además de infiltrar el microambiente de las NMJs en el músculo esquelético, infiltran los nervios periféricos de la vía motora descendente, y de esta manera contribuyen a la degeneración axonal característica de la ELA.

Resultados

- Estudiando cortes histológicos de nervio ciático de ratas sintomáticas (15 días post-parálisis) con azul de toluidina, observamos que los mastocitos infiltran el endoneuro de los nervios en degeneración. Esta infiltración está acompañada de una degranulación significativa en comparación con los estadios iniciales y animales no transgénicos.
- Los mastocitos que infiltran el nervio ciático, expresan triptasa, c-Kit, e interactúan espacialmente con macrófagos que expresan CSF-1R, cuya infiltración de la vía motora también aumenta de forma significativa luego del comienzo de los síntomas.
- Además los mastocitos forman agregados multicelulares con neutrófilos, que también infiltran de forma masiva el nervio ciático en degeneración. Esta infiltración se correlaciona directamente con la progresión de la parálisis.
- Los neutrófilos contribuyen con los macrófagos a la fagocitosis de los ovoides de mielina. Además, observamos que los agregados de neutrófilos están estrechamente asociados a la agregación de SOD1 mal plegada.

- El tratamiento con masitinib iniciado luego del comienzo clínico de los síntomas, previene de forma significativa la infiltración de mastocitos, neutrófilos y macrófagos.
- La disminución de los niveles inflamatorios previene la degeneración axonal de forma significativa, así como la degeneración de las vainas de mielina.
- La reactividad de las células de Schwann, característica de la degeneración de tipo Walleriana, disminuye de forma significativa luego del tratamiento con masitinib.
- Finalmente y por primera vez identificamos un aumento post-parálisis de los ligandos de c-Kit y CSF-1R, el "*stem cell factor* (SCF)", y CSF1 e IL-34 respectivamente, en la vía motora en degeneración en las ratas $SOD1^{G93A}$. Observamos un aumento de expresión de SCF en los macrófagos que infiltran el endoneuro y un aumento de la expresión de CSF1 e IL-34 en las células de Schwann.

Conclusiones

Estos estudios muestran por primera vez que la infiltración de mastocitos y neutrófilos contribuyen a la degeneración de los axones de la vía motora en un modelo animal de ELA. Esta infiltración ocurre masivamente luego del comienzo de la parálisis correlacionándose con la progresión de la parálisis. Las células de Schwann que se actúan luego de la denervación parecen iniciar la reacción inflamatoria a través de la expresión de CSF1 e IL-34. El bloqueo específico de la inflamación periférica con masitinib previene la degeneración de los axones motores y las vainas de mielina que ocurre a medida que la enfermedad progresa, sugiriendo el efecto deletéreo del infiltrado inflamatorio.

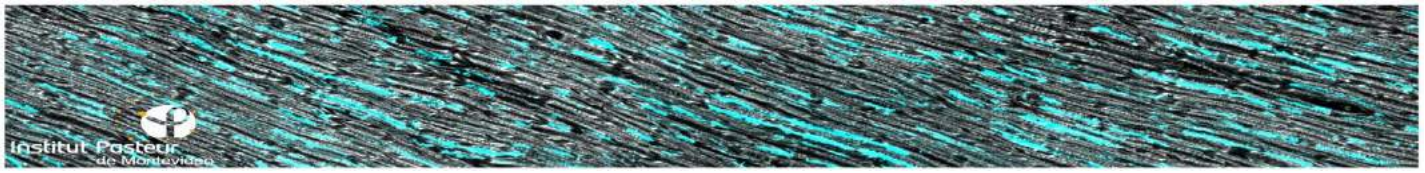

Evidence for mast cell and neutrophil-driven sciatic nerve pathology associated to paralysis progression in an inherited ALS model

Emiliano Trias[1], Valentina Varela[1], Romina Barreto-Núñez[1], Sofía Ibarburu[1], Mariángeles Kovacs[1], Olivier Hermine[2,3,4,5,6,7,8,9,10], Joseph S. Beckman[11], Luis Barbeito[1,†]

Progressive spreading of skeletal muscle paralysis is a clinical feature of Amyotrophic lateral sclerosis (ALS), a neurodegenerative disease with an average survival of 2 to 5 years. Evidence in rodent models expressing ALS-linked SOD1 mutations indicate that specific glial and immune cells emerging after paralysis onset can adversely accelerate disease progression. Pharmacological inhibition of the tyrosine kinase receptors c-Kit and CSF-1R downregulates activated spinal cord microglia as well as skeletal muscle mast cells, thus reducing the rate of post-paralysis motor neuron loss, NMJ denervation and disease progression. However, it is presently unknown whether mast cells and neutrophils play a pathogenic role during peripheral nerve degeneration. Here, we have analyzed the progression of sciatic nerve pathology in SOD1^{G93A} rats in a window of time between hind limb onset and advanced paralysis after 15 days. We report a yet unknown infiltration of degranulating mast cells into the endoneurium, the number of which sharply increased after paralysis onset and correlated with progression of nerve pathology. Remarkably, chymase-positive mast cells formed large heterotypic multicellular aggregates with elastase-positive neutrophils that were aligned along the sciatic nerve endoneurium in close contact with misfolded SOD1 and fragmented myelin ovoids. Mast cells also interacted with macrophages, which expressed the c-Kit receptor ligand stem cell factor (SCF), essential for mast cell differentiation. CSF-1R agonists, IL34 and CSF1, were expressed in GFAP-positive Schwann cells. Pharmacological inhibition of c-Kit and CSF-1R with masitinib during 15 days (30 mg/kg/d p.o.), starting at paralysis onset, prevented the appearance of mast cell/neutrophil aggregates and decreased the number of non-phagocytic macrophages. Remarkably, masitinib treatment also significantly decreased axonal pathology and demyelination, as compared to vehicle-treated rats. These findings provide further evidence for mast cell and neutrophil-driven pathology of the sciatic nerve, effectors likely contributing to aggravate distal axonopathy that can be therapeutically targeted with masitinib.

1 Institut Pasteur de Montevideo, Uruguay
2 Imagine Institute, Hôpital Necker, Paris, France
3 INSERM UMR 1163, Laboratory of Cellular and Molecular Mechanisms of Hematological Disorders and Therapeutic Implications, Paris, France.
4 Paris Descartes–Sorbonne Paris Cité University, Imagine Institute, Paris, France
5 CNRS ERL 8254, Paris, France
6 Laboratory of Excellence GR-Ex, Paris, France
7 Equipe Labélisée par la Ligue Nationale contre le cancer
8 AB Science
9 Department of Hematology, Necker Hospital, Paris, France
10 Centre national de référence des mastocytoses (CEREMAST), Paris, France
11 Linus Pauling Institute, Department of Biochemistry and Biophysics, Environmental Health Sciences Center, Oregon State University

†Correspondence to: Luis Barbeito
Institut Pasteur de Montevideo
Mataojo 2020, Montevideo 11.400, Uruguay
(00 598) 2 522 0910
barbeito@pateur.edu.uy

Keywords: ALS, sciatic nerve degeneration, mast cells, neutrophils, masitinib, c-Kit, CSF-1R

Abbreviations: SCF: Stem cell factor; CSF1: Colony stimulating factor 1; ALS: Amyotrophic Lateral Sclerosis; CSF-1R: Colony stimulating factor receptor 1; IL-34: Interleukin 34.

Introduction

Motor neuron degeneration and distal motor axonopathy are among the best recognized pathological features of amyotrophic lateral sclerosis (ALS), a progressive paralytic neurodegenerative disease. Survival after diagnosis is typically between 3 to 5 years and largely determined by the rate of spread of motor neuron pathology along the neuroaxis (Brown and Al-Chalabi, 2017). Despite decades of research, the etiology of most ALS cases remains unknown and there is a poor understanding of the pathological mechanisms underlying the disease onset and subsequent progressive spreading. Finally, there still exists an urgent unmet medical need for therapeutic actions to slow or stop the paralysis progression early after diagnosis, with the hope of turning this fatal disease into a chronic condition.

Evidence in ALS patients and murine models expressing ALS-linked SOD1 mutations indicate that lower motor neuron degeneration starts peripherally as a distal axonopathy before overt loss of motor neuron cell bodies (Kennel et al., 1996; Frey et al., 2000; Fischer et al., 2004). This early "dying back" motor neuropathy could potentially be more easily targeted by therapeutic interventions. Degeneration of motor axons in ALS has been associated with defective axonal transport, mitochondria function and/or stabilization of neuromuscular junctions (Kong and Xu, 1998; Millecamps and Julien, 2013; Arbour et al., 2015; Campanari et al., 2016). More recently, it has become clear that activation of peripheral immune cells may influence the vulnerability of motor nerve terminals (Van Dyke et al., 2016; Trias et al., 2017). A subset of ALS patients exhibits abnormally activated circulating monocytes (Zhang et al., 2011; Zhao et al., 2017) and downregulation of LyC6 monocytes ameliorate survival in ALS mice (Butovsky et al., 2012), suggesting a systemic pathogenic role of these cells in ALS. Monocyte-derived macrophages have been also reported infiltrating peripheral nerves and skeletal muscle of ALS patients and transgenic mice (Chiu et al., 2009). However, there is conflicting evidence as to whether macrophage infiltration in ALS degenerating nerves is deleterious (Martinez-Muriana et al., 2016), or protective (Nardo et al., 2016). The multiple and simultaneous functional phenotypes of macrophages mediating cytotoxicity, phagocytosis or regeneration obfuscates the identification of many macrophages associated to motor nerve degeneration in ALS.

Recent evidence indicate that mast cells and macrophages accumulate in neuromuscular compartments undergoing denervation in symptomatic SOD1^{G93A} rats (Van Dyke et al., 2016; Trias et al., 2017). Mast cells are granulated hematopoietic-derived immune cells, which precursors migrate within tissues reaching maturation and differentiation under influence of SCF and other local produced cytokines (Erb et al., 1996). Because mast cells are a significant source of mediators that can orchestrate inflammation, vascular changes, leukocyte infiltration and even modulation of nerve terminals (Kleij and Bienenstock, 2005; Mizisin and Weerasuriya, 2011; Frenzel and Hermine, 2013), the possibility exists that mast cells also play a pathogenic role in ALS by aggravating distal axonopathy. In support to this hypothesis, pharmacological targeting of mast cells in ALS rats with the tyrosine kinase inhibitor masitinib, is associated to delayed progression of NMJ denervation and motor functions (Trias et al., 2017). Nonetheless, scarce information exists about the pathological role of mast cells interacting with motor nerves along the descending motor pathway including ventral roots and nerves. Such interactions have the potential to trigger local chronic inflammation aggravating damage of distal motor axons.

Previously, we have shown evidence that post-paralyis ibition of tyrosine kinase receptors with masitinib prolongs post-paralysis survival, delaying motor neuron death and NMJ denervation in SOD1G93A rats (Trias et al., 2016; Trias et al., 2017). Masitinib is a multifaceted drug that inhibits type III tyrosine kinase receptors, including c-Kit, colony-stimulating factor 1 receptor (CSF-1R) and platelet-derived growth factor receptors (PDGF-R) (Dubreuil et al., 2009; Anastassiadis et al., 2011). By targeting CSF-1R and c-Kit, masitinib can prevent excessive aberrant microgliosis in the spinal cord and exacerbated accumulation of mast cells in the skeletal muscles of symptomatic SOD1^{G93A} rats, respectively (Trias et al., 2016; Trias et al., 2017). Moreover, masitinib has been clinically tested in a phase 3 clinical trial in ALS patients, showing promising therapeutic effects in a significant subset of patients (Mora et al., 2017). Thus, the characterization of masitinib's cellular targets in ALS may lead to a better understanding of pathogenic mechanism underlying disease progression in the central and peripheral nervous system.

Here, we investigated for the occurrence of mast cells and their cell-cell interactions in the sciatic nerve of SOD1^{G93A} rats during a window of time between hind limb onset and advanced paralysis observed in the following 15 days. This short period is characterized by overt systemic inflammatory reaction that likely underlies the rapid paralysis progression occurring in rats, resembling, at least in part, the recognized low-grade inflammation reported in ALS patients (Keizman et al., 2009). We report a sharp post-paralysis increase in mast cell number and degranulation in the sciatic nerve, forming yet unknown multicellular aggregates with neutrophils. Pharmacological inhibition of mast cells with masitinib prevented both immune cell infiltration, and axonal loss and myelin disruption in ALS rats.

Materials and Methods

Animals.

Male SOD1^{G93A} progeny were used for further breeding to maintain the line. Rats were housed in a centralized animal facility with a 12-h light-dark cycle with ad libitum access to food and water. Perfusion with fixative was performed under 90% ketamine – 10% xylazine anesthesia and all efforts were made to minimize animal suffering, discomfort or stress. All procedures using laboratory animals were performed in accordance with the national and international guidelines and were approved by the Institutional Animal Committee for animal experimentation. This study was carried out in strict accordance with the Institut Pasteur de Montevideo Committee's requirements and under the

current ethical regulations of the Uruguayan Law N° 18.611 for animal experimentation that follow the Guide for the Care and Use of Laboratory Animals of the National Institutes of Health (USA).

Experimental conditions.

At least 5 rats were analyzed for each experiment. Four different conditions were studied as follow: 1) non-transgenic (NonTg) rats of 160-180 days; 2) transgenic $SOD1^{G93A}$ rats of 180-190 days (symptomatic, onset); 3) transgenic $SOD1^{G93A}$ rats of 195-210 days treated with vehicle (symptomatic, 15d-vehicle) and 4) transgenic $SOD1^{G93A}$ rats of 195-210 days treated with 30 mg/kg/d of masitinib during 15 days (symptomatic, 15d-masitinib).

Determination of disease onset.

All rats were weighed and evaluated for motor activity daily as described (Trias et al., 2016; Trias et al., 2017). Disease onset was determined for each animal when pronounced muscle atrophy was accompanied by abnormal gait, typically expressed as subtle limping or dragging of one hind limb.

Masitinib administration.

As described previously (Trias et al., 2017), only transgenic rats showing weakness and gait alterations in hind limbs as the first clinical sign were selected for masitinib treatment studies. Male rats were divided randomly into the masitinib or vehicle-treated groups. Masitinib mesylate (AB1010), freshly prepared in drinking sterilized water, was administrated daily at a dose of 30 mg/kg using a curved stainless steel gavage needle with 3-mm ball tip. Dosing was defined in accordance to previous studies in the same rat model of ALS that was shown to be safe for chronic treatments (Trias et al., 2016; Trias et al., 2017). Rats were treated from day-1 post-paralysis for an additional 15 days, when they were then euthanized.

Sciatic nerve cryopreserved sections.

Paraformaldehyde (4%) fixed sciatic nerve was cryopreserved in 30% sucrose (Sigma) at 4 °C. The 72h preserved sciatic nerve was embedded in TissueTek (Sakura), sectioned (longitudinal and transverse) at 8-10 µm using a cryostat, and collected on gelatin-coated slides.

Immunohistochemistry of sciatic nerve slices.

Sections were blocked for 2 h at room temperature (5% BSA, 0.5% Triton X-100 in PBS), incubated with primary antibodies overnight at 4°C in 1% BSA, 0.3%Triton X-100 in PBS. Antibodies used were: 1:250 mouse monoclonal anti-Chymase (abcam, #ab2377), 1:250 rat polyclonal anti-c-Kit-biotin (abcam, #ab25022), 1:200 rabbit polyclonal anti-Tryptase (abcam, #ab134932), 1:200 mouse monoclonal anti-CD11b (BD Bioscience, #BD550299), 1:200 rabbit polyclonal anti-CSF-1R (Santa Cruz Biotechnology, #sc-692), 1:200 mouse monoclonal anti-CSF-1R (Santa Cruz Biotechnology, #sc-46662), 1:250 mouse monoclonal anti-CD68 (abcam, #ab31630), 1:300 rabbit monoclonal anti-CD34 (abcam, #ab81289), 1:300 Isolectin-Biotin probe (Thermo Fisher Scientific, #I21414), 1:400 mouse monoclonal anti-GFAP (Sigma, #G3893), 1:400 rabbit polyclonal anti-GFAP (Sigma, #G9269), 1:300 mouse monoclonal anti-S100 (Sigma, #S2532), 1:300 mouse monoclonal anti-neurofilament200-AlexaFluor555 (Thermo Fisher Scientific, #MAB5256A5), 1:200 rabbit polyclonal anti-IL34 (Santa Cruz Biotechnology, #sc-135176), 1:250 rabbit polyclonal anti-MCSF (Thermo Fisher Scientific, #PA5-42558), 1:300 rabbit polyclonal anti-Elastase (abcam, #ab21595), 1:250 mouse monoclonal anti-misfSOD1 (MÉDIMABS, #MM-0070), 1:300 Myelin-AlexaFluor488 or AlexaFluor546 probes (Thermo Fisher Scientific, #F34652), 1:250 rabbit polyclonal SCF (Thermo Fisher Scientific, #PA5-20746). After incubation with primary antibodies, slices were washed with PBS 3 times for 10 min, incubated with secondary antibodies for 2 h at room temperature, 1:500 goat anti-rabbit-AlexaFluor488 (Thermo Fisher Scientific, #A21052), 1:500 goat anti-mouse-AlexaFluor546 (Thermo Fisher Scientific, #A11035), 1:500 goat anti-mouse-AlexaFluor633 (Thermo Fisher Scientific, #A21052), 1:500 Streptavidin-AlexaFluor405 or AlexaFluor633 (Thermo Fisher Scientific, #S21375), washed with PBS 3 times for 5 min, and mounted in DPX mounting medium (Sigma).

Toluidine blue staining.

Mast cell analysis was based in metachromasia observation as previously described (Trias et al., 2017), using 8-10 µm sections of paraformaldehyde-fixed sciatic nerves were cryostat sliced and mounted in gelatin-coated slides. Sections were washed and hydrated twice in distilled water for 10 minutes and embedded in 1% toluidine blue solution during 10 minutes. Then, slides were washed in distilled water three times for 5 minutes and dehydrated during 3 minutes in 70% ethanol, 3 minutes in 95% ethanol and finally 2 minutes in 100% ethanol. Slides were cleared in xylene twice, 3 minutes each and finally mounted in DPX (Sigma). 10x, 20x, 40x and 100x images were acquired using an Olympus CX41 microscope connected to a EvolutionTMLC Color camera and using ImagePro Express software for acquisition. The number of toluidine blue-positive metachromatic mast cells
was counted using the ImageJ software, in at least 50 fields per nerve (1 cm long) per animal using a magnification of 10x. Degranulating mast cells, characterized by extensive metachromatic granules being released by an isolated mast a cell, were counted using 20x magnification in serial pictures of each nerve section.

Fluorescence Imaging.

Fluorescence imaging was performed with a laser scanning Zeiss LSM 800 confocal microscope with either a 25x (1.2 numerical aperture) objective or 63x (1.3 numerical aperture) oil-immersion objective using Zeiss Zen Black

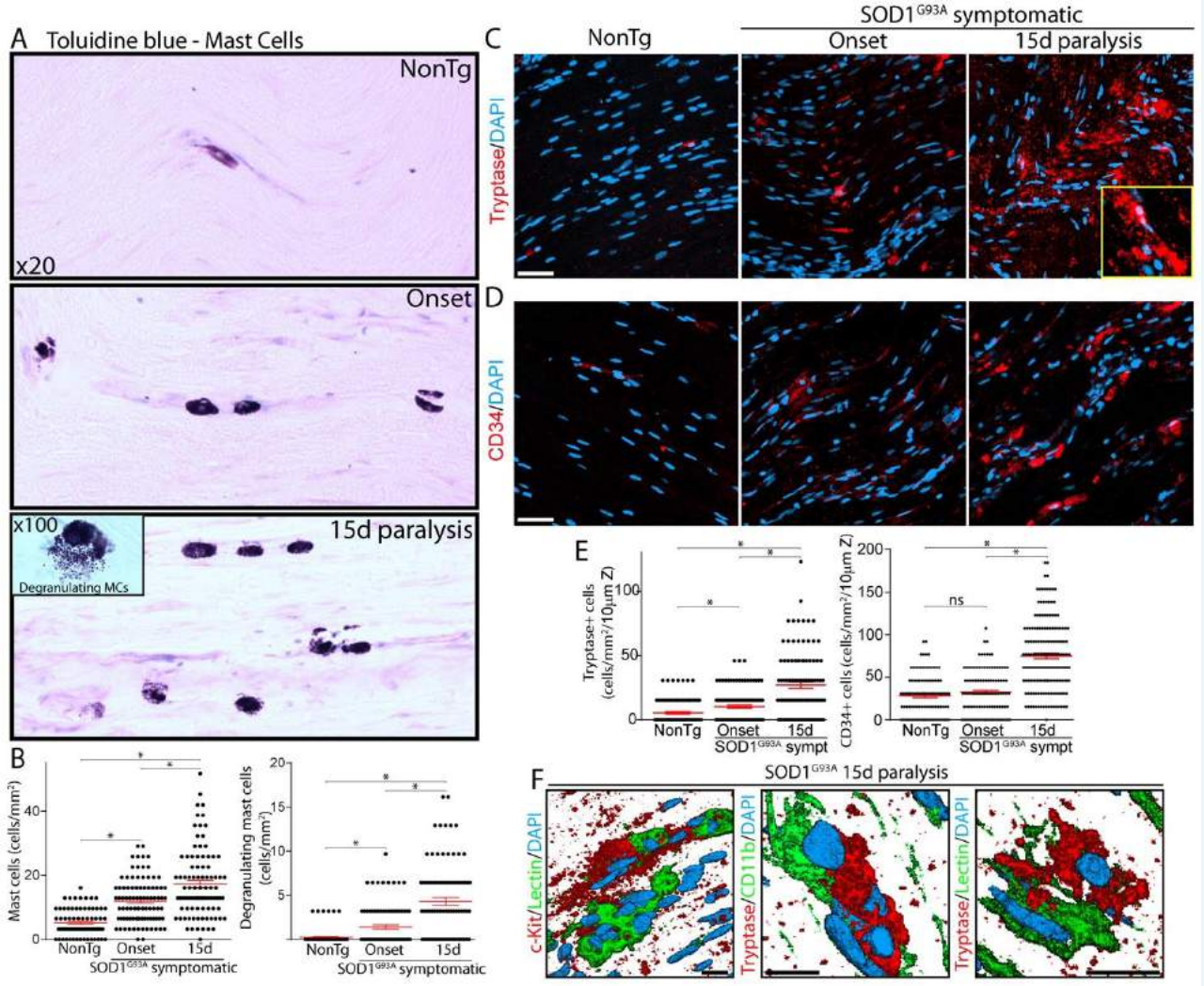

Figure 1. Infiltration and degranulation of mast cells into the sciatic nerve endoneurium after paralysis onset. Longitudinal cryostat sections of NonTg and SOD1^{G93A} rat sciatic nerve at different stages of paralysis. (A) Using toluidine blue staining, few endoneurium mast cells displaying metachromasia were observed in NonTg and mSOD1-onset sciatic nerve as compared to numerous mast cells 15d after paralysis onset. (B) Quantitative analysis of total mast cell and degranulating mast cell numbers. Note the sharp increase in mast cells between onset and advanced paralysis. (C) Confocal representative images comparing the infiltration of tryptase-positive mast cells (red) among conditions. Few mast cells tryptase-positive cells are observed in NonTg and mSOD1-onset conditions when compared with advanced paralysis. D) Confocal representative images comparing CD34-positive cell infiltration (red) among conditions. E) Quantitative analysis of Tryptase- and CD34-positive cells (red) that infiltrate the degenerating sciatic nerve during paralysis progression. Note the sharp increase of both populations after 15d of paralysis when compared with NonTg and onset. F) 3D representative reconstruction showing how Tryptase-positive mast cells spatially interact with CD11b- and Lectin-positive macrophages (green) in the endoneurium of the sciatic nerve during advanced paralysis. All quantitative data are expressed as mean ± SEM; data were analyzed by Kruskal-Wallis followed by Dunn's multiple comparison test, $p < 0.01$ was considered statistical significant. n=4-5 animals/condition. Scale bars in C, D) 50 µm and in F) 10 µm.

software. Maximum intensity projections of optical sections were created with Zeiss Zen software. Maximum intensity projections of optical sections as well as 3D reconstructions were created with Zeiss Zen software.

Statistics analysis.

Quantitative data were expressed as mean ± SEM. Two-tailed Mann-Whitney test or Kruskal-Wallis followed by Dunn's multiple comparison test were used for statistical analysis, with $p<0.01$ considered significant. GraphPad Prism 7.03 software was used for statistical analyses.

Study Approval.

All experimental procedures were approved by the Ethical Committee for the use of Experimental Animals (CEUA) of the Institut Pasteur de Montevideo, Uruguay.

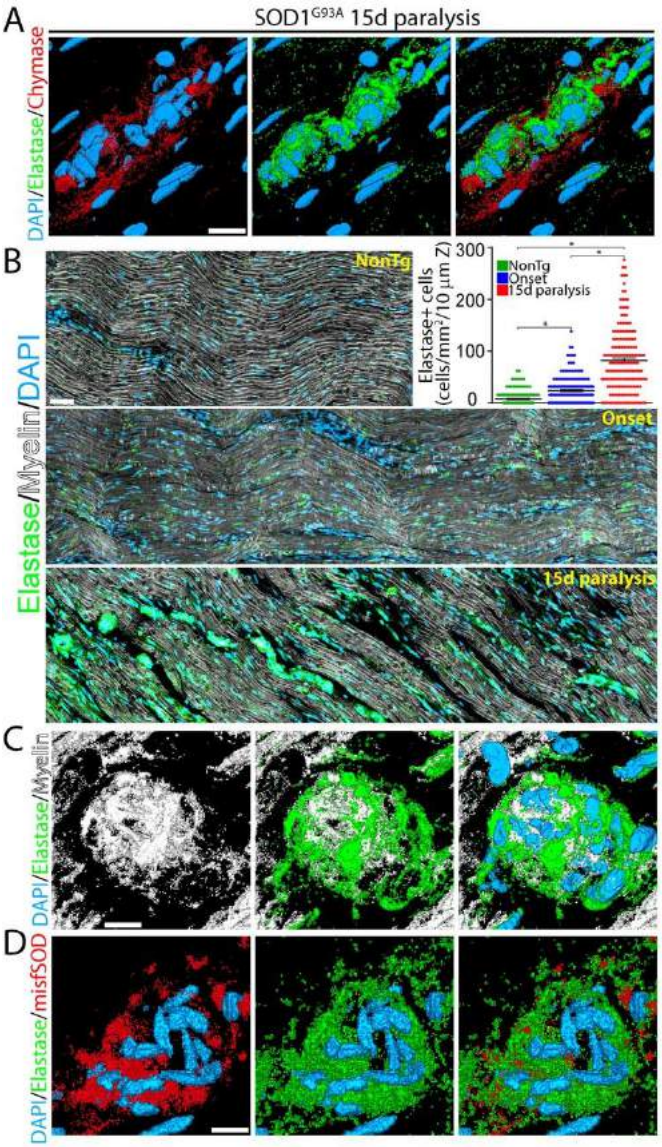

Figure 2. Mast cells form multicellular aggregates with neurotrophils. Longitudinal 8-10 mm sciatic nerve cryosections stained for neutrophil and mast cell markers. A) 3D representative reconstruction of mast cell/neutrophil aggregates observed in the sciatic nerve 15 days after paralysis onset. Note Chymase-positive mast cells (red) organizing in the surface of elatase-positive neutrophil aggregates (green) that aligned in the endoneurium. B) Tile reconstruction of a representative section of sciatic nerve comparing Elastase-positive neutrophil infiltration among conditions. The graph in the upper panel shows the quantitative analysis of Elastase-positive cells. Note the significant increase of neutrophils after onset, correlating with paralysis progression. Data are expressed as mean ± SEM; data were analyzed by Kruskal-Wallis followed by Dunn's multiple comparison test, $p < 0.01$ was considered statistical significant. n=4-5 animals/condition. C) Representative 3D reconstruction of Elastase+ neutrophils (green) while phagocyte myelin ovoids (white) in the endoneurium. D) Representative 3D reconstruction of Elastase+ aggregates displying high levels of misfolded SOD1. Scale bar in B) 50 µm and in A, C, D) 10 µm.

Results

Endoneural infiltration and degranulation of mast cells after paralysis onset.

We analyzed the mast cell phenotypic features in histological sections of the SOD1^{G93A} rat sciatic nerves after hind limb paralysis onset as compared with advanced paralysis observed 15 days after onset. In healthy sciatic nerves from non-transgenic rats, mast cells were rarely found in the endoneural space but occurred in low number around blood vessels at the peryneurium and epineurium. In contrast, endoneural mast cells were grouped and arranged aligned on the apparent trajectory of degenerating axons, sharply increasing after paralysis onset (Fig. 1A). Mast cells

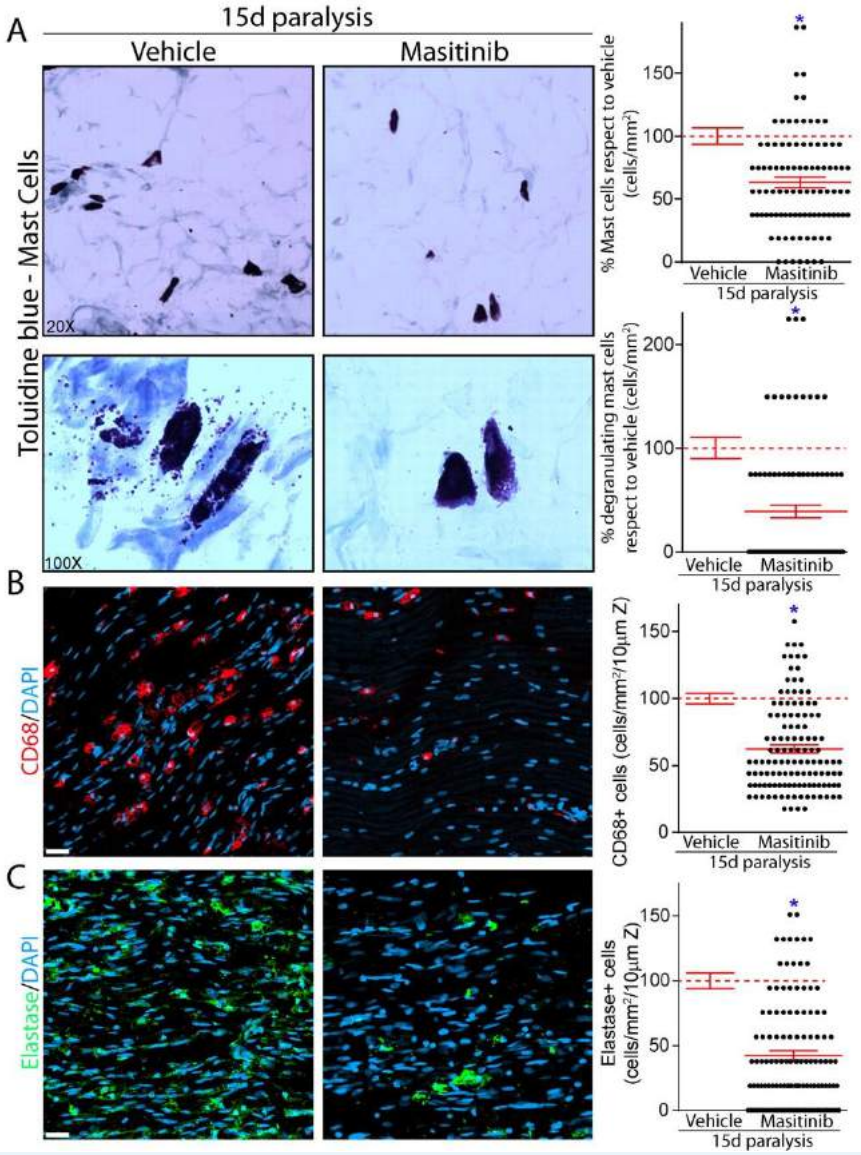

Figure 3. Masitinib treatment reduces mast cell infiltration and degranulation into degenerating sciatic nerve after 15d of paralysis. Masitinib (30 mg/kg/d) or vehicles were orally administered during 15 days after paralysis onset and rats were processed for histochemical analysis of the sciatic nerves. A) Representative microscopic fields of transversal sections of sciatic nerve stained with toluidine blue, showing the number and degranulation of mast cells. Note the sharp reduction in mast cell number, size and degranulating pictures in masitinib-treated rats as compared with controls. The graphs to the right show the quantitative analysis of the number of total mast cells (upper) and degranulating mast cells (lower) assessed in toluidine blue stained sections. Total and degranulating mast cell number was expressed as percent of vehicle treated rats. B) Representative microscopic fields of longitudinal sections of sciatic nerve immunostained for CD68. The reduction of endoneurium macrophages that infiltrate the sciatic nerve 15d after paralysis onset in masitinib-treated rats as compared with controls is observed in the quantitative analysis to the right. Values for advanced paralysis-masitinib are expressed as percent respect to 15d paralysis-vehicle. C) Confocal representative images comparing the infiltration of Elastase+ neutrophils (green) between vehicle- and masitinib-treated rats. The graph to the right shows the quantitative analysis of neutrophil infiltration. Note the significant reduction of elastase-positive cells after masitinib treatment. All quantitative data are expressed as mean ± SEM; data were analyzed by Mann-Whitney test, 2-tailed, $p < 0.01$ was considered statistical significant. n=4-5 animals/condition.

displayed increased size and abundant metachromatic granules, with frequent occurrence of explosive degranulation (Fig. 1A). The number of mast cells were increased by 2-fold at paralysis onset respect to age-matched non-transgenic healthy control (11,96 vs 5,2 cells/mm2), sharply augmented by 3-fold in the following two weeks of paralysis progression (17,3 cells/mm2) (Fig. 1B). Remarkably, the density of degranulating mast cells, a more relevant measure of mast cell activity, increased significantly at paralysis onset and advanced paralysis, as compared to non-transgenic animals (Fig. 1B). Additionally, immunostaining with tryptase, confirmed the progressive mast cells infiltration of sciatic nerve but also a

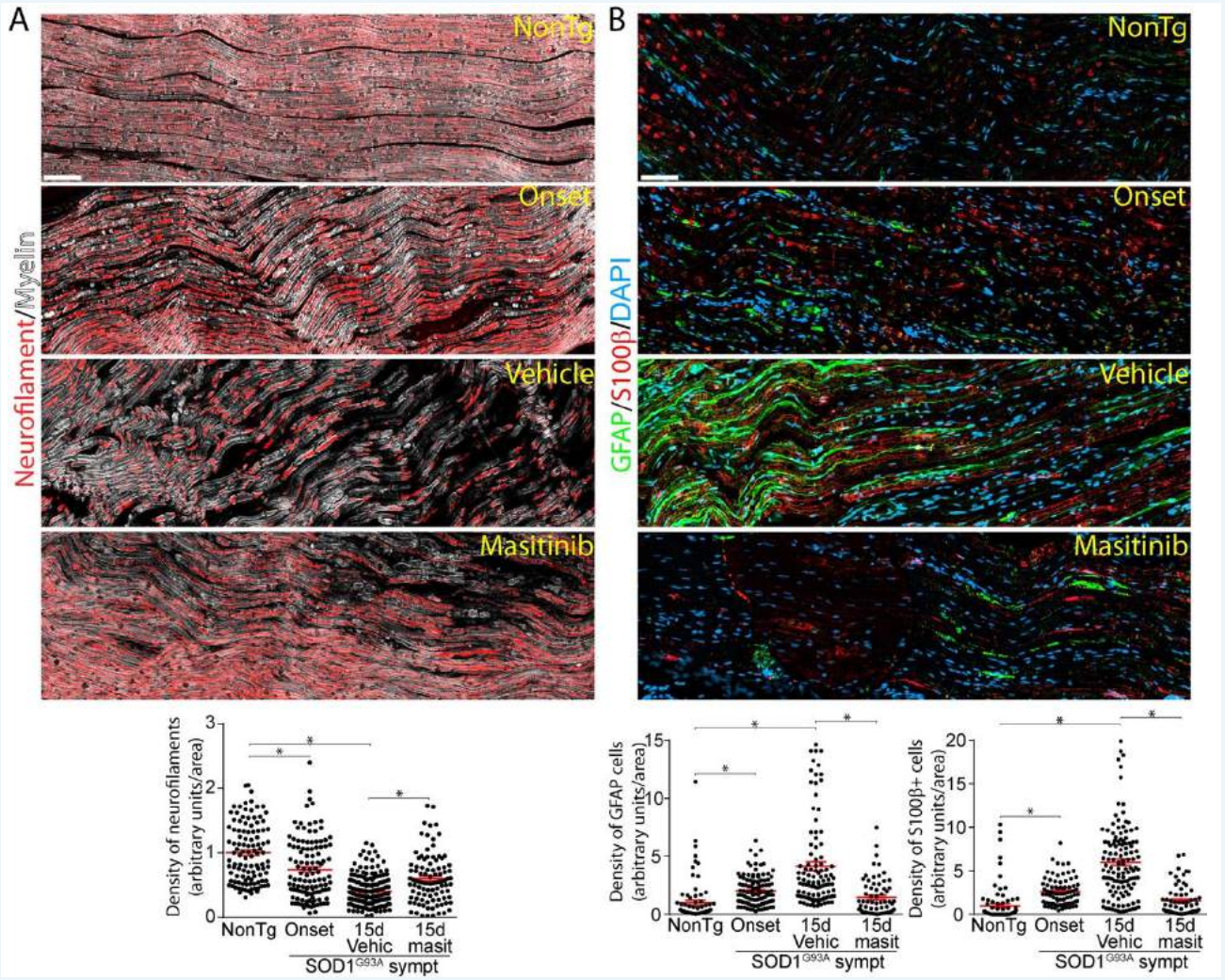

Figure 4. Post-paralysis treatment with masitinib prevents axonal and myelin degeneration and Schwann cell reactivity in the degenerating sciatic nerve. Confocal representative images of the sciatic nerve of NonTg and SOD1 symptomatic rats (Onset, 15d paralysis-vehicle and 15d paralysis-mastitinib. 30 mg/kg/d of masitinib was administered after paralysis onset and continued during 15 days. A) 10 µm sciatic nerve sections were stained for neurofilaments (red) or fluoromyelin (white) to analyze axonal and myeling structure among conditions. Density of axon and myelin per area was analyzed and quantify in the graph below. Note how masitinib treatment significantly prevents axonal and myelin degeneration 15d after onset. B) Sciatic nerve representative confocal images showing 2 staining for Schwann cells, GFAP (green) and S100β (red). Few Schwann cells are observed in NonTg animals and S100β signal is restricted to Schmidt-Lanterman clefts. A significant glial reactivity is observed as disease progresses. Masitinib treatment significantly prevents Schwann cell reactivity. Graphs below show the quantitative analysis of the density of Schwann cells per area. All quantitative data are expressed as mean ± SEM; data were analyzed by Kruskal-Wallis followed by Dunn's multiple comparison test, $p < 0.01$ was considered statistical significant. n=4-5 animals/condition. Scale bar in A, B) 50 µm.

great abundance of tryptase-positive granules invading the neighboring tissue (Fig. 1C, E). Immunostaining for CD34 displayed an even more abundant sub-set of mast cells or progenitor hematopoietic-derived mononuclear cells that sharply increased after paralysis onset (Fig 1D, E).

Mast cells infiltrating the degenerating sciatic nerves were frequently observed in contact with CD11b- and isolectin-positive macrophages (Fig. 1F) and close to phagocytic CD68-positive macrophages that massively infiltrated the nerve during paralysis and mostly displayed phagocytosis of myelin debris.

Mast cell-neutrophil interactions characterize the sciatic nerve pathology during paralysis progression.

As shown in Figure 2A, chymase-positive mast cells interacted with neutrophils labeled with a specific antibody for elastase, a serine protease stored in large quantities in neutrophil cytoplasmic granules (Korkmaz et al., 2010). Such mast cell-neutrophil heterotypic aggregates were

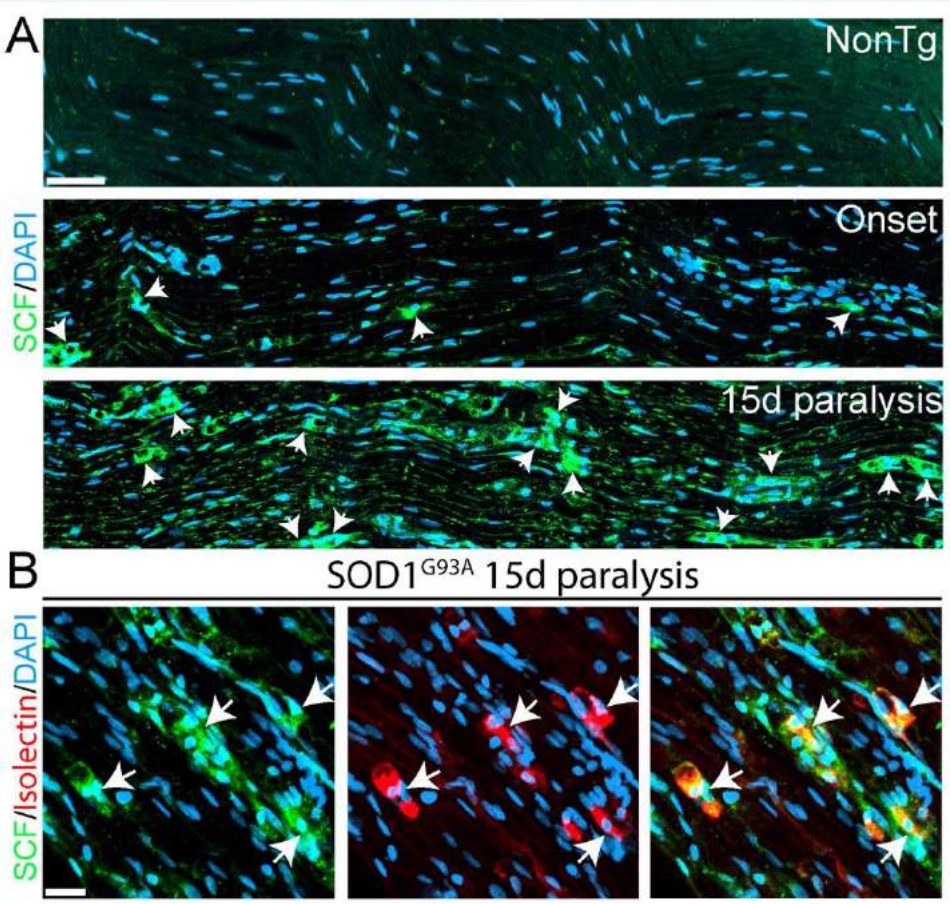

Figure 5. Stem cell factor expression is upregulated in infiltrating macrophages after paralysis onset. Longitudinal 8-10 mm sciatic nerve cryosections stained for c-Kit ligand, SCF. A) Confocal representative images of the sciatic nerve of NonTg and SOD1 symptomatic rats (Onset and 15d paralysis) stained with SCF antibody. SCF expression (green) significantly increase according paralysis progresses. Arrows show SCF-positive cells infiltrating along the sciatic nerve endoneurium. Note how scf-positive cells increase significantly after paralysis onset. All quantitative data are expressed as mean ± SEM; data were analyzed by Kruskal-Wallis followed by Dunn's multiple comparison test, $p < 0.01$ was considered statistical significant. n=4-5 animals/condition. B) Confocal representative images of the 15d-paralysis sciatic nerve where the co-expression of Lectin (red) and SCF (green) was assessed. SCF is expressed by infiltrating Lectin+ macrophages. Scale bar in A) 50 µm and in B) 20 µm.

typically formed of 6 to 12 compacted neutrophils surrounded by a few mast cells expressing chymase, a protease with recognized chemoattractant ability for neutrophils and inflammatory cells (He and Walls, 1998; Halova et al., 2012). Staining for elastase-positive neutrophil aggregates was a remarkable feature of sciatic nerve post-paralysis pathology, increasing 5-fold from paralysis onset to advanced paralysis (Fig 2B). Neutrophils were frequently associated to myelin debris and displayed myelin phagocytosis (Fig. 2C), which is in agreement with their role in myelin clearance in Wallerian degeneration (Lindborg et al., 2017). Finally, neutrophil aggregates also displayed immunoreactivity for human misfolded SOD1 (Fig. 2D), which appeared to be degraded in an intracellular compartment.

Post-paralysis tyrosine kinase inhibition with masitinib prevents mast cell and neutrophil accumulation into the sciatic nerve.

Masitinib potently inhibits the SCF/c-Kit pathway in mast cells and CSF-1R in macrophage and microglial cells (Dubreuil et al., 2009; Trias et al., 2017). To determine the pathogenic contribution of masitinib-responsive immune cells to sciatic nerve pathology, we administered masitinib (30 mg/kg/d) during 15 days after paralysis onset and then measured nerve pathology analyzing inflammatory cell recruitment.

Figure 3A shows representative transversal sections of the sciatic nerve in advanced paralysis from $SOD1^{G93A}$ rats treated with vehicle or masitinib. Compared to vehicle-treated rats, masitinib decreased the number and degranulation of mast cells by 37% and 60% respectively. Masitinib treatment also decreased by 38% and 57% the number of CD68-positive macrophages and neutrophils infiltrating the sciatic nerve, as compared with vehicle

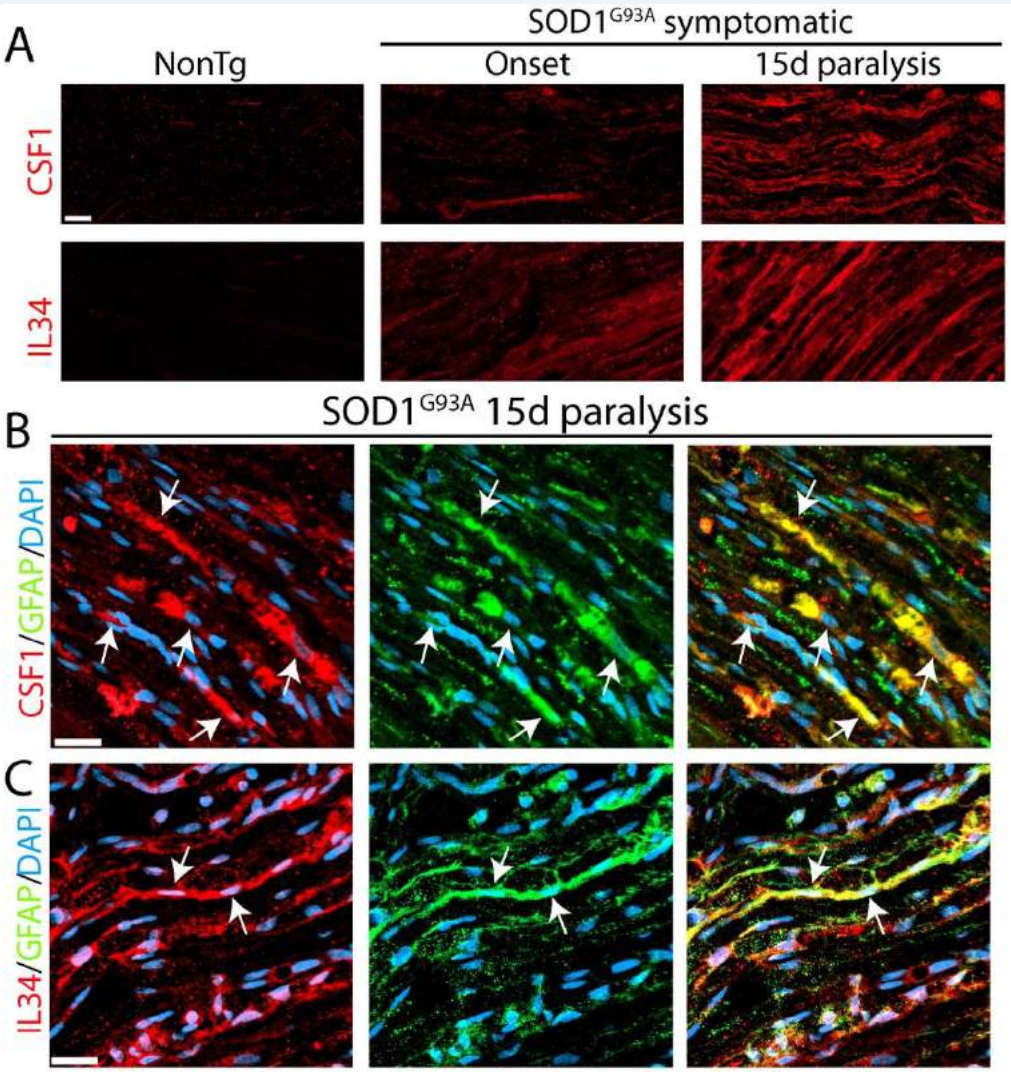

Figure 6. Schwann cells upregulate the expression of CSF1 and IL-34 in the degenerating sciatic nerve. Longitudinal 8-10 mm sciatic nerve sections stained for the CSF-1R ligands, CSF1 and IL-34. A) Confocal representative images showing the upregulation of CSF1 and IL-34 in the degenerating sciatic nerve. Note how the expression of CSF-1R ligands increase significantly in the windows of time between onset and advanced paralysis stage. The graphs below show the quantitatite analysis of the expression of CSF1 and IL-34. B) Confocal images showing the co-expression of GFAP-positive Schwan cells (green) with CSF1 (red). C) GFAP-positive Schwann cells (green) express IL-34 ligand during the symptomatic stage of the disease. Scale bar in A) 20 mm and in B, C) 25 mm.

treatment (Fig. 3B, C). These results are consistent with a synergistic action of masitinib downregulating inflammatory activity of c-Kit-positive mast cells and CSF-1R-positive macrophages.

Masitinib-induced reduction of immune cell infiltration was associated with preserved nerve pathology.

Paralysis progression in ALS correlates with Wallerian-like axon degeneration pathology (Conforti et al., 2014), we have analyzed the effect of masitinib on the number and morphology of axons, myelin ovoids, and denervated Schwann cells. Frequent axonal swelling was the predominant pathological finding at disease onset (Fig 4A). In comparison, a significant number of axons were lost and replaced by myelin ovoids in the subsequent 15 days of paralysis progression. Neurofilament immunoreactivity decreased by 40% between paralysis onset and advanced paralysis. Remarkably, masitinib treatment significantly prevented axonal pathology in large areas of the sciatic nerve as estimated by reduced neurofilament immunoreactivity with respect to vehicle (Fig. 4A). The protection of sciatic nerve pathology by masitinib was also evidenced by the estimate of demyelinating Schwann cells typically expressing GFAP and S100β (Fig. 4B), which typically peaked after paralysis onset and decreased by 60% with respect to vehicle-treated rats.

Post-paralysis upregulation of SCF in macrophages.

The protective effect of masitinib on mast cell infiltration into the sciatic nerve via inhibition of c-Kit, anticipates an increased expression of stem cell factor (SCF), a c-Kit agonist that mediates growth, differentiation and chemotaxis of mast cells (Okayama and Kawakami, 2006). As shown in Figure 5A, SCF immunoreactivity sharply increased after paralysis onset, being mainly expressed by isolectin-positive macrophages that infiltrate the degenerating nerve (Fig. 5B).

Post-paralysis upregulation of CSF1 and IL-34 in Schwann cells.

Masitinib also inhibits the tyrosine kinase receptor CSF-1R expressed in monocytes and subset of macrophages, which is differentially activated by the growth factors CSF1 and IL-34 (Stanley and Chitu, 2014). By analyzing the post-paralysis expression of CSF1 and IL-34 during paralysis progression, we found an increased immunoreactivity for both factors, starting at paralysis onset and increasing significantly 15 days later (Fig. 6A). While both proteins were not detected in the healthy sciatic nerve from non-transgenic rats, the immunoreactivity appeared at paralysis onset and further increased at advanced paralysis. Remarkably, both CSF1 and IL-34 were highly expressed by denervated Schwann cells expressing GFAP and S100β (Fig. 6B, C), further supporting the importance of intercellular crosstalk in the triggering of sciatic nerve immune cell infiltration.

Discussion

In agreement with previous evidence obtained in the skeletal muscle of SOD1^{G93A} rat (Trias et al., 2017), here we report a significant infiltration of degranulating mast cells into the endoneurium of the degenerating sciatic nerve that correlates with paralysis progression. Mast cells infiltration installed in only two weeks after paralysis onset, the time course being strikingly similar to that occurring in the skeletal muscle, suggesting a concerted systemic inflammatory reaction. In accordance, neutrophils, CD34-positive cells and phagocytic macrophages also increased in the endoneurium, an inflammatory response orchestrated in part by mast cells. Pharmacological downregulation of immune cells with masitinib delayed the rate of axonal loss, myelin disruption and activated GFAP- and S100β-positive Schwann cells, suggesting a local pathogenic role of immune cell infiltrate. These findings provide an additional mechanism of action for masitinib protecting the peripheral motor pathway. Moreover, they could also have diagnostic and therapeutic significance if translated to ALS patients that are responsive to masitinib.

Previous reports have showed monocyte and macrophage infiltration in the ALS degenerating nerves of human patients and murine models (Kerkhoff et al., 1993; Chiu et al., 2009; Kano et al., 2012; Nardo et al., 2016). However, the endoneurial infiltration of degranulating mast cells has not been previously observed in ALS cases or animal models. After paralysis onset, mast cells progressively accumulated along apparent degenerating fibers, indicating a direct interaction with motor axons and the surrounding Schwann cells. Perivascular mast cells are considered a resident cell type in peripheral nerves and they likely contribute to local tissue repair (Mizisin and Weerasuriya, 2011). Mast cell activation and degranulation in mammalian nerves have been reported in animal models of diabetic neuropathy (Zheng et al., 2012), autoimmune neuritis and Wallerian degeneration following nerve injury (Olsson, 1967; Esposito et al., 2002), in accordance with their role to trigger inflammation in response to local damage (Dai and Korthuis, 2011; Theoharides et al., 2012). The finding of frequent mast cell degranulation in the degenerating sciatic nerve anticipates multiple inflammatory pathways mediated by secreted metachromatic heparin derivatives, proteases, cytokines, trophic factors and vasoactive mediators (Dai and Korthuis, 2011). Mast cells can also release nerve growth factor (NGF) species (Leon et al., 1994), which can stimulate myelination through activation of p75NTR receptors expressed in non-myelinating Schwann cells (Chan et al., 2004). Thus, activated and degranulating mast cells have the potential to directly or indirectly modify the cellular microenvironment in ALS degenerating nerves.

The finding of mast cell interacting with neutrophil aggregates is intriguing. Both cell types cluster together in the endoneurium with 8-15 neutrophils localized in the core surrounded by few chymase+ mast cells. Mast cells and macrophages can increase vascular permeability (Zhuang et al., 1996; Sprague and Khalil, 2009) and attract blood neurotrophils to damaged tissues through the release of a variety of factors such as histamine, tryptase, cytokines/chemokines, nitric oxide, TNFα, among others (Brown and Hatfield, 2012; Theoharides et al., 2012). Chymase, a protease expressed and released by mast cells also the ability to attract neutrophils in response to damage (He and Walls, 1998; Tani et al., 2000). Clustering of neutrophils could be facilitated by the characteristic extracellular traps originated after cell lysis (Zawrotniak and Rapala-Kozik, 2013; Papayannopoulos, 2017). Also, we found a direct interaction between neutrophils and misfolded human SOD1, suggesting the protein may be oxidized by activated neutrophils undergoing oxidative burst. It is unknown whether misfolded SOD1 could further stimulates inflammation and initiate an autoimmune response. Neutrophil aggregates were also associated with myelin ovoids and phagocytic macrophages, suggesting their role in the clearance of myelin as previously observed in Wallerian degeneration (Lindborg et al., 2017). Finally, neutrophil infiltration to the sciatic nerve could also be also influenced by the systemic inflammatory reaction observed in different cohorts of ALS patients, in part involving an increased number of circulating neutrophils that increase over disease progression (Murdock et al., 2016; Murdock et al., 2017).

Systemic treatment with masitinib was used to determine

the causal effect of mast cell and associated immune cell infiltration on the post-paralysis sciatic nerve pathology. Masitinib targets mast cells and macrophages/microglia through the inhibition of receptors c-Kit and CSF-1R, respectively (Trias et al., 2016; Trias et al., 2017). In accordance with previous results in skeletal muscle from SOD1G93A rats, we found that masitinb prevented the excessive infiltration of mast cells and associated immune cells occurring in sciatic nerve over paralysis progression. In parallel, masitinib significantly decreased axonal pathology, myeling disruption and the number of Schwann cells, further suggesting the adverse influence of immune cell infiltration on sciatic nerve. Thus, the remarkable effect of masitinib on SOD1G93A rat post-paralysis survival (Trias et al., 2016) might be explained by its synergistic effects on deleterious inflammatory cell populations that invade the lower motor neuron cell body and their axonal trajectory through the nerves to the muscular motor nerve terminals. Because masitinib inhibits various tyrosine kinases receptors including c-Kit, CSF-1R, PDGF-R, Lyn and Fyn, it can potentially downregulate several cell types including microglia, astrocytes, NG2 cells, mast cells monocytes and macrophage.

To better understand the origin of mast cell infiltration in the sciatic nerve, we have analyzed the expression of SCF, which mediates mast cell differentiation and activation through activation of c-Kit receptor (Galli et al., 1994; Galli et al., 1995). We found that SCF was progressively upregulated in the degenerating sciatic nerve during advanced paralysis, being mainly expressed by CD68-positive macrophages. Although, previous reports have shown increased SCF expression in glial cells following CNS injury (Zhang and Fedoroff, 1999), this is the first report showing SCF upregulation in macrophages invading the degenerating sciatic nerve. In turn, we found that CSF1 and IL-34, both recognized as agonists for CSF-1R, were also upregulated in advanced paralysis and expressed by Schwann cells. Recently, dorsal root ganglia together with sciatic nerve axons were shown to express CSF1 and IL-34 after nerve injury (Guan et al., 2016; Okubo et al., 2016). This upregulation also occurs in dorsal and ventral spinal neurons that promote microglia proliferation and activation in the central nervous system (Guan et al., 2016). These results suggest a mechanism by which denervated Schwann cells produce CSF1 and IL-34 to attract macrophages, which in turn produce the SCF, leading to a complex inflammatory response involving neutrophils and other immune cells.

In conclusion, the present study shows further evidence for the role of mast cells orchestrating inflammation in the cellular microenvironment of the peripheral motor axons with the potential to accelerate distal axonopathy and motor neuron degeneration after paralysis onset. Moreover, pharmacological downregulation of mast cells, neutrophils and macrophages with masitinib, administered after paralysis onset, decreased sciatic nerve pathology, suggesting an additional mechanism of action for selective tyrosine kinase inhibitors.

Acknowledgments

We want to thank the staff from the Transgenic and Experimental Animal Unit from Institut Pasteur de Montevideo.

Funding

This work was supported by Institut Pasteur de Montevideo – FOCEM Mercosur (COF 03/11), the Amyotrophic Lateral Sclerosis Association (00482), Department of Defense (AL140108), Agencia Nacional de Investigación e Innovación (ANII), Programa de Desarrollo de las Ciencias Básicas (PEDECIBA), ECOS-Sud Program (U014S02) and CSIC-Universidad de la República (Grupo I+D 1104 Neuroinflamación y glía). Partial funding was received from ABScience

References

Anastassiadis T, Deacon SW, Devarajan K, Ma H, Peterson JR. Comprehensive assay of kinase catalytic activity reveals features of kinase inhibitor selectivity. Nat Biotechnol 2011; 29(11): 1039-45.

Arbour D, Tremblay E, Martineau E, Julien JP, Robitaille R. Early and persistent abnormal decoding by glial cells at the neuromuscular junction in an ALS model. J Neurosci 2015; 35(2): 688-706.

Brown MA, Hatfield JK. Mast Cells are Important Modifiers of Autoimmune Disease: With so Much Evidence, Why is There Still Controversy? Front Immunol 2012; 3: 147.

Brown RH, Jr., Al-Chalabi A. Amyotrophic Lateral Sclerosis. N Engl J Med 2017; 377(16): 1602.

Butovsky O, Siddiqui S, Gabriely G, Lanser AJ, Dake B, Murugaiyan G, et al. Modulating inflammatory monocytes with a unique microRNA gene signature ameliorates murine ALS. J Clin Invest 2012; 122(9): 3063-87.

Campanari ML, Garcia-Ayllon MS, Ciura S, Saez-Valero J, Kabashi E. Neuromuscular Junction Impairment in Amyotrophic Lateral Sclerosis: Reassessing the Role of Acetylcholinesterase. Front Mol Neurosci 2016; 9: 160.

Chan JR, Watkins TA, Cosgaya JM, Zhang C, Chen L, Reichardt LF, et al. NGF controls axonal receptivity to myelination by Schwann cells or oligodendrocytes. Neuron 2004; 43(2): 183-91.

Chiu IM, Phatnani H, Kuligowski M, Tapia JC, Carrasco MA, Zhang M, et al. Activation of innate and humoral immunity in the peripheral nervous system of ALS transgenic mice. Proc Natl Acad Sci U S A 2009; 106(49): 20960-5.

Conforti L, Gilley J, Coleman MP. Wallerian degeneration: an emerging axon death pathway linking injury and disease. Nat Rev Neurosci 2014; 15(6): 394-409.

Dai H, Korthuis RJ. Mast Cell Proteases and Inflammation. Drug Discov Today Dis Models 2011; 8(1): 47-55.

Dubreuil P, Letard S, Ciufolini M, Gros L, Humbert M, Casteran N, et al. Masitinib (AB1010), a potent and selective tyrosine kinase inhibitor targeting KIT. PLoS One 2009; 4(9): e7258.

Erb KJ, Holloway JW, Le Gros G. Mast cells in the front line. Innate immunity. Curr Biol 1996; 6(8): 941-2.

Esposito B, De Santis A, Monteforte R, Baccari GC. Mast cells in Wallerian degeneration: morphologic and ultrastructural

changes. J Comp Neurol 2002; 445(3): 199-210.

Fischer LR, Culver DG, Tennant P, Davis AA, Wang M, Castellano-Sanchez A, et al. Amyotrophic lateral sclerosis is a distal axonopathy: evidence in mice and man. Exp Neurol 2004; 185(2): 232-40.

Frenzel L, Hermine O. Mast cells and inflammation. Joint, bone, spine: revue du rhumatisme 2013; 80(2): 141-5.

Frey D, Schneider C, Xu L, Borg J, Spooren W, Caroni P. Early and selective loss of neuromuscular synapse subtypes with low sprouting competence in motoneuron diseases. J Neurosci 2000; 20(7): 2534-42.

Galli SJ, Tsai M, Wershil BK, Tam SY, Costa JJ. Regulation of mouse and human mast cell development, survival and function by stem cell factor, the ligand for the c-kit receptor. Int Arch Allergy Immunol 1995; 107(1-3): 51-3.

Galli SJ, Zsebo KM, Geissler EN. The kit ligand, stem cell factor. Adv Immunol 1994; 55: 1-96.

Guan Z, Kuhn JA, Wang X, Colquitt B, Solorzano C, Vaman S, et al. Injured sensory neuron-derived CSF1 induces microglial proliferation and DAP12-dependent pain. Nat Neurosci 2016; 19(1): 94-101.

Halova I, Draberova L, Draber P. Mast cell chemotaxis - chemoattractants and signaling pathways. Front Immunol 2012; 3: 119.

He S, Walls AF. Human mast cell chymase induces the accumulation of neutrophils, eosinophils and other inflammatory cells in vivo. Br J Pharmacol 1998; 125(7): 1491-500.

Kano O, Beers DR, Henkel JS, Appel SH. Peripheral nerve inflammation in ALS mice: cause or consequence. Neurology 2012; 78(11): 833-5.

Keizman D, Rogowski O, Berliner S, Ish-Shalom M, Maimon N, Nefussy B, et al. Low-grade systemic inflammation in patients with amyotrophic lateral sclerosis. Acta Neurol Scand 2009; 119(6): 383-9.

Kennel PF, Finiels F, Revah F, Mallet J. Neuromuscular function impairment is not caused by motor neurone loss in FALS mice: an electromyographic study. Neuroreport 1996; 7(8): 1427-31.

Kerkhoff H, Troost D, Louwerse ES, van Dijk M, Veldman H, Jennekens FG. Inflammatory cells in the peripheral nervous system in motor neuron disease. Acta Neuropathol 1993; 85(5): 560-5.

Kleij HP, Bienenstock J. Significance of Conversation between Mast Cells and Nerves. Allergy, asthma, and clinical immunology : official journal of the Canadian Society of Allergy and Clinical Immunology 2005; 1(2): 65-80.

Kong J, Xu Z. Massive mitochondrial degeneration in motor neurons triggers the onset of amyotrophic lateral sclerosis in mice expressing a mutant SOD1. J Neurosci 1998; 18(9): 3241-50.

Korkmaz B, Horwitz MS, Jenne DE, Gauthier F. Neutrophil elastase, proteinase 3, and cathepsin G as therapeutic targets in human diseases. Pharmacol Rev 2010; 62(4): 726-59.

Leon A, Buriani A, Dal Toso R, Fabris M, Romanello S, Aloe L, et al. Mast cells synthesize, store, and release nerve growth factor. Proc Natl Acad Sci U S A 1994; 91(9): 3739-43.

Lindborg JA, Mack M, Zigmond RE. Neutrophils Are Critical for Myelin Removal in a Peripheral Nerve Injury Model of Wallerian Degeneration. The Journal of neuroscience: the official journal of the Society for Neuroscience 2017; 37(43): 10258-77.

Martinez-Muriana A, Mancuso R, Francos-Quijorna I, Olmos-Alonso A, Osta R, Perry VH, et al. CSF1R blockade slows the progression of amyotrophic lateral sclerosis by reducing microgliosis and invasion of macrophages into peripheral nerves. Sci Rep 2016; 6: 25663.

Millecamps S, Julien JP. Axonal transport deficits and neurodegenerative diseases. Nat Rev Neurosci 2013; 14(3): 161-76.

Mizisin AP, Weerasuriya A. Homeostatic regulation of the endoneurial microenvironment during development, aging and in response to trauma, disease and toxic insult. Acta Neuropathol 2011; 121(3): 291-312.

Mora JS, Barbeito L, Hermine O. Masitinib as an add-on therapy to riluzole is beneficial in the treatment of amyotrophic lateral sclerosis (ALS) with acceptable tolerability: Results from a randomized controlled phase 3 trial. Video Lectures http://videolecturesnet/encals2017_barbeito_mora_hermine_therapy/ September 2017.

Murdock BJ, Bender DE, Kashlan SR, Figueroa-Romero C, Backus C, Callaghan BC, et al. Increased ratio of circulating neutrophils to monocytes in amyotrophic lateral sclerosis. Neurol Neuroimmunol Neuroinflamm 2016; 3(4): e242.

Murdock BJ, Zhou T, Kashlan SR, Little RJ, Goutman SA, Feldman EL. Correlation of Peripheral Immunity With Rapid Amyotrophic Lateral Sclerosis Progression. JAMA neurology 2017.

Nardo G, Trolese MC, de Vito G, Cecchi R, Riva N, Dina G, et al. Immune response in peripheral axons delays disease progression in SOD1G93A mice. Journal of neuroinflammation 2016; 13(1): 261.

Okayama Y, Kawakami T. Development, migration, and survival of mast cells. Immunol Res 2006; 34(2): 97-115.

Okubo M, Yamanaka H, Kobayashi K, Dai Y, Kanda H, Yagi H, et al. Macrophage-Colony Stimulating Factor Derived from Injured Primary Afferent Induces Proliferation of Spinal Microglia and Neuropathic Pain in Rats. PLoS One 2016; 11(4): e0153375.

Olsson Y. Degranulation of mast cells in peripheral nerve injuries. Acta Neurol Scand 1967; 43(3): 365-74.

Papayannopoulos V. Neutrophil extracellular traps in immunity and disease. Nat Rev Immunol 2017.

Sprague AH, Khalil RA. Inflammatory cytokines in vascular dysfunction and vascular disease. Biochem Pharmacol 2009; 78(6): 539-52.

Stanley ER, Chitu V. CSF-1 receptor signaling in myeloid cells. Cold Spring Harb Perspect Biol 2014; 6(6).

Tani K, Ogushi F, Kido H, Kawano T, Kunori Y, Kamimura T, et al. Chymase is a potent chemoattractant for human monocytes and neutrophils. J Leukoc Biol 2000; 67(4): 585-9.

Theoharides TC, Alysandratos KD, Angelidou A, Delivanis DA, Sismanopoulos N, Zhang B, et al. Mast cells and inflammation. Biochim Biophys Acta 2012; 1822(1): 21-33.

Trias E, Ibarburu S, Barreto-Nunez R, Babdor J, Maciel TT,

Guillo M, et al. Post-paralysis tyrosine kinase inhibition with masitinib abrogates neuroinflammation and slows disease progression in inherited amyotrophic lateral sclerosis. J Neuroinflammation 2016; 13(1): 177.

Trias E, Ibarburu S, Barreto-Nunez R, Varela V, Moura IC, Dubreuil P, et al. Evidence for mast cells contributing to neuromuscular pathology in an inherited model of ALS. JCI Insight 2017; 2(20).

Van Dyke JM, Smit-Oistad IM, Macrander C, Krakora D, Meyer MG, Suzuki M. Macrophage-mediated inflammation and glial response in the skeletal muscle of a rat model of familial amyotrophic lateral sclerosis (ALS). Exp Neurol 2016; 277: 275-82.

Zawrotniak M, Rapala-Kozik M. Neutrophil extracellular traps (NETs) - formation and implications. Acta Biochim Pol 2013; 60(3): 277-84.

Zhang R, Hadlock KG, Do H, Yu S, Honrada R, Champion S, et al. Gene expression profiling in peripheral blood mononuclear cells from patients with sporadic amyotrophic lateral sclerosis (sALS). J Neuroimmunol 2011; 230(1-2): 114-23.

Zhang SC, Fedoroff S. Expression of stem cell factor and c-kit receptor in neural cells after brain injury. Acta Neuropathol 1999; 97(4): 393-8.

Zhao W, Beers DR, Hooten KG, Sieglaff DH, Zhang A, Kalyana-Sundaram S, et al. Characterization of Gene Expression Phenotype in Amyotrophic Lateral Sclerosis Monocytes. JAMA Neurol 2017; 74(6): 677-85.

Zheng JM, Yao GH, Cheng Z, Wang R, Liu ZH. Pathogenic role of mast cells in the development of diabetic nephropathy: a study of patients at different stages of the disease. Diabetologia 2012; 55(3): 801-11.

Zhuang X, Silverman AJ, Silver R. Brain mast cell degranulation regulates blood-brain barrier. J Neurobiol 1996; 31(4): 393-403.

Discusión

En este trabajo de doctorado hemos realizado algunos aportes significativos a la comprensión de la patogenia y tratamiento de la ELA. El descubrimiento de una sub-población de células gliales con fenotipo aberrante y con gran capacidad proliferativa, neurotóxica e inflamatoria, significó un cambio profundo en la comprensión de las causas de la muerte de motoneuronas, así como de la progresión de la enfermedad a lo largo del neuroeje. Se establece así una hipótesis que denominamos “de la glía aberrante” para explicar la progresión de la ELA. A su vez, la hipótesis de la glía aberrante permitió identificar un fármaco anti-neoplásico de la familia de los inhibidores de tirosin-quinasas (masitinib) como una forma para retardar la neuroinflamación, la muerte progresiva de motoneuronas y por lo tanto el avance de la parálisis. Masitinib bloquea la activación y proliferación de microglías y células gliales aberrantes por inhibición del receptor CSF-1R. Sin embargo, también bloquea otros receptores y tirosin-quinasas como c-Kit y Fyn, que controlan la diferenciación y activación de los mastocitos. Esto nos llevó, en un segunda parte de nuestra investigación, a investigar el papel patogénico de los mastocitos en la ELA. Demostramos por primera vez, que estas células efectoras infiltran masivamente el sistema nervioso periférico en la fase sintomática de las ratas que desarrollan ELA, siguiendo el trayecto de los axones motores en degeneración hasta las terminaciones pre-sinápticas musculares. A su vez, demostramos cómo los mastocitos interactúan con macrófagos y con neutrófilos, organizando un microambiente celular inflamatorio potencialmente patogénico, que parece acelerar la axonopatía distal que caracteriza a esta enfermedad. De esta manera, en el transcurso de este trabajo de tesis describimos nuevos mecanismos patogénicos en la ELA, tanto a nivel central como periférico, identificando un fármaco anti-neoplásico con potencialidad terapéutica multifacética en la neurodegeneración. Basados en nuestros estudios pre-clínicos, el masitinib ya ha sido analizado en un ensayo Fase III en pacientes con ELA, con resultados promisorios que deberán ser confirmados en nuevos estudios.

Si bien al comienzo se pensó que la glía aberrante aislada de ratas ELA correspondía a cambios degenerativos de los astrocitos, nuestros estudios posteriores, basados en separación celular ("*cell sorting"*) de células CD11b de cultivos primarios de la médula espinal, mostraron que las células gliales aberrantes surgen de una transformación fenotípica de microglías activadas que rodean a las motoneuronas en la etapa sintomática de la enfermedad[20]. Debido a su alta tasa proliferativa, la glía aberrante parece sufrir una expansión significativa a lo largo de neuroeje, lo cual podría explicar el curso acelerado de la parálisis en el modelo de rata[70]. Nuestro trabajo sobre el trasplante de células gliales aberrantes en ratas no-transgénicas, evidencia su capacidad intrínseca para inducir microgliosis y astrocitosis, seguramente a través de la secreción de factores solubles aún no identificados, y podrían actuar tanto en forma autócrina y parácrina.

Estudios previos han mostrado la plasticidad fenotípica de las microglías en respuesta a condiciones patológicas de neurodegeneración, así como en modelos de daño agudo o incluso en patologías oncológicas gliales[120-124]. En este contexto, es posible anticipar que la transformación aberrante pueda ser dependiente de la expresión de la SOD1 mutada, que podría conferir una respuesta inflamatoria exacerbada o una inestabilidad fenotípica acentuada. Otros estudios previos han demostrado cambios fenotípicos de la microglía en la ELA con capacidad patogénica. El grupo liderado por Stanley Appel realizó cultivos de microglía adulta, a partir de la médula espinal de ratones $SOD1^{G93A}$ en etapas sintomáticas de la enfermedad[125]. Los autores mostraron que la microglía sufre una transformación fenotípica y funcional que la hace neurotóxica. El grupo liderado por Tom Maniatis mostró que la microglía proveniente de ratones $SOD1^{G93A}$ presenta un perfil de expresión génica diferente al de microglías en patologías inflamatorias agudas[126]. La microglía que expresa mutaciones de la SOD1 difiere completamente de la microglía no transgénica cuando es sometida a diferentes estímulos inflamatorios[126], sugiriendo que el fenotipo aberrante de la microglía en la ELA estaría condicionada por la expresión SOD1 mutante así como por el microambiente en el que se encuentra.

Otros autores han demostrado que la activación inflamatoria de la microglía es suficiente para inducir la muerte de las motoneuronas a través de la vía clásica inflamatoria NFκB[127]. Por lo tanto, el diseño de estrategias terapéuticas para inhibir selectivamente la respuesta microglial exacerbada, se ha convertido en uno de los campos de mayor crecimiento en neurodegeneración.

Otros autores han confirmado la emergencia de otros tipos de glía aberrante en modelos de ELA. Un estudio liderado por Ben Barres ha mostrado la existencia de un fenotipo astrocitario neurotóxico al que ellos llamaron A1[128]. Este fenotipo es inducido como consecuencia del microambiente en el que se encuentran, principalmente por factores secretados por la microglía activada. Los astrocitos con fenotipo A1 se vuelven tóxicos para las motoneuronas y oligodendrocitos.

En otro estudio, Melanie Das y Clive Svendsen aislaron una población aparentemente de astrocitos senescentes en ratas $SOD1^{G93A}$ sintomáticas que, al igual que la glía aberrante, expresan altos niveles de GFAP y S100β y que son tóxicos para las motoneuronas[129]. La demostración de fenotipos senescentes de glía es muy significativa puesto que estas células podrían estar dando lugar a células secretorias SASP (del inglés "*senescence-associated secretory phenotype*") que secretan una variedad de factores solubles pro-inflamatorios. El fenotipo astrocitario senescente ha sido directamente relacionado a diversas patologías neurodegenerativas como el Alzheimer y el Parkinson[130-132]. Por tanto, sería importante determinar si la glía aberrante que nosotros aislamos corresponde a un fenotipo SASP.

Estudios preliminares llevados a cabo en nuestro laboratorio muestran que, durante la fase sintomática de la enfermedad, existe un aumento en el número de células senescentes en el microambiente que rodea a las motoneuronas en degeneración, pero no hemos logrado identificar formalmente el fenotipo SAPS. Por lo tanto, durante la fase sintomática en la ELA, las células con fenotipos SASP podrían constituir una fuente de factores que expliquen el aumento explosivo de la inflamación y la emergencia de varios tipos de glía

aberrante en los linajes de microglía y macroglía. Nuevos estudios serán necesarios para determinar si existe una subpoblación de glía aberrante con fenotipo SASP que module y perpetúe la constitución del microambiente degenerativo en la médula espinal en la ELA.

Nuestro trabajo de tesis no estuvo enfocado en estudiar el origen de la neurotoxicidad inducida por las células gliales aberrantes ni en identificar los factores solubles involucrados. A pesar de que la toxicidad de células gliales viene siendo estudiado por diversos grupos a nivel mundial[133-138], los mecanismos últimos de toxicidad para motoneuronas permanecen desconocidos.

El concepto de células gliales aberrantes con alta capacidad proliferativa nos llevó a estudiar fármacos anti-neoplásicos que pudieran prevenir o disminuir la aparición de estos fenotipos aberrantes en la fase sintomática de la ELA. Fue así que identificamos una familia de fármacos inhibidores de tirosin-quinasas capaces de bloquear la proliferación y la migración de las células gliales aberrantes *in vitro* e *in vivo*.

Cuando es administrado luego del comienzo clínico de la enfermedad en ratas SOD1, el masitinib previene la muerte masiva de motoneuronas, disminuye significativamente la microgliosis, la emergencia de células gliales aberrantes, y retrasa en aproximadamente un 40% la progresión de la enfermedad[139]. Masitinib es único comparado con decenas de fármacos ensayados en modelos de ELA, pues es efectivo cuando se administra luego del comienzo clínico de la enfermedad y no en etapas asintomáticas, como ha sucedido para otros fármacos[51,140-143]. Esto lo hace potencialmente más adaptado a la realidad clínica de los pacientes con ELA. Nuestros resultados con masitinib también contrastan con un gran número de ensayos pre-clínicos realizados en modelos murinos de ELA, que si bien mostraban protección en el modelo animal, fallaron al momento de ser trasladados a la clínica[143,144]. Recientemente, un nuevo fármaco ha sido aprobado para el tratamiento de la ELA, un “scavenger” de radicales libres: la Edevarona[145], que podría tener un

efecto protector en un reducido porcentaje de los pacientes. Se desconoce si la Edevarona actúa sobre las células gliales.

Nuestras investigaciones sugieren que la modulación de las microglías activadas y sus fenotipos aberrantes puede ser obtenida por la inhibición del receptor CSF-1R con masitinib[139]. El masitinib es un inhibidor de la clase III de tirosina quinasas, específicamente c-Kit, CSF-1R y PDGF-R[146]. A su vez, CSF-1R es expresado por macrófagos, microglía y osteoclastos[147] y presenta dos ligandos endógenos: CSF1 e IL-34[148]. Estos regulan la proliferación, diferenciación y sobrevida de las microglías. Los ratones que no expresan CSF-1R o IL-34, presentan una muy escasa población de macrófagos y microglía[149-151]. Esto posiciona a los receptores de tirosina-quinasas en las microglías como blancos moleculares para el desarrollo de estrategias terapéuticas alternativas en la neurodegeneración. Otras aproximaciones terapéuticas centradas en disminuir la reactividad de microglías han tenido resultados negativos en la clínica. Por ejemplo, el antibiótico minociclina tiene un potente efecto supresor de la actividad glial en modelos preclínicos[51]. Sin embargo, su uso en pacientes con ELA demostró tener un efecto contraproducente, agravando la progresión de la enfermedad[152]. Estos resultados confirman que la supresión genérica de las células microgliales no es adecuada para el tratamiento de la ELA y plantean la necesidad de profundizar el estudio de fármacos que actúen específicamente en fenotipos aberrantes y neurotóxicos.

Basados en estos estudios pre-clínicos llevados a cabo en nuestro laboratorio, la empresa francesa ABScience lanzó un ensayo clínico en pacientes con ELA utilizando el masitinib. En mayo del presente año, culminó la Fase III de este ensayo con resultados significativamente alentadores. El ensayo, que incluyó a 394 pacientes, liderado por Mora, Genge y colaboradores mostró que, en relación al tratamiento con placebo, la administración de masitinib 4.5 mg/Kg/día tiene un efecto terapéutico en un subgrupo mayoritario de pacientes tratados con riluzole, enlenteciendo la progresión de la enfermedad un 27%[153]. Es importante destacar que este efecto es significativo cuando se toman en cuenta solamente los pacientes que cursan una progresión “normal”. Sin

embargo, cuando se analizan los casos de progresión “rápida”, el masitinib no mostró efectos significativos sobre la progresión. De todas maneras, es de destacar que la población de pacientes que presentan progresión “normal” constituye aproximadamente el 70% de los pacientes. Este estudio sugiere que el masitinib tiene un efecto modificador de la progresión de la ELA.

En los últimos años, otras investigaciones han estudiado el uso de inhibidores de tirosina-quinasas como tratamiento para diferentes enfermedades neurodegenerativas y obtenido resultados que apoyan nuestros hallazgos. En 2016, Martínez-Muriana y colaboradores mostraron que la inhibición de CSF-1R, utilizando el GW2580, un inhibidor específico, retrasa significativamente la progresión de la enfermedad en un modelo murino de ELA SOD1$^{G93A\ 154}$. Los autores mostraron que la microgliosis en la médula espinal de estos ratones se correlaciona con un aumento de la expresión de CSF-1R y su ligando CSF1. El tratamiento con GW2580 reduce la proliferación de la microglía en el SNC y de los macrófagos en el SNP, disminuyendo la muerte de motoneuronas y prolongando la sobrevida de los ratones[154]. Esto constituye una nueva evidencia de que la inhibición de los receptores de tirosina-quinasas es una estrategia válida y novedosa para el tratamiento de las enfermedades neurodegenerativas.

Otros inhibidores de tirosina-quinasas, entre ellos imatinib y dasitinib, han mostrado un efecto benéfico, previniendo la muerte de motoneuronas en la ELA, inhibiendo la vía Src/c-Abl[155-157], dos tirosina-quinasas asociadas a la muerte neuronal [158-161].

Por otro lado, la inhibición farmacológica del receptor CSF-1R demostró ser efectiva en el tratamiento de la enfermedad de Alzheimer, actuando sobre la proliferación de microglía dependiente de CSF1[162], disminuyendo la acumulación de placas β-amiloides y retrasando los déficits conductuales y motores[163,164]. Además, el inhibidor de tirosina-quinasas “nilotinib” protege a las neuronas dopaminérgicas inhibiendo la vía c-Abl, en un modelo de enfermedad de parkinson[165,166].

Por lo tanto, el desarrollo de inhibidores de tirosina-quinasas que controlan las células inflamatorias en el SNC y posiblemente también en la periferia, podría suponer un avance significativo en el tratamiento de la progresión de enfermedades neurodegenerativas.

El masitinib es un fármaco que afecta a múltiples blancos celulares a través de múltiples receptores de tirosin-quinasas. Esto nos hizo suponer que la microglía y las células gliales aberrantes no deberían ser las únicas inhibidas por masitinib en la ELA. Al mismo tiempo postulamos que masitinib podría actuar en otra población de células inflamatorias, los mastocitos, que notablemente contralan el estado de activación de monocitos, macrófagos y microglias[167-172]. Los precursores de mastocitos y mastocitos maduros expresan el receptor de tirosin-quinasa c-Kit, que regula su desarrollo, migración y activación[173,174]. El masitinib ha demostrado un efecto terapéutico en casos de mastocitosis y tumores de mastocitos, en donde el receptor c-Kit se encuentra activado constitutivamente, generando la proliferación oncológica de las células[175-178]. Además de su reconocido papel en las respuestas alérgicas o anafilácticas, los mastocitos están asociados a un gran número de patologías caracterizadas por la inflamación crónica, donde estas células desempeñan un rol clave[168,179]. Representan una parte importante en el desencadenamiento de la inflamación en el SNC y en la comunicación glía-sistema inmune[180-182]. Además, pueden liberar sustancias quimioatrayentes para reclutar eosinófilos y monocitos[167,168,183]. Algunas patologías del sistema nervioso, como la esclerosis múltiple están acompañadas por un gran aumento en el número de mastocitos en el SNC[184]. Los mastocitos activados pueden provocar la desmielinización e inducir apoptosis de los oligodendrocitos[185-187]. Pueden producir y liberar factor de crecimiento nervioso (NGF) y además, responder al mismo de forma autócrina/parácrina. Esto puede generar el reclutamiento de linfocitos T, los cuales incrementan el proceso inflamatorio[188,189].

En este contexto, enfocamos nuestra investigación más reciente a un posible efecto patogénico de los mastocitos en la ELA. Hasta la actualidad existían dos reportes que mostraban evidencia de que los mastocitos podrían contribuir a la neuroinflamación en la médula espinal en pacientes con ELA[100,190]. Sin

embargo, estos estudios no son concluyentes, y se contradicen con otros reportes que no logran identificar mastocitos en la médula espinal[191].

Nuestros resultados en el modelo de ratas ELA, indican que los mastocitos no infiltran significativamente la médula espinal en estadios sintomáticos de la enfermedad. Sin embargo, descubrimos una significativa infiltración y degranulación de mastocitos en el músculo esquelético y el nervio ciático de las ratas $SOD1^{G93A}$ sintomáticas[192]. En el músculo, en particular, esta infiltración se observa, en mayor medida, en el microambiente que rodea a las placas motoras, las uniones neuromusculares y, en menor medida, en el parénquima carente de terminales nerviosas o placas. La infiltración de mastocitos ocurre luego de comenzados los síntomas motores y aumenta a medida que avanza la parálisis, estando correlacionada con una denervación masiva de las placas motoras y pérdida de NMJs que tiene lugar durante la etapa sintomática de la enfermedad. La infiltración de mastocitos está asociada temporal y espacialmente a la infiltración de macrófagos y neutrófilos que ocurre tanto en el músculo como el microambiente que rodea los axones motores del nervio ciático en degeneración. El tratamiento con masitinib previno la infiltración masiva de estos tipos celulares, enlenteciendo la denervación, la degeneración axonal y los déficits motores[192].

Nuestras investigaciones son las primeras en mostrar el reclutamiento y la contribución patogénica de los mastocitos en la axonopatía distal de la ELA. Si bien los mecanismos moleculares involucrados aún no han sido establecidos, postulamos que los mastocitos actúan a través del reclutamiento y activación de otras efectores inflamatorios como macrófagos o neutrófilos, entre otros[193]. En parte, los mastocitos regulan la permeabilidad vascular facilitando la extravasación de células sanguíneas[194], secretando proteasas, triptasa, metaloproteasas MMP-9, quimasas, y factores tróficos[195]. Además, identificamos una infiltración característica de neutrófilos en los nervios ciáticos que degeneran. El aumento de estas células inflamatorias se correlaciona con la progresión de la enfermedad. Observamos que los neutrófilos se agrupan en asociación con los mastocitos y contribuyen con la fagocitosis de la mielina. No fue hasta hace poco tiempo que se demostró que los neutrófilos, en

colaboración con los macrófagos y las células de Schwann, contribuyen a la fagocitosis durante la degeneración Walleriana[196]. Si bien esta función fagocítica podría tener efectos benéficos para el sistema, otros autores han mostrado que los neutrófilos contribuyen en otros procesos neurodegenerativos[197,198]. También, en los pacientes con ELA, el equipo liderado por Feldman demostró que la población de neutrófilos circulantes aumenta significativamente en estos pacientes cuando se los compara con los controles. El aumento de esta población celular, junto con la de monocitos, está correlacionado con la severidad de los síntomas a medida que la enfermedad progresa[16,199]. Los neutrófilos activados son la fuente circulante más importante de especies reactivas del oxígeno (ROS)[200,201].

En pacientes con enfermedad de Parkinson, se han evidenciado mayores niveles de ROS cuando son comparados con controles, una observación que se correlaciona con un mayor número de neutrófilos circulantes[202], los cuales, transportando sustancias pro-oxidativas, pueden causar daño oxidativo en el microambiente que infiltran[200,201]. Este daño oxidativo es una característica central de las enfermedades neurodegenerativas, especialmente en la ELA[203]. Las concentraciones fisiológicas de óxido nítrico (NO), claves en la señalización celular, pueden promover y amplificar el daño oxidativo cuando reaccionan con superóxido, produciendo peroxinitrito[204,205]. En la ELA, este mecanismo nitro-oxidativo ha sido muy bien estudiado durante los últimos 20 años por el grupo de Beckman[203], quienes han mostrado que los niveles fisiológicos de NO pueden promover la sobrevida de las motoneuronas, pero estas mismas concentraciones son capaces de estimular la apoptosis de las mismas en las condiciones del microambiente celular inflamatorio[206,207]. Estos mecanismos patogénicos incluyen el diálogo de varios tipos celulares, donde los neutrófilos podrían jugar un papel central contribuyendo con el daño oxidativo. De esta forma, en el intento de comprender los mecanismos de acción sistémicos del masitinib en la ELA hemos descubierto nuevos mecanismos patogénicos en el sistema nervioso periférico con insospechadas repercusiones en el diagnóstico, pronóstico y tratamiento de la ELA.

Conclusiones

Este proyecto de doctorado aportó nuevos conocimientos al campo de los mecanismos patogénicos de la neurodegeneración. Mostramos evidencia de que durante la fase sintomática de la ELA en el modelo de rata, se constituye un microambiente celular neurodegenerativo de gran complejidad, involucrando células neurales de estirpe glial y células no neurales de estirpe inmune. Esto ocurre en la médula espinal, así como a lo largo de toda la vía motora, desde el nervio ciático hasta las unidades motoras del músculo esquelético. También aportamos evidencia de que el microambiente celular degenerativo implica la activación de receptores de tirosin-quinasas (al menos CSF-1R y c-Kit), anticipando un aumento simultáneo en la expresión de los agonistas endógenos SCF y CSF1 e IL-34. Por lo tanto, nuestro trabajo sienta bases racionales para el uso de fármacos inhibidores de tirosina-quinasas como el masitinib tanto en la ELA como en otras enfermedades neurodegenerativas caracterizadas por neuroinflamación.

Por fin, nuestros aportes generan una gran cantidad de nuevos escenarios e hipótesis que deberán ser analizadas en el mediano plazo. Por ejemplo, las células mielinizantes y sus precursores tanto en el SNC como en el SNP, podrían ser blancos potencialmente terapéuticos del masitinib. En la médula espinal degenerante, las células NG2 que proliferan masivamente y han sido asociadas a la neurodegeneración[208,209], expresan el receptor PDGF-Rα, siendo por lo tanto un potencial blanco de masitinib. De la misma forma, masitinib podría modular una subpoblación de células de Schwann no mielinizantes que expresan SCF, a través de la inhibición de PDFG-R.

Referencias

1. McGeer PL, McGeer EG. The inflammatory response system of brain: implications for therapy of Alzheimer and other neurodegenerative diseases. *Brain Res Brain Res Rev.* 1995;21(2):195-218.
2. Tian L, Ma L, Kaarela T, Li Z. Neuroimmune crosstalk in the central nervous system and its significance for neurological diseases. *Journal of neuroinflammation.* 2012;9:155.
3. Ransohoff RM, Brown MA. Innate immunity in the central nervous system. *The Journal of clinical investigation.* 2012;122(4):1164-1171.
4. Aloisi F. The role of microglia and astrocytes in CNS immune surveillance and immunopathology. *Advances in experimental medicine and biology.* 1999;468:123-133.
5. Ousman SS, Kubes P. Immune surveillance in the central nervous system. *Nature neuroscience.* 2012;15(8):1096-1101.
6. Russo MV, McGavern DB. Immune Surveillance of the CNS following Infection and Injury. *Trends in immunology.* 2015;36(10):637-650.
7. Walsh JG, Muruve DA, Power C. Inflammasomes in the CNS. *Nature reviews Neuroscience.* 2014;15(2):84-97.
8. Debye B, Schmulling L, Zhou L, Rune G, Beyer C, Johann S. Neurodegeneration and NLRP3 inflammasome expression in the anterior thalamus of SOD1(G93A) ALS mice. *Brain pathology.* 2016.
9. Johann S, Heitzer M, Kanagaratnam M, et al. NLRP3 inflammasome is expressed by astrocytes in the SOD1 mouse model of ALS and in human sporadic ALS patients. *Glia.* 2015;63(12):2260-2273.
10. McGeer PL, McGeer EG. Inflammation and the degenerative diseases of aging. *Ann N Y Acad Sci.* 2004;1035:104-116.
11. McGeer PL, McGeer EG. Innate immunity, local inflammation, and degenerative disease. *Sci Aging Knowledge Environ.* 2002;2002(29):re3.
12. McGeer PL, McGeer EG. Inflammatory processes in amyotrophic lateral sclerosis. *Muscle Nerve.* 2002;26(4):459-470.
13. McGeer PL, McGeer EG. Glial cell reactions in neurodegenerative diseases: pathophysiology and therapeutic interventions. *Alzheimer Dis Assoc Disord.* 1998;12 Suppl 2:S1-6.
14. McGeer PL, McGeer EG. Mechanisms of cell death in Alzheimer disease--immunopathology. *J Neural Transm Suppl.* 1998;54:159-166.
15. Butovsky O, Siddiqui S, Gabriely G, et al. Modulating inflammatory monocytes with a unique microRNA gene signature ameliorates murine ALS. *J Clin Invest.* 2012;122(9):3063-3087.
16. Murdock BJ, Zhou T, Kashlan SR, Little RJ, Goutman SA, Feldman EL. Correlation of Peripheral Immunity With Rapid Amyotrophic Lateral Sclerosis Progression. *JAMA neurology.* 2017.
17. Napoli I, Neumann H. Protective effects of microglia in multiple sclerosis. *Exp Neurol.* 2010;225(1):24-28.

18. Napoli I, Neumann H. Microglial clearance function in health and disease. *Neuroscience.* 2009;158(3):1030-1038.
19. Barbeito LH, Pehar M, Cassina P, et al. A role for astrocytes in motor neuron loss in amyotrophic lateral sclerosis. *Brain Res Brain Res Rev.* 2004;47(1-3):263-274.
20. Trias E, Diaz-Amarilla P, Olivera-Bravo S, et al. Phenotypic transition of microglia into astrocyte-like cells associated with disease onset in a model of inherited ALS. *Front Cell Neurosci.* 2013;7:274.
21. Diaz-Amarilla P, Olivera-Bravo S, Trias E, et al. Phenotypically aberrant astrocytes that promote motoneuron damage in a model of inherited amyotrophic lateral sclerosis. *Proc Natl Acad Sci U S A.* 2011;108(44):18126-18131.
22. Evans MC, Couch Y, Sibson N, Turner MR. Inflammation and neurovascular changes in amyotrophic lateral sclerosis. *Molecular and cellular neurosciences.* 2013;53:34-41.
23. Ellwardt E, Zipp F. Molecular mechanisms linking neuroinflammation and neurodegeneration in MS. *Exp Neurol.* 2014.
24. Brown RH, Jr., Al-Chalabi A. Amyotrophic Lateral Sclerosis. *N Engl J Med.* 2017;377(16):1602.
25. Liu YJ, Fan HB, Jin Y, et al. Cannabinoid receptor 2 suppresses leukocyte inflammatory migration by modulating the JNK/c-Jun/Alox5 pathway. *The Journal of biological chemistry.* 2013;288(19):13551-13562.
26. Gurney ME, Pu H, Chiu AY, et al. Motor neuron degeneration in mice that express a human Cu,Zn superoxide dismutase mutation. *Science.* 1994;264(5166):1772-1775.
27. McGoldrick P, Joyce PI, Fisher EM, Greensmith L. Rodent models of amyotrophic lateral sclerosis. *Biochimica et biophysica acta.* 2013;1832(9):1421-1436.
28. Philips T, Rothstein JD. Rodent Models of Amyotrophic Lateral Sclerosis. *Curr Protoc Pharmacol.* 2015;69:5 67 61-21.
29. Van Den Bosch L. Genetic rodent models of amyotrophic lateral sclerosis. *J Biomed Biotechnol.* 2011;2011:348765.
30. Bruijn LI, Houseweart MK, Kato S, et al. Aggregation and motor neuron toxicity of an ALS-linked SOD1 mutant independent from wild-type SOD1. *Science.* 1998;281(5384):1851-1854.
31. Wong PC, Pardo CA, Borchelt DR, et al. An adverse property of a familial ALS-linked SOD1 mutation causes motor neuron disease characterized by vacuolar degeneration of mitochondria. *Neuron.* 1995;14(6):1105-1116.
32. Taylor JP, Brown RH, Jr., Cleveland DW. Decoding ALS: from genes to mechanism. *Nature.* 2016;539(7628):197-206.
33. Zetterstrom P, Stewart HG, Bergemalm D, et al. Soluble misfolded subfractions of mutant superoxide dismutase-1s are enriched in spinal cords throughout life in murine ALS models. *Proc Natl Acad Sci U S A.* 2007;104(35):14157-14162.
34. Trumbull KA, Beckman JS. A role for copper in the toxicity of zinc-deficient superoxide dismutase to motor neurons in amyotrophic lateral sclerosis. *Antioxidants & redox signaling.* 2009;11(7):1627-1639.

35. Roberts BR, Tainer JA, Getzoff ED, et al. Structural characterization of zinc-deficient human superoxide dismutase and implications for ALS. *Journal of molecular biology.* 2007;373(4):877-890.
36. Estevez AG, Crow JP, Sampson JB, et al. Induction of nitric oxide-dependent apoptosis in motor neurons by zinc-deficient superoxide dismutase. *Science.* 1999;286(5449):2498-2500.
37. Cassina P, Pehar M, Vargas MR, et al. Astrocyte activation by fibroblast growth factor-1 and motor neuron apoptosis: implications for amyotrophic lateral sclerosis. *Journal of neurochemistry.* 2005;93(1):38-46.
38. Pehar M, Cassina P, Vargas MR, et al. Astrocytic production of nerve growth factor in motor neuron apoptosis: implications for amyotrophic lateral sclerosis. *Journal of neurochemistry.* 2004;89(2):464-473.
39. Pehar M, Vargas MR, Cassina P, Barbeito AG, Beckman JS, Barbeito L. Complexity of astrocyte-motor neuron interactions in amyotrophic lateral sclerosis. *Neurodegener Dis.* 2005;2(3-4):139-146.
40. Cassina P, Cassina A, Pehar M, et al. Mitochondrial dysfunction in SOD1G93A-bearing astrocytes promotes motor neuron degeneration: prevention by mitochondrial-targeted antioxidants. *J Neurosci.* 2008;28(16):4115-4122.
41. Cassina P, Peluffo H, Pehar M, et al. Peroxynitrite triggers a phenotypic transformation in spinal cord astrocytes that induces motor neuron apoptosis. *J Neurosci Res.* 2002;67(1):21-29.
42. Pehar M, Martinez-Palma L, Peluffo H, Kamaid A, Cassina P, Barbeito L. Peroxynitrite-induced cytotoxicity in cultured astrocytes is associated with morphological changes and increased nitrotyrosine immunoreactivity. *Neurotox Res.* 2002;4(2):87-93.
43. Pehar M, Vargas MR, Robinson KM, et al. Peroxynitrite transforms nerve growth factor into an apoptotic factor for motor neurons. *Free Radic Biol Med.* 2006;41(11):1632-1644.
44. Williams JR, Trias E, Beilby PR, et al. Copper delivery to the CNS by CuATSM effectively treats motor neuron disease in SOD(G93A) mice co-expressing the Copper-Chaperone-for-SOD. *Neurobiology of disease.* 2016;89:1-9.
45. Diaz-Amarilla P, Miquel E, Trostchansky A, et al. Electrophilic nitro-fatty acids prevent astrocyte-mediated toxicity to motor neurons in a cell model of familial amyotrophic lateral sclerosis via nuclear factor erythroid 2-related factor activation. *Free radical biology & medicine.* 2016;95:112-120.
46. Miquel E, Cassina A, Martinez-Palma L, et al. Neuroprotective effects of the mitochondria-targeted antioxidant MitoQ in a model of inherited amyotrophic lateral sclerosis. *Free radical biology & medicine.* 2014;70:204-213.
47. Miquel E, Cassina A, Martinez-Palma L, et al. Modulation of astrocytic mitochondrial function by dichloroacetate improves survival and motor performance in inherited amyotrophic lateral sclerosis. *PloS one.* 2012;7(4):e34776.
48. Rothstein JD, Van Kammen M, Levey AI, Martin LJ, Kuncl RW. Selective loss of glial glutamate transporter GLT-1 in amyotrophic lateral sclerosis. *Annals of neurology.* 1995;38(1):73-84.
49. Vermeiren C, Hemptinne I, Vanhoutte N, Tilleux S, Maloteaux JM, Hermans E. Loss of metabotropic glutamate receptor-mediated regulation of glutamate

transport in chemically activated astrocytes in a rat model of amyotrophic lateral sclerosis. *Journal of neurochemistry.* 2006;96(3):719-731.

50. Kawamata T, Akiyama H, Yamada T, McGeer PL. Immunologic reactions in amyotrophic lateral sclerosis brain and spinal cord tissue. *The American journal of pathology.* 1992;140(3):691-707.
51. Kriz J, Nguyen MD, Julien JP. Minocycline slows disease progression in a mouse model of amyotrophic lateral sclerosis. *Neurobiology of disease.* 2002;10(3):268-278.
52. Nguyen MD, D'Aigle T, Gowing G, Julien JP, Rivest S. Exacerbation of motor neuron disease by chronic stimulation of innate immunity in a mouse model of amyotrophic lateral sclerosis. *The Journal of neuroscience : the official journal of the Society for Neuroscience.* 2004;24(6):1340-1349.
53. Gowing G, Lalancette-Hebert M, Audet JN, Dequen F, Julien JP. Macrophage colony stimulating factor (M-CSF) exacerbates ALS disease in a mouse model through altered responses of microglia expressing mutant superoxide dismutase. *Experimental neurology.* 2009;220(2):267-275.
54. Henkel JS, Engelhardt JI, Siklos L, et al. Presence of dendritic cells, MCP-1, and activated microglia/macrophages in amyotrophic lateral sclerosis spinal cord tissue. *Annals of neurology.* 2004;55(2):221-235.
55. Vaknin I, Kunis G, Miller O, et al. Excess circulating alternatively activated myeloid (M2) cells accelerate ALS progression while inhibiting experimental autoimmune encephalomyelitis. *PloS one.* 2011;6(11):e26921.
56. Zhao W, Beers DR, Appel SH. Immune-mediated mechanisms in the pathoprogression of amyotrophic lateral sclerosis. *Journal of neuroimmune pharmacology : the official journal of the Society on NeuroImmune Pharmacology.* 2013;8(4):888-899.
57. Boillee S, Vande Velde C, Cleveland DW. ALS: a disease of motor neurons and their nonneuronal neighbors. *Neuron.* 2006;52(1):39-59.
58. Boillee S, Yamanaka K, Lobsiger CS, et al. Onset and progression in inherited ALS determined by motor neurons and microglia. *Science.* 2006;312(5778):1389-1392.
59. Bruijn LI, Becher MW, Lee MK, et al. ALS-linked SOD1 mutant G85R mediates damage to astrocytes and promotes rapidly progressive disease with SOD1-containing inclusions. *Neuron.* 1997;18(2):327-338.
60. Bruijn LI, Cleveland DW. Mechanisms of selective motor neuron death in ALS: insights from transgenic mouse models of motor neuron disease. *Neuropathology and applied neurobiology.* 1996;22(5):373-387.
61. Clement AM, Nguyen MD, Roberts EA, et al. Wild-type nonneuronal cells extend survival of SOD1 mutant motor neurons in ALS mice. *Science.* 2003;302(5642):113-117.
62. Ilieva H, Polymenidou M, Cleveland DW. Non-cell autonomous toxicity in neurodegenerative disorders: ALS and beyond. *J Cell Biol.* 2009;187(6):761-772.
63. Yamanaka K, Boillee S, Roberts EA, et al. Mutant SOD1 in cell types other than motor neurons and oligodendrocytes accelerates onset of disease in ALS mice. *Proceedings of the National Academy of Sciences of the United States of America.* 2008;105(21):7594-7599.

64. Yamanaka K, Chun SJ, Boillee S, et al. Astrocytes as determinants of disease progression in inherited amyotrophic lateral sclerosis. *Nature neuroscience.* 2008;11(3):251-253.
65. Charcot J-M, Joffroy A. Deux cas d'atrophie musculaire progressive : avec lésions de la substance grise et des faisceaux antérolatéraux de la moelle épinière. *Arch de physiol norm et path.* 1869;1 vol. (50 p.) : 3 p. de pl. ; in-8°:pp. 354-369; 629-649; pp. 744-760.
66. Brown RH, Al-Chalabi A. Amyotrophic Lateral Sclerosis. *N Engl J Med.* 2017;377(2):162-172.
67. Renton AE, Chio A, Traynor BJ. State of play in amyotrophic lateral sclerosis genetics. *Nat Neurosci.* 2014;17(1):17-23.
68. Gurney ME. Transgenic-mouse model of amyotrophic lateral sclerosis. *The New England journal of medicine.* 1994;331(25):1721-1722.
69. Bruijn LI, Beal MF, Becher MW, et al. Elevated free nitrotyrosine levels, but not protein-bound nitrotyrosine or hydroxyl radicals, throughout amyotrophic lateral sclerosis (ALS)-like disease implicate tyrosine nitration as an aberrant in vivo property of one familial ALS-linked superoxide dismutase 1 mutant. *Proc Natl Acad Sci U S A.* 1997;94(14):7606-7611.
70. Howland DS, Liu J, She Y, et al. Focal loss of the glutamate transporter EAAT2 in a transgenic rat model of SOD1 mutant-mediated amyotrophic lateral sclerosis (ALS). *Proc Natl Acad Sci U S A.* 2002;99(3):1604-1609.
71. Quail DF, Joyce JA. Microenvironmental regulation of tumor progression and metastasis. *Nat Med.* 2013;19(11):1423-1437.
72. Hanahan D, Weinberg RA. Hallmarks of cancer: the next generation. *Cell.* 2011;144(5):646-674.
73. Hainaut P, Plymoth A. Targeting the hallmarks of cancer: towards a rational approach to next-generation cancer therapy. *Curr Opin Oncol.* 2013;25(1):50-51.
74. Vargas MR, Pehar M, Diaz-Amarilla PJ, Beckman JS, Barbeito L. Transcriptional profile of primary astrocytes expressing ALS-linked mutant SOD1. *J Neurosci Res.* 2008;86(16):3515-3525.
75. Panatier A, Robitaille R. Astrocytic mGluR5 and the tripartite synapse. *Neuroscience.* 2016;323:29-34.
76. Bezzi P, Volterra A. A neuron-glia signalling network in the active brain. *Curr Opin Neurobiol.* 2001;11(3):387-394.
77. Sofroniew MV, Vinters HV. Astrocytes: biology and pathology. *Acta neuropathologica.* 2010;119(1):7-35.
78. Ang LC, Bhaumick B, Juurlink BH. Neurite promoting activity of insulin, insulin-like growth factor I and nerve growth factor on spinal motoneurons is astrocyte dependent. *Brain Res Dev Brain Res.* 1993;74(1):83-88.
79. Peluffo H, Estevez A, Barbeito L, Stutzmann JM. Riluzole promotes survival of rat motoneurons in vitro by stimulating trophic activity produced by spinal astrocyte monolayers. *Neuroscience letters.* 1997;228(3):207-211.
80. Pekny M, Pekna M. Astrocyte reactivity and reactive astrogliosis: costs and benefits. *Physiol Rev.* 2014;94(4):1077-1098.
81. Ridet JL, Malhotra SK, Privat A, Gage FH. Reactive astrocytes: cellular and molecular cues to biological function. *Trends Neurosci.* 1997;20(12):570-577.

82. Falsig J, Porzgen P, Lund S, Schrattenholz A, Leist M. The inflammatory transcriptome of reactive murine astrocytes and implications for their innate immune function. *J Neurochem.* 2006;96(3):893-907.
83. Dong Y, Benveniste EN. Immune function of astrocytes. *Glia.* 2001;36(2):180-190.
84. Shih AY, Fernandes HB, Choi FY, et al. Policing the police: astrocytes modulate microglial activation. *J Neurosci.* 2006;26(15):3887-3888.
85. Barbierato M, Facci L, Argentini C, Marinelli C, Skaper SD, Giusti P. Astrocyte-microglia cooperation in the expression of a pro-inflammatory phenotype. *CNS Neurol Disord Drug Targets.* 2013;12(5):608-618.
86. Xie L, Yang SH. Interaction of astrocytes and T cells in physiological and pathological conditions. *Brain Res.* 2015;1623:63-73.
87. Kim SU, de Vellis J. Microglia in health and disease. *J Neurosci Res.* 2005;81(3):302-313.
88. Hall ED, Oostveen JA, Gurney ME. Relationship of microglial and astrocytic activation to disease onset and progression in a transgenic model of familial ALS. *Glia.* 1998;23(3):249-256.
89. Gehrmann J, Matsumoto Y, Kreutzberg GW. Microglia: intrinsic immuneffector cell of the brain. *Brain Res Brain Res Rev.* 1995;20(3):269-287.
90. Alexianu ME, Kozovska M, Appel SH. Immune reactivity in a mouse model of familial ALS correlates with disease progression. *Neurology.* 2001;57(7):1282-1289.
91. Graber DJ, Hickey WF, Harris BT. Progressive changes in microglia and macrophages in spinal cord and peripheral nerve in the transgenic rat model of amyotrophic lateral sclerosis. *J Neuroinflammation.* 2010;7:8.
92. Sanagi T, Yuasa S, Nakamura Y, et al. Appearance of phagocytic microglia adjacent to motoneurons in spinal cord tissue from a presymptomatic transgenic rat model of amyotrophic lateral sclerosis. *J Neurosci Res.* 2010;88(12):2736-2746.
93. Yrjanheikki J, Keinanen R, Pellikka M, Hokfelt T, Koistinaho J. Tetracyclines inhibit microglial activation and are neuroprotective in global brain ischemia. *Proc Natl Acad Sci U S A.* 1998;95(26):15769-15774.
94. Beers DR, Henkel JS, Xiao Q, et al. Wild-type microglia extend survival in PU.1 knockout mice with familial amyotrophic lateral sclerosis. *Proceedings of the National Academy of Sciences of the United States of America.* 2006;103(43):16021-16026.
95. Garbuzova-Davis S, Sanberg PR. Blood-CNS Barrier Impairment in ALS patients versus an animal model. *Front Cell Neurosci.* 2014;8:21.
96. Winkler EA, Sengillo JD, Sagare AP, et al. Blood-spinal cord barrier disruption contributes to early motor-neuron degeneration in ALS-model mice. *Proc Natl Acad Sci U S A.* 2014;111(11):E1035-1042.
97. Engelhardt JI, Tajti J, Appel SH. Lymphocytic infiltrates in the spinal cord in amyotrophic lateral sclerosis. *Archives of neurology.* 1993;50(1):30-36.
98. Rentzos M, Evangelopoulos E, Sereti E, et al. Alterations of T cell subsets in ALS: a systemic immune activation? *Acta neurologica Scandinavica.* 2012;125(4):260-264.

99. Beers DR, Zhao W, Wang J, et al. ALS patients' regulatory T lymphocytes are dysfunctional, and correlate with disease progression rate and severity. *JCI Insight.* 2017;2(5):e89530.
100. Graves MC, Fiala M, Dinglasan LA, et al. Inflammation in amyotrophic lateral sclerosis spinal cord and brain is mediated by activated macrophages, mast cells and T cells. *Amyotroph Lateral Scler Other Motor Neuron Disord.* 2004;5(4):213-219.
101. Fischer LR, Glass JD. Axonal degeneration in motor neuron disease. *Neurodegener Dis.* 2007;4(6):431-442.
102. Fischer LR, Culver DG, Tennant P, et al. Amyotrophic lateral sclerosis is a distal axonopathy: evidence in mice and man. *Exp Neurol.* 2004;185(2):232-240.
103. Kennel PF, Finiels F, Revah F, Mallet J. Neuromuscular function impairment is not caused by motor neurone loss in FALS mice: an electromyographic study. *Neuroreport.* 1996;7(8):1427-1431.
104. Frey D, Schneider C, Xu L, Borg J, Spooren W, Caroni P. Early and selective loss of neuromuscular synapse subtypes with low sprouting competence in motoneuron diseases. *J Neurosci.* 2000;20(7):2534-2542.
105. Williamson TL, Cleveland DW. Slowing of axonal transport is a very early event in the toxicity of ALS-linked SOD1 mutants to motor neurons. *Nature neuroscience.* 1999;2(1):50-56.
106. Strom AL, Gal J, Shi P, Kasarskis EJ, Hayward LJ, Zhu H. Retrograde axonal transport and motor neuron disease. *Journal of neurochemistry.* 2008;106(2):495-505.
107. Magrane J, Cortez C, Gan WB, Manfredi G. Abnormal mitochondrial transport and morphology are common pathological denominators in SOD1 and TDP43 ALS mouse models. *Human molecular genetics.* 2014;23(6):1413-1424.
108. Salvadores N, Sanhueza M, Manque P, Court FA. Axonal Degeneration during Aging and Its Functional Role in Neurodegenerative Disorders. *Frontiers in neuroscience.* 2017;11:451.
109. Kano O, Beers DR, Henkel JS, Appel SH. Peripheral nerve inflammation in ALS mice: cause or consequence. *Neurology.* 2012;78(11):833-835.
110. Van Dyke JM, Smit-Oistad IM, Macrander C, Krakora D, Meyer MG, Suzuki M. Macrophage-mediated inflammation and glial response in the skeletal muscle of a rat model of familial amyotrophic lateral sclerosis (ALS). *Exp Neurol.* 2016;277:275-282.
111. Chiu IM, Phatnani H, Kuligowski M, et al. Activation of innate and humoral immunity in the peripheral nervous system of ALS transgenic mice. *Proc Natl Acad Sci U S A.* 2009;106(49):20960-20965.
112. Riva N, Chaabane L, Peviani M, et al. Defining peripheral nervous system dysfunction in the SOD-1G93A transgenic rat model of amyotrophic lateral sclerosis. *J Neuropathol Exp Neurol.* 2014;73(7):658-670.
113. Nardo G, Trolese MC, de Vito G, et al. Immune response in peripheral axons delays disease progression in SOD1G93A mice. *Journal of neuroinflammation.* 2016;13(1):261.
114. Arbour D, Vande Velde C, Robitaille R. New perspectives on amyotrophic lateral sclerosis: the role of glial cells at the neuromuscular junction. *J Physiol.* 2017;595(3):647-661.

115. Arbour D, Tremblay E, Martineau E, Julien JP, Robitaille R. Early and persistent abnormal decoding by glial cells at the neuromuscular junction in an ALS model. *J Neurosci.* 2015;35(2):688-706.
116. Lobsiger CS, Boillee S, McAlonis-Downes M, et al. Schwann cells expressing dismutase active mutant SOD1 unexpectedly slow disease progression in ALS mice. *Proceedings of the National Academy of Sciences of the United States of America.* 2009;106(11):4465-4470.
117. Elmore MR, Najafi AR, Koike MA, et al. Colony-stimulating factor 1 receptor signaling is necessary for microglia viability, unmasking a microglia progenitor cell in the adult brain. *Neuron.* 2014;82(2):380-397.
118. Segaliny AI, Tellez-Gabriel M, Heymann MF, Heymann D. Receptor tyrosine kinases: Characterisation, mechanism of action and therapeutic interests for bone cancers. *J Bone Oncol.* 2015;4(1):1-12.
119. Rosnet O, Birnbaum D. Hematopoietic receptors of class III receptor-type tyrosine kinases. *Crit Rev Oncog.* 1993;4(6):595-613.
120. Yokoyama A, Sakamoto A, Kameda K, Imai Y, Tanaka J. NG2 proteoglycan-expressing microglia as multipotent neural progenitors in normal and pathologic brains. *Glia.* 2006;53(7):754-768.
121. Yokoyama A, Yang L, Itoh S, Mori K, Tanaka J. Microglia, a potential source of neurons, astrocytes, and oligodendrocytes. *Glia.* 2004;45(1):96-104.
122. Noristani HN, Gerber YN, Sabourin JC, et al. RNA-Seq Analysis of Microglia Reveals Time-Dependent Activation of Specific Genetic Programs following Spinal Cord Injury. *Front Mol Neurosci.* 2017;10:90.
123. Huysentruyt LC, Akgoc Z, Seyfried TN. Hypothesis: are neoplastic macrophages/microglia present in glioblastoma multiforme? *ASN Neuro.* 2011;3(4).
124. Persson A, Englund E. Phagocytic properties in tumor astrocytes. *Neuropathology.* 2012;32(3):252-260.
125. Liao B, Zhao W, Beers DR, Henkel JS, Appel SH. Transformation from a neuroprotective to a neurotoxic microglial phenotype in a mouse model of ALS. *Experimental neurology.* 2012;237(1):147-152.
126. Chiu IM, Morimoto ET, Goodarzi H, et al. A neurodegeneration-specific gene-expression signature of acutely isolated microglia from an amyotrophic lateral sclerosis mouse model. *Cell Rep.* 2013;4(2):385-401.
127. Frakes AE, Ferraiuolo L, Haidet-Phillips AM, et al. Microglia induce motor neuron death via the classical NF-kappaB pathway in amyotrophic lateral sclerosis. *Neuron.* 2014;81(5):1009-1023.
128. Liddelow SA, Guttenplan KA, Clarke LE, et al. Neurotoxic reactive astrocytes are induced by activated microglia. *Nature.* 2017;541(7638):481-487.
129. Das MM, Svendsen CN. Astrocytes show reduced support of motor neurons with aging that is accelerated in a rodent model of ALS. *Neurobiology of aging.* 2015;36(2):1130-1139.
130. Bhat R, Crowe EP, Bitto A, et al. Astrocyte senescence as a component of Alzheimer's disease. *PLoS One.* 2012;7(9):e45069.
131. Chinta SJ, Lieu CA, Demaria M, Laberge RM, Campisi J, Andersen JK. Environmental stress, ageing and glial cell senescence: a novel mechanistic link to Parkinson's disease? *J Intern Med.* 2013;273(5):429-436.

132. Golde TE, Miller VM. Proteinopathy-induced neuronal senescence: a hypothesis for brain failure in Alzheimer's and other neurodegenerative diseases. *Alzheimers Res Ther.* 2009;1(2):5.
133. Qian K, Huang H, Peterson A, et al. Sporadic ALS Astrocytes Induce Neuronal Degeneration In Vivo. *Stem cell reports.* 2017;8(4):843-855.
134. Nagai M, Re DB, Nagata T, et al. Astrocytes expressing ALS-linked mutated SOD1 release factors selectively toxic to motor neurons. *Nature neuroscience.* 2007;10(5):615-622.
135. Almad AA, Doreswamy A, Gross SK, et al. Connexin 43 in astrocytes contributes to motor neuron toxicity in amyotrophic lateral sclerosis. *Glia.* 2016;64(7):1154-1169.
136. Haidet-Phillips AM, Hester ME, Miranda CJ, et al. Astrocytes from familial and sporadic ALS patients are toxic to motor neurons. *Nat Biotechnol.* 2011;29(9):824-828.
137. Valbuena GN, Tortarolo M, Bendotti C, Cantoni L, Keun HC. Altered Metabolic Profiles Associate with Toxicity in SOD1G93A Astrocyte-Neuron Co-Cultures. *Sci Rep.* 2017;7(1):50.
138. Papadeas ST, Kraig SE, O'Banion C, Lepore AC, Maragakis NJ. Astrocytes carrying the superoxide dismutase 1 (SOD1G93A) mutation induce wild-type motor neuron degeneration in vivo. *Proc Natl Acad Sci U S A.* 2011;108(43):17803-17808.
139. Trias E, Ibarburu S, Barreto-Nunez R, et al. Post-paralysis tyrosine kinase inhibition with masitinib abrogates neuroinflammation and slows disease progression in inherited amyotrophic lateral sclerosis. *J Neuroinflammation.* 2016;13(1):177.
140. Petrov D, Mansfield C, Moussy A, Hermine O. ALS Clinical Trials Review: 20 Years of Failure. Are We Any Closer to Registering a New Treatment? *Front Aging Neurosci.* 2017;9:68.
141. Gurney ME. The use of transgenic mouse models of amyotrophic lateral sclerosis in preclinical drug studies. *J Neurol Sci.* 1997;152 Suppl 1:S67-73.
142. DeLoach A, Cozart M, Kiaei A, Kiaei M. A retrospective review of the progress in amyotrophic lateral sclerosis drug discovery over the last decade and a look at the latest strategies. *Expert Opin Drug Discov.* 2015;10(10):1099-1118.
143. Mitsumoto H, Brooks BR, Silani V. Clinical trials in amyotrophic lateral sclerosis: why so many negative trials and how can trials be improved? *Lancet Neurol.* 2014;13(11):1127-1138.
144. Pandya RS, Zhu H, Li W, Bowser R, Friedlander RM, Wang X. Therapeutic neuroprotective agents for amyotrophic lateral sclerosis. *Cellular and molecular life sciences : CMLS.* 2013;70(24):4729-4745.
145. Writing G, Edaravone ALSSG. Safety and efficacy of edaravone in well defined patients with amyotrophic lateral sclerosis: a randomised, double-blind, placebo-controlled trial. *Lancet Neurol.* 2017;16(7):505-512.
146. Dubreuil P, Letard S, Ciufolini M, et al. Masitinib (AB1010), a potent and selective tyrosine kinase inhibitor targeting KIT. *PLoS One.* 2009;4(9):e7258.
147. Patel S, Player MR. Colony-stimulating factor-1 receptor inhibitors for the treatment of cancer and inflammatory disease. *Curr Top Med Chem.* 2009;9(7):599-610.

148. Lin H, Lee E, Hestir K, et al. Discovery of a cytokine and its receptor by functional screening of the extracellular proteome. *Science.* 2008;320(5877):807-811.
149. Li J, Chen K, Zhu L, Pollard JW. Conditional deletion of the colony stimulating factor-1 receptor (c-fms proto-oncogene) in mice. *Genesis.* 2006;44(7):328-335.
150. Wang Y, Szretter KJ, Vermi W, et al. IL-34 is a tissue-restricted ligand of CSF1R required for the development of Langerhans cells and microglia. *Nature immunology.* 2012;13(8):753-760.
151. Erblich B, Zhu L, Etgen AM, Dobrenis K, Pollard JW. Absence of colony stimulation factor-1 receptor results in loss of microglia, disrupted brain development and olfactory deficits. *PLoS One.* 2011;6(10):e26317.
152. Gordon PH, Moore DH, Miller RG, et al. Efficacy of minocycline in patients with amyotrophic lateral sclerosis: a phase III randomised trial. *Lancet Neurol.* 2007;6(12):1045-1053.
153. Mora J, Barbeito L, Hermine O. Masitinib as an add-on therapy to riluzole is beneficial in the treatment of amyotrophic lateral sclerosis (ALS) with acceptable tolerability: Results from a randomized controlled phase 3 trial. In. ENCALS Meeting 2017. abstract book2017:pp.37.
154. Martinez-Muriana A, Mancuso R, Francos-Quijorna I, et al. CSF1R blockade slows the progression of amyotrophic lateral sclerosis by reducing microgliosis and invasion of macrophages into peripheral nerves. *Sci Rep.* 2016;6:25663.
155. Imamura K, Izumi Y, Watanabe A, et al. The Src/c-Abl pathway is a potential therapeutic target in amyotrophic lateral sclerosis. *Sci Transl Med.* 2017;9(391).
156. Rojas F, Gonzalez D, Cortes N, et al. Reactive oxygen species trigger motoneuron death in non-cell-autonomous models of ALS through activation of c-Abl signaling. *Front Cell Neurosci.* 2015;9:203.
157. Katsumata R, Ishigaki S, Katsuno M, et al. c-Abl inhibition delays motor neuron degeneration in the G93A mouse, an animal model of amyotrophic lateral sclerosis. *PLoS One.* 2012;7(9):e46185.
158. Mojsilovic-Petrovic J, Jeong GB, Crocker A, et al. Protecting motor neurons from toxic insult by antagonism of adenosine A2a and Trk receptors. *J Neurosci.* 2006;26(36):9250-9263.
159. Ellis CE, Schwartzberg PL, Grider TL, Fink DW, Nussbaum RL. alpha-synuclein is phosphorylated by members of the Src family of protein-tyrosine kinases. *J Biol Chem.* 2001;276(6):3879-3884.
160. Schlatterer SD, Acker CM, Davies P. c-Abl in neurodegenerative disease. *J Mol Neurosci.* 2011;45(3):445-452.
161. Jing Z, Caltagarone J, Bowser R. Altered subcellular distribution of c-Abl in Alzheimer's disease. *J Alzheimers Dis.* 2009;17(2):409-422.
162. Olmos-Alonso A, Schetters ST, Sri S, et al. Pharmacological targeting of CSF1R inhibits microglial proliferation and prevents the progression of Alzheimer's-like pathology. *Brain.* 2016;139(Pt 3):891-907.
163. Spangenberg EE, Lee RJ, Najafi AR, et al. Eliminating microglia in Alzheimer's mice prevents neuronal loss without modulating amyloid-beta pathology. *Brain.* 2016;139(Pt 4):1265-1281.

164. Dagher NN, Najafi AR, Kayala KM, et al. Colony-stimulating factor 1 receptor inhibition prevents microglial plaque association and improves cognition in 3xTg-AD mice. *J Neuroinflammation.* 2015;12:139.
165. Karuppagounder SS, Brahmachari S, Lee Y, Dawson VL, Dawson TM, Ko HS. The c-Abl inhibitor, nilotinib, protects dopaminergic neurons in a preclinical animal model of Parkinson's disease. *Sci Rep.* 2014;4:4874.
166. Pagan F, Hebron M, Valadez EH, et al. Nilotinib Effects in Parkinson's disease and Dementia with Lewy bodies. *Journal of Parkinson's disease.* 2016;6(3):503-517.
167. Theoharides TC, Alysandratos KD, Angelidou A, et al. Mast cells and inflammation. *Biochim Biophys Acta.* 2012;1822(1):21-33.
168. Frenzel L, Hermine O. Mast cells and inflammation. *Joint, bone, spine : revue du rhumatisme.* 2013;80(2):141-145.
169. Theoharides TC, Stewart JM, Panagiotidou S, Melamed I. Mast cells, brain inflammation and autism. *Eur J Pharmacol.* 2016;778:96-102.
170. Polyzoidis S, Koletsa T, Panagiotidou S, Ashkan K, Theoharides TC. Mast cells in meningiomas and brain inflammation. *J Neuroinflammation.* 2015;12:170.
171. Beghdadi W, Madjene LC, Benhamou M, et al. Mast cells as cellular sensors in inflammation and immunity. *Front Immunol.* 2011;2:37.
172. Hsu CL, Neilsen CV, Bryce PJ. IL-33 is produced by mast cells and regulates IgE-dependent inflammation. *PLoS One.* 2010;5(8):e11944.
173. Pittoni P, Piconese S, Tripodo C, Colombo MP. Tumor-intrinsic and -extrinsic roles of c-Kit: mast cells as the primary off-target of tyrosine kinase inhibitors. *Oncogene.* 2011;30(7):757-769.
174. Grimbaldeston MA, Chen CC, Piliponsky AM, Tsai M, Tam SY, Galli SJ. Mast cell-deficient W-sash c-kit mutant Kit W-sh/W-sh mice as a model for investigating mast cell biology in vivo. *Am J Pathol.* 2005;167(3):835-848.
175. Lortholary O, Chandesris MO, Bulai Livideanu C, et al. Masitinib for treatment of severely symptomatic indolent systemic mastocytosis: a randomised, placebo-controlled, phase 3 study. *Lancet.* 2017;389(10069):612-620.
176. Smrkovski OA, Essick L, Rohrbach BW, Legendre AM. Masitinib mesylate for metastatic and non-resectable canine cutaneous mast cell tumours. *Veterinary and comparative oncology.* 2015;13(3):314-321.
177. Moura DS, Sultan S, Georgin-Lavialle S, et al. Depression in patients with mastocytosis: prevalence, features and effects of masitinib therapy. *PloS one.* 2011;6(10):e26375.
178. Paul C, Sans B, Suarez F, et al. Masitinib for the treatment of systemic and cutaneous mastocytosis with handicap: a phase 2a study. *American journal of hematology.* 2010;85(12):921-925.
179. Graziottin A, Skaper SD, Fusco M. Mast cells in chronic inflammation, pelvic pain and depression in women. *Gynecol Endocrinol.* 2014;30(7):472-477.
180. Yuan H, Zhu X, Zhou S, et al. Role of mast cell activation in inducing microglial cells to release neurotrophin. *J Neurosci Res.* 2010;88(6):1348-1354.
181. Zhang S, Zeng X, Yang H, Hu G, He S. Mast cell tryptase induces microglia activation via protease-activated receptor 2 signaling. *Cell Physiol Biochem.* 2012;29(5-6):931-940.

182. Rodewald HR, Dessing M, Dvorak AM, Galli SJ. Identification of a committed precursor for the mast cell lineage. *Science.* 1996;271(5250):818-822.
183. Nakamura Y, Kambe N, Saito M, et al. Mast cells mediate neutrophil recruitment and vascular leakage through the NLRP3 inflammasome in histamine-independent urticaria. *J Exp Med.* 2009;206(5):1037-1046.
184. Conti P, Kempuraj D. Important role of mast cells in multiple sclerosis. *Mult Scler Relat Disord.* 2016;5:77-80.
185. Medic N, Lorenzon P, Vita F, et al. Mast cell adhesion induces cytoskeletal modifications and programmed cell death in oligodendrocytes. *J Neuroimmunol.* 2010;218(1-2):57-66.
186. Elieh-Ali-Komi D, Cao Y. Role of Mast Cells in the Pathogenesis of Multiple Sclerosis and Experimental Autoimmune Encephalomyelitis. *Clin Rev Allergy Immunol.* 2017;52(3):436-445.
187. Costanza M, Colombo MP, Pedotti R. Mast cells in the pathogenesis of multiple sclerosis and experimental autoimmune encephalomyelitis. *Int J Mol Sci.* 2012;13(11):15107-15125.
188. Leon A, Buriani A, Dal Toso R, et al. Mast cells synthesize, store, and release nerve growth factor. *Proc Natl Acad Sci U S A.* 1994;91(9):3739-3743.
189. Levi-Montalcini R, Skaper SD, Dal Toso R, Petrelli L, Leon A. Nerve growth factor: from neurotrophin to neurokine. *Trends Neurosci.* 1996;19(11):514-520.
190. Fiala M, Chattopadhay M, La Cava A, et al. IL-17A is increased in the serum and in spinal cord CD8 and mast cells of ALS patients. *J Neuroinflammation.* 2010;7:76.
191. Staats KA, Schonefeldt S, Van Helleputte L, et al. C-kit is important for SOD1(G93A) mouse survival independent of mast cells. *Neuroscience.* 2015;301:415-420.
192. Trias E, Ibarburu S, Barreto-Nunez R, et al. Evidence for mast cells contributing to neuromuscular pathology in an inherited model of ALS. *JCI Insight.* 2017;2(20).
193. Mizisin AP, Weerasuriya A. Homeostatic regulation of the endoneurial microenvironment during development, aging and in response to trauma, disease and toxic insult. *Acta Neuropathol.* 2011;121(3):291-312.
194. Kalichman MW, Powell HC, Calcutt NA, Mizisin AP. Mast cell degranulation and blood-nerve barrier permeability in rat sciatic nerve after 7 days of hyperglycemia. *Am J Physiol.* 1995;268(2 Pt 2):H740-748.
195. Caughey GH. Mast cell proteases as protective and inflammatory mediators. *Adv Exp Med Biol.* 2011;716:212-234.
196. Lindborg JA, Mack M, Zigmond RE. Neutrophils Are Critical for Myelin Removal in a Peripheral Nerve Injury Model of Wallerian Degeneration. *The Journal of neuroscience : the official journal of the Society for Neuroscience.* 2017;37(43):10258-10277.
197. Zenaro E, Pietronigro E, Della Bianca V, et al. Neutrophils promote Alzheimer's disease-like pathology and cognitive decline via LFA-1 integrin. *Nat Med.* 2015;21(8):880-886.
198. Whalley K. Neurodegenerative disease: A neutrophil invasion. *Nat Rev Neurosci.* 2015;16(9):510.

199. Murdock BJ, Bender DE, Kashlan SR, et al. Increased ratio of circulating neutrophils to monocytes in amyotrophic lateral sclerosis. *Neurology(R) neuroimmunology & neuroinflammation.* 2016;3(4):e242.
200. Babior BM, Lambeth JD, Nauseef W. The neutrophil NADPH oxidase. *Arch Biochem Biophys.* 2002;397(2):342-344.
201. Vignais PV. The superoxide-generating NADPH oxidase: structural aspects and activation mechanism. *Cell Mol Life Sci.* 2002;59(9):1428-1459.
202. Vitte J, Michel BF, Bongrand P, Gastaut JL. Oxidative stress level in circulating neutrophils is linked to neurodegenerative diseases. *J Clin Immunol.* 2004;24(6):683-692.
203. Drechsel DA, Estevez AG, Barbeito L, Beckman JS. Nitric oxide-mediated oxidative damage and the progressive demise of motor neurons in ALS. *Neurotox Res.* 2012;22(4):251-264.
204. Pehar M, Vargas MR, Robinson KM, et al. Mitochondrial superoxide production and nuclear factor erythroid 2-related factor 2 activation in p75 neurotrophin receptor-induced motor neuron apoptosis. *J Neurosci.* 2007;27(29):7777-7785.
205. Beckman JS. Understanding peroxynitrite biochemistry and its potential for treating human diseases. *Arch Biochem Biophys.* 2009;484(2):114-116.
206. Beckman JS, Estevez AG, Crow JP, Barbeito L. Superoxide dismutase and the death of motoneurons in ALS. *Trends Neurosci.* 2001;24(11 Suppl):S15-20.
207. Beckman JS, Carson M, Smith CD, Koppenol WH. ALS, SOD and peroxynitrite. *Nature.* 1993;364(6438):584.
208. Kang SH, Li Y, Fukaya M, et al. Degeneration and impaired regeneration of gray matter oligodendrocytes in amyotrophic lateral sclerosis. *Nat Neurosci.* 2013;16(5):571-579.
209. Kang SH, Fukaya M, Yang JK, Rothstein JD, Bergles DE. NG2+ CNS glial progenitors remain committed to the oligodendrocyte lineage in postnatal life and following neurodegeneration. *Neuron.* 2010;68(4):668-681.